

The Open University's repository of research publications
and other research outputs

Biophysical studies of TIMP-1

Thesis

How to cite:

Hodges, Deborah Jane (1995). Biophysical studies of TIMP-1. PhD thesis The Open University.

For guidance on citations see [FAQs](#).

© 1995 The Author

Version: Version of Record

Copyright and Moral Rights for the articles on this site are retained by the individual authors and/or other copyright owners. For more information on Open Research Online's data [policy](#) on reuse of materials please consult the policies page.

oro.open.ac.uk

Biophysical Studies of TIMP-1.

Deborah Jane Hodges.

**A thesis submitted in fulfilment of the requirements of the
Open University for the degree of Doctor of Philosophy.**

June 1995

**Addenbrooke's NHS Trust, Rheumatology Research Unit, in
collaboration with SmithKline Beecham Pharmaceuticals**

Author's number : P9268915

Date of submission : June 1995

Date of award : 22nd September 1995

ON INSTRUCTION

FROM

THE UNIVERSITY THE

PUBLISHED PAPERS

HAVE NOT BEEN

SCANNED

"Before proceeding up the hall, study all the doorways.

You never know when an enemy will be present."

The sayings of Odinn, taken from the Hávamál.

(The Poetic Edda, tr. by H.A. Bellows).

Table of Contents.

	Page
Contents.	i
Acknowledgements.	vi
Declaration.	vii
Summary.	viii
Abbreviations.	x
Publications.	xiv
Preface.	xv
Chapter 1.	1
An Introduction to Matrix Metalloproteinases and the Tissue Inhibitors of Metalloproteinases.	1
1.1. Matrix Metalloproteinases.	2
1.1.1. What Makes an MMP?.....	2
1.1.2 Metal Requirement.....	10
1.1.3. Activation and Latency.....	11
1.1.4 Structures.	14
1.2. An Inhibitor of Metalloproteinases.	14
1.2.1. A Family of Inhibitors.	15
1.3. Sequences and Relationships.....	16
1.3.1. Homologies.....	17
1.4. Physical Properties.....	18
1.4.1. Amino Acid Composition.....	18
1.4.2. Glycosylation	19
1.4.3. Disulphide Pattern.....	20
1.4.4. Stability.....	21
1.4.5 Proteolysis and Peptide Mapping.....	23
1.4.6. Solution Structure of the N-Terminal Domain of TIMP-2.....	25

1.5. Regulation of Expression.....	26
1.5.1. Regulation at the gene level.....	26
1.5.2. RNA stability.....	29
1.5.3. Regulation by Cytokines.....	29
1.6. Localisation.....	32
1.7. Inhibition of the Matrix Metalloproteinases.....	33
1.7.1. TIMP and Enzyme Latency.....	33
1.7.2. Inhibition of Enzyme Activity.....	36
1.7.3. Identifying Important Residues.....	39
1.8. TIMP as a Growth Factor.....	42
1.9. MMPs and TIMPs in Disease States.....	44
1.10. The Development of New Therapeutic Agents.....	45
1.10.1. Compounds Used In Vivo.....	45
1.10.2. Compounds Used In Vitro.....	46
1.11. Summary.....	47
Chapter 2.....	48
General Methods and Materials.....	48
2.1. Assays.....	48
2.1.1. Collagenase and TIMP Bioassays.....	48
2.2. Enzyme-Linked Immunosorbent Assays (ELISAs).....	50
2.3. Protein Assays.....	52
2.3.1. Absorbance.....	52
2.3.2. BCA Protein Assay.....	52
2.4. SDS-PAGE.....	52
2.5. Western Blotting.....	54
2.6. Other Materials.....	56
Chapter 3.....	57
Purification Of TIMP-1.....	57
3.1. Introduction.....	57

3.2. Methods	58
3.2.1. Materials	58
3.2.2. Experimental Methods	58
3.3. Results	62
3.3.1. Purification of TIMP-1 Using Multi-Step Procedure	62
3.3.2. 1D NMR Spectrum of Purified TIMP-1	67
3.3.3. Development of a Monoclonal Antibody Affinity Matrix.....	67
3.3.4. Large Scale Purification of TIMP-1	72
3.4. Discussion	76
Chapter 4.	78
Evaluation of Expression Systems for TIMP-1 in Escherichia Coli.....	78
4.1. Introduction.....	78
4.2. Methods	81
4.2.1. Materials	81
4.2.2. Experimental Details	84
4.3. Results	87
4.3.1. Assessment of the pEZZ18 vector system for TIMP-1 and Δ TIMP-1	87
4.3.2. Assessment of the pASK60-strep Vector System for TIMP- 1 and Δ TIMP-1	99
4.4. Discussion	106
4.4.1. Alternative strategies.....	109
Chapter 5.	110
Secondary Structure and Thermostability of TIMP-1.	110
5.1. Introduction.....	110
5.2. Methods	112
5.2.1. Materials.....	112
5.2.2. Experimental Details	112
5.3. Results	115

5.3.1. Secondary Structure Determination.....	115
5.3.2. Secondary structure Prediction.....	127
5.4. Discussion.....	130
Chapter 6.	134
Some Surface Features of TIMP-1.....	134
6.1. Introduction.....	134
6.2. Methods.....	137
6.2.1. Materials.....	137
6.2.2. Methods.....	138
6.3. Results.....	142
6.3.1. Carbohydrate Analysis.....	142
6.3.2. NMR Paramagnetic Probe Experiments.....	152
6.3.3. ANS Binding Study.....	156
6.4. Discussion.....	164
Chapter 7.	169
Study of a Peptide Derived From the N-terminus of TIMP-1.....	169
7.1. Introduction.....	169
7.2. Methods.....	172
7.2.1. Materials.....	172
7.2.2. Experimental Details.....	172
7.3. Results.....	174
7.3.1. Inhibitory Activity.....	174
7.3.2. NMR studies of the Cyclised form of Cys-3 - Cys-13.....	174
7.4. Discussion.....	193
Chapter 8.	198
The Suitability of TIMP-1 for Further NMR Studies.....	198
8.1. Introduction.....	198
8.2. Methods.....	200
8.2.1. Materials.....	200

8.2.2. Experimental Procedures	200
8.3. Results	201
8.3.1. Solubility, Stability and 1D Spectra	201
8.3.2. pH Stability	203
8.3.3. 2D Spectra.....	203
8.4. Discussion.....	206
Chapter 9.	208
Concluding Discussion.....	208
References.	218
Appendices.	252

Acknowledgements.

I would firstly like to thank my supervisors, Dr. Tim Cawston and Dr. David Reid for all their efforts since this project began.

Many thanks go to all the members of the Rheumatology Research Unit for making these last few years an enjoyable and instructive experience. In particular I would like to acknowledge the efforts of Dr. Mary O'Hare in the development of the TIMP-1 expression systems.

My grateful thanks go to SmithKline Beecham Pharmaceuticals for the funding of this project, in particular, to Dr. Greg Harper. Thanks also to all the staff of the Analytical Sciences department for their guidance with the spectroscopy and HPLC.

Finally, I would like to thank Ben for his endless support and patience. Maybe I'll let you borrow my sword one day.

Declaration.

This thesis is based on research performed in the Rheumatology Research Unit, Addenbrookes Hospital Cambridge. Except for commonly held concepts, and where specific reference is made to other work, the content of this thesis is original. No part of this thesis has been submitted for the award of any other degree.

Please return this form to the Research Degrees Office of the Open University. All students should complete Part 1. Part 2 applies only to PhD students.

Student: DEBORAH J. HODGES PI: P9268915

Sponsoring Establishment: RHEUMATOLOGY RESEARCH UNIT, CAMBRIDGE

Degree for which the thesis is submitted: Ph.D.

Thesis title: BIOPHYSICAL STUDIES OF TIMP -1.

Part 1 Open University Library Authorisation (to be completed by all students)

I confirm that I am willing for my thesis to be made available to readers by the Open University Library, and that it may be photocopied, subject to the discretion of the Librarian.

Signed: [Signature] Date: 20/9/95

Part 2 British Library Authorisation (to be completed by PhD students only)

If you want a copy of your thesis to be held by the British Library, you must sign a British Doctoral Thesis Agreement Form and return it to the Research Degrees Office of the University together with this form. You are also required to provide the University with an unbound copy of the thesis. The British Library will use this to make their microfilm copy: it will not be returned. Information on the presentation of the thesis is given with the Agreement form.

If your thesis is part of a collaborative group project, you will need to obtain the signatures of others involved for the Agreement Form.

The University has decided that the lodging of your thesis at the British Library should be voluntary. Please tick either (a) or (b) below to indicate your intentions.

(a)

I am willing for the Open University to supply the British Library with a copy of my thesis

(b)

I do not wish the Open University to supply a copy of my thesis to the British Library

Signed: [Signature] Date: 20/9/95

Summary.

This study had two aspects. The first was the production and purification of TIMP-1. The second was a series of biophysical studies of TIMP-1 and a TIMP-1 derived peptide.

A monoclonal antibody affinity column was developed and used to purify large quantities of human TIMP-1 for further experiments. Two *E.coli* expression systems were studied to determine whether they would be suitable for large scale production of recombinant protein. In the first system TIMP-1 was to be secreted as a fusion protein which could be cleaved, leaving a free N-terminus. It was discovered that it was not possible to cleave off the fusion protein. In the second system, the protein was secreted, without additions to the periplasm. Although active protein, with the correct N-terminus, was obtained, the yields were too low to be of use for large scale expression.

Secondary structure analysis by CD and FTIR showed TIMP-1 to be a mostly β -sheet protein (approaching 50%) with around 20% α -helix. A temperature study using these techniques found that little change occurs until temperatures of over 60°C where the protein aggregates. The small changes appear to be a general loosening of the structure.

In analyses of the surface of TIMP-1, additional carbohydrate was identified (other than the two N-linked chains) using Con-A probing of Western blots. TIMP-1 purified from WI-38 foetal lung fibroblast cells can be separated into two pools by Concanavalin A-Sepharose chromatography. These two pools were found to have a different set of pIs and a different monosaccharide composition.

The use of NMR paramagnetic probes identified a hydrophobic region exposed on the surface of TIMP-1. This region probably includes a tyrosine residue and either a tryptophan or phenylalanine. The presence of an exposed hydrophobic region was also shown in binding studies using the fluorescent probe ANS. These studies identified a single, low affinity binding site. An additional study with the N-terminal fragment of

type-1 collagenase found no binding sites on the enzyme, but a change in fluorescence occurred when TIMP-1 was present.

A peptide was designed based on the N-terminal sequence of TIMP-1. High homology, susceptibility to mutation and an interesting resemblance to the Bowman-Birk family of inhibitors suggested that this peptide might be inhibitory. It was found to have only a weak inhibitory activity against gelatinase. NMR studies of this peptide in water showed a large number of conformers as a result of stabilisation of the *cis* isomer of its proline residues. This preference for the *cis* form was retained for one proline in the solvent, TFE.

Preliminary NMR studies were also carried out which concluded that TIMP-1 should be suitable for further structural studies using isotopic labelling.

Abbreviations

1D/2D	one-dimensional / two-dimensional
ANS	8-anilino-1-napthalene sulphonate
AP (1) AP (2)	activating protein
APMA	aminophenyl-mercuric-acetate
APS	ammonium persulphate
Bac coll	bacterial collagenase
BBI	Bowman-Birk inhibitor
BCA	bicinchoninic acid
BSA	bovine serum albumin
CAB	Concanavalin A binding
CD	circular dichroism / circular dichroic
CHO	chinese hamster ovary
Con A	Concanavalin A
COSY	correlated spectroscopy
cpm/dpm	counts/disintegrations per minute
DFP	di-isopropyl fluorophosphate
DEPC	diethyl-pyrocabonate
DMARDs	disease modifying anti-rheumatic drugs
DQF	double quantum filtered
Δ TIMP-1	TIMP-1 residues 1-125
DTT	di-thiothreitol

<i>E.coli</i>	<i>Escherichia coli</i>
EDTA	ethylenediaminetetraacetic acid
EGF	epidermal growth factor
ELISA	enzyme linked immunosorbent assay
EMBL	european molecular biology laboratory
EPA	erythroid potentiating activity
FID	free induction decay
FSB	final sample buffer
FTIR	fourier transform infra red
GOR	Gibrat, Garnier and Robson
(rp) HPLC	(reverse phase) high performance liquid chromatography
HRP	horse-radish peroxidase
IEF	iso-electric focusing
IFN	interferon
IL	interleukin
IPTG	isopropyl- β -D-thiogalactoside
L-AMP	LB-ampicillin
LB	Luria - Bertani
MeI	methyl iodide
MMP	matrix metalloproteinase
NCAB	non-Concanavalin A binding
NMR	nuclear magnetic resonance

NOE	nuclear Overhauser effect
NOESY	nuclear Overhauser effect spectroscopy
NSAID	non-steroidal anti-inflammatory drug
OH-TEMPO	4-hydroxy-2,2,6,6-tetramethylpiperidiny-N-oxyl
OPD	0-phenylene-diamine
PBS	phosphate buffered saline
PCR	polymerase chain reaction
PEA	polyoma enhancer A3
PMNL	polymorphonuclear leucocyte
PMSF	phenylmethylsulphonyl fluoride
PNGaseF	Glycopeptidase F
PVDF	polyvinylidene difluoride
ROESY	rotating frame NOESY
RT	room temperature
SB	SmithKline Beecham Pharmaceuticals
SDS	sodium dodecyl sulphate
SDS-PAGE	SDS - polyacrylamide gel electrophoresis
SOPM	self optimised prediction method
Strep	streptavidin
TAE	Tris-acetate-EDTA
TBS	Tris buffered saline
TCA	tri-chloro-acetic acid
TEMED	NNN'N'-tetramethylethylenediamine

TFA	tri-fluoro-acetic acid
TFE-d2	Tri-fluoro-ethanol (partially deuterated)
TGF	transforming growth factor
TIMP	tissue inhibitor of metalloproteinases
TNF	tumour necrosis factor
TOCSY	total correlation spectroscopy
TPA	12-O-tetradecanoylphorbol-13-acetate
TRE	TPA-responsive element
ZZ	pair of IgG binding domains

Publications.

Hodges, D.J. Lee, D.C., Salter, C.J., Reid, D.G., Harper, G.P., Cawston. T.E.
Purification and secondary structural analysis of tissue inhibitor of metalloproteinases-1.
(1994) *Biochim. Biophys. Acta.* 1208, 94-100.

Poster Presentations.

Deborah J. Hodges, David C. Lee, Cclin L. Salter, David G. Reid and Tim E. Cawston.
Structural Analysis of TIMP-1 by NMR, CD and FTIR. British Connective Tissue
Society/British Society of Rheumatology meeting September 1992

Deborah J. Hodges, Tim E. Cawston and David G. Reid. Spectroscopic Studies of a
Peptide Derived from Tissue Inhibitor of Metalloproteinases-1 (TIMP-1). XVith
International conference on magnetic resonance in biological systems. Veldhoven, The
Netherlands 1994.

Preface.

The tissue inhibitors of metalloproteinases are a small family of proteins which specifically inhibit the matrix metalloproteinases. They are found in many tissues and have an essential role in the regulating the turnover of the extracellular matrix.

To maintain healthy extracellular matrix, an even balance between synthesis and degradation must be retained. When this balance is disturbed the result is seen as a number of disease states. Overproduction of matrix is associated with fibrotic type diseases, whilst excessive matrix breakdown is seen in arthritic conditions. The matrix metalloproteinases, together, have the capability to break down all the components of the extracellular matrix. Since the TIMPs are specific inhibitors, they represent an important potential source of therapeutics. Compounds designed to mirror the inhibition by the TIMPs could be used to target the MMPs and control their activity in destructive pathologies.

If such compounds are to be developed, it is essential to understand the mechanism of MMP inhibition by the TIMPs. Part of this is to determine the structure of all of the proteins involved. Since the important regions for inhibition are found on the surface of the protein it is important that this is carefully characterised, both alone and in an enzyme-inhibitor complex.

This study has been devoted to TIMP-1, the first of the family to be discovered. At the outset of this work, very little was known about its structure. It was known to be highly stable (to temperature and pH), with six characterised disulphide bonds and two glycosylation sites where a total of 8 kDa of carbohydrate was attached.

The aims of the study were twofold. The first was to develop an expression system that would guarantee a supply of TIMP-1 for all further studies. The second was to obtain as much structural information about the TIMP-1 molecule as possible using a number of spectroscopic techniques, including NMR.

Chapter 1.

An Introduction to Matrix Metalloproteinases and the Tissue Inhibitors of Metalloproteinases.

The matrix metalloproteinases (MMPs) are a large family of enzymes involved in the breakdown of connective tissue components [1, 2]. Their normal function is in the turnover of extracellular matrix materials such as collagens and proteoglycans. Together, they can break down all of the components of the extracellular matrix. To maintain a balance between synthesis and breakdown it is essential that the MMPs are closely regulated. The regulation is complex, with several regulatory mechanisms involved at different stages. The production, activation and extracellular activity is controlled through stimulation by cytokines, transcriptional and translational controls, the maintenance of enzyme latency, the activation process and the direct inhibition of the active form.

Malfunctions in connective tissue turnover can lead to a variety of disease states. Reduced enzyme activity is seen in fibrotic conditions such as alcohol induced liver fibrosis [3]. Excessive, or undesirable activity is seen in the degenerative processes of the rheumatic diseases and the metastatic activity of tumour cells. A greater understanding of the mechanisms of connective tissue turnover and the enzymes and inhibitors involved may lead to the development of new therapeutics.

The tissue inhibitors of metalloproteinases (TIMPs) are very important, specific inhibitors of the MMPs. The TIMPs inhibit the active form of the enzymes, and in certain cases are involved with maintenance of the latent state. To understand the function of these inhibitors it is also necessary to understand the nature and function of the MMPs.

1.1. Matrix Metalloproteinases.

Vertebrate collagenolytic activity was first identified in tadpole tails [4], where a metallo-enzyme was found that broke down the collagen of the tail during the resorption process. Over the next thirty years a range of different metalloproteinases was identified in many species, that degraded either collagen or other connective tissue matrix proteins. To date there are at least ten named enzymes, although there are almost certainly others that remain to be identified.

1.1.1. What Makes an MMP?

Table 1.1 (below) lists the known matrix metalloproteinases. Some of the enzymes have acquired a number of alternative names. This was a result of differing naming strategies and the circumstances of the original identification, these names are included in the table. Also included are the substrate specificities of each enzyme.

Enzyme	Alternative names	MW	Substrates
Collagenases			
Interstitial Collagenase	MMP-1 Vertebrate Collagenase Fibroblast Collagenase	55 kDa	Collagen I,II,III, X. gelatin. proteoglycan core protein
Neutrophil Collagenase	MMP-8	75 kDa	As MMP-1
Collagenase-3	MMP-13	54 kDa	Collagen I
Gelatinases			
Gelatinase A	MMP-2 72 kDa gelatinase Type IV collagenase	72 kDa	Gelatins type I, II, III Collagens type IV, V, VII, X, XII Aggrecan, Elastin.
Gelatinase B	MMP-9 92 kDa gelatinase Type IV Collagenase	92 kDa	As gelatinase A

Stromelysins			
Stromelysin-1	MMP-3 Transin Proteoglycanase Procollagenase activator	60/55 kDa	Aggrecan, link protein, fibronectin, laminin. Gelatins I, III, IV, V. Cross-link collagens II, IV, IX pro-collagens Activates pro-collagenase and gelatinase B
Stromelysin-2	MMP-10 Transin-2	60/55 kDa	As for stromelysin-1.
Stromelysin-3	MMP-11	58 kDa	N-terminal fragment is a weak caseinase. Also laminin, fibronectin and aggrecan.
Matrilysin	MMP-7 PUMP-1 Uterine metalloproteinase	28 kDa	As for stromelysin-1. Elastin.
Other Enzymes			
Metalloelastase	MMP-12	53 kDa	Elastin, Fibronectin
Membrane Type Metalloproteinase	MMP-14	63 kDa	Activates Gelatinase A

Table 1.1. The Matrix metalloproteinases and their substrates. Most of the information in this table is derived from Murphy et al [5].

There are several features that distinguish the MMPs as a unique class of enzyme. The first of these is that their sequences should be strongly homologous to that of collagenase [6]. Sequences for the human forms of each of the MMPs have been determined, except for MMP-12 (murine form only) and are shown aligned in Appendix 1.

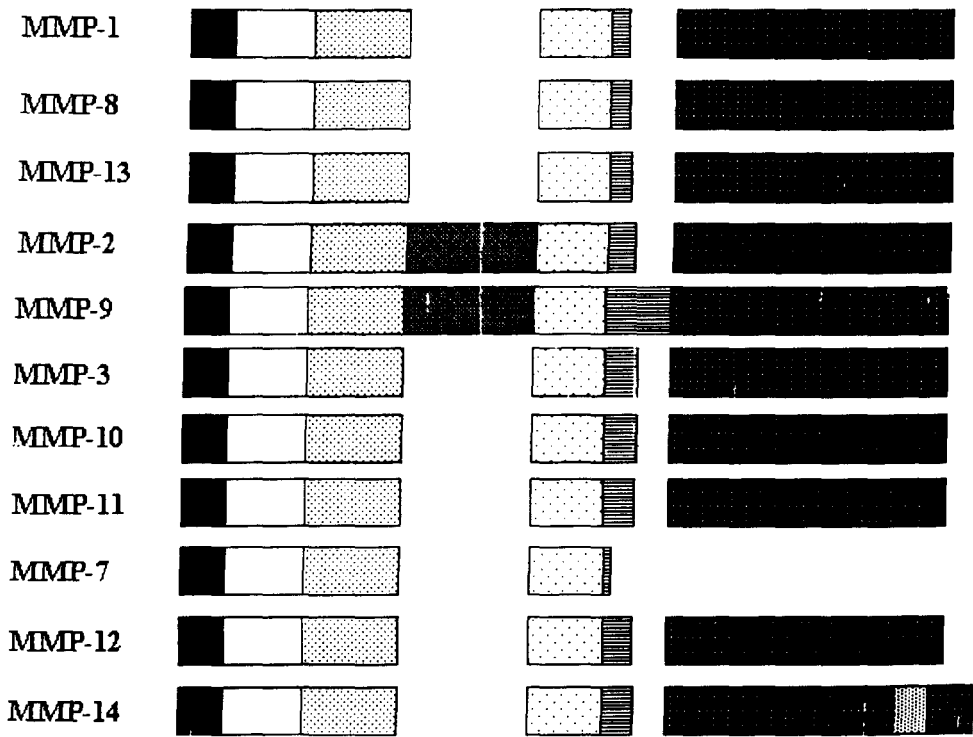
All the MMPs are based around a very similar modular structure. The basic pattern is of a hydrophobic signal sequence, which is necessary since the MMPs are secreted [7]. A conserved propeptide, which is involved in maintaining the latent state of the secreted enzyme, must be removed for the enzyme to attain activity [8]. The catalytic domain contains a highly conserved consensus sequence which forms a zinc binding site [9]. Next, is a proline rich hinge region that is also essential for activity. The C-terminal domain consists of four repeats that resemble hemopexin and vitronectin [10]. In both of the gelatinases (72 kDa and 92 kDa) three repeats of a type II fibronectin like domain are inserted before the zinc binding site [11]. Matrilysin is unusual in that it is a truncated MMP [12]. It does not have the pexin domain and the hinge region is much shorter than in the other MMPs. The membrane metalloproteinase, (MMP14) also has an additional transmembrane anchoring domain. Through variations on this theme they have a range of molecular weights between 28 kDa (matrilysin) and 92 kDa (92 kDa gelatinase or MMP-9). Figure 1.1 shows the different domains and relative sizes of the MMPs.

The final unique feature that distinguishes the MMPs, is that they can all be inhibited by one or more of the TIMP family.

Another feature of the MMPs is not unique to them, but includes them in a larger group of proteinases. This is the highly conserved sequence in the catalytic domain that forms the catalytic domain zinc binding site [13]. The consensus sequence, HEXXH draws in other proteins such as thermolysin, peptidase N and the tetanus toxin. An extension of this consensus sequence and the inclusion of a methionine turn later in the sequence refines the group to a superfamily named the metzincins [14]. This includes very similar proteins such as astacin and some of the snake venom metalloproteinases.

The Collagenases.

There are now three known human collagenases, fibroblast collagenase (MMP-1), neutrophil collagenase (MMP-8) and collagenase-3 (MMP-13). Of all the enzymes, only the collagenases are capable of cleaving triple helical collagen to give the characteristic $\frac{1}{4}$ - $\frac{3}{4}$ fragments [15, 16]. Of the three, fibroblast collagenase is the most






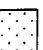



-  Signal peptide
-  Propeptide
-  Fibronectin like domain
-  Catalytic domain
-  Hinge
-  Pexin like domain
-  Transmembrane anchor

Figure 1-1 Representative diagram showing the multi-domain structure of the Matrix Metalloproteinases.

widespread, being produced by a number of cells [1] including skin [17], and macrophages [18]. The expected molecular weight is 52 kDa with an apparent molecular weight of 52 or 56 kDa in the secreted, latent form [19]. The variation is due to heterologous glycosylation. MMP-8 is only produced by PMN-leucocyte cells [20] and has a slightly different specificity from fibroblast collagenase. It is larger than fibroblast collagenase (75 kDa - precursor form) but is also glycosylated. Recently a third protein was added to this group on the basis of its collagenolytic activity, and close sequence homology to the other collagenases. This is collagenase-3 or MMP-13 [21]. It has a sequence of 471 amino-acids and an apparent molecular weight of 65 kDa by SDS-PAGE. This MMP is unusual in that so far it has only been identified in breast carcinomas and no other human tissue. Its role may therefore be unique to the processes of invasive breast cancer. The only other MMPs that resemble this was originally identified as MMP-1 in rats [22] and mice [23]. However, its activity and sequence were unusual for an MMP-1 (it has the ability to cleave other sites in the collagen molecule). The rat and mice collagenases have a greater homology with the human MMP-13, and no equivalent to MMP-1 has been identified in these species.

The site where the α chains are cleaved in triple helical collagen, is unique even though the cleaved residues (Gly-775 - Ile/Leu-776) occur in other regions of the molecule. The sequences on either side of the scissile bond appear to be important in determining the cleavage site [24]. This region may be structurally different to the rest of the collagen molecule, unfolding to allow enzyme access [25].

The unique action of the collagenases is not associated with a particular domain but requires both the N- and C- terminal domains of the enzyme. It is essential that the entire molecule is present. Experiments with chimeric proteins have shown that triple helical collagenolytic activity cannot be re-created by mixing the N- and C- terminal domains of different MMPs [26, 27].

Once active, (human fibroblast) collagenase can break down into two fragments by way of an autolytic cleavage between Pro-250 and Ile-251 (numbered from the first residue of the pro-peptide) [28]. The larger 26 kDa fragment is inactive, but the smaller 22 kDa fragment retains all activity bar that of a triple helical collagenase. Truncation mutants of neutrophil collagenase suggest that the specificity is associated with a 62 residue sequence in the C-terminal domain [29]. Chemical modification of neutrophil collagenase indicates that a tyrosine residue and a lysine residue are essential for the enzyme activity [30].

The Gelatinases.

There are only two members of the gelatinase family, gelatinase A (MMP-2) and gelatinase B (MMP-9). Unlike the collagenases they are able to degrade type IV collagen as well as denatured triple helical collagens. Gelatinase A is the smaller of the two enzymes (72 kDa in its secreted form) and is generally not glycosylated. It is produced by many connective tissue cells, including bone [31], epithelia [32] endothelia [33] and skin [34]. The larger protein, gelatinase B is a 92 kDa glycoprotein. It is less widespread than the 72 kDa gelatinase, being produced by keratinocytes [35], leucocytes [36], monocytes and macrophages [37]. It is also found in a number of transformed cells.

The additional fibronectin like domain consists of three contiguous repeats of the fibronectin type II unit. Fusion of a single repeat of this unit to β -galactosidase allowed it to bind gelatin [38]. Deletion mutants of gelatinase A, where the fibronectin domain was absent had many of the normal properties such as TIMP binding, activation by APMA and k_{cat} for a synthetic substrate. [39] These mutants could not bind to collagen type IV and had a lower activity against casein and gelatin. The fibronectin domain appeared to be responsible for the high affinity of the gelatinases for gelatin and the gelatinolytic activity. Further study [38] has found that the first and last of these three repeats are responsible for the most of the binding activity. The three units are not entirely conserved and the difference in binding affinity is due to variation in a non-conserved region.

The type IV collagen cleavage by the gelatinases has been partially characterised. Gelatinases cleave the molecule at approximately $\frac{1}{4}$ of the distance from its N-terminus [40] at the Gly-446 - Ile-447 scissile bond [41] which is probably part of a triple helical portion of the molecule.

The Stromelysins.

There are three enzymes that have been named as stromelysins, stromelysin-1 (MMP-3), stromelysin-2 (MMP-10) and stromelysin-3 (MMP-11).

The first two stromelysins are closely related in both sequence, [42] and specificity [43, 44, 45]. The differences are that stromelysin-1 also degrades the proteoglycan link protein, laminin, procollagen peptides and type X collagen. Both enzymes are capable of activating pro-collagenase.

Stromelysin-3 was identified by screening a cDNA library and was classified as a stromelysin on the basis of its location in the stromal cells of breast carcinomas [46]. However, its sequence is unusual, having a relatively low similarity to the other stromelysins and the MMPs (40% homology to other stromelysins and collagenase, compared with 79% between the two stromelysins and 56% for the similarity between stromelysin-1 and collagenase-1). In a phylogenetic analysis of the MMP family, stromelysin-3 appears as a very early branch off the main line [42]. It is also found on a different chromosome to the majority of the MMPs, locating to the q11.2 region of chromosome 22 [47] rather than chromosome 11 q22-q23 [48]. The difference between the sequence of stromelysin-3 and the remainder of the metalloproteinases implied that there could be differences in the activity or mechanism. This was borne out on expressing the murine stromelysin-3 gene in *E.coli* [49]. The gene product was a 57 kDa protein that did not show any enzymatic activity, and could not be activated by the conventional methods. However treatment with organomercurials generated 55/58 and 27/28 kDa forms. The short form had lost the propeptide and much of the C-terminal domain. This N-terminal piece was found to have very weak caseinase activity as well as degrading

fibronectin, laminin and proteoglycan. It has no type I collagenolytic activity, gelatinolytic activity is very weak and type IV collagen was only degraded at 37°C. Like the other stromelysins it is able to potentiate the activation of collagenase by trypsin and can be inhibited by TIMP-1.

Other MMPs.

The remaining MMPs have not been characterised sufficiently to be described as either a collagenase, a gelatinase or a stromelysin. Some do not fit the descriptions of any category. Matrilysin (MMP-7) is the best described of the remaining MMPs. This short form metalloproteinase was originally identified in uterine tissue on the basis of its substrate specificity and response to certain inhibitors [50]. Its activity is similar to that of the stromelysins, degrading gelatins, proteoglycan and fibronectin. It also has the ability to activate procollagenase [12]. Unlike the other stromelysins it can not degrade type X collagen. Although the C-terminal domain is absent, it behaves much as any other MMP, being secreted as a latent pro-enzyme that can be activated by organo-mercurials and inhibited by 1,10-phenanthroline and TIMP-1.

Metalloelastase (MMP-12) has the same domain structure as the rest of the family and is approximately the same size (53 kDa in pro- form and 45 kDa when active). However it does not show a wide spectrum of activity. Its only substrate identified to date is elastin [51]. The most recent addition to the MMP family is the only one that is not secreted from the cell to the matrix. Instead it is found on the cell membrane. This is MMP-14 or membrane type matrix metalloproteinase [52]. The predicted amino acid sequence shows that it also follows the basic multi-domain structure of the other MMPs but contains two differences. The first of these is an insertion of 10 residues similar to one seen in stromelysin-3. The second is a sequence in the haemopexin domain that is very rich in hydrophobic residues and could thus act as the transmembrane anchor. The function of this enzyme appears to be the activation of the 92 kDa pro-gelatinase A at the cell surface.

1.1.2 Metal Requirement.

Both zinc and calcium are required for activity. Early experiments showed that zinc was present in the collagenase molecule and that it was essential for the enzyme's activity [53]. Initially there were no quantitative determinations of the amount of zinc present in each molecule. A conserved sequence in the catalytic domain looked like a promising candidate for a zinc binding site. The catalytic zinc atom is found at the active site, in all of the known MMP structures forming ligands to the three conserved histidine residues, His-218, His-222 and His-228 (numbered according to the human fibroblast collagenase sequence). Further studies of stromelysin showed that two moles of zinc were present per mole of enzyme [54]. This is probably the case for all the MMPs. The function of the additional zinc was revealed on the publication of the first crystal structure of a truncated MMP [55]. It has a structural, rather than catalytic function in the enzyme. Calcium is also found to interact with the enzyme and is again essential for its activity, increasing its overall stability [56]. Stromelysin-1 has been shown to require a minimum of 2 mM calcium to maintain the thermostability of the enzyme and prevent autolysis [57]. This concentration of calcium is also important for the activation of the enzyme. Evidence from the structure of full length human fibroblast collagenase (T.E. Cawston personal communication) has found 3 calcium atoms in the N-terminal domain and 1 in the C-terminal domain. The hinge region and part of the fibronectin inserts in the gelatinases have regions that are rich in Glu/Asp and subsequently are good candidates for calcium binding sites in this group of MMPs.

1.1.3. Activation and Latency.

All of the MMPs are secreted in a latent pro-enzyme form that requires activation. On activation the molecular mass of the enzyme decreases by around 10 kDa. Early evidence could not determine whether this was a result of the removal of a propeptide [58], or the loss of an inhibitor [59].

A number of chemical agents have been found that can activate the MMPs. These include organo-mercurials such as p-aminophenylmercuric acetate (APMA) [60], chaotropic ions including sodium thiocyanate and sodium iodide [61], and detergents [62]. Many proteinases can also activate the MMPs. Trypsin [63], several serine proteinases [64], bacterial proteinases [65], plasmin [66], mast cell chymase [67] collagen (gelatinase only) [68] and other MMPs that have already been activated [69, 70].

All of the zymogen forms of the MMPs have a pro-peptide that is lost during the processing to the active species. This peptide has an essential role in maintaining the latent state. Part of the pro-peptide sequence is highly conserved throughout the MMPs. The consensus sequence of this conserved region is MRKPRCGVPD. Peptides containing this sequence were found to inhibit active 72 kDa gelatinase [71]. The same effect was also seen for free cysteine alone. This pointed to the importance of the pro-peptide cysteine residue in the latency, and activation of the MMPs. The initial work suggested that the cysteine in the pro-peptide could co-ordinate with the zinc atom at the active site. This was supported by studies of mutants lacking Cys-73 [72]. Fibroblast collagenase that was secreted without Cys-73 either exhibited more autoactivation or could be more easily activated than the wild type protein. The final confirmation was the identification of the Cys-Zn ligand in stromelysin [54]. The presence of the peptide would serve to partially block access to the active site. In addition, the cysteine ligand occupies a site normally occupied by a water molecule that is essential for catalysis. For

the MMPs to be activated this interaction must be perturbed and a resulting conformational change lead to the completion of the activation process.

The involvement of the Cys-Zn ligand in the latency of the MMPs has given rise to the cysteine switch model of activation [73]. The dissociation of the cysteine from the zinc as a result of external influences acts as a switch, turning the zinc atom from an inactive state, into a catalytic one, allowing autolytic activation to occur. Another experiment identified the formation of a covalent complex between the cysteine residue and the Hg atom of APMA during the activation process, supporting the switch model [74]. This model describes the activation process for most of the MMPs under most circumstances. Interestingly the activation of stromelysin-1 required more than the disruption of the Cys-Zn coordination. Dissociation by modification of the Cys residue did not activate the protein and further APMA or proteinase treatment was required [75]. The reaction appears to be due to other structural changes.

Although the final product of the activation is essentially the same, the fine details of the mechanism differ for the chemical and proteolytic methods.

For stromelysin-1, proteolytic activation can be by a number of proteinases that generally cleave the pro-peptide at an exposed sequence [63]. The exact site varies between different proteinases and is followed by a second autolytic cleavage at the His-82 - Phe-83 bond. This stepwise activation appears to be universal throughout the MMPs, including matrilysin which lacks the C-terminal domain [76].

Stromelysin-1 has been found to activate 92 kDa gelatinase (MMP-9) in a two stage reaction, the first cleavage exposing the second cleavage site [69]. Stromelysin-1 (MMP-3) has also been shown to activate pro-collagenase [77]. When APMA was included in the reaction the final activity was greater than that of either MMP-3 or APMA alone. In this case the initial activation (by APMA or other proteinases) leads to a reduction in molecular weight and some activity. Stromelysin-1 cleaves the Gln-80 - Phe-

81 bond resulting in increased activity [78]. This superactivation appears to be related to the formation of a salt bridge between the N-terminal NH group and Asp-232 [79].

Of the chemical activators, the mechanism of activation by APMA has been best studied. The activation by organo-mercurials is dependent on their concentration. In the activation of the 72 kDa pro-gelatinase, residues 1-80 are cleaved at a specific locus leaving a single N-terminus for the active 63 kDa protein [80]. This cleavage is autoproteolytic, and for enzyme activity to be present there must be some rearrangement of the proteins structure to allow it. A similar picture is seen for the activation of polymorphonuclear leucocyte collagenase (PMNL). Rather than a single cleavage, the reaction occurred via three steps, giving a final N-terminus of either Met-80 or Leu-81 [81].

When HgCl_2 is used as the activating compound for 92 kDa gelatinase the cleavage of the N-terminal pro-peptide occurred in several steps [82]. Four individual cleavage reactions occurred giving an N-terminus at residue 76 and the conserved sequence containing the active cysteine of the pro-peptide remained intact. An additional set of three cleavages took place at the C-terminus removing other cysteine residues. It is possible that the 92 kDa gelatinase has a different mechanism of activation, using a disulphide rearrangement rather than the destabilisation of the cysteine-zinc ligand. The function of the Hg atom in either an organo-mercurial or in HgCl_2 alone is to destabilise the Cys-Zn ligand by altering the equilibrium so that the Cys forms a ligand or covalent complex with the mercury atom. This allows the water molecule to return to the zinc atom, restoring activity. The other compounds that activate the MMPs are all thought to act in a similar manner. Mercurials, thiol reagents, metal ions and oxidants directly disrupt the Cys-Zn ligand [1]. Other agents such as chaotropes and detergents (e.g SDS) have a general effect on the proteins structure, inducing large scale conformational changes that would shift the equilibrium of the Cys-Zn towards the active state.

1.1.4 Structures.

It has proved to be very difficult to determine the structure of the MMPs. The full length active enzyme (collagenase in particular) tends to fragment. To date the only completed structures are those of N-terminal fragments, produced using recombinant techniques. The recent developments in NMR technology have meant that the truncated proteinase was suitable for solution studies. The first structural details to appear were the secondary structure assignments of truncated stromelysin-1 [83]. The 19 kDa catalytic domain is composed of a five stranded β -sheet with four parallel and one anti-parallel strand and three helices. The secondary structure is very similar to that of astacin, a related proteinase [84]. The crystal structures of truncated human fibroblast and neutrophil collagenases give the overall structure [55, 85]. When complexed with a low molecular weight inhibitor, the structure of neutrophil collagenase is essentially spherical with a small cleft separating the main portion from a smaller C-terminal subdomain. The first zinc is found at the bottom of the active site cleft, whilst the second is packed onto the top of the sheet along with two calcium ions. The fibroblast collagenase structure is extremely similar to this [86]. All of the N-terminal structures solved so far share the same topology and it is likely that other MMP structures will share the same overall fold. However, the C-terminal domains may show greater variability.

1.2. An Inhibitor of Metalloproteinases.

During the latter part of the 1970's collagenase inhibitory activity was identified in various mammalian body fluids and tissues. Woolley et al [87] discovered a small (40 kDa) protein in serum that showed high specificity to collagenase, but did not inhibit any other class of enzyme. Sellers et al [88] described another inhibitor in the medium of rabbit foetal bone cultures. This showed inhibitory activity against stromelysin and gelatinase as well as collagenase. The protein appeared to have a molecular weight of 30 kDa by gel filtration. It was also shown to be inactivated by trypsin, chymotrypsin and by

boiling for 15 minutes. A closely similar inhibitor was identified in tissues from gravid uterus [89]. These inhibitors were produced in the early stages of the culture (days 1-3) [90] during the log phase, and before collagenase could be detected in the medium. They also showed a cross species specificity, inhibiting murine and porcine collagenases [88]. Tissues from several different species were also shown to contain collagenase inhibitors (reviewed in detail by Reynolds et al) [91], including, chick bone [92] porcine smooth muscle [93], porcine gingiva [94] bovine nasal cartilage [95], bovine aorta [96], human skin fibroblasts [97], human rheumatoid synovium [98], human tendon [99], and human gingiva [100]. All of these inhibitors showed several distinctive features in common, which can be used as an aid in identifying new proteins as TIMPs. They were stable at high temperatures for short periods, e.g. 60°C for 10 minutes, but were destroyed at high temperatures. They were also resistant to low pH (as low as pH 2.0) [96] and lyophilisation [101]. Inhibitory activity could also be abolished by 30 mg/ml trypsin [102], reduction and alkylation [93] and 3M KSCN [100]. The molecular weight of the proteins as determined by various gel filtrations and gel electrophoresis ranged from 22 kDa [95] to 45 kDa [96], although most estimates were in the high twenties. Woolley et al named their inhibitor β_1 -anticollagenase from its original identification as a β -serum protein [87]. In the paper by Cawston et al [103], describing the purification scheme for rabbit bone inhibitor, the name, tissue inhibitor of metalloproteinases (TIMP) was proposed for this protein. This inhibitor is now known as TIMP-1. Other related inhibitors are numbered in order of discovery.

1.2.1. A Family of Inhibitors.

There are three identified tissue inhibitors of metalloproteinases TIMP-1, TIMP-2 and TIMP-3. They have been identified in many species and tissues, and it is likely that the TIMPs are ubiquitous throughout the mammals.

During the preparation of the 28.5 kDa inhibitor (TIMP-1), occasionally other inhibitory activities were seen. One was seen at a lower molecular weight of around 22

kDa [104]. This did not bind to Concanavalin A. Another [105], had an apparent molecular weight of 75 kDa, and was eventually shown to be an inhibitory enzyme-inhibitor complex. The second member of the TIMP family was confirmed by two separate groups, in 1989 when the sequences of human [106], and bovine [107] 22 kDa TIMP-2 were published concurrently. Previously, a bovine inhibitor with an apparent molecular weight of 28 kDa by gel filtration, had been partially sequenced [108]. This sequence was identical to that of the published TIMP-2, although it was not identified as a distinct protein at the time.

The most recent addition to the TIMP family was initially identified in chicken embryo fibroblasts [109], as a protein produced during the early stages of cell transformation. It is one of a series of metalloproteinase inhibitors that were identified in the media and extracellular matrix of the cell cultures. Again it is a protein of approximately 21 kDa, and like TIMP-2, is not glycosylated. However, its sequence [110], differs sufficiently from those of TIMP-1 and TIMP-2 for it to be classed as a third, distinct TIMP, TIMP-3.

1.3. Sequences and Relationships.

In 1983 the first 23 N-terminal residues were determined by Stricklin et al [111] for a 28.5 kDa inhibitor from human skin fibroblasts. They also suggested that the protein contained no free thiols, but did contain a large number of disulphides (although this number was initially overestimated).

The first complete TIMP sequence to be published was the nucleotide sequence of TIMP-1 from human cells [112]. This indicated a protein of 184 residues with an N-terminal sequence of 23 residues cleaved during processing. Two potential glycosylation sites were identified at Asn-30 and Asn-78. Also of note was the large number of

cysteine residues (12). The amino acid sequence of human TIMP-1, as derived from its nucleotide sequence, is shown below (table 1·2).

1	CTCVPPHPQT	AFCNSDLVIR	AKFVGTPEVN	QTTLYQRYEI	KMTKMYKGF
50	ALGDAADIRF	VYTPAMESVC	GYFHRSHNRS	EEFLIAGKLQ	DGLLHITCS
100	FVAPWNSLSL	AQRRGFTKTY	TVGCEECTVF	PCLSIPCKLQ	SGTHCLWTD
150	LLQGSEKGFQ	SRHLACLPRE	PGLCTWQSLR	SQIA	

Table 1·2. Amino acid sequence of human TIMP-1.

This sequence is identical to the partial sequence described by Stricklin et al [111].

There are now complete TIMP-1 sequences for mouse [113], human [112], bovine [114] sheep [115], rat [116], rabbit [117], pig [118] and baboon [119]. TIMP-2 sequences have been determined for mouse [120], human [106], bovine [107] and rat [121] inhibitors. Three sequences for TIMP-3 in different species have also been generated in quick succession, the original, chick [122], human [123], and mouse [124].

1.3.1. Homologies.

Computer analysis of the TIMP sequences gives the relative homologies between the different molecules within, and between species. In humans, TIMP-1 and TIMP-2 share a 41% direct homology, with a further 29% of residues as conservative substitutions [106]. TIMP-3 has a 37% and a 42% direct homology to TIMP-1 and TIMP-2 respectively.[123]. In all three proteins, across all species, the cysteine residues are entirely conserved, implying that these residues are essential to the structure, and subsequently the inhibitory process. In addition all three tryptophan residues are entirely conserved. Particular regions show a higher than average degree of conservation. Most notably, the N-terminal stretch of 24 residues which has a 66% identity between the three TIMPs. The three sequences aligned using the Clustal program are shown in Appendix 2.

The equivalent analysis for the murine forms of TIMP gives an identity of 35·7% and 36·8% with TIMP-1 for TIMP-2 and TIMP-3 respectively and 43·0% between

TIMPs 2 and 3 (calculated using the method of Lipman and Pearson [125]). Again the cysteines and tryptophans and strong N-terminal homology are retained. A Clustal alignment showing all the known TIMP sequences is included as Appendix 3.

It is interesting, that the pre-sequences of TIMPs 1 and 2 also show a high degree of homology [126] which may point to an important role for the pre-sequence in the *in vivo* processing of the protein. The presequence of TIMP-3 [122, 123] is also very similar having a run of lysine residues and ending with an alanine before the N-terminal cysteine.

1.4. Physical Properties.

Since TIMP-1 was identified several years before the other members of the TIMP family, much more is known about its structure and physico-chemical properties. Subsequently this description of the physical properties concentrates primarily on TIMP-1.

1.4.1. Amino Acid Composition.

The amino acid composition of TIMP-1 is set out in table 1.3.

Ala	Cys	Asp	Glu	Phe
11	12	5	9	10
Gly	His	Ile	Lys	Leu
12	6	7	8	18
Met	Asn	Pro	Gln	Arg
3	4	10	12	10

Ser	Thr	Val	Trp	Tyr
13	16	9	3	6

Table 1-3. Amino acid composition of human TIMP-1. When compared with the mean composition of 1465 proteins [127], TIMP-1 is rich in cysteine, glutamine and threonine, but has relatively little asparagine and aspartic acid.

1.4.2. Glycosylation

TIMP-1 is a glycoprotein, and will bind to Concanavalin A [128]. The other TIMPs are apparently non-glycosylated, having no clear glycosylation consensus sequences, or anomalously high molecular weights on SDS-PAGE. However towards the C-terminus of TIMP-3 is the sequence Asn Ala Thr, which is a potential glycosylation site. Although the chicken TIMP-3 was not found to be glycosylated, there may be situations where carbohydrate is attached.

The amino acid sequence of TIMP-1 has two sites at Asn-30 and Asn-78, which are part of consensus sequences for N-linked glycosylation (Asn-Xaa-Thr/Ser). TIMP-1, with 184 amino-acids would be expected to have a molecular weight of 20.5 kDa. The actual molecular weight of 28.5 kDa is made up of extensive glycosylation at both N-linked sites. This is indicated by the appearance of an intermediate band of approximately 25 kDa, when the protein is treated with N-glycosidase [129]. A further indication that both sites are glycosylated is that both asparagine residues are not seen during sequencing unless the protein is deglycosylated [130]. The N-terminal fragment of TIMP-1 expressed in mouse myeloma cells shows more than one molecular weight which is reduced to a single SDS PAGE band by deglycosylation. From the appearance

of tryptic fragments on rpHPLC it would appear that the primary glycosylation site is Asn-30, and that this glycosylation is heterologous [131].

Human skin fibroblast TIMP-1 was found to contain 13 hexose residues per molecule [111], although this does not account for the total extra mass. The most detailed study of the sugar composition of TIMP-1 was carried out using TIMP-1 (apparent Mw 29 kDa) from bovine dental pulp [132]. This showed TIMP-1 to contain complex-type oligosaccharides composed of a substantial quantity of glucosamine, with large proportions of mannose and galactose, with fucose, glucose and sialic acid as minor components. The binding to Concanavalin A indicates that α -D-mannopyranosyl or α -D-glucopyranosyl is available. TIMP-1 does not bind to wheat germ lectin Sepharose, indicating that there are no free N-acetyl glucosaminyl residues [128].

The isoelectric focusing pattern of TIMP-1 shows considerable heterogeneity. Bovine TIMP-1 gives two pIs of 5.6 and 6.5 [132], rabbit bone TIMP-1^{has} values of 5.9, 6.4 and 6.6 [133]. Human TIMP-1 also shows a number of different pIs [134]. Neuraminidase treatment reduces the number of these isoforms and results in pIs of between 8 and 9. However the value predicted by computer analysis of the sequence is close to 7 (my calculation) which has implications for the tertiary arrangement of acidic and basic residues. Concanavalin A purification of foetal lung fibroblast TIMP-1 has identified a form of TIMP-1 that does not bind to the lectin, but is otherwise identical to the binding form [135]. These facts would suggest that the glycosylation pattern is heterogeneous, with most of the heterogeneity due to variable sialation.

1.4.3. Disulphide Pattern

The absence of free thiols [111] indicates that all of the cysteines in TIMP-1 are found as disulphide bonds. Determination of the amino acid composition [111] showed the presence of twelve cysteines, and thus, six disulphide bonds. The arrangement of the disulphides was determined by rpHPLC analysis of trypsin degradation fragments, identifying disulphide bonded fragments by differences occurring on reduction [136].

This gives disulphide pairs of Cys-1 - Cys-70, Cys-3 - Cys-99, Cys-13 - Cys-124, Cys-127 - Cys-174, Cys-132 - Cys-137 and Cys-145 - Cys-166. The arrangement of the disulphides is such that TIMP-1 has two apparent domains. The first domain is between Cys-1 and Cys-124, the second from Cys-127 to the C-terminus, with a linker of Glu-125 - Glu-126 between. Since the cysteines are entirely conserved, this pattern is assumed to be consistent throughout the TIMP family [137]. The nature of the linker between the two domains is variable, with one or two small, often acidic residues present.

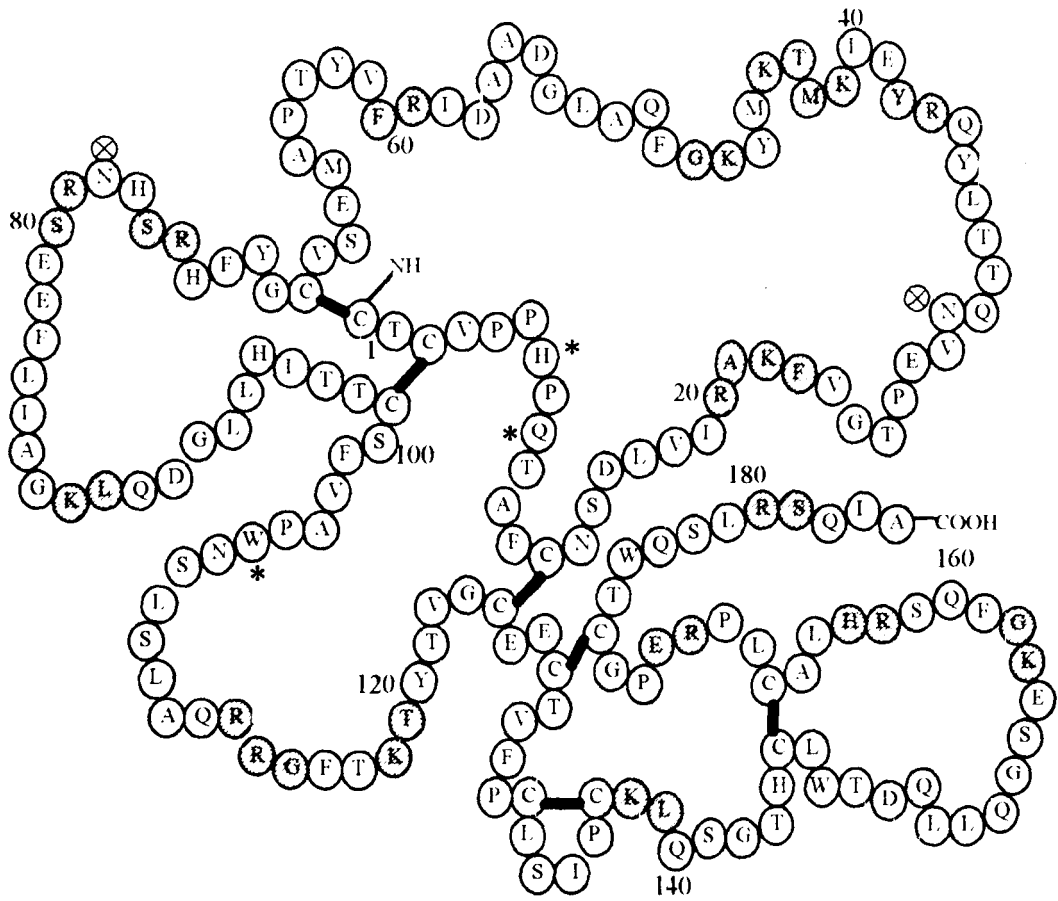
The order of the disulphides is such that it is possible to draw a representative diagram of TIMP-1 (Figure 1.2), where none of the loops have to cross in three dimensions.

Although the disulphide pattern has only been determined for human TIMP-1, the cysteine residues are conserved throughout the TIMP family. Thus, it is assumed that the pattern holds true for all of the other TIMPs [137], and similar structures can be created using the equivalent, assumed disulphide pairs.

1.4.4. Stability.

One of the notable features of the TIMP family is the exceptional stability of the proteins under extreme conditions. Although the biophysical properties of TIMP-3 have yet to be fully determined it is likely that it will be similar.

TIMP-1 from many different species and tissues shows a high degree of thermal stability. TIMP-1 can survive for an hour at temperatures of up to 60°C [133]. However, boiling for extended periods does destroy the activity [93]. It is also very resistant to low pH, being almost unaffected by incubations at pH values as low as 2 [93]. Much of this stability is attributed to the high number of disulphide



- ⊗ Glycosylation site
- * Residue implicated in MMP inhibition
- Disulfide bond
- Tryptic cleavage site

Figure 1-2. Representative Diagram of TIMP-1 Showing Features of Interest.

bonds present, although it is possible that TIMP-1 can sustain substantial damage without any immediate effect on its inhibitory capabilities.

1.4.5 Proteolysis and Peptide Mapping.

TIMP-1 has differing susceptibilities to degradation by proteases [138]. It is sensitive to trypsin and α -chymotrypsin, which break TIMP-1 down into a series of small fragments. This degradation was originally used in conjunction with thermostability tests to identify TIMP like inhibitors. Human neutrophil elastase also destroys the activity at a relatively low concentration (10 μ g/ml). Other proteinases had little or no effect on TIMP-1, even at high concentrations. Plasmin, thrombin, and plasma kallikrein do not affect the activity in any way, whilst cathepsin G and pancreatic elastase require high enzyme concentrations to give only a partial inactivation. These enzymes do not affect the molecular weight of TIMP-1 on a non-reducing PAGE, but only when the disulphides are reduced, do smaller polypeptides appear. This suggests that the conformation is held very firmly by the disulphides, and the proteolysis only affects activity when sections of the protein are removed by multiple cleavages.

The trypsin cleavage used to identify the disulphide bonded fragments also identified an insoluble tryptic core [136]. This core included five out of the six disulphide pairs (all but Cys-145 - Cys-166). A further study of the tryptic fragments generated a detailed peptide map [139] shown in table 1.4.

Tryptic cleavage of the non-reduced form of TIMP-1 produced insoluble peptides of residues 1-20, 60-75, 89-113, 119-138 and 170-180, with the remaining peptides in a soluble fraction. Analysis of the rate of cleavage in the whole protein and N-terminal fragment of TIMP-1 (Cys-1 - Glu-126) identified particular peptides that are released faster and hence are more accessible than others. The last four residues (180-184) were released first, but only require one cut, rather than two. Evidence from the quick release of peptides suggests that the C-terminus, and the region Arg-113 - Lys-118 are exposed. The region Lys-23 - Arg-59 is also exposed, but to a lesser extent, with the three

Residue Numbers	Sequence
1-20	CTCVPPHPQTAFCSNDLVIR
21-22	AK
23-37	FVGTPEVNQTTLYQR
38-41	YEIK
42-44	MTK
45-47	MYK
48-59	GFQALGDAADIR
60-75	FVYTPAMESVCGYFHR
76-79	SHNR
80-88	SEEFLLIAGK
89-113	LQDGLLHITTCSEFVAPWNSLSLAQR
114	R
115-118	GFTK
119-138	TYTVGCEECTVFPCLSLPCK
139-157	LQTGTHCLWTDQLLQGSEK
158-162	GFQSR
163-169	HLACLPR
170-180	EPGLCTWQSLR
181-184	SQIA

Table 1-4. Tryptic Cleavage Fragments of TIMP-1. This table has been modified from the original paper and includes Ser-76 - Arg-79, Ala-21 - Lys-22 and Arg-114 which were not detected but their existence is derived from the data.

peptides it contains being released in a distinct sequence. It has been noted that TIMP-1 preparations that became bacterially contaminated are also cleaved in this region (between Gly-53 and Asp54) [Clark, I.M. unpublished results].

Interestingly, TIMP-3 has a different sensitivity to TIMP-1. Whilst susceptible to chymotrypsin and the non-specific action of Pronase, it is resistant to trypsin degradation [140]. It is also resistant to the proteinases produced by transforming cells, but since these would include matrix metalloproteinases, each enzyme would need to be assayed individually.

1.4.6. Solution Structure of the N-Terminal Domain of TIMP-2.

A recent publication has described the partial solution structure of the N-terminal domain of TIMP-2 [141]. Expression in a mammalian cell system meant that isotopic labelling was not possible and all the data were obtained using homonuclear, three-dimensional NMR methods. The overall fold is that of a five stranded, antiparallel β -barrel, where β -sheet comprises 40 % of the total secondary structure content. Two short stretches of helix are also found. The remainder of structure consists of ill determined loops. This structure is similar to the fold seen in the OB (oligosaccharide/oligonucleotide) binding family of proteins.

The highly conserved VIRAK sequence forms part of a structurally important helix. Folding studies of N-terminally truncated TIMP-1 and TIMP-2 (wild type and mutants) indicate that Ala-21 in particular is important for the structural stability [142].

1.5. Regulation of Expression.

1.5.1. Regulation at the gene level.

Chromosomal Location.

Each of the genes for the human TIMPs is found on a different chromosome. TIMP-1 is found on the X-chromosome [143], as part of a conserved linkage group that includes the genes for ornithine transcarbamylase, synapsin-1 and one of the *raf* oncogene family. The gene for human TIMP-1 has been mapped to position Xp11·1-p11·4 [144, 145].

The gene for human TIMP-2 has been localised to the end of chromosome 17, at position 17q25 [146]. Other genes in this region include galactokinase, avian erythroblastic leukaemia viral oncogene homologue 2-like (ERBA 2L) and the thyroid hormone binding protein. The murine equivalent has been found on chromosome 11 close to a protein kinase gene, and again to the ERBA gene.

The human TIMP-3 gene has been identified on chromosome 22, at position q12·1-q13·2 [123]. In this case the position was determined by *in situ* hybridisation so there is no information as to other closely linked genes.

There is a form of regulation that is unique to the X chromosome, X-linked inactivation. Early in female development one of the X-chromosomes is shut down, with a large number of its genes being inactivated. Although the TIMP-1 gene lies close to one of the genes that are expressed, analysis of mRNA production from active and inactive X chromosomes indicates that the active chromosome mRNA production is one hundred times that of the inactive chromosome [147].

Gene Structure and Regulatory Sequences.

Much of the early work on the TIMP-1 promoter region was carried out using the murine genome. The murine TIMP-1 gene was originally identified as 16C8, which

was co-induced with IFN β 1 on infection with Newcastle Disease virus [148, 149]. The gene could also be induced by serum and phorbol esters [150]. Analysis of the upstream sequence and comparison with the human TIMP-1 cDNA identified an arrangement of six introns, five exons and a number of regulatory sites [151].

The exact size of the upstream regulatory region is unknown. A length of 230 bp is sufficient to allow expression [113, 151], and deletion of the region -230 to -52 abolishes transcription. The β -galactosidase gene under the control of a region of the TIMP-1 promoter (from -2158 to -58) shows normal expression and control suggesting that distal sequences have a role in the full regulation of the gene [152].

There is no clear TATA box and to date, eight possible transcription start sites have been identified [151]. The induction by Newcastle Disease virus is associated with four CCAAT boxes present in intron 1 which increase the level of transcription when present [153]. Intron 1 itself is not translated. Phorbol ester (e.g. 12-*O*-tetradecanoylphorbol-13-acetate) and serum responses are associated with a non-consensus AP1 (activating protein 1) site at position -59/-53 [154]. Interestingly this partial site only functions correctly in the context of the TIMP-1 gene. Close to this downstream site, and also involved in the serum/phorbol response is a 24 bp dyad of symmetry which contains a PEA3 (polyoma enhancer A3) site [155]. These two sites make up the TRE (TPA-responsive element). It is thought that the TRE is responsible for the basal level of TIMP-1 gene transcription. The TRE site is flanked by a pair of sp1 sites (GC boxes) which are commonly found in housekeeping genes [155]. Further upstream is a true AP1 enhancer site flanked by a further two possible PEA3 sites [155]. Also present, between the TRE and are two potential AP2 sites surrounding another potential sp1 site [153].

The set of regulatory regions (including potential sites) in the murine TIMP-1 promoter is summarised in Figure 1.3.

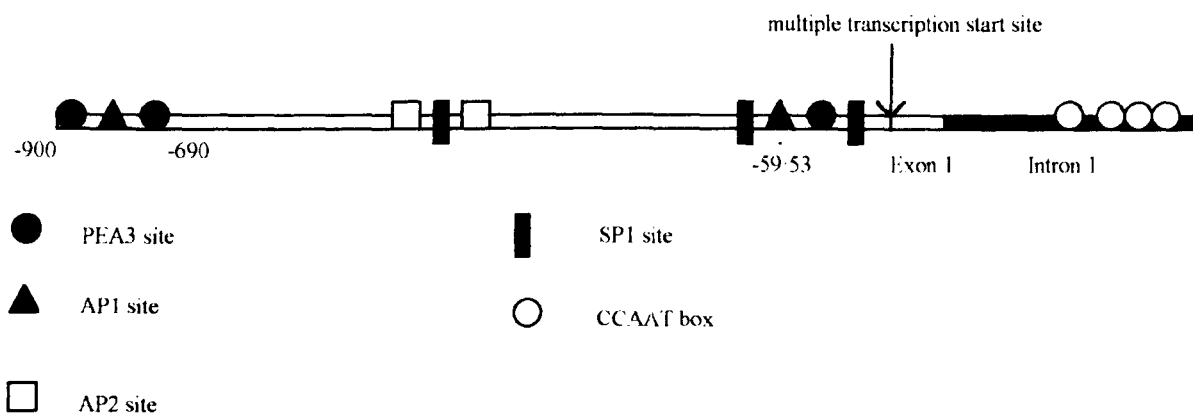


Figure 1-3. Regulatory Elements of the murine TIMP-1 Promotor.

Evidence from constructs with reporter genes suggests that all of these regions are important for transcription. However only the AP1 site at -59 has been shown to bind nuclear AP1 factors.

The presence of housekeeping regulatory elements as well as inducible elements in the TIMP-1 gene agrees well with the observation that in many cell lines TIMP-1 is produced at a basal level, but can also be induced by a number of different substances. In contrast TIMP-2 appears to be a constitutive gene which does not respond significantly to inducing agents [120].

Although there have been detailed studies of the murine promoter less is known about the nature of the human TIMP promoters. However a study of the human TIMP-2 gene suggested that by comparison with the murine TIMP-1 gene, TIMP-1 and TIMP-2 are differentially regulated [156]. The human TIMP-2 gene shows characteristics that are very typical of a housekeeping or constitutive gene. In this case a TATA like element is found, along with a number of possible transcription start sites. There are several sp1 motifs, a CpG island, an AP2 site and an AP1 site that forms part of a negative control element.

A study of the TIMP-1 gene in T-cells infected with the human T-cell leukaemia virus (HTLV) has shown that TIMP-1 can be induced by the viral tax1 protein [157]. This induction is associated with the presence of an AP1 site that is conserved between the human and mouse sequences.

1.5.2. RNA stability

It has been reported that the mRNA transcripts of TIMP-1 from TPA transformed/induced cells have an increased stability in the cytoplasm [158]. Differently sized mRNA transcripts of the TIMP-1 gene have been seen. Northern blotting using a poly-dT oligo, showed them to be due to variations in the length of the poly-A tail over time, reaching a minimum after 12 hours [148].

1.5.3. Regulation by Cytokines.

When TIMP-1 was first identified it was produced in the early stages of a serum free cell culture, normally for the first few days [88]. This expression was either at a basal level or was a result of stimulation by agents produced by the cultured cells. There are now many compounds produced *in vivo* that are known to affect the expression of TIMP-1. Usually the effect is the upregulation of TIMP-1 production, although in certain circumstances down-regulation may occur. The *in vivo* regulation of TIMP-1 would appear to be very complex, different cells may or may not produce TIMP-1 at a detectable level and their response to different regulatory substances also varies with cell type.

Interleukin-1 is a 17 kDa peptide produced by a range of cells, including monocytes and leukocytes. It acts on many cell types and is involved in upregulating the inflammatory response. The presence of IL-1 in cartilage cultures induces cartilage breakdown [159]. IL-1 has very little effect on TIMP-1 production in articular chondrocytes [160], although there is a greater response than that to TNF- α . No significant stimulation is seen in porcine synovial fibroblasts [161], human rheumatoid

synovial fibroblasts [162] or normal chondrocytes [163]. Although most cells do not show a significant increase in TIMP-1 production with IL-1 there are reports that TIMP-1 is elevated in IL-1 treated cervical fibroblasts and that protein kinase C is involved in the response [164]. Tumour necrosis factor- α is another inflammatory cytokine secreted by macrophage and monocyte cell lines which has cytotoxic and protein regulatory properties. TNF induces TIMP-1 expression in human skin fibroblasts [165] but has no effect on the expression of TIMP-1 in articular chondrocytes [166]. The effect of TNF is seen at low concentrations in fibroblasts (0.005 ng/ml) but a suppressive effect is seen at higher concentrations. Thus the effect is bifunctional, both stimulating and suppressing [167]. TNF alone could not increase the expression of TIMP-1 in endothelial cells, but when EGF was added a synergistic effect was seen [168] and TIMP-1 production was increased.

Transforming growth factor- β has been implicated in the regulation of connective tissue matrix regulation. When TGF- β is present it results in the deposition of more matrix [169]. When included in cultures of human fibroblasts an increase in TIMP-1 production was seen [170]. This increase could be small and was increased when other growth factors were also present [171]. TGF- β induction of TIMP-1 is accompanied by a concomitant decrease in the production of collagenase [172]. The induction of TIMP-1 was also seen in rat calvarial osteoblasts; where one line could be significantly induced and the other, with a much higher basal level of expression did not respond [170]. Synovial cells will also produce TIMP-1 on exposure to TGF- β [173]. Other cells such as articular chondrocytes [174], calvarial osteoblasts (in the presence of $1,25(\text{OH})_2\text{D}_3$) [175], and hepatomas [176] respond similarly. It has also been shown to partially prevent the IL-1 induced degradation of bovine cartilage [159].

There have been differing reports on the effect of interleukin 6 (IL-6) on the production of TIMP-1. Most show an increase in synthesis, although the opposite has been seen in the same cell type. Upregulation is seen in human skin and cervical fibroblasts [177] and shows a linear dose dependency. It has also been seen in human

articular chondrocytes, synoviocytes [178] and hepatoma cells [176]. However another study showed no IL-6 response in skin fibroblasts. High levels of IL-6 have been seen in the synovial fluid of patients with rheumatoid arthritis [179]. Since IL-6 does not stimulate the production of MMPs [177] this finding could suggest that there is an attempt by the affected tissues to prevent cartilage breakdown.

The actions of oncostatin M, leukemia inhibitory factor (LIF) and interleukin 11 are closely linked to that of IL-6. They all act on cells via the same signal transducer, GP130 [180, 181]. Each of these agents has been shown to increase the production of TIMP-1. Interleukin 11 is a very recently discovered cytokine that has been shown to increase TIMP-1 synthesis. Oncostatin M selectively upregulates TIMP-1 in human fibroblasts without an associated increase in MMP production [182]. This increase is also notable in that it is much greater than that produced by IL-6 or any other stimulatory cytokine. LIF also increases the expression of TIMP-1 without an accompanying increase in the production of MMPs.

Progesterone and 17 β -estradiol are steroid hormones which have been shown to increase the production of TIMP-1 in rabbit uterine cervical fibroblasts [183]. Progesterone also stimulates TIMP-2 production in rabbit cervical fibroblasts [184]. Prostaglandins acting on granulosa cells can stimulate inhibitor activity. This activity can be inhibited by the antiprogestosterone RU486 [185]. Other hormones such as leuteinising hormone stimulate the production of TIMP-1 in rat ovarian tissue. This is thought to have an important role in the connective tissue changes accompanying ovulation [186].

Prostaglandins might also be involved in the increased level of TIMP-1 and TIMP-2 mRNA found in menstrual tissue [187]. Interestingly prostaglandin E2 does not affect the production of TIMP-1 in other cell lines such as dermal fibroblasts [188], and osteogenic sarcoma cells [189]. This implies a specific receptor mediated response.

Retinoic acid has been shown to stimulate the production of TIMP-1 in human synovial fibroblasts [190].

1.6. Localisation.

TIMP-1 was originally identified in serum where it makes up less than 5% of the anti-metalloproteinase activity present [87]. Its concentration was determined at $1.03 \pm 0.27 \mu\text{g/ml}$ [191]. Subsequently in the circulatory system other MMP inhibitors are dominant. The most important of these is $\alpha 2$ -macroglobulin, which is responsible for more than 95% of the total metalloproteinase inhibitor activity in human plasma [87]. The $\alpha 2$ -macroglobulin is a general proteinase inhibitor that forms irreversible complexes with all four classes of proteinases, including the MMPs, on cleavage of a bait region. This eventually leads to removal of the inactive enzyme-inhibitor complexes via the liver [192]. However this inhibitor is very large, forming a tetrameric complex of approximately 750 kDa. This makes access to tissue spaces difficult, restricting activity to the circulatory system and inflammatory body fluids such as rheumatoid synovial fluid. This leaves the TIMPs as the primary regulators of MMP activity away from the circulatory system.

One of the most notable features of the TIMPs is their ubiquity. TIMP-1 in particular is found in a large range of cells, tissues and body fluids. In most cases the presence of one or more of the TIMPs is usually associated with the expression of the MMPs which are in turn found wherever the connective tissue matrix is being remodelled. TIMPs have been associated with fibroblast cells [193], mesangial cells [194], endothelial cells [195], smooth muscle cells [196], macrophages [197], osteoblasts [198] and tissues undergoing osteogenesis [199], corneal tissue [200], in the roots of growing hairs [201], teeth [202], periodontal tissue and crevicular fluid [203]. It is particularly prevalent in ovarian tissue including the follicular fluid [204], amniotic fluid [205], granulosa and luteal tissues [206] where MMP (and subsequently TIMP) activity is strongly associated with the processes of ovulation [207] and the endometrial remodelling processes associated with menstruation and embryonic implantation [208]. TIMP is also found in areas of active growth such as the growth plate of bone [209] and

in various foetal tissues where control of the extracellular matrix is essential during development [210].

In pathological states it has been found in synovial fluids [211, 212] and the cells of the rheumatoid synovium [213], scarring [214] and fibrotic tissues [3]. There is a strong association with cancerous tissues and cells. TIMPs have been identified in many tumour cells including pulmonary carcinomas [215], colorectal tumours [216], non-Hodgkins lymphomas [217] and transformed fibroblasts [218].

1.7. Inhibition of the Matrix Metalloproteinases.

1.7.1. TIMP and Enzyme Latency.

The TIMPs have been found to regulate enzyme activity at two levels. Mostly regulation is by directly inhibiting the fully active enzyme. However, regulation by the TIMPs has been identified prior to the activation of the enzyme. Here they have been found to be involved in the control of activation for some of the MMPs.

Both TIMP-1 and TIMP-2 have been shown to form exclusive inhibitor-zymogen complexes with the 92 kDa and 72 kDa pro-gelatinases respectively, but for no other MMP. TIMP-1 forms a complex with the pro-enzyme form of the 92 kDa and TIMP-2 forms a complex with the 72 kDa form [219, 220]. These complexes are produced by a range of cells and have also been identified in synovial fluids [221]. Of the two it is the TIMP-2/72 kDa gelatinase that has been studied in most detail.

The TIMP-2/72 kDa pro-gelatinase complex has two interesting features. The first is that it is possible for activation to occur whilst the inhibitor is still present in the complex [220]. No dissociation is necessary, although it is possible that the inhibitor could be dissociating for long enough for activation to take place. Activation is still possible using conventional materials such as APMA [222]. It has been shown that

stromelysin can activate the TIMP-2/72 kDa pro-gelatinase complex [223] and that APMA will further increase the activity. A protein based activator of 72 kDa gelatinase has also been associated with cell membranes [224, 225]. This may be the membrane metalloproteinase identified recently [52].

The addition of extra free TIMP-1 or TIMP-2 will inhibit both the activation and the activity of the activated enzyme. The ability of additional TIMP to form a further complex with the TIMP-2/72 kDa pro-gelatinase complex suggests that an additional binding site is present on one or both of the molecules. Non-denaturing SDS-PAGE and cross linking experiments suggest that higher order (tetrameric) complexes can also form [226].

The second feature is that this complex is itself an inhibitor of the MMPs. This activity was originally identified as an additional inhibitory peak in gel filtration profiles of foetal lung fibroblast media [220] and it has also been found in synovial fluids [227]. This also suggests that TIMP-2 may have more than one binding site for the 72 kDa pro-gelatinase. One site that is involved in the direct inhibition of the active enzyme and another that binds the latent enzyme, leaving the inhibitory domain free to inhibit additional molecules of active gelatinase. Further confirmation comes from the fact that TIMP-2 will still bind to 72 kDa pro-gelatinase in the presence of 1,10-phenanthroline [228]. This hypothesis has been supported by the identification of inactive ternary complexes consisting of two molecules of gelatinase bound with a single molecule of TIMP-2 [229]. This showed that if the TIMP-2 molecule was binding to both enzymes simultaneously then by deduction there must be two functional sites on the TIMP-2 molecule. Deletion studies of the TIMP-1 molecule have shown that the C-terminus of the protein is involved in the second interaction with the 92 kDa pro-gelatinase [230]. The same has been found for the TIMP-2/72 kDa gelatinase complex (unpublished results cited in [231]).

Data from studies using peptides have located an additional binding site in the C-terminal portion of the gelatinase molecule. It was found some distance away from the active site (in the region starting at residue 414). The presence of a second site in the C-terminus of pro-gelatinase has also been shown in experiments with deletion mutants. Here, inhibition was reduced in C-terminal deletion mutants and a separately expressed C-terminal piece was found to bind to TIMP-2 [232]. This second site has been described as a stabilisation site [228]. The dissociation constants have been determined for both sites. For the active site the K_d is 0.72 nM and the stabilisation site has a K_d of 0.42 nM, both of which indicate tight binding complexes.

The function of the TIMP-2 molecule here appears to be to prevent the autodegradation of the enzyme [233]. The capacity to bind the additional site appears to be lost once the enzyme has been fully activated. This would allow a pool of stable, inactive enzyme to remain in the tissues alongside a store of TIMP-2. Once activated this TIMP-2 would then be immediately available as an inhibitor at the active site. In addition there is evidence that TIMP-2 will not bind pro-gelatinase that lacks the C-terminal domain and that this mutant pro-enzyme can not be activated by membrane preparations [231]. In this instance the role of TIMP-2 may be to regulate the activation of the 72 kDa gelatinase by cell membranes.

Cross linking studies of TIMP-2/72 kDa pro-gelatinase complexes suggest that 79% of the material is in the form of a binary complex and that the remainder is in the form of a ternary complex consisting of two molecules each of TIMP-2 and gelatinase [233]. When the cross-linked binary complex is activated it has normal activity but is less susceptible to inhibition by free TIMP-2. This suggests that occupation of one site partly prevents occupation of the second.

1.7.2. Inhibition of Enzyme Activity.

The three different TIMPs that have been described so far have different specificities for the different MMPs. Although they are likely to share the same overall topology it is not guaranteed that they will share the same mechanism. Subsequently it is important to consider the structure and function of the enzymes involved and the details of the interactions of each with the MMPs.

With the exception of the complexes formed between TIMPs 1 and 2 and the latent gelatinases all of the TIMP-MMP interactions have a 1:1 stoichiometry. A number of studies have looked for the sites on both the TIMPs and the MMPs that are involved in the interaction.

Whilst it is possible for both TIMP-1 and TIMP-2 to inhibit all of the MMPs (the details of TIMP-3 are not fully determined) there is a variation in the relative specificity of each inhibitor for certain enzymes. TIMP-1 binds preferentially to the 92 kDa active form of gelatinase whilst TIMP-2 binds the active 72 kDa form [219, 220]. Also the smallest of the MMPs, matrilysin has, a K_i of 4.5×10^{-9} M (binding TIMP-1) compared with that of the binding constant for the interaction of TIMP-1 with stromelysin ($K_i = 8.3 \times 10^{-10}$ M) [234]. Matrilysin differs from the other MMPs in not having a C-terminal domain, consisting only of a pro-peptide and a catalytic domain [12]. This differential binding is an indication that the C-terminus of the enzymes is involved in the interaction with the TIMPs in addition to the assumed binding site in the active site.

One study of the differential binding used C-terminal deletion mutants of stromelysin and collagenase [26]. The K_i was determined using a synthetic substrate in the enzyme assay which gave approximate values. This indicated that there was no difference in the interaction of TIMP-1 with stromelysin with and without the C-terminal fragment. However, a difference of an order of magnitude was found when the K_i of TIMP-1 binding to intact collagenase was compared with that of TIMP-1 binding to the C-terminally truncated form (<0.2 nM, compared with 1.2 nM). The autoproteolytically

generated N-terminus of fibroblast collagenase was shown to have a significantly reduced ability to be inhibited by TIMP-1 [28].

Another study of stromelysin mutants did find a difference in the relative abilities of intact and C-terminal deleted mutants to bind TIMP-1. This gave a K_i 14% that of the intact enzyme ($8.3 \times 10^{-10}M$ intact, 5.95×10^{-9} truncated) [234]. Analysis of the association rates of TIMPs 1 and 2, and stromelysin in contrast showed that the C-terminal domain has no effect on the rate of association [235].

Similar experiments using C-terminal deletion mutants have been carried out for the 72 kDa gelatinase. Again it was found that the truncated enzyme had altered binding affinities for the inhibitors. In this case TIMP-2 showed greatly reduced binding and TIMP-1 did not bind at all [231]. This suggests that the C-terminus of some of the MMPs is important in the interaction with TIMP-1 in addition to the N-terminus.

The role of the different domains of the TIMPs in relation to the formation of higher order TIMP/gelatinase complexes has already been discussed (see section on latency). The N-terminus of TIMP-1 alone has been shown to inhibit the MMPs [230]. The C-terminus appears to be involved in the interaction with some of the MMPs and not with others. There is little effect on the rate of binding of TIMP-1 and TIMP-2 to stromelysin-1, whereas the interaction with the 72 kDa gelatinase is much more dependent on the presence of the C-terminal domain [235].

Mechanism of Action.

In all studies of the TIMPs, the binding to the MMPs has been shown to be reversible. TIMP molecules are not consumed in the reaction, nor is an irreversible covalent complex formed with the MMP. In all cases studied so far it is possible to retrieve active TIMPs from the various complexes. The most probable mode of action is a steric hindrance preventing access to the active site by the substrate.

The association constants are very high, such that the complex once formed is unlikely to dissociate. Estimates made over a period of time have increased the value as the methodology has improved. Initial calculation of the binding constant for the TIMP-1 - collagenase interaction gave a K_d of 1.4×10^{-10} M [236], another calculation gave a figure of 1×10^{-9} M. A more recent analysis using surface plasmon resonance technology estimated the K_d to be 4.1×10^{-9} M [237]. However when α 2-macroglobulin is present the majority of collagenase molecules will bind to this in preference to TIMP-1 [238]. This is due to a faster binding rate than for TIMP-1.

Although the interaction is very tight it is possible for other small molecules to enter the TIMP-1-collagenase complex. A small collagen based peptide coupled to a chelating hydroxamate group can both block complex formation and encourage the dissociation of TIMP-1 from collagenase [239]. A biological factor, endothelial cell stimulating angiogenesis factor (ESAF) is also able to release TIMP-1 from enzyme-inhibitor complexes [240].

There has only been one detailed kinetic study of the interaction of TIMPs and MMPs. This was a study using a variety of deletion mutants of TIMP-1 and TIMP-2 and the 72 kDa gelatinase [241]. In this case the reaction is a simple bimolecular association with a k_{on} that is not unexpected for such an interaction. Again the k_{on} seen for both of the C-terminal deletion mutants (TIMP-1 and TIMP-2) was similar to that seen for other interactions of this type, although the rates for both were up to three orders of magnitude lower than for the native protein. TIMP-2 has a series of charged residues at its C-terminal tail (interestingly, a feature it has in common with TIMP-3). The kinetic study showed that this portion was important in maintaining the k_{on} . If these charged residues were removed, the k_{on} was four times slower than before. This ties in with the inverse relationship between the inhibitory activity of TIMP-2 and ionic strength. Ionic interactions are also involved in the inhibition of 72 kDa gelatinase by the N-terminal of TIMP-2, since the sensitivity to salt remains even in the absence of the C-terminal

peptide. This effect is not seen for TIMP-1, suggesting that for gelatinase inhibition, alternative binding mechanisms (such as hydrophobic interactions) are involved.

In another study, the glutamic acid residue at the active site of the 72 kDa gelatinase (Glu-375) was mutated to either Asp (same charge), Ala (replacing an acidic side chain with a hydrophobic one) or Gln (uncharged equivalent) [242]. None of these changes affected the ability of TIMP-1 to bind to the activated 72 kDa gelatinase indicating that Glu-375 is not involved in the interaction between TIMP-1 and the active site.

1.7.3. Identifying Important Residues.

Sequence Homologies.

Various regions of the TIMPs have been proposed as being potentially important for activity on the basis of the strong conservation of their sequences. The largest of these is the N-terminal sequence where most residues are identical throughout all of the TIMPs. Even where there are variations in the absolute homology the difference is normally a conservative substitution. These highly conserved sequences may be important to the ability of TIMPs to inhibit MMPs. It is also possible that they are essential to the general structure of the TIMP family. As mentioned previously, all of the cysteines are conserved and there is a high degree of conservation amongst the residues surrounding the cysteines. To look for conservations that are retained within one of the TIMP family across different species, but differ in the other TIMPs might indicate regions of the molecules that are important to the individual specificity and function of each of the TIMPs.

Appendix 3 shows the alignment of all the fifteen known TIMP sequences along with an indication of the extent of conservation, within each TIMP type and across the whole family. Over all the TIMPs only a few key residues are conserved entirely. All twelve of the cysteine residues are entirely conserved, reflecting the importance of the

disulphide bonding to the overall structure of the proteins. Residues adjacent or close to the cysteines also tend to be conserved. The VIRAK sequence identified by Woessner is also entirely conserved. In the solution structure of TIMP-2 this sequence forms part of a helix which is presumably essential to the overall TIMP structure. The other conserved residues are scattered throughout the sequence and probably represent key points in a common fold.

TIMP-1 does not have many residues that are unique and conserved. This in part reflects the larger number of sequences studied. The sequences V-29NQTTLYQ-36 and L-151LQGSEK-157 (human) are unlike the other TIMPs, and are mostly conserved across the different species. Many other sequences are shared with TIMP-2 or TIMP-3. Among the four known TIMP-2 sequences, there is a very high degree of conservation, with only ten of the 194 residues showing any variation. Interesting features include the sequences G-37NPIKRIQ-44, K-89AEG-93, T-152EKSING-158 and Q-185EFLDIE-193, which are unique to TIMP-2. TIMP-3 also appears to be highly conserved, although only three sequences were available for alignment. The sequence SNFGHS stands out as being different from other TIMPs. Some of these features, particularly in the C-terminal domains, may be associated with the growth factor properties of the TIMPs. In the case of TIMP-2 the unique sequences may be involved in its additional binding site for 72 kDa gelatinase. The overall lack of clearly unique sequences could suggest (and agrees with peptide and antibody competition studies described later) that the inhibitory action of the TIMPs is associated with large parts of the molecule rather than a single region.

Modifications and Mutagenesis.

In addition to the proteolytic analyses, chemical methods have been used to identify surface residues that may be involved in the inhibitory process. This method is more specific, identifying functional residues, rather than those that are simply exposed. Mutagenesis has also been used to identify important regions and residues. On large scale, the N-terminal domain of TIMP-1 has been cloned and expressed separately (Cys-

1 - Glu-126), and shown to be fully active [230]. On a smaller scale, individual residues and short stretches of sequence have been altered or deleted.

It was found that diethylpyrocarbonate (DEPC) inactivated TIMP-1 [243]. DEPC carboxylates nucleophiles, primarily histidine (although other residues can be carboxylated) under certain conditions. At 50% inactivation of TIMP-1, only 1.5 molecules of carboxyl groups were bound per TIMP-1 molecule suggesting a specific inactivation mechanism. Peptide mapping identified His-95, His-144 and His-154 as carboxylated after DEPC treatment [131], one other could not be identified. If the inhibitory activity is purely due to the N-terminal domain [230], then, if a histidine was important for the activity it is unlikely to be His-144 or His-154. Another study where site directed mutations were found that affected the activity of TIMP-1 suggested that His-95, was not essential for inhibition. Instead His-7 was singled out as important [244]. It is interesting to note that both His-7 and His-95 are conserved. DEPC modification of mutant TIMPs has not clarified the situation. A His-95 mutant (His95Gln), which remains active [244] is affected by DEPC treatment. However, His-7 which shows reduced activity when mutated to Ala-7 [244], also remains sensitive to DEPC [131]. Unfolding experiments have suggested that the DEPC modified protein is not significantly less stable than the wild type, so any structural perturbations caused by the carboxylation are local, and do not affect the overall structure or stability.

One sequence is highly conserved throughout all of the TIMPs, this is the VIRAK sequence from close to the N-terminus (18-22). The high degree of conservation could indicate that this region has a functional importance. Deletion of this sequence results in no significant yield of protein indicating that its function may be structural rather than inhibitory [230].

It is possible that the mechanism of interaction cannot be explained by a simplistic model of a few spatially close residues. This idea is supported by a recent study using peptide competition and identifying the epitopes of antibodies that block inhibition [237].

These results suggest that a large part of the TIMP-1 sequence may be involved in the MMP interaction. Residues 2-45, 70-145 and 165-184 were implicated in competition experiments using long peptides. Shorter peptides refined this to residues 2-25 and 121-136. This would suggest that the C-terminal, previously thought to be unimportant, may have a function in the inhibitory process. Of particular interest was the 'hinge' region between the two domains. This does not agree with other work that shows the inhibitory activity to be based solely in the N-terminal domain [230]. Previous studies of tryptic susceptibility show no protection of the N-terminus by the C-terminus [139]. Subsequently it may be possible that the C-terminus has a function in direct inhibition that has not been defined.

Structure and Inhibition.

Not all of the structure is necessary for inhibition but it appears that all of it is required for normal kinetics and the formation of higher order complexes.

It is also not necessary for the structure to be intact for inhibition to occur. TIMP-1 that had been cleaved by bacterial proteinases [Clark I.M. unpublished results] was found to retain its activity. TIMP-2 has been purified in a two chain form that has also been shown to be active in spite of a proteolytic cleavage [245]. Interestingly, this two chain form does not bind to the 72 kDa progelatinase.

1.8. TIMP as a Growth Factor.

Although TIMP-1 was first identified on the basis of its inhibitory activity an entirely different line of investigation identified TIMP-1 not as an inhibitor, but as a growth factor. A factor was identified that had the ability to stimulate the differentiation of erythroid precursors [246, 247]. This proteinaceous factor was called 'erythroid potentiating activity' or EPA. Many of the early studies on the regulation of the TIMP gene were carried out before the co-identity was known. Only when the complete

sequence of TIMP-1 was determined and compared with the N-terminal sequence of EPA [248], were they found to be the same protein.

TIMP-1 is produced by the stromal cells of human bone marrow [249] where local release allows direct stimulation of the erythropoietic precursor cells. A wide ranging study found that the stimulatory activity extends beyond the erythropoietic cell lines causing cell proliferation in all of those tested [250]. Cell lines shown to respond to TIMP-1 stimulation were human gingival fibroblasts, Burkitts lymphoma cells, human lymphoblasts, epithelial cell, smooth muscle cells, chondrocytes, leukaemia cells and transformed human lung cells. TIMP-1 has also been found to stimulate keratinocytes [251]. A monoclonal antibody was found that blocked both the proliferative and potentiating activities of TIMP-1 in an erythroleukaemia cell line [252] showing that the two activities are closely linked.

Initial assays of the ability of TIMP-2 to stimulate cell proliferation did not show any activity [250]. It was originally thought that the stimulatory activity of TIMP-1 was connected to a region of the N-terminal sequence that had a high homology to granulocyte-macrophage colony stimulating factor [253]. TIMP-2 does not share this homology. However a later study found that TIMP-2 could stimulate the differentiation of the same erythroid cells as TIMP-1 (BFU-E) [254] as well as the proliferation of a human fibroblast line [255]. This would suggest that the region of the TIMPs involved in these growth factor properties is one shared by both TIMP-1 and TIMP-2. TIMP-2 also appears to be more potent than TIMP-1 at stimulating a range of cells, requiring a tenth the concentration of protein to achieve the same degree of promotion [256]. When TIMP-1 or TIMP-2 are complexed with the progelatinase B or progelatinase A respectively, no stimulation of proliferation is seen. However this growth promoting activity is found in the reduced, alkylated forms of the proteins. Evidence has also been found for the presence of TIMP-2 receptors on the surface of cells from a lymphoma line.

1.9. MMPs and TIMPs in Disease States.

MMP and TIMP activity is seen in an enormous number of cells and tissues. Their role in controlling the turnover of connective tissue components is an extremely important one. Wherever there are changes occurring in the tissue matrix the MMPs and the TIMPs are likely to be involved. An error at any point in the control structure can lead to a number of diseases.

The degradation of cartilage that occurs in arthritis is associated with an imbalance in the enzyme-inhibitor ratio that results in excessive MMP activity [257]. MMPs have been identified in the synovial fluid of patients with arthritis [258] and localised in rheumatoid synovium [259]. TIMP is not always absent from sites of matrix breakdown (it has also been found as a complex with collagenase in synovial fluids [212]).

MMPs have been identified in metastatic tumour cells, and are often found with TIMPs. The breakdown of the basement membrane collagens (type IV) in particular allows cells to escape the confines of their original location and move to new sites. The problem here is also one of an imbalance between matrix breakdown and enzyme inhibition. In experimental models treatment with additional TIMP (both TIMP-1 and TIMP-2) can prevent the metastatic process [260, 261].

MMPs are also associated with periodontal disease [262]. The quantity of collagenase found in periodontal tissues is generally related to the severity of the condition. TIMP-1 has also been found in dental material (see section on localisation) again indicating that the problem is an imbalance rather than an absence of inhibitor.

There is evidence that malfunctions in the TIMP gene are associated with familial otosclerosis [263]. Stromelysin has also been linked to this condition [264]. MMPs are involved in the processes of fibrosis and inflammation development. The ubiquity of the MMPs and TIMPs, their crucial role in connective tissue turnover and the potential for

serious illness resulting from a malfunction in their activity means that it is essential that we fully understand the nature and control of the enzymes and their inhibitors. With this information we can make new advances in the treatment of disease.

1.10. The Development of New Therapeutic Agents.

This study has been carried out against a background of research into the mechanisms involved in arthritis. Its long term aim is to contribute information that will be useful in the development of new anti-rheumatic drugs. Since MMP activity is also associated with the processes underlying tumour metastasis compounds that can modulate their activity may also prove useful in the treatment of cancer.

1.10.1. Compounds Used *In Vivo*.

Patients with arthritis are commonly treated with drugs from one or more of the non-steroidal anti-inflammatory (NSAID), steroidal or disease modifying anti-rheumatic drugs (DMARDS). The NSAIDs are benzoic acid derivatives the commonest of which is salicylic acid (aspirin). Their primary action is the inhibition of prostaglandin synthesis, although dependant on the dosage used, other processes are inhibited. These include histamine release, transmembrane anion transport, mitochondrial metabolism and various membrane proteinase activities [265]. Although very effective, these compounds are associated with gastrointestinal problems where they can cause ulceration in the stomach and duodenum [266]. The DMARDS are a group of unrelated drugs with the ability to affect the progress of the disease. The best known are methotrexate, gold, penicillamine, sulfasalazine and the anti-malarials [267]. Other treatments use immunosuppression (cyclosporine) [268] dietary modifications, immunotherapy, interferon treatment [269] and humanised monoclonal antibodies that target T-cells [270].

Many of these treatments rely on modifying the inflammatory response. An alternative approach would be direct modulation of MMP/TIMP activity. One method

would be cytokine therapy, using them to tip the balance of enzyme-inhibitor away from a net breakdown of matrix. However the functions of the cytokines are very complex, being involved in many physiological processes where modifications might not be desirable. Another approach that has attracted a great deal of interest is to specifically inhibit one, or more of the MMPs.

1.10.2. Compounds Used *In Vitro*.

Many compounds have now been identified that will inhibit the MMPs *in vitro*. Compounds that chelate the zinc atoms such as EDTA and 1,10 - phenanthroline and compounds that reduce the disulphide bridges (DTT and β -mercaptoethanol) will destroy enzyme activity. More specific inhibitors have been designed, based on the cleavage site in the collagen molecule. These include the peptide hydroxamic acids which are based on the tripeptide (Pro)-Leu-Gly [271, 272]. Phosphoramidate and phosphoramidate inhibitors [273, 274] have also been based around a peptide. In these cases the peptide was Leu/Ile-Ala-Gly. The inhibition is thought to be a result of the interaction of the phosphoryl atom with the active site zinc. Sulphur-based substrate analogues, again with a similar peptide sequence have also been found to be effective [275].

Other inhibitors have been found amongst the antibiotics. Tetracycline is known to have an anti-inflammatory action connected to the inhibition of collagenase activity. This may be an indirect effect rather than a direct inhibition. Actinonin is a pseudopeptide antibiotic produced by actinomycetes which has a K_i of 1.4×10^{-6} M against collagenase. The incorporation of a zinc ligand into a synthetic substrate has proven to be relatively effective in a series of inhibitors designed by Roche ($I_{50} = 17$ nM) [276]. The ACE inhibitor, captopril has been shown to inhibit both the 72 kDa and the 92 kDa gelatinases [277]. Again it is thought to act by the chelation of the zinc atom at the active site.

Another strategy is to mimic the action of the TIMPs. A good mimic could be based on either the structure/sequence of one of the TIMPs. Alternatively it might be an

entirely novel molecule based on the specific interaction of a TIMP molecule with an MMP.

1.11. Summary.

In pathological conditions the delicate balance of connective tissue breakdown and synthesis is perturbed, often with serious and debilitating consequences. A detailed understanding of the mechanism of connective tissue turnover may identify key points at which the process can be modified by suitable therapeutic agents. The matrix metalloproteinases and their inhibitors play a vital role in connective tissue turnover. To understand their function it is essential to include detailed structural and functional studies.

TIMP-1 has only been produced in sufficient quantities for this type of study in recent years. Subsequently only a few details are known of its structure and mechanism. Attempts to crystallise wild type TIMP-1 have been unsuccessful, possibly due to its extensive glycosylation. However a mutant TIMP-1 where the glycosylation sites are removed has crystallised [278]. Recent developments in NMR technology have increased the upper size limit of suitable proteins to over 20 kDa. Since TIMP-1 has a protein molecular weight of 20.5 kDa it should be possible to determine its structure using multidimensional NMR spectroscopy. This requires that an expression system is available to produce large quantities of isotopically labelled, non-glycosylated TIMP-1.

This study uses a variety of spectroscopic techniques to elucidate structural features of TIMP-1 including its secondary structure content, surface properties and interactions with collagenase. Also included are the developments of expression and purification protocols designed to maintain a reliable supply of recombinant TIMP-1 for continuing studies.

Chapter 2.

General Methods and Materials.

2.1. Assays.

2.1.1. Collagenase and TIMP Bioassays.

The biological activity of collagenase and TIMP is measured using a modification of the diffuse collagen fibril assay [279].

At 37°C type I collagen dissociates into individual fibrils. Collagenase breaks triple helical collagen and fibrils into well characterised $\frac{1}{4}$ and $\frac{3}{4}$ fragments of the whole molecule. On centrifugation these cleaved fragments remain in the supernatant and the undigested fibrils form a pellet at the bottom of the tube. If the collagen fibrils are radiolabelled, collagenase activity can be assayed by assessing the radioactivity of the supernatant containing the cleaved fragments.

Controls for this assay are a blank to assess the residual radioactivity in the supernatant after the intact, radio-labelled fibrils have been removed from solution. Trypsin breaks down any collagen fibrils that are unwound (damaged) and subsequently accessible to other proteinases, and is included as a control for the quality of the collagen fibrils. A bacterial collagenase control is included to cleave all of the collagen fibrils. This shows the radioactivity to be expected from supernatants where all of the collagen is cleaved (100% lysis), and is used in calculating the collagenase activity of a test sample.

Collagenase activity is calculated from the raw counts as overpage:

$$\frac{100}{\text{Bac. Cell (cpm)}} \times \frac{1000}{\text{Sample volume } (\mu\text{l})} \times \frac{1}{\text{time (minutes)}} = \text{assay factor}$$

$$\text{enzyme activity} = \text{assay factor} \times (\text{Sample cpm} - \text{blank cpm})$$

One unit of collagenase activity is defined as the amount that digests 1 μg of collagen per minute at 37°C.

To assay inhibitory activity a known amount of collagenase, sufficient to give approximately 70% lysis is added to each sample and used as an additional control.

Inhibitory activity is calculated using the equation below:

$$\text{inhibitory activity} = \text{assay factor (as above)} \times (\text{enzyme cpm} - \text{sample cpm})$$

One unit of inhibitory activity is defined as the amount of inhibitor that reduces the activity of two units of enzyme by 50%.

Materials.

Microcentrifuge tubes are from Hughes and Hughes, Romford, UK. ^3H type I calf skin collagen is produced by the Rheumatology Research Unit Cambridge UK [279]. Trypsin and *clostridium histolyticum* collagenase are from Sigma Chemicals, Poole, UK. Scintillation fluid is Optiphase 'Hisafe' II, from LKB Instruments Ltd, Surrey, UK. Other chemicals are analytical grade reagents from standard sources.

Experimental Details.

Radiolabelled type I calf skin collagen is prepared by dissolving the collagen in a Borate buffer, 200 mM NaCl, 0.02% (w/v) NaN₃, pH 9 and labelling with ³H-acetic anhydride. The final activity is approximately 2.5 x 10⁵ dpm mg⁻¹.

Porcine collagenase purified in the Rheumatology Research Unit is activated by the addition of APMA to 0.7 mM [280].

Control tubes are, (1) buffers and collagen only, (2) 10 µl of 1mg/ml trypsin in 1 mM HCl, (3) 20 µg of bacterial collagenase, and for the inhibitor assay, sufficient active enzyme to produce approximately 70% lysis of the collagen.

100 µl of 50 mM Tris, 1 mM CaCl₂ pH 7.9 is added to all tubes. Sample volumes range from 10-50 µl. All samples and controls are made up to 200 µl with 25 mM sodium cacodylate, 0.05% (v/v) Brij-35, pH 7.6. 100 µl of ³H collagen is added to each tube, which is then mixed and incubated for 16 hours in a waterbath at 37°C.

After the incubation sample tubes are centrifuged for 10 minutes at 13700 rpm, 4°C. 200 µl of each supernatant is transferred to scintillation vials and mixed with 3 ml of scintillation fluid. Activity is counted for 15 seconds per vial on either an LKB Rackbeta scintillation counter or a Wallac 1410 liquid scintillation counter.

2.2. Enzyme-Linked Immunosorbent Assays (ELISAs).

The exact quantity of TIMP-1 in samples is determined using a sandwich enzyme linked immunosorbent assay (ELISA) [135] developed in the Rheumatology Research Unit. Plastic 96 well plates are coated with a monoclonal anti- TIMP-1 antibody, then blocked with BSA to prevent non-specific adsorption of the samples to the plastic. The sequence of incubations is first the samples, then a second, biotinylated monoclonal antibody to TIMP-1 and finally streptavidin linked horse-radish peroxidase. The

detection method uses horse-radish peroxidase, which breaks down OPD to give a yellow product. The colour development is stopped by the addition of sulphuric acid. The quantity of TIMP present is determined from the absorbance of the final product at 492 nm in comparison with a standard curve.

Materials.

Ninety-six well maxisorp microtitre plates are from Nunc. Monoclonal, and biotinylated monoclonal antibodies are prepared in the Rheumatology Research Unit [135]. Horse-radish peroxidase conjugated streptavidin is from Dako Ltd, High Wycombe, Bucks, UK. Citrate phosphate buffer and phosphate buffers are made up from capsules and tablets purchased from Sigma. OPD is from Sigma. Wash buffer consists of phosphate buffered saline plus 0.1% (w/v) thimerosal. Protein diluent is wash buffer plus 0.5 mg/ml bovine serum albumen (BSA, from Sigma). Blocking buffer is 10 mg/ml BSA in PBS, plus 0.02% (w/v) NaN_3 .

Experimental Details

Assay plates are coated with 100 μl per well of G10C6 anti-TIMP-1 antibody at 4 $\mu\text{g/ml}$ in PBS. Plates are incubated overnight at 4°C, the antibody solution removed, then they are blocked for a minimum of 1 hour with 150 $\mu\text{l/well}$ of blocking buffer. Before use the coated plates are washed automatically with wash buffer using a Titertek plus M96 washer (ICN Flow). Samples are diluted in protein diluent and applied in duplicate to the plate at 100 $\mu\text{l/well}$. A standard curve of TIMP-1 at 5-50 ng/ml is prepared in the same diluent.

Samples are incubated for two hours at room temperature then the plate is washed three times. 100 μl of biotinylated P2H10 monoclonal antibody is added to each well at 200 ng/ml and the plate incubated for a further two hours. It is then washed again three times and 100 μl of HRP linked streptavidin added to each well at a 1/5000 dilution (in protein diluent). The plate is incubated for a further 30 minutes followed by three

washes. Colour is developed in the dark by the addition of 100 μl /well of OPD (one 15 mg tablet in 12 ml phosphate-citrate buffer). The reaction is stopped when sufficient colour has developed (normally 2-15 minutes) by the addition of 50 μl /well 2M H_2SO_4 . The absorbance of the samples is read on a Titertek multiscan plus MK II plate reader (ICN Flow) at 492 nm and results calculated from the standard curve using the TiterSoft analysis package.

2.3. Protein Assays.

2.3.1. Absorbance.

The absorbance of protein solution at 280 nm are determined on a Cecil 6600 UV/vis spectrophotometer, using either quartz or disposable polymethyl methacrylate UV grade cuvettes from Jencons Scientific. Protein concentrations are approximated on the assumption that an A_{280} of 1.0 corresponds to a concentration of 1 mg/ml.

2.3.2. BCA Protein Assay.

The bicinchoninic acid binding assay is used to determine the protein concentration for some samples of mixed proteins and when an immunoassay is not suitable [281]. This is performed using the BCA assay kit from Pierce-Wallac following the manufacturers' instructions.

2.4. SDS-PAGE.

Materials.

SDS gel electrophoresis is routinely carried out using the mini-protean II system from Bio-Rad Laboratories Ltd, Hemel-Hempsted, Herts, UK. Large gels are produced using the Bio-Rad protean system. Polyacrylamide-bis-acrylamide is purchased as a 40%

(w/v) (39:1 - acrylamide:bis) solution from Amresco. Ammonium persulphate (APS) is purchased in 0.2 g sachets from BDH Ltd, Upminster, Essex, UK and used at 0.2 gm/ml. TEMED is from BDH. 4x lower gel buffer consists of 1.5 M Tris, 0.4% (w/v) SDS, pH 8.8. 4x upper gel buffer consists of 0.5 M Tris, 0.4% (w/v) SDS, pH 6.8. 5x final sample buffer consists of 250 mM Tris pH 6.8, 40% (v/v) glycerol, 10% (w/v) sodium dodecyl sulphate (SDS), 0.5% (w/v) bromophenol blue. 5x running buffer consists of 125 mM Tris, 1M glycine, 5% (w/v) SDS. Coomassie stain contains 2.5% (w/v) Coomassie blue G-250 in 40% (v/v) methanol, 60% (v/v) H₂O. Destain contains 5% (v/v) acetic acid and 40% (v/v) methanol. Proteins for molecular weight markers and all other materials are of good quality, from standard sources.

Experimental Details.

All SDS PAGE is based on the method of Laemmli [282]. Lower gels of 0.75 and 1.0 mm are prepared at an acrylamide concentration of 12%. Upper gels are prepared at a concentration of 4.5%. Gels are set using 60 µl 0.2 g/ml APS and 20 µl TEMED per 12 ml of gel.

Samples requiring concentration are treated in one of two ways. For one method two volumes of acetone are added to the sample which is then incubated at -20°C for a minimum of 30 minutes. The sample is centrifuged for 10 minutes at 13700 rpm to form a pellet of precipitated protein, the solvent is decanted and the protein dried under vacuum. In the second method 600 µl methanol, 200 µl chloroform and 200 µl water are added to 300 µl of the sample. The sample is centrifuged at 13700 rpm for 2 minutes, the upper layer removed, taking care not to disturb the protein at the interface, and 750 µl of methanol added. After a final 5 minute centrifugation (at 13700 rpm) the supernatant is decanted and the pellet vacuum dried. All precipitated samples are taken up in FSB diluted to the working concentration. Samples not requiring concentration are prepared by the addition of FSB (to the working concentration). All samples are boiled for 4 minutes prior to loading on the gel.

Samples are electrophoresed at 200 V for approximately 45 minutes (until the dye front passes the end of the gel). Gels are Coomassie stained for a minimum of 10 minutes, destained, photographed and dried under vacuum.

2.5. Western Blotting.

Immunoblotting and transfer to PVDF membrane for Protein Sequencing.

Materials.

Western blotting is carried out using an LKB 2117 multiphor II semi-dry blotter (LKB Instruments Ltd, Surrey, UK). Transfer buffer contains 39 mM glycine, 48 mM Tris, 0.037% (w/v) SDS, 20% (v/v) methanol. Filter paper is 1F grade, from LKB. Nitrocellulose (2 μ m) is from Schleicher and Schuell, Dassell, Germany. PVDF membrane (Immobilon-p) is from Millipore Corporation Bedford M.A. USA. Pre-stained molecular weight markers (low range) are from Bio-Rad Laboratories Ltd, Hemel-Hempsted, Herts, UK. Wash buffer is Tris-buffered saline (TBS) with 0.1% (v/v) TWEEN, pH 7.6. Blocking and antibody buffers contain TBS-TWEEN with 5% (w/v) non-fat milk (Marvel). Polyclonal anti-TIMP-1 and anti-collagenase antibodies are produced from rabbit, at the Rheumatology Research Unit [135, 283]. Horse-radish peroxidase linked, swine antibodies to rabbit immunoglobulins are obtained from Dako Ltd, High Wycombe, Bucks, UK. 4-chloronaphthol is from Sigma. Alkaline phosphatase linked goat antibodies to rabbit immunoglobulins are obtained from Bio-Rad Laboratories Ltd, Hemel-Hempsted, Herts, UK. Alkaline phosphatase colour development kit is also from Bio-Rad.

Experimental Details

SDS PAGE gels are run as described using 5-10 μ l of pre-stained markers in one lane. All materials are soaked in transfer buffer prior to use. A sandwich is formed on the

anode of the blotter of, 9 sheets of filter paper, 1 sheet of nitrocellulose/PVDF, the SDS gel and finally a further 9 sheets of filter paper. A current of 200 mA is applied through the sandwich for 45-60 minutes and the blot transferred immediately to blocking buffer for 1 hour.

For immunoblotting the membrane is then incubated overnight with the polyclonal antibody at a concentration of 1.5 µl/ml. It is then washed (3 x 10 minutes) in wash buffer and incubated for a further 4 hours in the HRP-linked antibody. The blot is then washed a further three times and the colour developed in 60 ml of developing buffer (1x15 mg tablet of 4-chloronaphthol dissolved in 10 ml methanol, 50 ml wash buffer, 33 µl H₂O₂).

Alternatively, for the alkaline phosphatase development the second antibody is used at a dilution of 1:3000, with an hour long incubation. The final wash before colour development does not contain TWEEN. The colour is developed using an alkaline phosphatase conjugate substrate kit from Bio-Rad Laboratories Ltd, Hemel-Hempsted, Herts, UK. This uses 50 µl of reagent A (nitroblue tetrazolium in aqueous dimethylformamide containing magnesium chloride) and 50 µl of reagent B (5-bromo-4-chloro-3-inolyl phosphate in dimethylformamide) in 20 ml of bicarbonate buffer pH 9.5. Colour development is stopped by washing with water.

For PVDF blots the membrane is pre-soaked in methanol, then washed with water. The transferred blot is passed quickly through Coomassie stain and immediately destained extensively.

2.6. Other Materials.

All other general laboratory chemicals where the source is not explicitly described are of analytical grade and obtained from either FSA Laboratory Supplies, Loughborough, Leics, UK, BDH Ltd, Upminster, Essex, UK or Sigma. Laboratory plastic-ware is obtained from ICN Flow Ltd, Rickmansworth, Herts, UK.

Chapter 3

Purification Of TIMP-1.

3.1. Introduction.

For detailed biochemical and structural studies it is necessary to have large quantities of highly purified protein that can be produced quickly with minimal losses. TIMP-1 was originally partially purified by gel filtration techniques [88]. Identifying it as a glycoprotein also aided the purification [128]. The protocol that was used for the initial TIMP-1 preparations was that devised by Cawston et al [103]. This used a series of filtration and affinity columns that result in a sample of very pure protein. Since the TIMP-1 was to be purified from human cell media, an initial chelating-Sepharose column was included as a first step to remove collagenase from the media prior to the TIMP-1 purification.

Another strategy for purifying a protein is to use either monoclonal or polyclonal antibodies to that protein, covalently attached to a support matrix. Solutions containing the protein of interest can then be passed down the affinity column and if the antibodies used were of high specificity, highly pure protein can be eluted in a single step. This strategy had previously been applied successfully for TIMP-1 by other workers [136].

To determine the most suitable matrix for an antibody affinity column, three different types of Sepharose with different linker groups for the ligand were tested. On the basis of these tests a much larger quantity of antibody coupled Sepharose was produced and used to purify a large quantity of TIMP-1 from human culture media. This approach is also shown to be applicable to the purification of recombinant TIMP-1.

3.2. Methods.

3.2.1. Materials

All cell culture media used for the purification of TIMP-1 came from WI-38 foetal lung fibroblast cells [284]. This was kindly produced in bulk by SB. Chelating-Sepharose, heparin-Sepharose, AcA44 gel filtration matrix, Concanavalin A-Sepharose, epoxy-activated Sepharose and activated CH-Sepharose are all from Pharmacia Fine Chemicals, Uppsala, Sweden. CNBr-activated Sepharose was also from Pharmacia and kindly provided in bulk by SB. Column chromatography equipment was purchased from Amicon, Upper-Mill, Gloucestershire, UK. Pumps and fraction collectors were from LKB Instruments Ltd, Surrey, UK. Monoclonal antibodies (P3G6) were developed in the Rheumatology Research Unit [135] and produced in bulk by SB. Dialysis tubing is from Medicell International, London UK. Concentrators and filtration membranes (Diaflow) are from Amicon. All other materials are of good quality from standard suppliers.

3.2.2. Experimental Methods.

At all stages of the purification the samples and column fractions are assayed for protein (by absorbance), inhibitory activity (by bioassay) and a specific ELISA for TIMP-1 (see General Methods). The purity of the sample is also determined during the preparation by analysis on SDS PAGE. For all purifications CaCl_2 (to 10 mM) is added to the bulk media and sodium azide added to 0.02%. It is then concentrated 10-20 fold, the medium adjusted to 50 mM Tris, 10 mM CaCl_2 , 0.02% NaN_3 , (pH 7.2) and passed down a chelating-Sepharose column. The chelating-Sepharose flow through pool contains TIMP-1 which does not bind to the column.

Multi-step Purification.

For this method the sample was dialysed into AcA column buffer (25 mM sodium cacodylate, 1M NaCl, 0.02% NaN_3 , 0.05% Brij-35 pH 7.2). Samples were concentrated to a minimum volume (2-40 ml) and loaded onto a 1.2 L gel filtration column of 4.5 cm

in diameter at a flow rate of 40 ml/hour. Fractions of 10 ml were collected. Those fractions identified as containing TIMP-1 were pooled, concentrated and dialysed into heparin-Sepharose buffer (25 mM sodium cacodylate 0.02% NaN₃, 0.05% Brij-35 pH 7.2). Samples were loaded onto a column of 50 ml at 40 ml/hour and 6 ml fractions taken. The column was washed with the loading buffer and bound proteins eluted with either a salt gradient of 0.1-0 M NaCl or a salt jump of 1M NaCl. Again TIMP-1 containing fractions were pooled and concentrated if necessary. The sample was then dialysed into the loading buffer for the Concanavalin A-Sepharose column (25 mM sodium cacodylate, 100 mM NaCl, 0.02% NaN₃, 0.05% Brij-35, 10 mM ZnCl₂, (used instead of MnCl₂ which could affect NMR studies) 10 mM MgCl₂, pH 7.2. It was loaded onto a 100 ml column at 60 ml/hour. The column was washed with the loading buffer taking fractions of 6 ml. Bound proteins were eluted using the loading buffer with the addition of 0.5 M glucopyranoside. For some samples an additional 'polishing' gel filtration step was used.

For some preparations Brij-35 was omitted from the latter stages of the purification. To remove residual detergent, the sample was dialysed into a 10 mM ammonium hydrogen-carbonate buffer and passed three times down a 10 ml column of Extractigel-D 0.05% Brij-35, washing with ammonium hydrogen-carbonate buffer. After each elution the sample was re-concentrated.

NMR Spectra.

One-dimensional NMR spectra were recorded on a Bruker AMX 360 spectrometer for a sample at approximately 8 mg/ml. For the 1D spectrum, 1024 FIDs were acquired into 16 K data blocks with a 60 degree excitation pulse of 6 ms, a spectral width of 7042 Hz, an acquisition time of 1.16 s and a relaxation delay of 1.5 s.

Preparation and Assessment of Antibody-Coupled Sepharose.

Coupling was performed according to the general instructions supplied by the manufacturer. For the coupling of P3G6-antibody to CNBr-activated Sepharose the matrix was swollen for 15 minutes in 3x the final expected volume of 1 mM HCl, then washed with 30 volumes of 1 mM HCl followed by 3 volumes of coupling buffer (0.1M NaHCO₃ 0.5 M NaCl, pH 8.3). Antibody was coupled at 1 mg/ml of gel in sufficient coupling buffer to give a soft slurry. The coupling mixture was incubated on an end over end mixer for either 16 hours at 4°C, or 2-4 hours at room temperature. To block remaining groups on the matrix the coupled gel was blocked with 1M ethanolamine for a further 2 hours at room temperature. The blocking agent and excess protein were washed off with alternate washes of 0.1M sodium acetate, 0.5 M NaCl pH 4.5 (acetate buffer), and coupling buffer. The matrix was finally washed with antibody column buffer (25 mM sodium cacodylate, 100 mM NaCl, 0.02% NaN₃ pH 7.2).

Activated CH-Sepharose was prepared and coupled to the antibody much as for CNBr-activated Sepharose. After the incubation with the antibody solution the matrix was washed with 10 volumes of coupling buffer, then incubated for 1 hour at room temperature in 50 mM Tris, 0.5M NaCl. pH 8.0 (Tris buffer). The matrix was given extensive alternate washes of Tris buffer and acetate buffer, and finally transferred to antibody column buffer.

Epoxy-activated Sepharose was prepared by swelling in an excess of distilled water for 15 minutes followed by extensive water washing. The ligand and matrix were incubated at 37°C (water bath) in coupling buffer for 16 hours with occasional gentle shaking. The coupled matrix was washed in 20 volumes of coupling buffer then given alternate washes of water, coupling buffer and acetate buffer. Remaining groups were blocked by a 1 hour incubation in 1M ethanolamine, the matrix washed extensively with water and transferred to column buffer.

Initially small columns (approximately 2 ml in volume) were prepared for each matrix type. Media known to contain TIMP-1 was passed down the columns under gravity and 1ml fractions collected manually. The columns were washed extensively with antibody column buffer. Proteins were eluted using a sodium citrate buffer at pH 3.0. Fractions were assayed for TIMP-1 by ELISA.

Purification of TIMP-1 on an Antibody Affinity Column.

A large quantity of antibody affinity matrix was prepared using CNBr-activated Sepharose. This was washed with antibody column buffer, and packed into an Amicon chromatography column (P70x250) with a total bed volume of 760 ml.

Culture medium from WI-38 foetal lung fibroblasts was processed as described to remove any collagenase present. Batches of the flow through pool were passed directly through the monoclonal antibody affinity column at 500 ml/hour. The column was washed extensively with antibody column buffer. TIMP-1 was eluted from this column using 3M NaI in either 50 mM Tris, 0.1 M NaCl, pH 7.2 (Tris buffer) or antibody column buffer. Fractions of 500 ml were collected and immediately transferred to dialysis against either 50 mM Tris 100 mM NaCl, pH 7.6, or antibody column buffer. Dialysed fractions were assayed for protein, TIMP-1 and inhibitory activity. Purity was determined by analysis of SDS PAGE gels using an LKB Ultrascan XL laser densitometer and accompanying software (LKB Instruments Ltd, Surrey, UK). For wild type TIMP-1 an additional Concanavalin A-Sepharose affinity column was used to separate different glycoforms.

Lyophilisation.

TIMP-1 for structural studies was dialysed into 10 mM ammonium bicarbonate and lyophilised.

3.3. Results.

3.3.1. Purification of TIMP-1 Using Multi-Step Procedure.

TIMP-1 was purified from WI-38 media in several batches. Figures 3-1, 3-2 and 3-3 show examples of column profiles for each step. Figure 3-4 shows an SDS-PAGE gel of the final purified products. Table 3-1 shows the respective yields for each stage. A total of 23.6 mg of TIMP-1 was purified in this manner.

	volume / ml	inhibitor / units	protein / mg	yield / %	Specific activity /units/mg
Concentrated Chelating-Sepharose Flow through Pool	156	515004	477.6	100	1078.3
Gel Filtration Pool	814	378376	75.3	73.5	5025.0
Heparin-Sepharose Pool	542	355488	32.4	69	10971.9
Con A-Sepharose Pool	337	227475	16	44	14217.2
Con A flow through Pool	150	106875	18.5	21	5777.0
Polishing AcA Pool	316	49088	7.6	9.5	6459.0

Table 3-1. Purification data for TIMP-1 derived from WI-38 media. The original volume of the chelating-Sepharose flow through was 7.5 L. Total quantity of purified TIMP-1 was 26.1 mg with a total activity of 334350 units (after Concanavalin A-Sepharose purification). The overall yield for the procedures was 44% for the CAB pool and 9.5% for the NCAB pool.

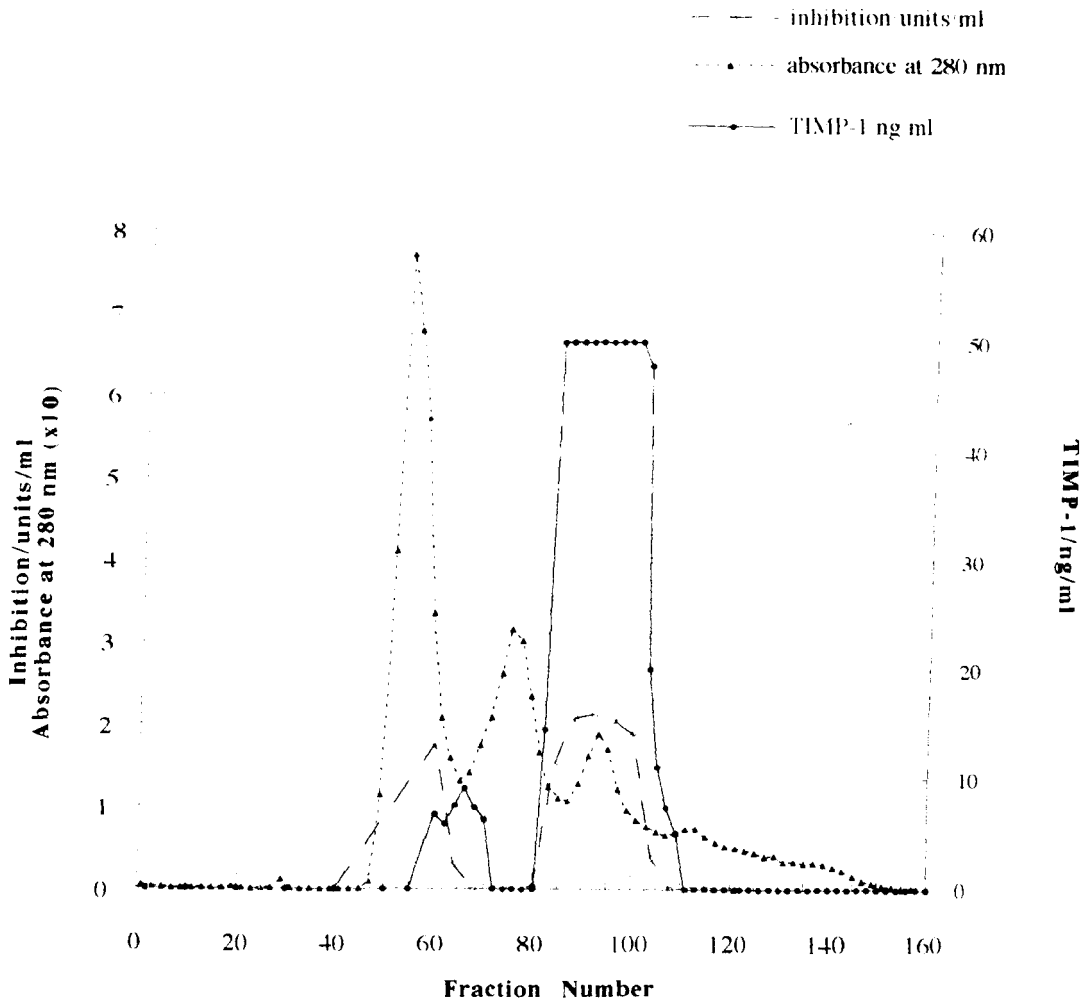


Figure 3-1. Example Gel Filtration (AcA44) Column Profile for TIMP-1 Purification.

WI-38 cell culture media is concentrated, dialysed into AcA column buffer and the column run at 60 ml/hr. The figure shows the profile for a 2L column, where 10 ml fractions are collected and assayed. Fractions are pooled to include the protein and inhibitory peaks. Fractions containing less than 20 ug/ml of TIMP-1 (by ELISA) are discarded.

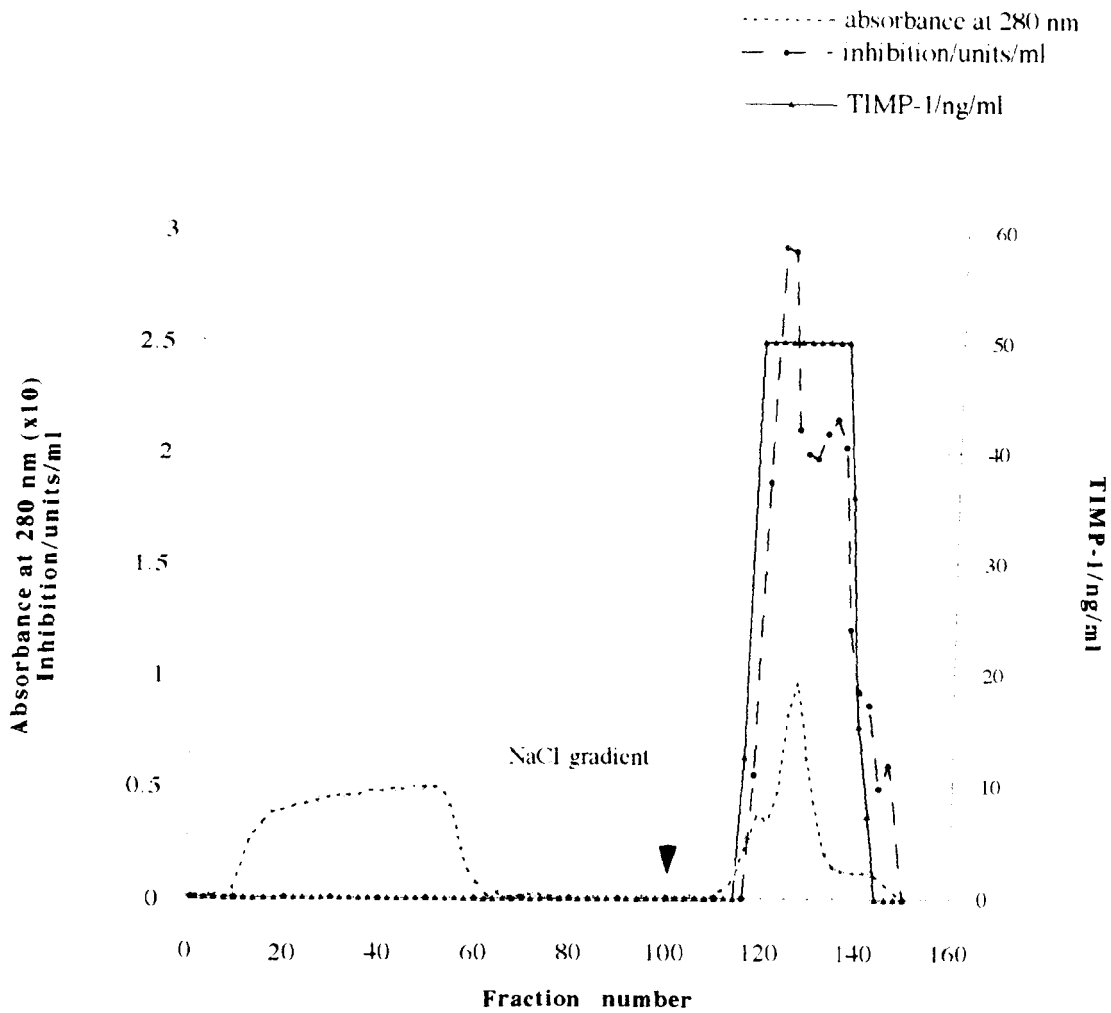


Figure 3-2. Heparin Sepharose Column Profile for TIMP-1 purification.

Material pooled from gel filtration is concentrated, dialysed into low salt buffer and the column run at 40 ml/hr. The figure shows the profile for a 100 ml column where 6 ml fractions are collected and assayed. Elution with a salt gradient gives the elution profile above. Fractions containing TIMP-1 are pooled.

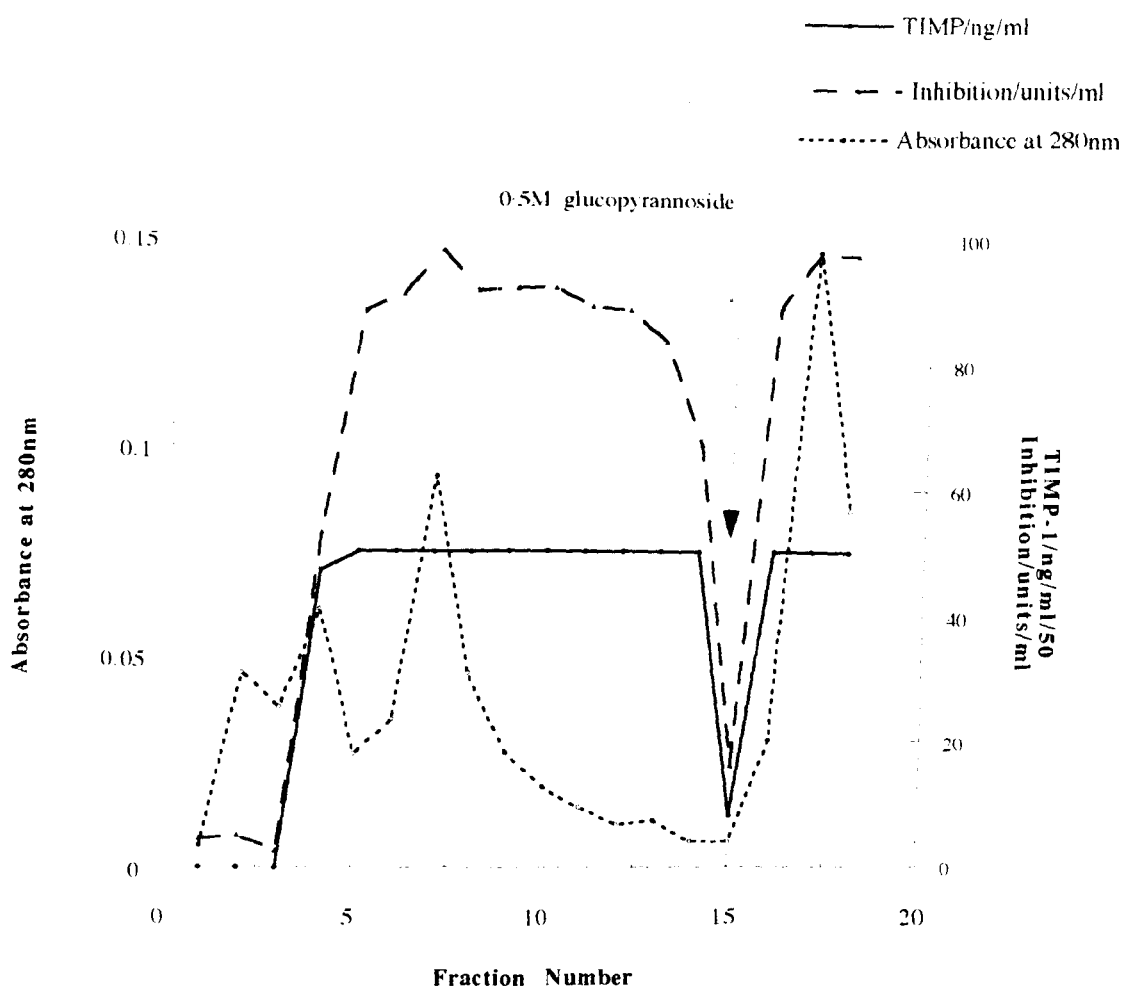


Figure 3-3. Example Concanavalin A Column Profile for TIMP-i Purification.

The pool from heparin-Sepharose is concentrated, dialysed into Con A-Sepharose buffer and loaded onto a 100 ml column at 60 ml/hr. Bound glycoproteins are eluted with 0.5M glucopyranoside. Fractions of 6ml are collected and assayed. The fractions are pooled as either NCAB (flow through prior to elution) or CAB (eluted).

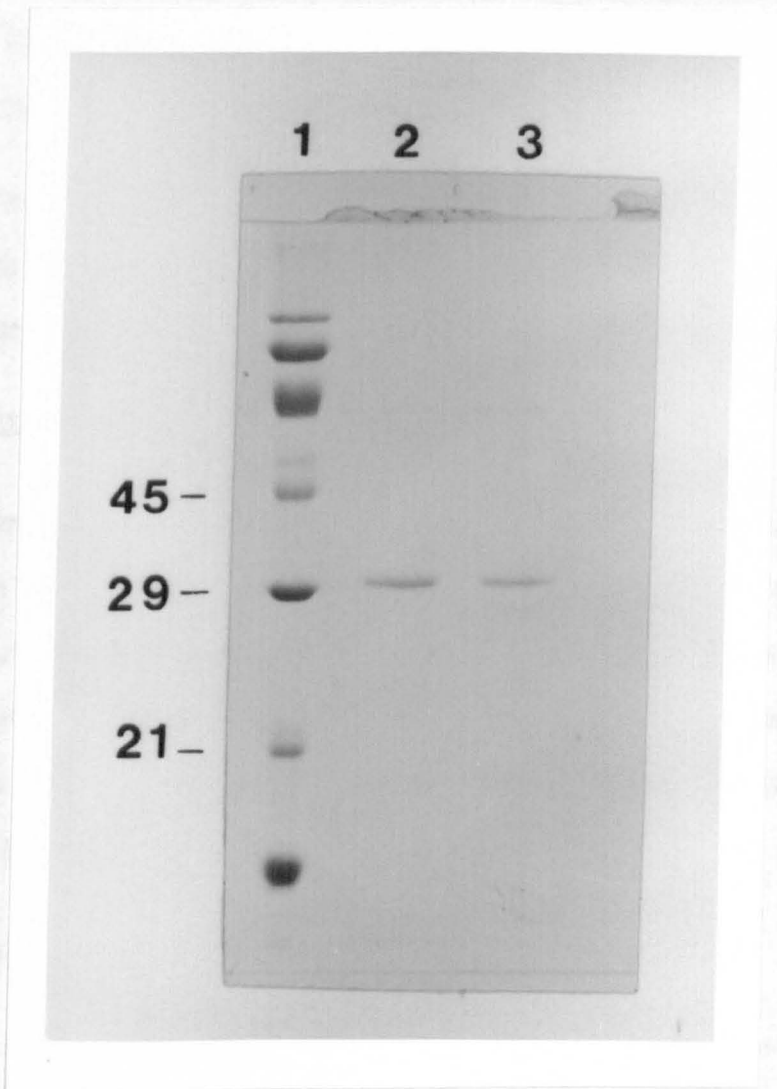


Figure 3·4. SDS PAGE of TIMP-1 Purified Using Gel Filtration and Affinity Chromatography.

Lane 1: molecular weight markers. Lane 2: NCAB TIMP-1 pool. Lane 3: CAB TIMP-1 pool. TIMP-1 runs as a single band close to the 29 kDa marker.

After passing through Concanavalin A-Sepharose matrix, the TIMP-1 is divided into two pools. The first does not bind to the matrix but is retarded. This can be seen on figure 3-3. This material is designated as non-Concanavalin A-Sepharose binding (NCAB) TIMP-1. The remainder of the material binds to the matrix and is eluted with the glucopyranoside buffer and is designated as Concanavalin A binding (CAB) TIMP-1.

Although the CAB TIMP is pure after Concanavalin A-Sepharose chromatography, the material that does not bind to the column (NCAB TIMP) is less pure (see figure 3-4). This material is subjected to an additional polishing step on another gel filtration column.

3.3.2. 1D NMR Spectrum of Purified TIMP-1.

A one-dimensional NMR spectrum of TIMP-1 purified using the original procedure is shown in figure 3-5. There are two strong peaks at 2.9 ppm and 0.8 ppm. These are not signals from the protein which has much weaker signals. The chemical shifts are indicative of a simple hydrocarbon. One-dimensional spectra were recorded for the different buffer components used during the purification, and this contaminant identified as Brij-35.

3.3.3. Development of a Monoclonal Antibody Affinity Matrix.

Three different Sepharose based support matrices were produced and tested to determine the most effective matrix for antibody coupling. Small columns (2ml) were prepared of P3G6 monoclonal anti-TIMP antibody coupled to CNBr-activated Sepharose, epoxy-activated Sepharose and activated CH-Sepharose. Equal volumes of the same TIMP-1 containing media were passed down the columns and the eluted material (neutralised by the addition of sufficient 1M Tris) assayed by ELISA or bioassay.

Column profiles for each of these matrices are shown in figures 3-6, 3-7 and 3-8. CNBr-activated Sepharose-P3G6 bound 650 units of inhibitory activity/ml of matrix. Epoxy-P3G6 Sepharose was found to have a binding capacity of 41 units/ml of

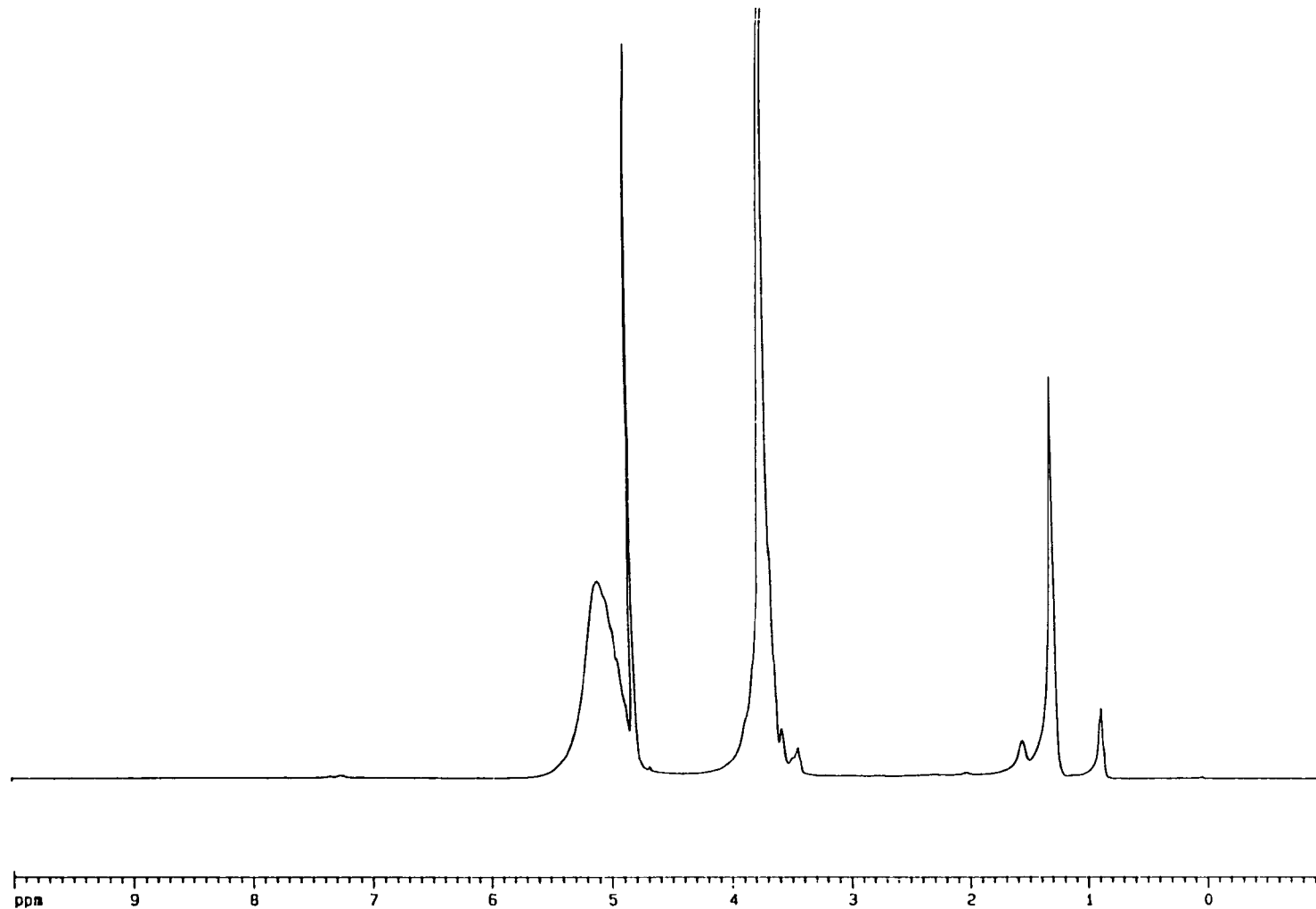


Figure 3-5. 1D NMR Spectrum of TIMP-1. The spectrum was recorded for a sample of TIMP-1 at 8 mg/ml. The signals from the protein are just visible as irregularities in the baseline around 7 ppm and 1.8 ppm. The main signals in this spectrum are the water close to 5 ppm and signals from the detergent Brij35 around 3.5 ppm and 1 ppm.

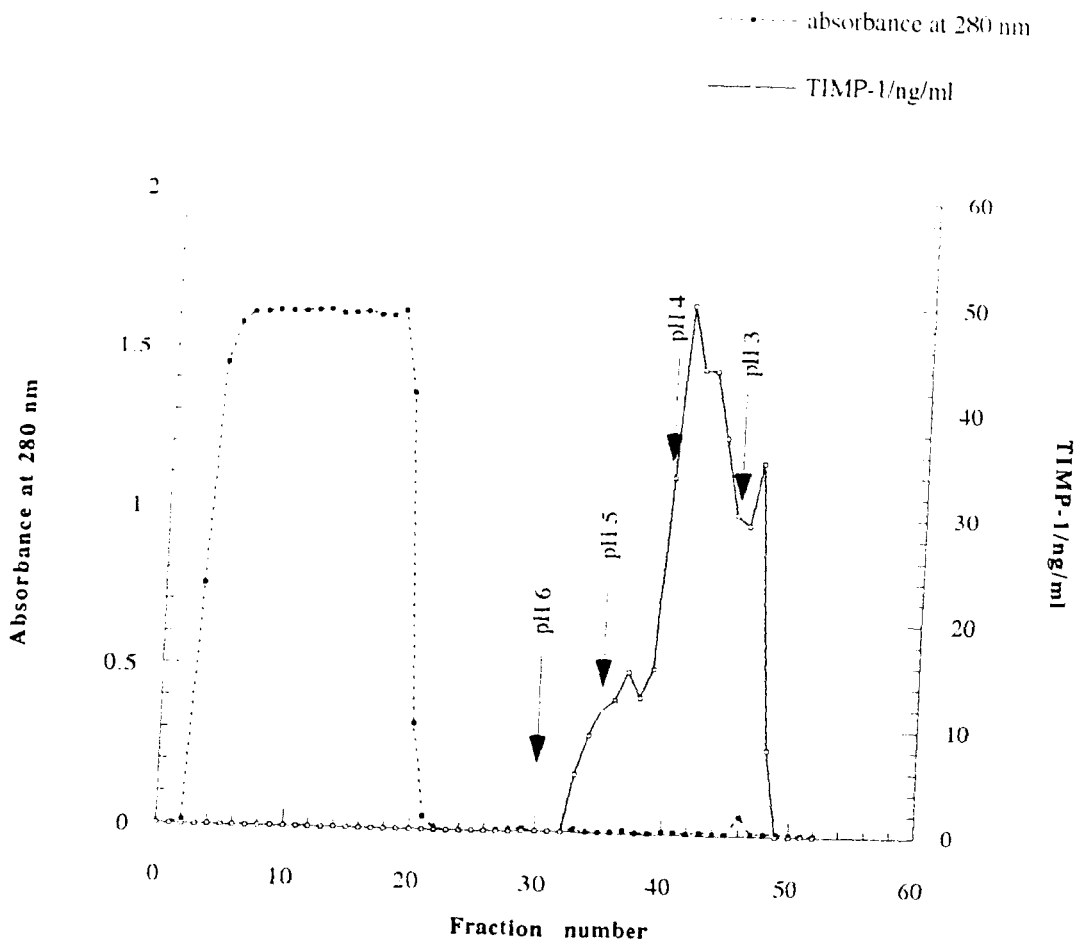


Figure 3-6. Column Profile for CN-Br-Activated Sepharose P3G6

Eluted with Citrate Buffer Over a pH Range of 3.0 - 6.0.

Pooled material from chelating-Sepharose is loaded directly onto the column.

The elution is carried out with buffers of different pH to identify the highest pH that elutes all of the protein. The majority of the protein is eluted at pH 4.0, however at pH 3.0 additional protein is eluted.

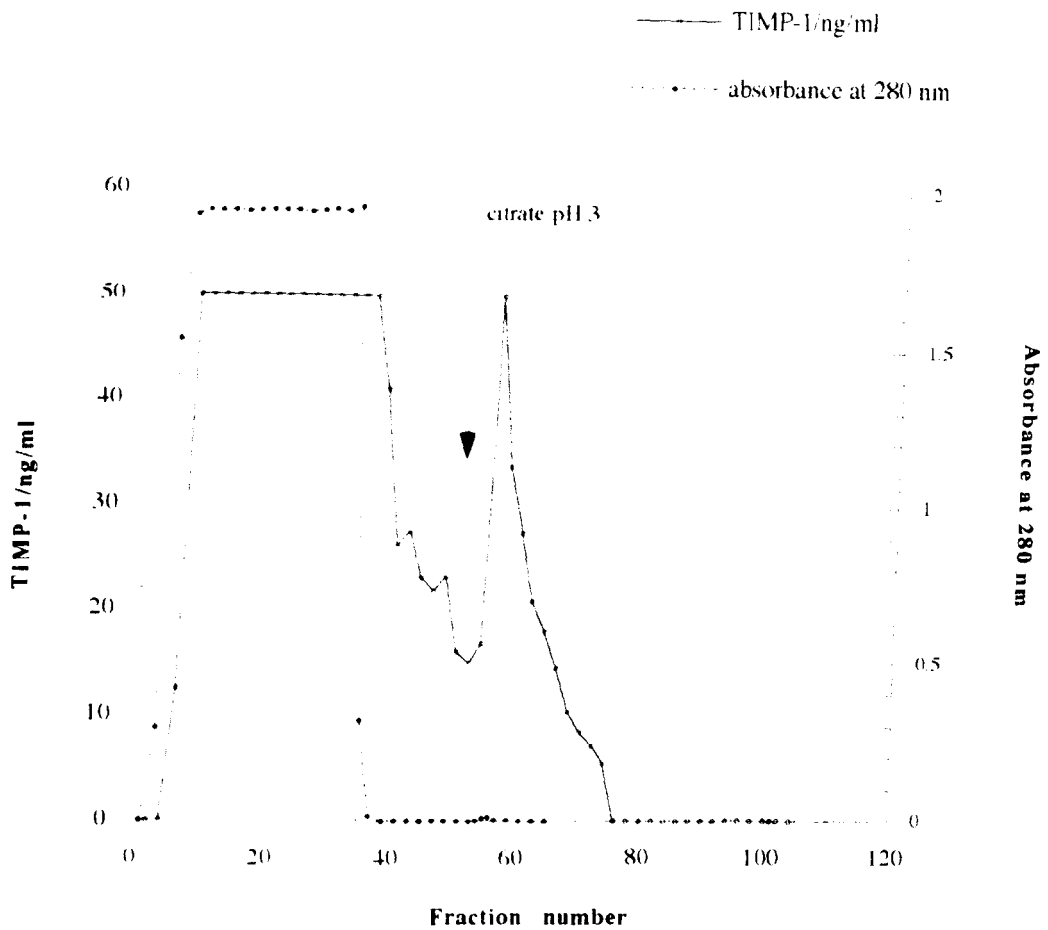


Figure 3-7. Column Profile for Epoxy-Activated Sepharose-P3G6.

Pooled material from chelating-Sepharose is loaded directly onto the column and eluted with citrate buffer at pH 3.0. From the figure it can be seen that most of the TIMP-1 passes straight through the column.

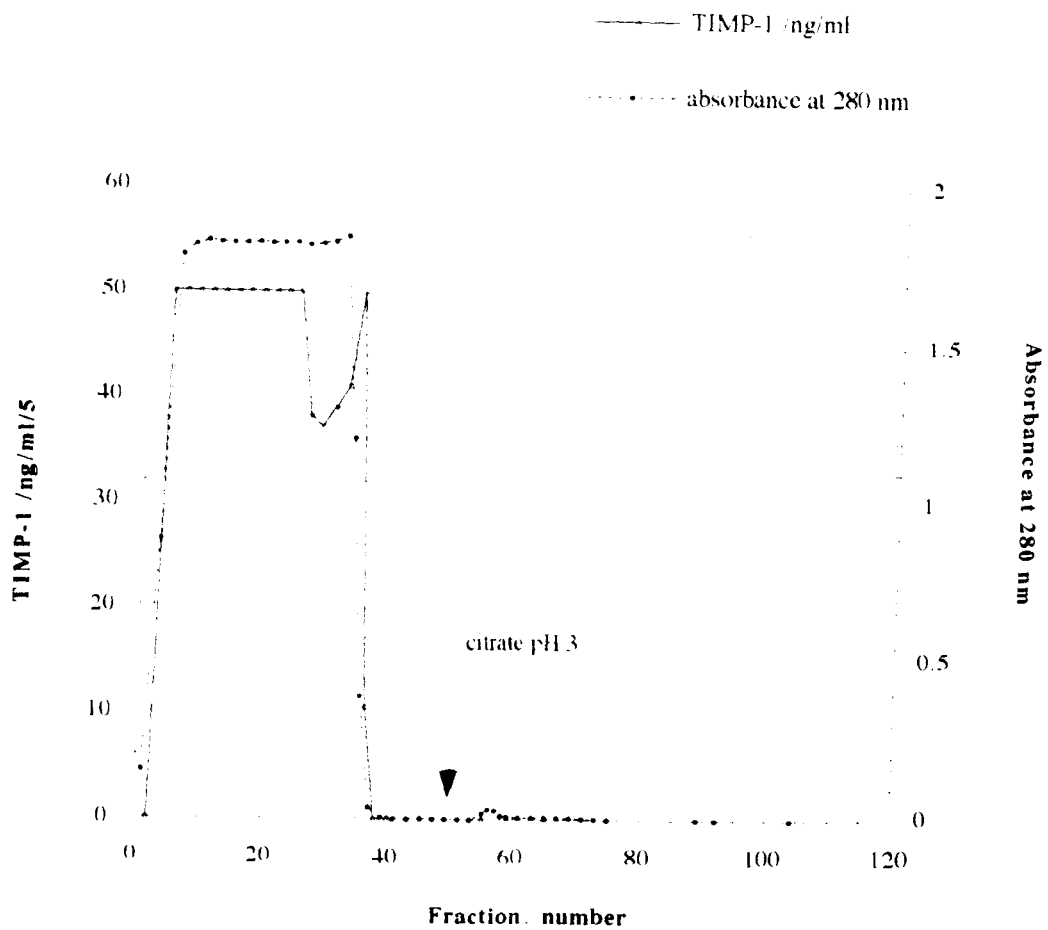


Figure 3-8. Column Profile for Activated CH-Sepharose-P3G6.

Pooled material from chelating-Sepharose is loaded directly onto the column and eluted with citrate buffer at pH 3.0. In this case none of the TIMP-1 is seen to bind the column. The small protein peak eluted is probably bound non-specifically.

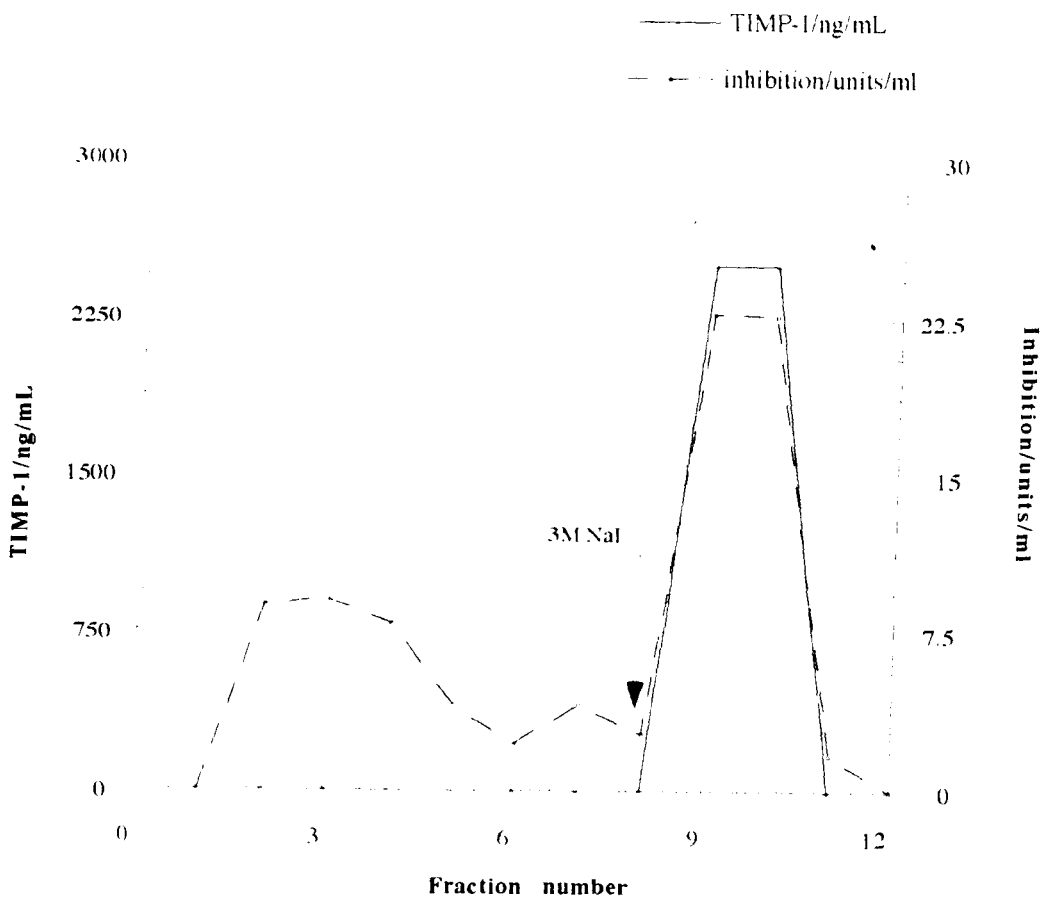
matrix. No TIMP-1, or inhibitory activity was found to bind to the activated CH-Sepharose-P3G6.

For the CNBr-activated Sepharose-P3G6, TIMP-1 could be eluted from the matrix over the entire pH range used although most material came off at pH 4 and any remainder came off at pH 3. For an initial sample loaded, of 500 ng of TIMP-1, 405 ng were recovered giving a yield of 81%.

A larger column of 25 ml of affinity matrix was prepared using the CNBr-activated Sepharose (taken from the large batch preparation) For this preparation the coupling efficiency was found to be 97% by comparing the E_{280} before and after the coupling reaction. Elution was with citrate buffer at pH 3.0. It was found that in this larger volume the protein was eluting very slowly giving many dilute fractions and an unacceptably large pool volume. Elution with 3M sodium iodide in the loading buffer gives the column profile shown in figure 3-9. This elutes all of the protein from the column using less than a column volume of elution buffer. The binding capacity of this matrix was calculated to be 0.14 mg/ml. As with the smaller columns, most of the yields were in the order of 80% (by both bioassay and ELISA).

3.3.4. Large Scale Purification of TIMP-1.

A total of 400 litres of WI-38 culture medium were concentrated and passed through a chelating-Sepharose column to remove the collagenase from the media. The resulting flow through pool had a total volume of 13 litres. A total of 8 litres of this product was passed in batches through the CNBr-activated Sepharose-P3G6 affinity column using 3M NaI as the elutant. This material was further purified by the separation of different glycoforms on a Concanavalin A-Sepharose column. This separation divided the material into two pools as with the previous purification, one that bound to the column



**Figure 3-9. Column Profile for CNBr-Activated Sepharose-P3G6
Column Used for Large Scale Purification of TIMP-1.**

Pooled material from chelating-Sepharose is loaded directly onto the column. The 760 ml column is run at 500 ml/hr taking 500 ml fractions. Elution is with 3M NaI. All of the TIMP-1 elutes in two fractions.

and a second that was retarded rather than entirely non-binding. The column profile for an example antibody affinity column run is shown in figure 3·9.

SDS PAGE gels of the purified TIMP-1 showed a single band and were determined to be 97% pure by gel-densitometry (figure 3·10).

A total of 90 mgs of TIMP-1 were prepared in this way and subdivided into Concanavalin A-Sepharose binding (CAB) material and non-Concanavalin A-Sepharose binding (NCAB) material. The yields for each batch on the monoclonal affinity column were greater than 80%. The subdivision of the purified material reduces the overall yield to 70% giving a pool of CAB TIMP-1 of 49·7 mg with a specific activity of 23875 units/mg and 28·5 mg of NCAB TIMP-1 with a specific activity of 27617 units/mg.

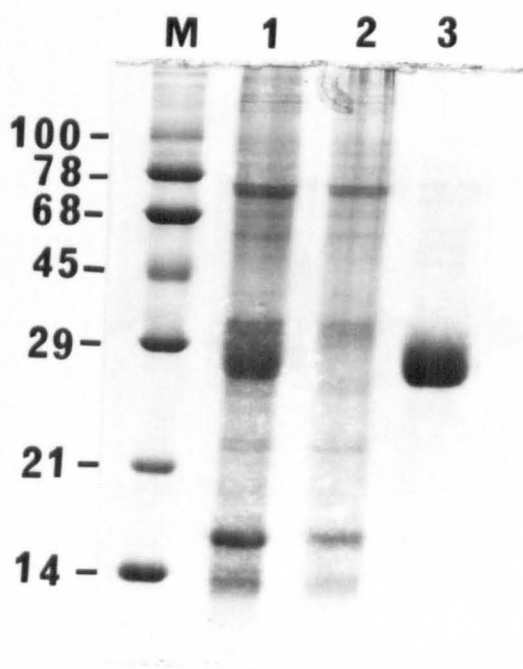


Figure 3-10. SDS-PAGE of TIMP-1 Purified Using an CNBr-Activated Sepharose-P3G6 Column.

Lane M: molecular weight markers. **Lane 1:** Chelating-Sepharose pool. **Lane 2:** Flow through from CNBr-Activated Sepharose-P3G6 Column. **Lane 3:** Eluted TIMP-1 from CNBr-Activated Sepharose-P3G6 Column.

3.4. Discussion.

The purification of TIMP-1 using the method of Cawston et al [103] produced material that gives a single band on an SDS PAGE gel. The overall yield for this procedure is 54%. Protein loss is occurring at each column, dialysis and concentration step. After extensive dialysis against ammonium hydrogen-carbonate buffer the mass of the initial preparation of lyophilised material was greater than expected. Analysis by NMR found this material to be chemically contaminated by the detergent Brij-35. The sample could be cleaned to chemical purity using Extractigel-D, a matrix with a high affinity for detergents. Dialysis under the condition used does not appear to be sufficient to remove all traces of detergent. This might be due either to some binding capacity of the dialysis tubing or to the structure of the detergent molecule being elongated inhibiting its passage through the tubing pores. Alternatively TIMP-1 may have an affinity for Brij35, which could suggest some degree of hydrophobic exposure at the surface.

To avoid this problem recurring, Brij-35 was omitted where possible and samples routinely treated to remove residual detergents.

A monoclonal antibody affinity column has been developed to purify TIMP-1 in a single step. Three different antibody-coupled Sepharose matrices were tested to determine which coupled matrix had the highest TIMP-1 binding capacity. Of the three, activated CH-Sepharose-P3G6 did not appear to bind TIMP-1 under the conditions used. Epoxy activated-Sepharose-P3G6 bound a small fraction of the TIMP-1 that had been loaded onto the column. CNBr-activated Sepharose-P3G6 matrix binds TIMP-1 with a capacity of 0.14 mg/ml of matrix.

P3G6 bound to CNBr-activated Sepharose proved to be the most effective for binding TIMP-1. On scaling up from a 2 ml column volume to a 25 ml, and 760 ml column, it was found that the original elutant (citrate pH 3.0) was not suitable. Elution with the low pH buffer did not give a sharp elution peak, instead the protein came off the column in an unacceptably large volume. The chaotropic salt NaI proved more effective,

giving a very sharp and predictable elution profile even for the largest column volume (760 ml).

This method gave an overall yield (before separation by Concanavalin A-Sepharose) of 80%. This is 20-30% greater than for the conventional method and is achieved in a single step. Purification from large volumes of cell culture medium provided 90 mg of highly pure TIMP-1, again with an overall yield of 80% before separation of glycoforms. The separation of the different forms on Concanavalin A-Sepharose does not alter the apparent molecular weight of TIMP-1 on SDS-PAGE. Although there is a difference in the specific activities of the two pools, this can be attributed to slight differences in purity and the accuracy of the inhibition assay.

The differences in the binding of TIMP-1 to Concanavalin A-Sepharose can be attributed to heterogeneity in the attached carbohydrates. Whether a carbohydrate will bind to the Concanavalin A-Sepharose lectin depends on its composition. Slight differences in the content, or arrangement of the sugars can alter the ability of the carbohydrate to bind to the matrix. A particular source for heterogeneity is the sialic acid residues at the ends of the carbohydrate chains. These are gradually hydrolysed in the extracellular environment, altering both the charge and structure of the carbohydrate moiety. Subsequently the ability of the protein to bind to Concanavalin A-Sepharose can be affected, dividing the wild type protein into pools containing one or more different glycoforms.

It should also be possible to purify large quantities of recombinant TIMP-1 in this manner.

Chapter 4.

Evaluation of Expression Systems for TIMP-1 in *Escherichia Coli*.

4.1. Introduction.

Detailed structural studies of proteins demand a ready supply of large quantities of material. For a protein such as TIMP which is produced *in vivo* in relatively small quantities the best solution is an over-expression system. The carbohydrates attached to TIMP-1 do not appear to have any function and would make analysis of NMR data extremely difficult. Signals from sugars are much sharper than those from the protein due to their high mobility, and overlap the region of an NMR spectrum where signals are found from residue side-chains. This makes expression in *E.coli* preferable since proteins are not glycosylated by the cells. Expression in *E.coli* can give a very high yield of protein per litre of growth medium, important when considering the production of TIMP-1 isotopically labelled for heteronuclear NMR studies.

Possibly the most difficult aspect of expressing TIMP-1 in *E.coli* is the need to form all six disulphide bonds correctly. The cytoplasm of *E.coli* is a reducing environment and others who have attempted to express TIMP-1 (murine) have found that it forms insoluble aggregates [285]. Attempts at refolding the insoluble human protein have met with varied success. One the most effective strategies so far has been to use a very careful renaturation procedure using oxidised glutathione and 4M urea in the refolding buffer [286]. Another group has reported the successful expression of human TIMP-1 in *E.coli*, again using a careful renaturing process [287]. However they do not give figures for the yield in terms of expression per litre of medium, an important figure when determining the feasibility of isotopically labelling a recombinant protein.

Baculovirus [288] and CHO cell [289] expression systems have also been used successfully to produce wild type TIMP-1 (murine and human). However these are not suitable for the expression of TIMP-1 for NMR structural studies. This is because in these systems, expressed proteins are normally glycosylated. Mutants of TIMP-1 where the glycosylation sites have been mutated out have been expressed in mouse myeloma cells [278]. However, isotopic labelling in these systems is currently prohibitively costly.

Two different strategies have been used in an attempt to produce soluble TIMP-1 in *E.coli*. The first used the pEZZ18 expression vector, which is based on pEMBL8+ [290]. This includes a synthetic version of part of the Staphylococcal protein A (SpA) as a fusion product with the protein of interest. SpA has the ability to bind to the Fc portion of most IgGs. This function is contained within five homologous IgG binding domains of around 58 residues each. In the pEZZ18 vector two IgG binding domains are present, based on the B domain of the original. This should allow the protein to be purified on IgG Sepharose. The inclusion of the N-terminal signal domain from SpA allows the fusion product to be secreted to the periplasm. Since the expression of the SpA gene in gram -ve strains of *E.coli* creates a leaky phenotype, proteins from the periplasm are secreted into the media. In the extracellular media the environment is not reducing and subsequently TIMP-1 should be able to fold correctly. To allow removal of the fusion protein a factor Xa cleavage site (IEGR) was inserted into the TIMP-1 cDNA before the N-terminal cysteine using PCR techniques. Factor Xa cleaves after the R of this sequence to give a free N-terminus. To generate a truncated TIMP-1 the cDNA was modified to create a stop codon after residue Glu-126, which lies in the linker region between the two domains.

The second strategy took advantage of the fact that the periplasmic space of *E.coli* contains a protein disulphide isomerase [291, 292]. The presence of a disulphide isomerase allows disulphide bonds to be re-arranged, increasing the amount of correctly folded protein. To do this the expression vector pASK60-strep was used. This utilises the N-terminal leader peptide (21 residues) of the *OmpA* protein which targets the

There are four different gene products expected in these experiments. From the pEZZ18 vector, full length, and truncated TIMP-1 are secreted to the media as fusion proteins with a pair of IgG binding domains at the N-terminus (abbreviated to ZZ-). From the pASK60 vector, full length and truncated TIMP-1 are produced with an N-terminal ompA signal sequence which directs the protein to the periplasm where the signal sequence is cleaved, leaving the N-terminal cysteine of TIMP. The expected molecular weights of these products (including those expected after successful cleavage of the fusion protein with factor Xa) are shown in the table below.

Product	Molecular Weight (kDa)	Weight after Xa Cleavage (kDa)
ZZ-TIMP-1	36	21
ZZ- Δ TIMP-1	28	13
(ompA) TIMP-1	21	n/a
(ompA) Δ TIMP-1	13	n/a

It should be noted that the ZZ-(Δ)TIMP-1 proteins do not run as expected on SDS PAGE. ZZ-TIMP-1 appears close to 45 kDa, whilst ZZ- Δ TIMP-1 appears close to 21 kDa.

protein to the periplasmic space. This peptide is cleaved as the protein is transported into the periplasm, leaving a free N-terminal residue. This vector also included a C-terminal strep-tag for easy purification of the final product. However, since an efficient purification system was already available and additional residues were undesirable, this C-terminal extension was removed. This method was also attempted with both full length, and truncated TIMP-1. Truncated TIMP-1 (Δ TIMP-1) was assessed alongside the full length systems to provide material for potential enzyme-inhibitor interaction studies and as a possible alternative, were the full length recombinant protein to prove unsuitable for NMR studies.

This chapter describes the development and assessment of these two strategies.

4.2. Methods.

4.2.1. Materials.

The TIMP-1 cDNA was a generous gift from Dr. Alan Galloway at British Biotechnology, Oxford UK. The pEZZ18 vector was from Pharmacia Biotech UK, St. Albans, Herts. The pASK-60 vector was from Biometra, Maidstone, Kent UK. HB101 cells were from Stratagene, Cambridge UK. TG1 cells were the generous gift of Dr. P. Alefounder, University of Cambridge UK. Large scale fermentations (10L) were performed at SmithKline Beecham Pharmaceuticals, Great Burgh, Surrey by Helen Edwards and Bob Imrie. Factor Xa was purchased from Denzyme Aps, Aarhus, Denmark. IgG Sepharose was from Pharmacia. Agar, yeast extract and bactotryptone were from Difco Labs, Molesy, Surrey, UK. Agarose was from Gibco BRL Ltd, Paisley, UK. DNA ligase, all restriction enzymes and restriction buffers were from Boehringer Mannheim UK, Lewes. Sussex. Mini gel apparatus was from International Biotechnologies Inc. Connecticut USA. Periplasmic extraction kit was from Biometra, Maidstone, Kent UK. Mini-prep spin kits were from QIAGEN, Dorking, Surrey, UK. Oligonucleotides were supplied by the Dept of Molecular Medicine Kings College London School of Medicine. Phosphoramidon, aprotinin, PMSF and ampicillin were from Sigma Chemical Company, Poole Dorset, UK. IPTG was from Northern Biologicals Ltd, Cramlington, UK. Falcon 2059 tubes were from FSA Lab Supplies, Loughborough, UK.

pEZZ18 vector for TIMP-1 and Δ TIMP-1.

The pEZZ18 vector used is shown as figure 4.1.

pASK-60 vector for TIMP-1.

The pASK60-strep vector used is shown in figure 4.2.

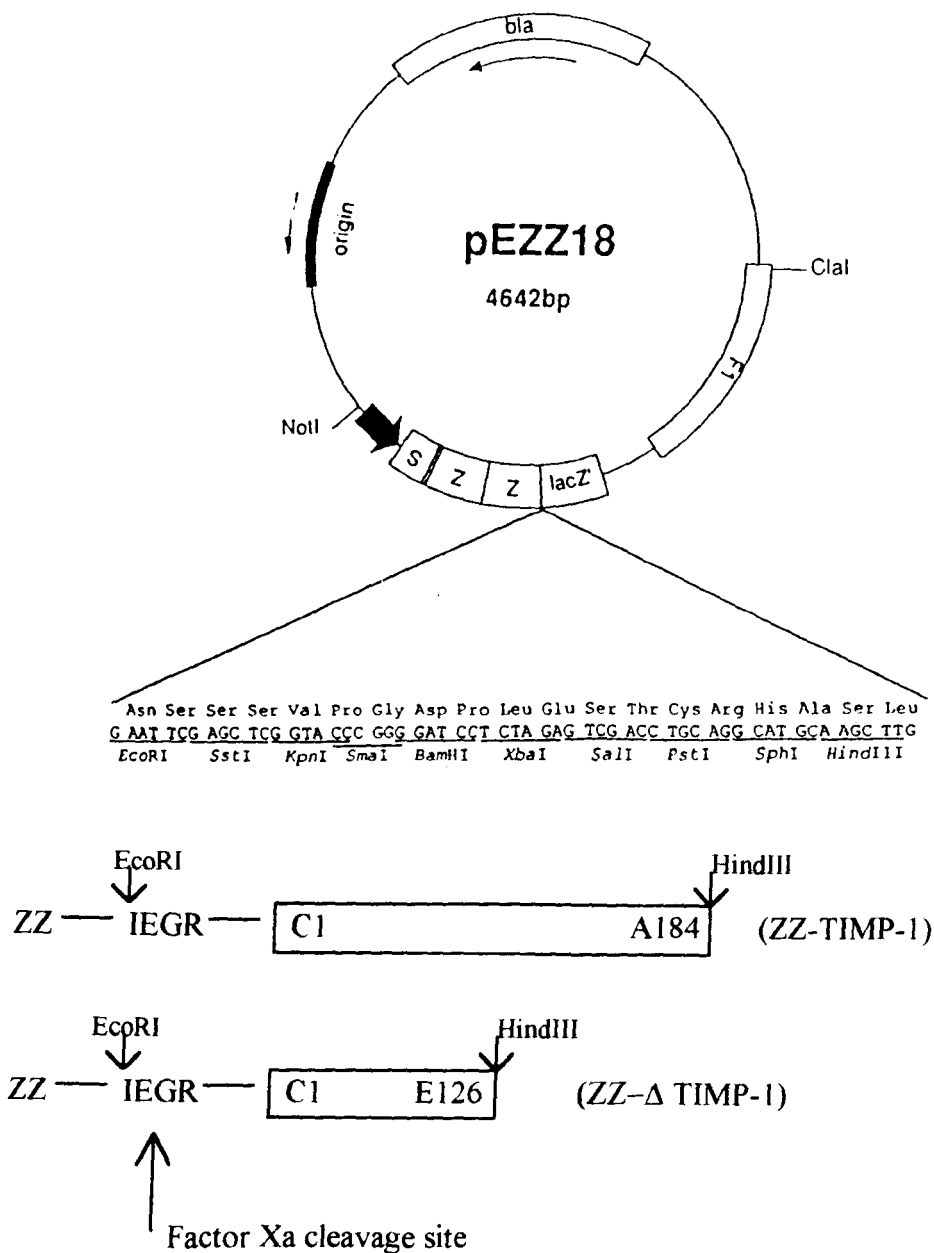
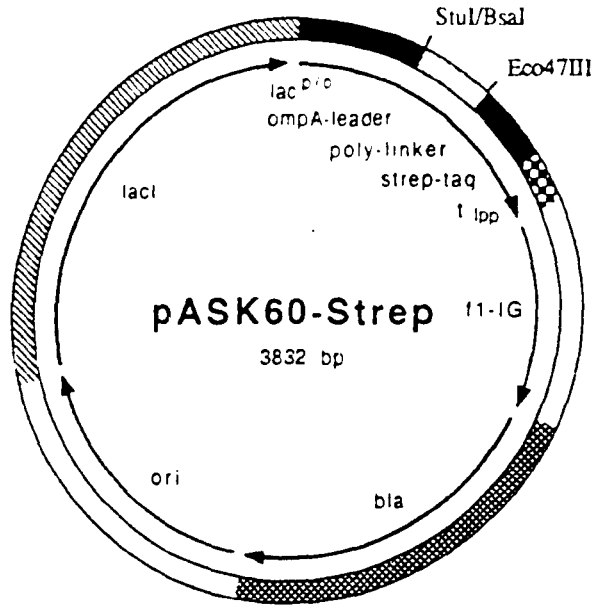


Figure 4-1. Diagrammatic representation of the pEZZ 18 Expression Vector and the TIMP-1/ Δ TIMP-1 Construct.

The vector contains two IgG binding domains (ZZ), a multiple, restriction site (shown expanded below the vector), the bla gene which confers ampicillin resistance, an origin of replication, the lacZ structural gene and the gene for F1 protein which is the recognition sequence for packing the DNA into phage particles after M13 or f1 infection. The TIMP constructs shown beneath the vector are inserted between the EcoRI and HindIII sites.



```

RBS                               XbaI   RBS
CACAGGAACAGCTATGACCATGATTACGAATTTCTAGATAACCGGGCAAAAAATGAAAAAGACAGCTATCGCG
LacZ: MetThrMetIleThrAsnPheEnd      OmpA: MetLysLysThrAlaIleAla

```

```

                               StuI  BsaI  EcoRI  SstI  KpnI  SmaI  BamHI
ATTGCAGTGGCACTGGCTGGTTTCGCTACCCTAGCGCAGCCCTAGACCAGAATTTCGAGCTCGGTACCCGGGGAT
IleAlaValAlaLeuAlaGlyPheAlaThrValAlaGlnAlaEnd

```

```

XhoI  SalI  PstI  Eco47III                               HindIII
CCCTCGAGGTGCGACCTGCAAGCCAGCGCTTGGCGTCACCCGCACTTCGGTGGTTAATAAGCTTGACCTGTGAAGTG
Strep-tag: SerAlaTrpArgHisProGlnPheGlyGlyEnd

```

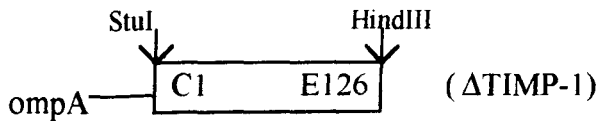


Figure 4-2. Diagrammatic representation of the pASK60-strep Expression Vector and the TIMP-1 ΔTIMP-1 Constructs.

The vector contains an origin of replication (ori); the ampicillin resistance gene (bla); the lac repressor gene (lacI); an expression cassette under the control of the lac promoter, containing a multiple restriction site (shown expanded below the vector), the ompA leader sequence and the strep tag, and an f1 origin as in figure 4-1. Here the TIMP-1 or ΔTIMP-1 construct is inserted between the StuI and HindIII sites in the multiple restriction site so that when the ompA leader sequence is cleaved in the periplasm the N-terminal amino acid is Cys1 of TIMP-1.

4.2.2. Experimental Details.

All modifications of TIMP-1 cDNA, vectors, PCR, and DNA sequencing was carried out by Dr. Mary O' Hare (at the Rheumatology Research Unit, Cambridge) and will not be discussed in detail here. To generate a truncated Δ TIMP-1 sequence a stop codon and an *EcoRI* site were inserted at base pair 379 using PCR. For the pEZZ18 vector, the TIMP-1 cDNA was modified to create a factor Xa cleavage site just before the first cysteine residue at the N-terminus of the TIMP-1/ Δ TIMP-1 coding sequence. The modified TIMP-1 cDNA was cloned in to the pEZZ18 vector between an *EcoRI* site and a *HindIII* site and the truncated TIMP-1 between a pair of *EcoRI* sites. For the pASK60-strep vector TIMP-1 and Δ TIMP-1 cDNAs were cloned into the vector between a *StuI* site and a *HindIII* site. The orientation and sequences were confirmed by double stranded dideoxy sequencing methodology. The pEZZ18 and pASK60-strep vectors containing the TIMP-1 cDNAs were initially introduced into the HB101 *E.coli* strain.

Cell cultures of up to 1L in volume were prepared by inoculating the relevant volume of LB (1% w/v bactotryptone, 1% w/v NaCl, 0.5% w/v yeast extract) at 1-2% v/v with an overnight preculture (in LB). All media was autoclaved and ampicillin added to 50 μ g/ml before use. Some cultures included 0.4% w/v glucose. This was to reduce premature expression from the lac promoter. Cultures for the pEZZ18 expression vector and all overnight pre-cultures were grown at 37°C with shaking at 250 rpm. Cultures for the pASK60-strep vector were grown as close to 22°C as possible shaking at 250 rpm. Expression was induced by the addition of IPTG to 1-2 mM. Cells were harvested from the media by centrifugation at 5000g for 10 minutes. Larger volumes (10L) were prepared at SB in either LB or minimal media (M9, 6.8g Na₂HPO₄, 3.0g KH₂PO₄, 0.5g NaCl, 1.0g NH₄Cl, 1L H₂O).

TIMP-1 and Δ TIMP-1 cDNAs were ligated into the pASK60-strep vector. Transformation of TG1 and HB101 cells was carried out in pre-chilled Falcon 2059 tubes. 100 μ l of competent cells were transferred to the tubes with 1.7 μ l β -mercapto-

ethanol. The cells were incubated on ice for 10 minutes with occasional swirling. 5 μ l of the ligation mixture was added to each tube, separate vector only controls were also prepared. The transformation mixture was incubated on ice for 30 minutes then subjected to a heat shock of 42°C for 45 seconds. The tubes were cooled on ice for 2 minutes then 0.9 ml of SOC medium added (20% w/v bactotryptone, 5% w/v yeast extract, 0.5% w/v NaCl, 2.5 mM KCl, 20 mM glucose, 50 μ l 1M MgCl₂). The cells were incubated at 37°C, 225 rpm for 1 hour then centrifuged for 10 minutes at 4000 rpm. The cell pellet was resuspended in 100 μ l of the supernatant and plated out onto L-Amp plates and grown at 37°C overnight.

L-AMP plates were prepared using 15 g/L bacto-agar dissolved in LB medium. Ampicillin was added to 50 μ g/ml before pouring the plates.

Plasmid preps (mini-preps) were prepared using the QIAprep spin kit which uses the NaOH SDS-lysis method [293].

Restriction digests were prepared using 10 units of each enzyme and its buffer, 10 μ l of DNA from a mini-prep and 6 μ l of water. The restriction mix was incubated at 37°C for 2 hours. 4ml of 6x sample buffer (0.25% (w/v) bromophenol blue, 40% (w/v) sucrose) was added to each sample then run out on an 8% agarose gel containing 50 μ l/L of a 10 mg/ml solution of ethidium bromide. Gels were run overnight at 25V in TAE running buffer (40 mM Tris-acetate, 1 mM EDTA, pH 8.0)

Periplasmic extraction was carried out on ice. The cell pellet was initially resuspended in sucrose buffer (0.5M sucrose, 0.1M Tris, 1 mM EDTA, pH 8.2). The cell pellet from a 10L fermentation was resuspended in 250 ml of sucrose buffer. 4ml of lysozyme (10mg/ml) was added with 250 ml of ice cold water and the cell slurry mixed and incubated on ice for 5 minutes. 9 ml of 1M MgSO₄ was added and the material centrifuged at 10,000 rpm for 20 minutes to remove cell debris and intact cells. For smaller culture volumes of the pASK60-strep expression systems the periplasm was extracted using a Biometra kit form of this procedure which omits the MgSO₄. Cytoplasmic extracts were obtained by sonication of the cell pellet resuspended in 50

mM Tris, 100 mM NaCl followed by centrifugation for 10 minutes at 37000 rpm to pellet remaining cell debris.

Purification of TIMP-1 containing material was carried out using either the CNBr-activated Sepharose-P3G6 column (as described in chapter 3), or an IgG Sepharose column for some preparations from the pEZZ18 vector. Where material was to undergo cleavage by factor Xa after purification the CNBr-activated Sepharose-P3G6 column was washed, eluted and the eluted fractions dialysed against Xa buffer (50 mM Tris, 100 mM NaCl, 1 mM CaCl₂, pH 8.0) instead of the previously described buffers. For purification using IgG-Sepharose, material was loaded onto a 10 ml IgG-Sepharose column at 100 ml/hr. The column was washed with a 50 mM Tris, 100 mM NaCl buffer pH 8.0 containing 1 mM EDTA and 1 mM PMSF. Protein was eluted using a two step elution of acetate buffer at pH 5.0 and then at pH 3.4. Fractions were returned to neutral pH by the addition of sufficient 3M Tris. Proteinase inhibitors (aprotinin to 10µg/ml, phosphoramidon to 1 mM, PMSF to 1 mM, and EDTA to 1 mM) were added to some samples during the purification process.

Cleavage of the fusion protein domain from TIMP-1 was attempted using the proteolytic enzyme, factor Xa. Protein samples were typically at 0.5-1 mg/ml. Factor Xa was stored as a 1mg/ml solution in 50% glycerol and used at a range of working concentrations of 1:10 (enzyme:protein) to 1:200. The cleavage reaction was carried out in Xa buffer at temperatures of 4°C, room temperature and 37°C. Incubation times ranged from 3 hours to 24 hours.

Western blotting to identify bands containing an IgG binding domain were carried out as described in the general methods, omitting the initial anti-TIMP-1 antibody incubation.

N-terminal sequence analysis was carried out at the microchemical facility at the Institute of Animal Physiology and Genetics Research, Babraham, Cambridge, UK by Pat Barker.

4.3. Results.

4.3.1. Assessment of the pEZZ18 vector system for TIMP-1 and Δ TIMP-1.

DNA sequence analysis of the vectors showed that the TIMP-1 and Δ TIMP-1 cDNAs had been correctly modified and inserted into the vector. The factor Xa cleavage site was also correct.

Expression tests were carried out using approximately 100 ml of medium from the cell cultures. The media from both the TIMP-1 and Δ TIMP-1 fermentations was passed down a CNBr-activated Sepharose-P3G6 column, and bound protein eluted as described (chapter 3). For the full length TIMP-1 system, TIMP-1 was detected (by ELISA) in the original medium, and in the material eluted from the column. TIMP-1 was also detected in the periplasm. The same pattern was seen for the Δ TIMP-1. None of this material showed any inhibitory activity in a bioassay.

Large volumes of media were produced to provide sufficient material to determine the conditions for cleavage of the fusion protein using factor Xa. Initial assay of the media by ELISA could not detect either the full length or the truncated molecule. Analysis of the medium by SDS PAGE, did not identify any protein overexpression in either the full length, or truncated TIMP-1 expression systems (figure 4.3).

Purification of full length ZZ-TIMP-1 from the media using CNBr-activated Sepharose-P3G6 gave a yield of 14 mg of material from a 10L fermentation. This purified material still showed several bands on a Western blot, although one band, at a little under 45 kDa was dominant (figure 4.4).

To determine the optimum conditions for cleavage of the full length ZZ-TIMP-1 fusion protein by factor Xa. The cleavage reaction was carried out using different temperatures and enzyme concentrations. For the lower temperatures no change was seen in the bands present on SDS-PAGE (figure 4.5). At higher temperatures (37°C and room temperature with higher enzyme concentrations) all of the bands present appeared

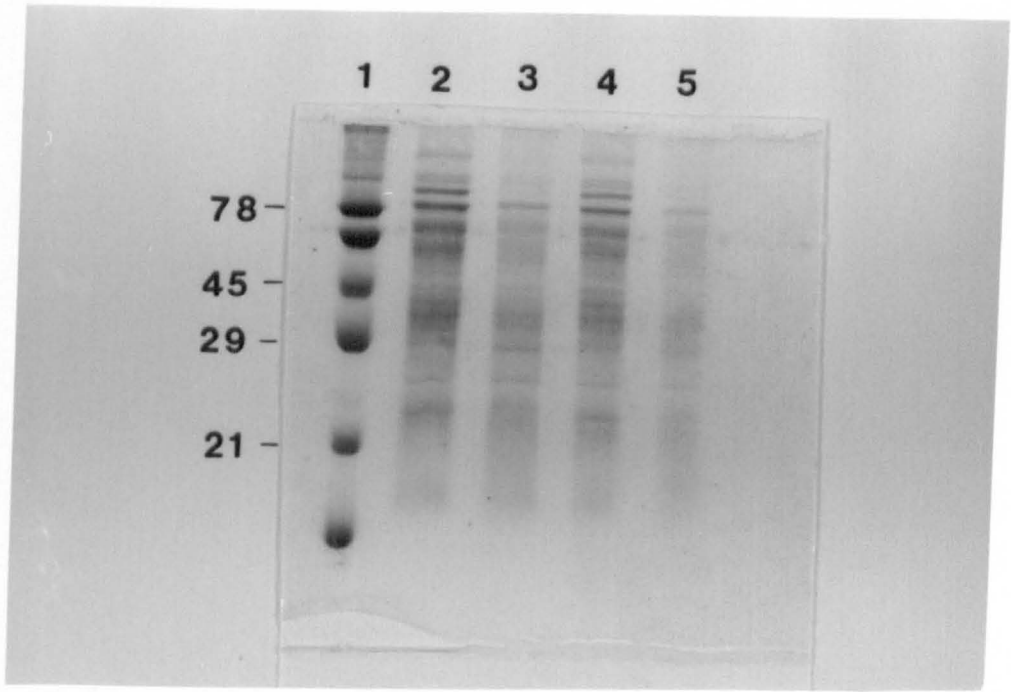


Figure 4.3. SDS-PAGE of Media From the ZZ-TIMP-1 and ZZ-ΔTIMP-1 Expression Systems.

Lane 1: Molecular weight markers. Lane 2: 15 μl ZZ-TIMP-1 media. Lane 3: 15 μl ZZ-ΔTIMP-1 media. Lane 4: 5 μl ZZ-TIMP-1 media. Lane 5: 5 μl ZZ-ΔTIMP-1 media.

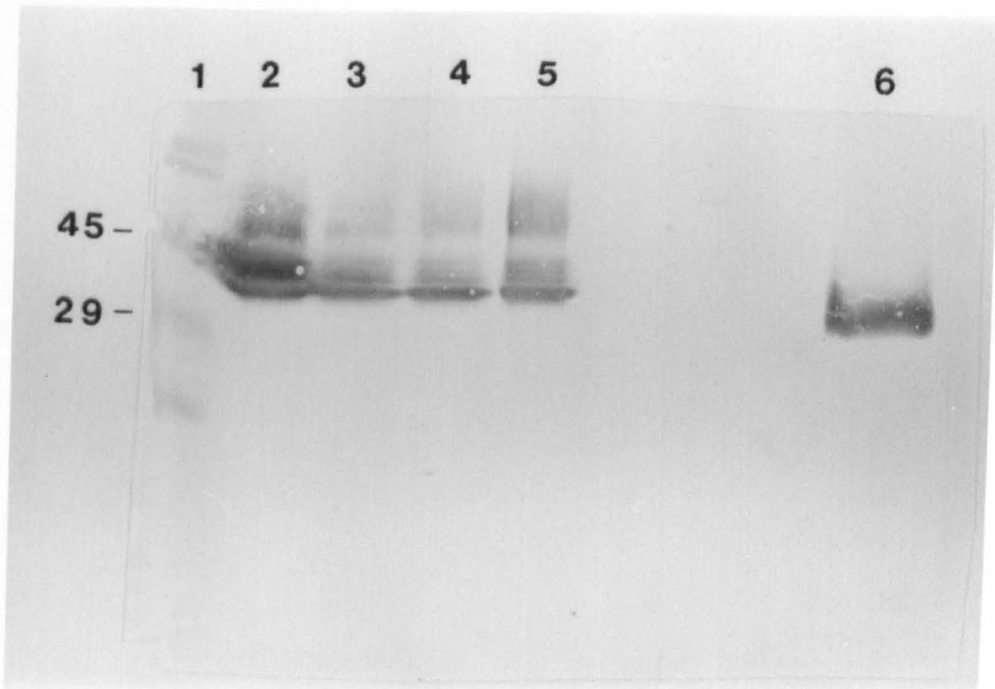


Figure 4-4. Western Blot of ZZ-TIMP-1 Purified By CNBr-activated Sepharose-P3G6 Chromatography.

Lane 1: Molecular weight markers. Lanes 2-5: Purified ZZ-TIMP-1. Lane 6: Wild type TIMP-1. The purified ZZ-TIMP-1 has a higher molecular weight than wild type TIMP-1 as would be expected.

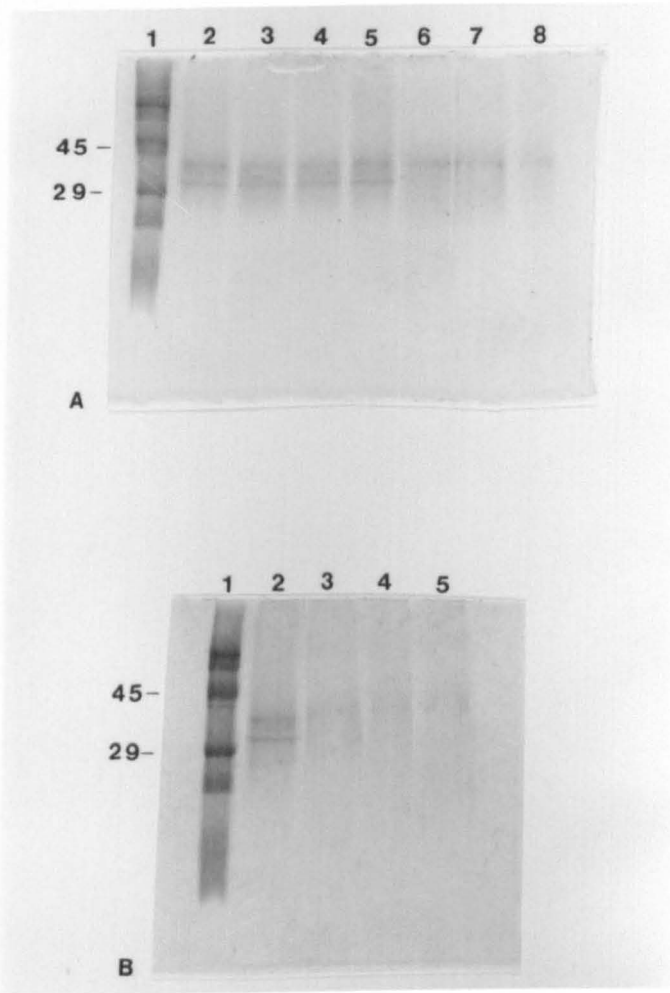


Figure 4-5. SDS-PAGE of Factor Xa Cleavage of ZZ-TIMP-1.

A. Lane 1: Molecular weight markers. Lane 2: Purified ZZ-TIMP-1. The remaining lanes contain ZZ-TIMP-1 treated with the following enzyme:protein ratios and incubation temperatures; Lane 3: 1:10, 4°C. Lane 4: 1:50, 4°C, Lane 5: 1:100, 4°C. Lane 6: 1:10, RT. Lane 7: 1:50, RT. Lane 8: 1:100, RT.

B. Lane 1: Molecular weight markers. Lane 2: Purified ZZ-TIMP-1. The remaining lanes contain ZZ-TIMP-1 treated with the following enzyme:protein ratios and incubation temperatures; Lane 3: 1:10, 37°C, Lane 4: 1:50, 37°C. Lane 5: 1:100, 37°C. The samples show signs of general proteolytic degradation at the higher temperatures.

to be degraded (figure 4.5). This degradation occurred more rapidly in material that had not been purified.

This breakdown is thought to be the result of proteinases from *E.coli* that are present in the media. Although the sample had been purified, residual contamination was sufficient to ensure total degradation of the protein.

No Δ TIMP-1 could be detected in the medium of the Δ TIMP-1 10L culture (by ELISA), or the fraction eluted from the affinity column. Analysis by SDS-PAGE showed that no intact proteins remained in the sample. It can be assumed that a short delay in processing this material resulted in complete degradation prior to assay. To prevent the breakdown of further samples, the proteinase inhibitors aprotinin and phosphoramidon were added to all subsequent preparations, other than those that were to be assayed for activity. These inhibitors were chosen because they do not inhibit factor Xa. Where a bioassay was necessary PMSF was added and allowed sufficient time to hydrolyse before any assays were performed.

The periplasm was extracted from the cell pellets (both approximately 70g in weight) harvested from the TIMP-1 and Δ TIMP-1 10 L fermentations described above. The periplasmic extract was found to contain TIMP-1/ Δ TIMP-1 (ELISA). There was some inhibitory activity found in the crude preparations, and no inhibitory activity was seen in fractions purified by CNBr-activated Sepharose-P3G6 chromatography (full length system) or purified using IgG Sepharose (Δ TIMP-1 system). A total of 1.9 mg of material was obtained from the purification of the TIMP-1 periplasm, and a yield of 11.8 mg of protein was obtained from the Δ TIMP-1 periplasm. A similar quantity of periplasm was obtained from both cell pellets.

The periplasmic preparations and column fractions from ZZ-TIMP-1 and ZZ- Δ TIMP-1 were analysed by SDS-PAGE and Western blotting. Both ZZ-TIMP-1 and ZZ- Δ TIMP-1 show many bands in the periplasmic extracts. In the ZZ-TIMP-1 sample a strong band is seen close to 45 kDa (4.6 A). No significant bands were seen in the ZZ- Δ TIMP-1 sample (Figure 4.6 C). After purification the ZZ-TIMP-1 sample shows one major band at 45 kDa and a number of

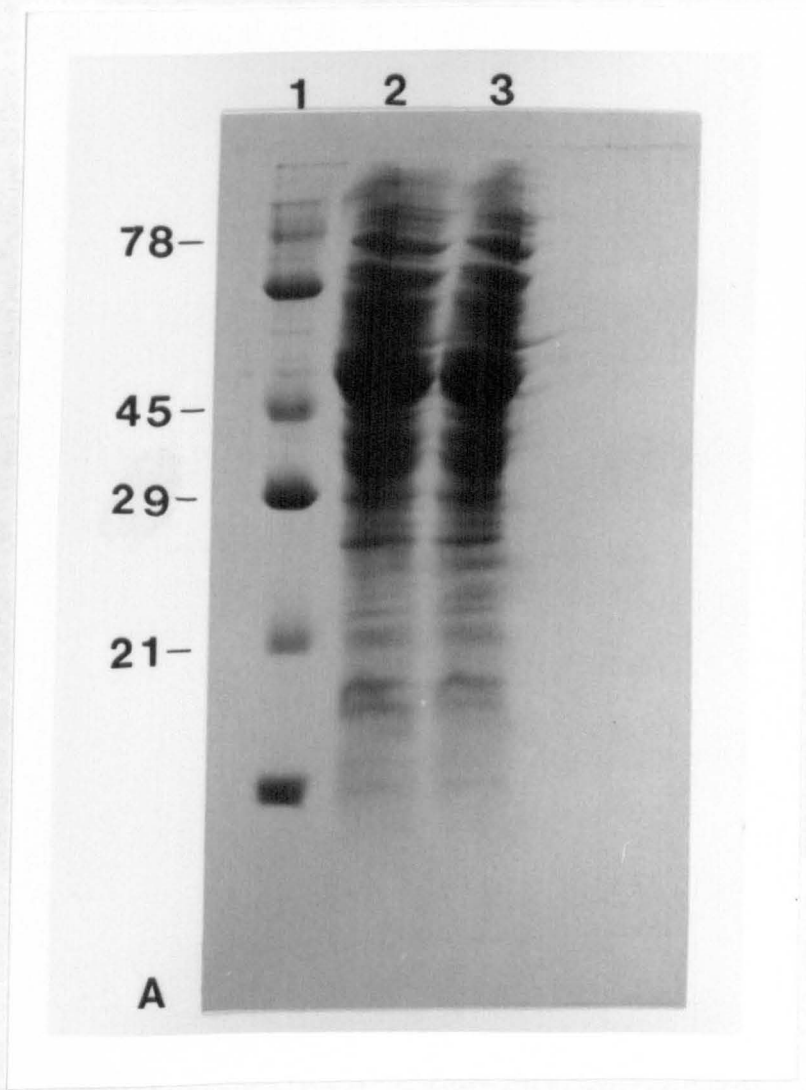


Figure 4-6. SDS-Page of Periplasmic Extracts and Purified ZZ-TIMP-1.

A. SDS-PAGE of periplasm from ZZ-TIMP-1. Lane 1: Molecular weight markers. Lane 2: Periplasm from ZZ-TIMP-1. Lane 3: Flow through from purification using CNBr-activated Sepharose-P3G6 Chromatography.

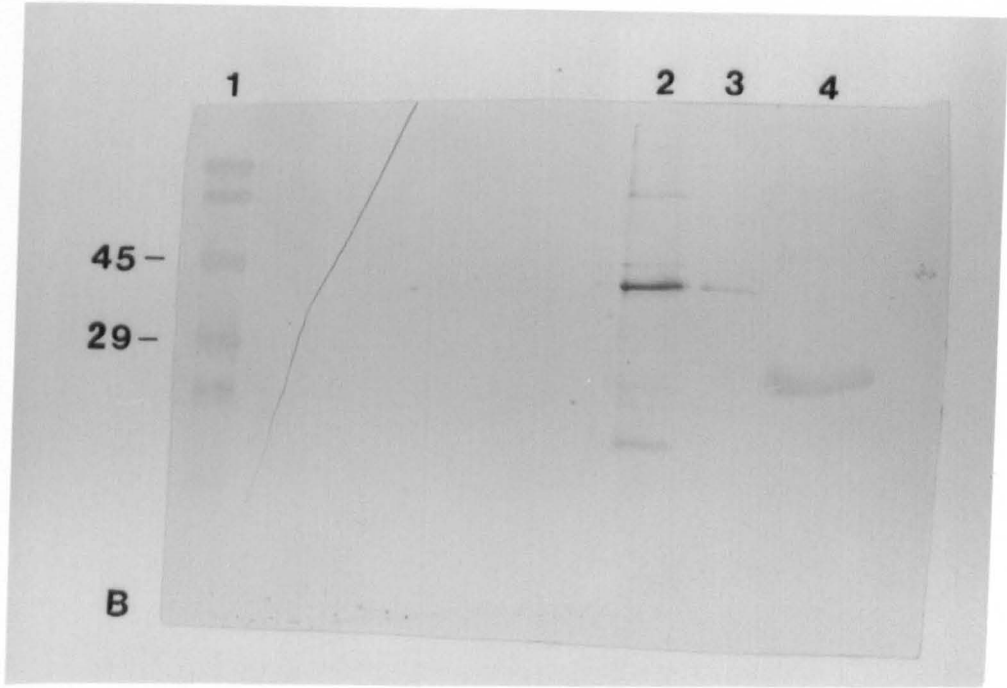
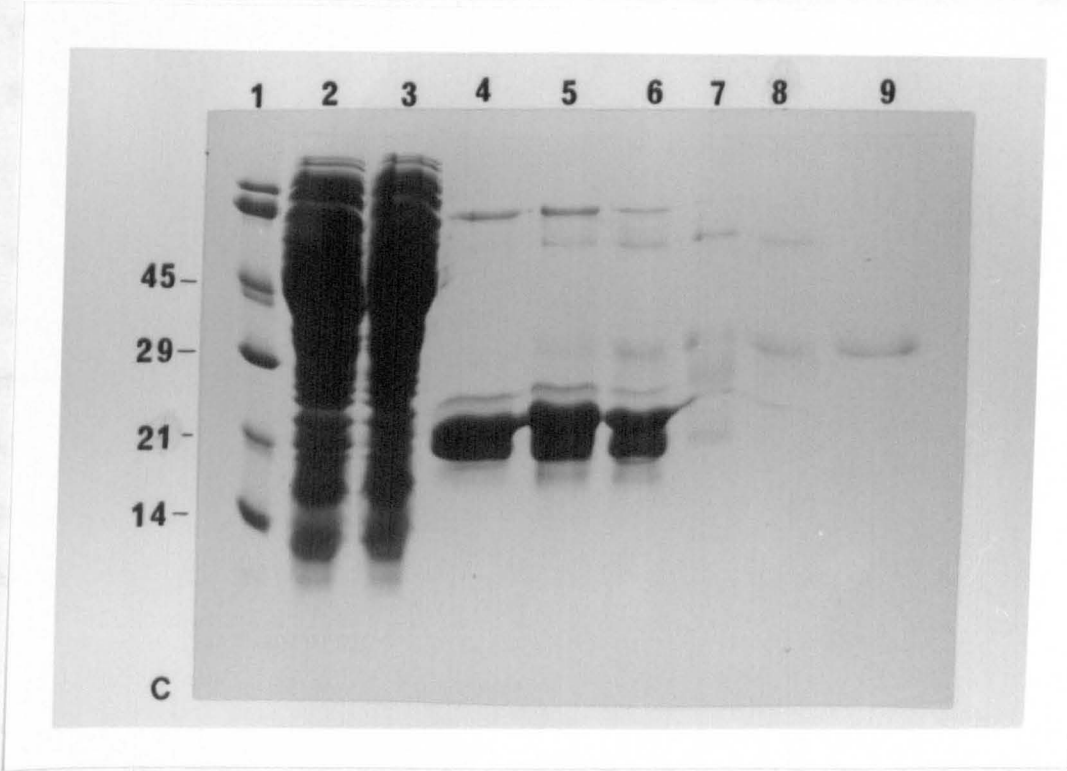


Figure 4-6. Western Blots of Periplasmic Extracts and Purified ZZ-TIMP-1.

B. Western blot (developed with 4-chloronaphthol) of purified ZZ-TIMP-1. Lane 1: Molecular weight markers. Lane 2: Concentrated pool eluted from CNBr-activated Sepharose-P3G6 column. Lane 3: Eluted pool prior to concentration. Lane 4: Wild type TIMP-1.

... (44 B). The ZZ-ΔTIMP-1 ... (44 C).

ZZ-ΔTIMP-1 was treated with factor Xa at various ... (44 D).



... (44 E) ... (44 F) ... (44 G) ... (44 H) ... (44 I) ... (44 J) ... (44 K) ... (44 L) ... (44 M) ... (44 N) ... (44 O) ... (44 P) ... (44 Q) ... (44 R) ... (44 S) ... (44 T) ... (44 U) ... (44 V) ... (44 W) ... (44 X) ... (44 Y) ... (44 Z) ... (44 AA) ... (44 AB) ... (44 AC) ... (44 AD) ... (44 AE) ... (44 AF) ... (44 AG) ... (44 AH) ... (44 AI) ... (44 AJ) ... (44 AK) ... (44 AL) ... (44 AM) ... (44 AN) ... (44 AO) ... (44 AP) ... (44 AQ) ... (44 AR) ... (44 AS) ... (44 AT) ... (44 AU) ... (44 AV) ... (44 AW) ... (44 AX) ... (44 AY) ... (44 AZ) ... (44 BA) ... (44 BB) ... (44 BC) ... (44 BD) ... (44 BE) ... (44 BF) ... (44 BG) ... (44 BH) ... (44 BI) ... (44 BJ) ... (44 BK) ... (44 BL) ... (44 BM) ... (44 BN) ... (44 BO) ... (44 BP) ... (44 BQ) ... (44 BR) ... (44 BS) ... (44 BT) ... (44 BU) ... (44 BV) ... (44 BW) ... (44 BX) ... (44 BY) ... (44 BZ) ... (44 CA) ... (44 CB) ... (44 CC) ... (44 CD) ... (44 CE) ... (44 CF) ... (44 CG) ... (44 CH) ... (44 CI) ... (44 CJ) ... (44 CK) ... (44 CL) ... (44 CM) ... (44 CN) ... (44 CO) ... (44 CP) ... (44 CQ) ... (44 CR) ... (44 CS) ... (44 CT) ... (44 CU) ... (44 CV) ... (44 CW) ... (44 CX) ... (44 CY) ... (44 CZ) ... (44 DA) ... (44 DB) ... (44 DC) ... (44 DD) ... (44 DE) ... (44 DF) ... (44 DG) ... (44 DH) ... (44 DI) ... (44 DJ) ... (44 DK) ... (44 DL) ... (44 DM) ... (44 DN) ... (44 DO) ... (44 DP) ... (44 DQ) ... (44 DR) ... (44 DS) ... (44 DT) ... (44 DU) ... (44 DV) ... (44 DW) ... (44 DX) ... (44 DY) ... (44 DZ) ... (44 EA) ... (44 EB) ... (44 EC) ... (44 ED) ... (44 EE) ... (44 EF) ... (44 EG) ... (44 EH) ... (44 EI) ... (44 EJ) ... (44 EK) ... (44 EL) ... (44 EM) ... (44 EN) ... (44 EO) ... (44 EP) ... (44 EQ) ... (44 ER) ... (44 ES) ... (44 ET) ... (44 EU) ... (44 EV) ... (44 EW) ... (44 EX) ... (44 EY) ... (44 EZ) ... (44 FA) ... (44 FB) ... (44 FC) ... (44 FD) ... (44 FE) ... (44 FF) ... (44 FG) ... (44 FH) ... (44 FI) ... (44 FJ) ... (44 FK) ... (44 FL) ... (44 FM) ... (44 FN) ... (44 FO) ... (44 FP) ... (44 FQ) ... (44 FR) ... (44 FS) ... (44 FT) ... (44 FU) ... (44 FV) ... (44 FW) ... (44 FX) ... (44 FY) ... (44 FZ) ... (44 GA) ... (44 GB) ... (44 GC) ... (44 GD) ... (44 GE) ... (44 GF) ... (44 GG) ... (44 GH) ... (44 GI) ... (44 GJ) ... (44 GK) ... (44 GL) ... (44 GM) ... (44 GN) ... (44 GO) ... (44 GP) ... (44 GQ) ... (44 GR) ... (44 GS) ... (44 GT) ... (44 GU) ... (44 GV) ... (44 GW) ... (44 GX) ... (44 GY) ... (44 GZ) ... (44 HA) ... (44 HB) ... (44 HC) ... (44 HD) ... (44 HE) ... (44 HF) ... (44 HG) ... (44 HH) ... (44 HI) ... (44 HJ) ... (44 HK) ... (44 HL) ... (44 HM) ... (44 HN) ... (44 HO) ... (44 HP) ... (44 HQ) ... (44 HR) ... (44 HS) ... (44 HT) ... (44 HU) ... (44 HV) ... (44 HW) ... (44 HX) ... (44 HY) ... (44 HZ) ... (44 IA) ... (44 IB) ... (44 IC) ... (44 ID) ... (44 IE) ... (44 IF) ... (44 IG) ... (44 IH) ... (44 II) ... (44 IJ) ... (44 IK) ... (44 IL) ... (44 IM) ... (44 IN) ... (44 IO) ... (44 IP) ... (44 IQ) ... (44 IR) ... (44 IS) ... (44 IT) ... (44 IU) ... (44 IV) ... (44 IW) ... (44 IX) ... (44 IY) ... (44 IZ) ... (44 JA) ... (44 JB) ... (44 JC) ... (44 JD) ... (44 JE) ... (44 JF) ... (44 JG) ... (44 JH) ... (44 JI) ... (44 JJ) ... (44 JK) ... (44 JL) ... (44 JM) ... (44 JN) ... (44 JO) ... (44 JP) ... (44 JQ) ... (44 JR) ... (44 JS) ... (44 JT) ... (44 JU) ... (44 JV) ... (44 JW) ... (44 JX) ... (44 JY) ... (44 JZ) ... (44 KA) ... (44 KB) ... (44 KC) ... (44 KD) ... (44 KE) ... (44 KF) ... (44 KG) ... (44 KH) ... (44 KI) ... (44 KJ) ... (44 KK) ... (44 KL) ... (44 KM) ... (44 KN) ... (44 KO) ... (44 KP) ... (44 KQ) ... (44 KR) ... (44 KS) ... (44 KT) ... (44 KU) ... (44 KV) ... (44 KW) ... (44 KX) ... (44 KY) ... (44 KZ) ... (44 LA) ... (44 LB) ... (44 LC) ... (44 LD) ... (44 LE) ... (44 LF) ... (44 LG) ... (44 LH) ... (44 LI) ... (44 LJ) ... (44 LK) ... (44 LL) ... (44 LM) ... (44 LN) ... (44 LO) ... (44 LP) ... (44 LQ) ... (44 LR) ... (44 LS) ... (44 LT) ... (44 LU) ... (44 LV) ... (44 LW) ... (44 LX) ... (44 LY) ... (44 LZ) ... (44 MA) ... (44 MB) ... (44 MC) ... (44 MD) ... (44 ME) ... (44 MF) ... (44 MG) ... (44 MH) ... (44 MI) ... (44 MJ) ... (44 MK) ... (44 ML) ... (44 MM) ... (44 MN) ... (44 MO) ... (44 MP) ... (44 MQ) ... (44 MR) ... (44 MS) ... (44 MT) ... (44 MU) ... (44 MV) ... (44 MW) ... (44 MX) ... (44 MY) ... (44 MZ) ... (44 NA) ... (44 NB) ... (44 NC) ... (44 ND) ... (44 NE) ... (44 NF) ... (44 NG) ... (44 NH) ... (44 NI) ... (44 NJ) ... (44 NK) ... (44 NL) ... (44 NM) ... (44 NN) ... (44 NO) ... (44 NP) ... (44 NQ) ... (44 NR) ... (44 NS) ... (44 NT) ... (44 NU) ... (44 NV) ... (44 NW) ... (44 NX) ... (44 NY) ... (44 NZ) ... (44 OA) ... (44 OB) ... (44 OC) ... (44 OD) ... (44 OE) ... (44 OF) ... (44 OG) ... (44 OH) ... (44 OI) ... (44 OJ) ... (44 OK) ... (44 OL) ... (44 OM) ... (44 ON) ... (44 OO) ... (44 OP) ... (44 OQ) ... (44 OR) ... (44 OS) ... (44 OT) ... (44 OU) ... (44 OV) ... (44 OW) ... (44 OX) ... (44 OY) ... (44 OZ) ... (44 PA) ... (44 PB) ... (44 PC) ... (44 PD) ... (44 PE) ... (44 PF) ... (44 PG) ... (44 PH) ... (44 PI) ... (44 PJ) ... (44 PK) ... (44 PL) ... (44 PM) ... (44 PN) ... (44 PO) ... (44 PP) ... (44 PQ) ... (44 PR) ... (44 PS) ... (44 PT) ... (44 PU) ... (44 PV) ... (44 PW) ... (44 PX) ... (44 PY) ... (44 PZ) ... (44 QA) ... (44 QB) ... (44 QC) ... (44 QD) ... (44 QE) ... (44 QF) ... (44 QG) ... (44 QH) ... (44 QI) ... (44 QJ) ... (44 QK) ... (44 QL) ... (44 QM) ... (44 QN) ... (44 QO) ... (44 QP) ... (44 QQ) ... (44 QR) ... (44 QS) ... (44 QT) ... (44 QU) ... (44 QV) ... (44 QW) ... (44 QX) ... (44 QY) ... (44 QZ) ... (44 RA) ... (44 RB) ... (44 RC) ... (44 RD) ... (44 RE) ... (44 RF) ... (44 RG) ... (44 RH) ... (44 RI) ... (44 RJ) ... (44 RK) ... (44 RL) ... (44 RM) ... (44 RN) ... (44 RO) ... (44 RP) ... (44 RQ) ... (44 RR) ... (44 RS) ... (44 RT) ... (44 RU) ... (44 RV) ... (44 RW) ... (44 RX) ... (44 RY) ... (44 RZ) ... (44 SA) ... (44 SB) ... (44 SC) ... (44 SD) ... (44 SE) ... (44 SF) ... (44 SG) ... (44 SH) ... (44 SI) ... (44 SJ) ... (44 SK) ... (44 SL) ... (44 SM) ... (44 SN) ... (44 SO) ... (44 SP) ... (44 SQ) ... (44 SR) ... (44 SS) ... (44 ST) ... (44 SU) ... (44 SV) ... (44 SW) ... (44 SX) ... (44 SY) ... (44 SZ) ... (44 TA) ... (44 TB) ... (44 TC) ... (44 TD) ... (44 TE) ... (44 TF) ... (44 TG) ... (44 TH) ... (44 TI) ... (44 TJ) ... (44 TK) ... (44 TL) ... (44 TM) ... (44 TN) ... (44 TO) ... (44 TP) ... (44 TQ) ... (44 TR) ... (44 TS) ... (44 TT) ... (44 TU) ... (44 TV) ... (44 TW) ... (44 TX) ... (44 TY) ... (44 TZ) ... (44 UA) ... (44 UB) ... (44 UC) ... (44 UD) ... (44 UE) ... (44 UF) ... (44 UG) ... (44 UH) ... (44 UI) ... (44 UJ) ... (44 UK) ... (44 UL) ... (44 UM) ... (44 UN) ... (44 UO) ... (44 UP) ... (44 UQ) ... (44 UR) ... (44 US) ... (44 UT) ... (44 UY) ... (44 UZ) ... (44 VA) ... (44 VB) ... (44 VC) ... (44 VD) ... (44 VE) ... (44 VF) ... (44 VG) ... (44 VH) ... (44 VI) ... (44 VJ) ... (44 VK) ... (44 VL) ... (44 VM) ... (44 VN) ... (44 VO) ... (44 VP) ... (44 VQ) ... (44 VR) ... (44 VS) ... (44 VT) ... (44 VU) ... (44 VV) ... (44 VW) ... (44 VX) ... (44 VY) ... (44 VZ) ... (44 WA) ... (44 WB) ... (44 WC) ... (44 WD) ... (44 WE) ... (44 WF) ... (44 WG) ... (44 WH) ... (44 WI) ... (44 WJ) ... (44 WK) ... (44 WL) ... (44 WM) ... (44 WN) ... (44 WO) ... (44 WP) ... (44 WQ) ... (44 WR) ... (44 WS) ... (44 WT) ... (44 WY) ... (44 WZ) ... (44 XA) ... (44 XB) ... (44 XC) ... (44 XD) ... (44 XE) ... (44 XF) ... (44 XG) ... (44 XH) ... (44 XI) ... (44 XJ) ... (44 XK) ... (44 XL) ... (44 XM) ... (44 XN) ... (44 XO) ... (44 XP) ... (44 XQ) ... (44 XR) ... (44 XS) ... (44 XT) ... (44 XU) ... (44 XV) ... (44 XW) ... (44 XX) ... (44 XY) ... (44 XZ) ... (44 YA) ... (44 YB) ... (44 YC) ... (44 YD) ... (44 YE) ... (44 YF) ... (44 YG) ... (44 YH) ... (44 YI) ... (44 YJ) ... (44 YK) ... (44 YL) ... (44 YM) ... (44 YN) ... (44 YO) ... (44 YP) ... (44 YQ) ... (44 YR) ... (44 YS) ... (44 YT) ... (44 YU) ... (44 YV) ... (44 YW) ... (44 YX) ... (44 YY) ... (44 YZ) ... (44 ZA) ... (44 ZB) ... (44 ZC) ... (44 ZD) ... (44 ZE) ... (44 ZF) ... (44 ZG) ... (44 ZH) ... (44 ZI) ... (44 ZJ) ... (44 ZK) ... (44 ZL) ... (44 ZM) ... (44 ZN) ... (44 ZO) ... (44 ZP) ... (44 ZQ) ... (44 ZR) ... (44 ZS) ... (44 ZT) ... (44 ZU) ... (44 ZV) ... (44 ZW) ... (44 ZX) ... (44 ZY) ... (44 ZZ)

Figure 4.6. SDS-PAGE of Periplasmic Extracts and Purified ZZ-ΔTIMP-1.
C. SDS-PAGE of periplasm and samples from the IgG-Sepharose purification of ZZ-ΔTIMP-1. Lane 1: Molecular weight markers. Lane 2: Periplasm from ZZ-ΔTIMP-1. Lane 3: Flow through pool from IgG-Sepharose column. Lanes 4 to 8: Fractions eluted from IgG-Sepharose column. Lane 9: Wild type TIMP-1.

weaker bands (4·6 B). The ZZ- Δ TIMP-1 sample has a strong doublet at approximately 21 kDa and some weak contaminant bands (4·6 C).

ZZ-TIMP-1 was treated with factor Xa at enzyme:protein ratios of 1:10 to 1:200 at 4°C, room temperature and 37°C, for up to 6 hours. No change was detected in any sample until after 3 hours (figure 4·7), when the band at 45 kDa could no longer be seen on a Western blot for any of the different temperatures or enzyme concentrations. This was not accompanied by the appearance of any additional bands.

ZZ- Δ TIMP-1 was treated with factor Xa at a ratio of 1:200 for 3 hours at room temperature and re-purified on IgG Sepharose. The flow through pool contained 3·53 mg of protein and the eluted pool contained 4·6 mg of protein. Analysis of the Δ TIMP-1 material by SDS PAGE and Western blotting shows a strong band at approximately 21 kDa that decreases in size after treatment with factor Xa (figure 4·8). However, after the second pass down IgG-Sepharose, both the original, and new bands are found in the eluted fraction. On assay, none of this material was found to have inhibitory activity.

Further 10L fermentations in LB, and minimal media were prepared for the ZZ-TIMP-1 system. Purification of this material by CNBr-activated Sepharose-P3G6 chromatography gave a yield of 18·5 mg protein for the LB culture and 12·8 mg from the cells in minimal media. A Western blot of the purified material is shown in figure 4·9. None of this material showed any inhibitory activity.

The cleavage reaction of the ZZ-TIMP-1 with factor Xa was carried out using enzyme:protein ratios of 1:50, 1:100 and 1:200 at room temperature and 37°C for a minimum of 3 hours for the preparations from minimal media and LB. Analysis by Western blotting (figure 4·9) and bioassay showed that there had not been a decrease in the molecular weight of any band on the gel, nor was any inhibitory activity generated.

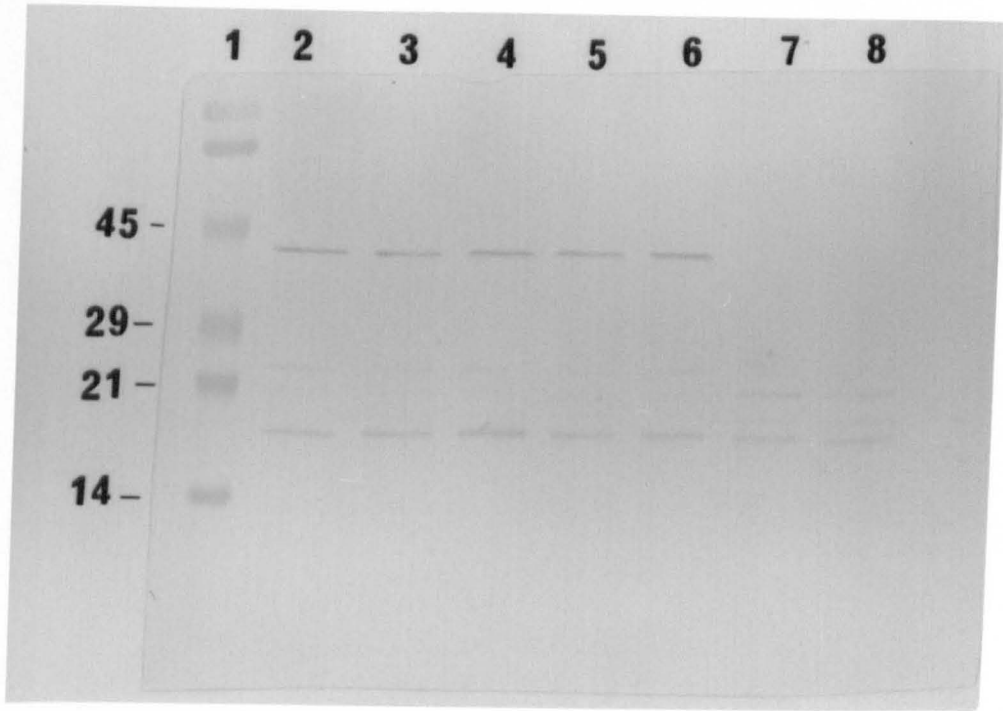


Figure 4-7. SDS-PAGE of Factor Xa Cleavage of ZZ-TIMP-1 (containing proteinase inhibitors).

Lane 1: Molecular weight markers. Lane 2: Purified ZZ-TIMP-1. The remaining lanes contain ZZ-TIMP-1 treated with the following enzyme:protein ratios incubation temperatures and incubation times; Lane 3: 1:10, RT, 1 hr. Lane 4: 1:50, RT, 1 hr. Lane 5: 1:100, RT, 1 hr. Lane 6: 1:200, RT, 1 hr. Lane 7: 1:10, RT, 3 hrs. Lane 8: 1:50, RT, 3hrs. Although the band at 45 kDa is absent in the longer incubations, no additional band is seen to indicate the release of the ZZ domains or the TIMP-1.

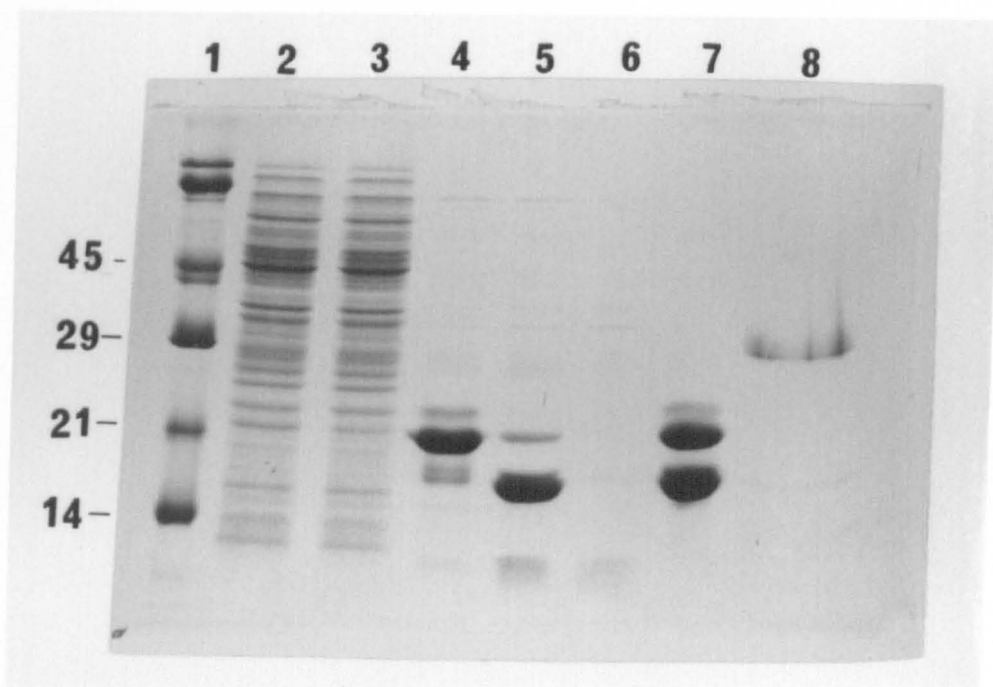


Figure 4-8. SDS-PAGE of ZZ- Δ TIMP-1 Periplasm, Purification and Factor Xa Cleavage.

Lane 1: Molecular weight markers. Lane 2: Periplasmic extract from ZZ- Δ TIMP-1. Lane 3: Flow through pool after IgG-Sepharose. Lane 4: Eluted pool from IgG-Sepharose. Lane 5: IgG pool treated with factor Xa (1:200) at RT for 3 hrs. Lane 6: Flow through from IgG-Sepharose column run of Xa treated ZZ- Δ TIMP-1. Lane 7: Eluted pool from second IgG-Sepharose column. Lane 8: Wild type TIMP-1.

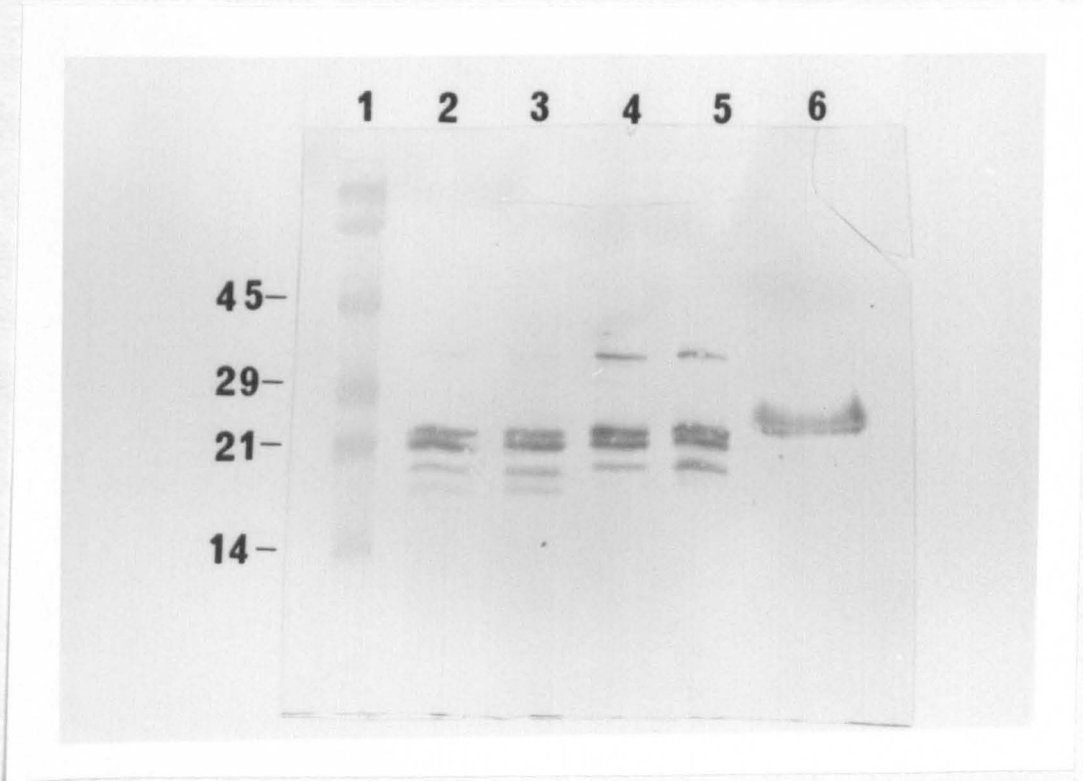


Figure 4-9. Western Blot (4-chloronaphthol stained) of ZZ-TIMP-1 purified from 10 L of LB, and minimal media and treated with factor Xa.

Lane 1: Molecular weight markers. Lane 2: ZZ-TIMP-1 from LB. Lane 3: ZZ-TIMP-1 from LB treated with factor Xa (1:200), RT, 3hrs. Lane 4: ZZ-TIMP-1 from minimal media. Lane 5: ZZ-TIMP-1 from minimal media treated with factor Xa (1:200), RT, 3hrs. Lane 6: Wild type TIMP-1.

The cleavage reaction was also carried out in the presence of 0.5 M urea, again to no effect. Treatment of the sample with thrombin also did not affect the molecular weight or activity observed.

Western blots of the culture media and periplasm extracted from both TIMP-1 and Δ TIMP-1 cultures, were prepared using only the second (HRP-linked anti-IgG) antibody. These blots showed the same pattern of bands as those prepared including the specific, anti-TIMP-1 first antibody (data not shown). This suggests that several different gene or processing products were present in the media, and that all of these products contain IgG binding domains. This was also seen for the Δ TIMP-1 sample that had shown an altered pattern of bands after treatment with factor Xa. This would imply that any cleavage that occurred was not generating free Δ TIMP-1.

4.3.2. Assessment of the pASK60-strep Vector System for TIMP-1 and Δ TIMP-1.

Several clones (15-20 of each) were tested for both the full length and the truncated TIMP-1 protein. Cultures of 10 ml were used for screening clones and larger cultures (up to 1L) were used for assessment of yield and N-terminal sequencing.

During initial expression tests of the full length pASK60-TIMP-1 vector in HB101 cells it was found that the cells grew very slowly at 22°C. Cultures inoculated at 2% required up to 10 hours to reach an A_{550} of 0.5 (suitable for induction by IPTG). Growth after induction was also very slow, normally requiring an overnight growth to reach a final A_{550} of between 1.0 and 2.0. Subsequently the vector+insert was transferred to competent TG1 cells where the induction point was reached in 2-4 hours and cells could be harvested after a further 6 hours.

Restriction digests of ^{plasmids from} cells transformed with the ligated vector identified 11 clones containing restriction products of the expected sizes. Analysis of periplasmic extracts of 10 ml cultures identified 5 clones that showed strong bands of approximately 21 kDa on a Western blot (figure 4.10). The two strongest of these were chosen for

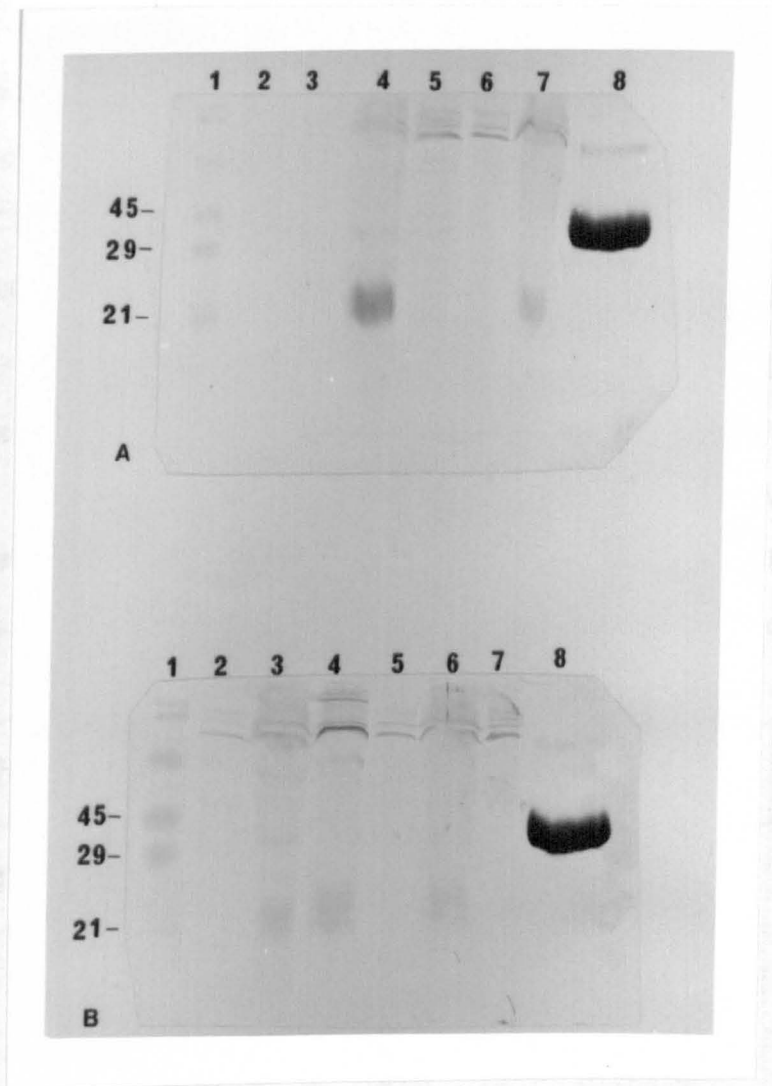


Figure 4-10. Western Blot (stained using alkaline phosphatase system) to Screen for TIMP-1 producing pASK60 clones.

A. Lane 1: Molecular weight markers. Lane 2: Clone 1. Lane 3: Clone 2. Lane 4: Clone 5. Lane 5: Clone 6. Lane 6: Clone 7. Lane 7: Clone 8. Lane 8: Wild type TIMP-1.

B. Lane 1: molecular weight markers. Lane 2: Clone 9. Lane 3: Clone 10. Lane 4: Clone 11. lane 5: Clone 12. Lane 6: Clone 13. Lane 7: Periplasm from cells containing the vector alone. Lane 8: Wild type TIMP-1.

further assessment of yields, activity and N-terminal sequence (clones numbered 5 and 8).

The medium, periplasmic extract and cytoplasmic extract from 50 ml cultures of both clones were assayed for the presence of TIMP-1 (by ELISA). TIMP-1 was found in both the periplasm and the cytoplasm but not in the medium. The periplasmic and cellular extracts were compared on Western blots against de-glycosylated wild type TIMP-1 (see chapter 6). The band at approximately 21 kDa ran alongside the de-glycosylated material indicating that the gene product was of a similar weight to that expected (figure 4.11).

Large cultures (1L) were produced to obtain sufficient material for N-terminal sequence analysis and assessment of yields. Parallel Western, and PVDF blots were prepared for clone 8 to identify clearly the band of interest on the PVDF membrane which was very faint. Clone 5 was not sequenced because the correct band could not easily be picked out on a blot. Sequence analysis of clone 8 did not produce a clear result (table 4.1).

Sequence Position	1	2	3	4	5	6
Sequencing Result	Ala	Asp	Gly	Asp	Glu	Arg
		Glu	Ile	Glu	Pro	Pro
		Thr	Gln		Thr	Gly
Possible Identity	X	Thr	X	X	Pro	Pro

Table 4.1. N-terminal sequence analysis of clone 8. Multiple options for each sequence position may be due to the presence of contaminating proteins of a similar molecular weight. Alternatively, weak signals from small quantities of protein for analysis can make distinguishing different residues difficult (cysteine does not appear as a possible residue identity because it cannot be detected by the sequencing methodology). Residues that agree with the expected sequence are shown on the last line of the table.

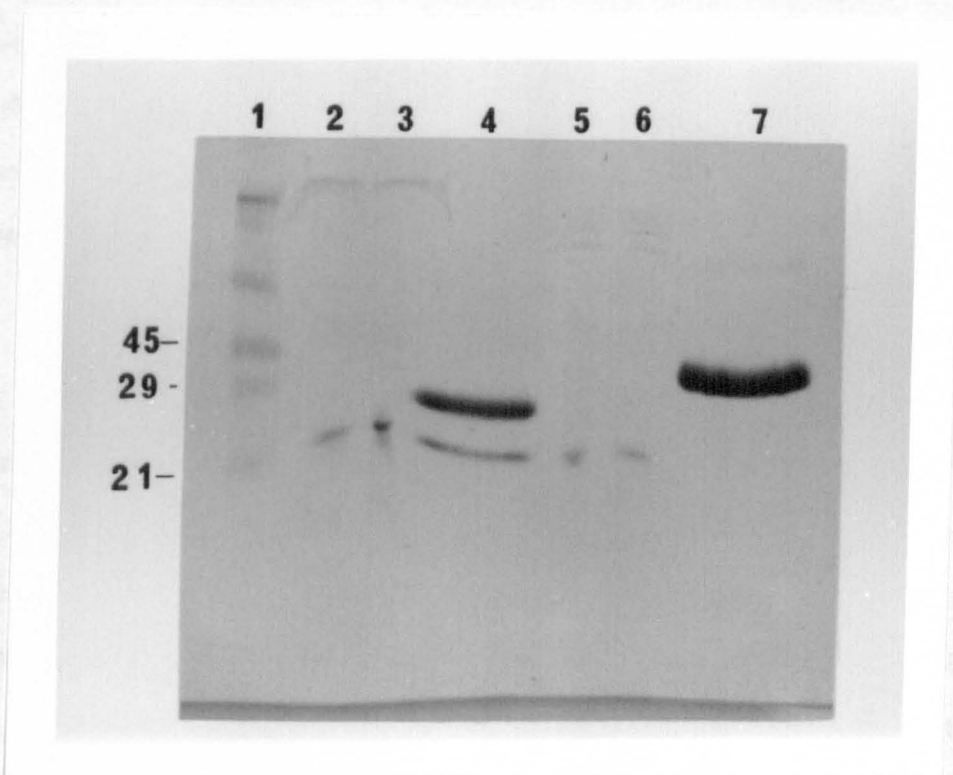


Figure 4-11. Western Blot (stained using alkaline phosphatase system) showing the comparison between the molecular weight of clones 5 and 8, and deglycosylated wild type TIMP-1.

Lane 1: Molecular weight markers. Lane 2: Periplasm from clone 5. Lane 3: Periplasm from clone 8. Lane 4: Deglycosylated TIMP-1. Lane 5: Cellular extract from clone 5. Lane 6: Cellular extract from clone 8. Lane 7: Wild type TIMP-1.

Of the different sequence options presented, threonine was indicated at position 2 and proline at position 5 and 6. This could indicate that the N-terminal sequence is cleaved correctly, but the sample used for sequencing probably contained other contaminating proteins, making the result more complex.

Low inhibitory activity was detected in both the periplasm, and cell extracts from clones 5 and 8. For a 50 ml culture with a final A_{550} of 2.0 a total of 1.5 ml of periplasm was extracted. The periplasm from clone 5 had an activity of 0.5 units/ml, and the cell extract, 1.44 units/ml. Clone 8 had 0.55 units/ml in the periplasmic extract and 1.13 units/ml.

The periplasmic material from 1L preparations of clones 5 and 8 were passed down a 10 ml CNBr-activated Sepharose-P3G6 column and eluted as described in chapter 3. Analysis of the column fractions by ELISA showed that some of the TIMP-1 came off in the flow through, whilst some bound to the matrix and could be released in the elution step. Clone 5 gave a yield of 780 ng/L from the purified periplasm and 2 μ g/L from the cytoplasm (not purified). Clone 8 gave 43 μ g/L from the purified periplasm and 0.3 μ g/L from the cytoplasmic extract (not purified). This gives the overall yields (extrapolated to 1litre) shown in table 4.2.

Truncated TIMP-1 was cloned into the pASK60 vector and introduced into HB101 cells. Restriction analysis of a selection of clones identified eleven that showed the correct plasmid and insertion profile. 10 ml cultures were prepared of each of these and the periplasm analysed by Western blotting. This identified five clones that appeared to produce an excess of protein of approximately 14 kDa Mw. One, (Δ 2a) appeared to be producing a large quantity of protein (figure 4.12). A 100 ml culture was prepared and the periplasm used for blotting onto PVDF for protein sequencing. The N-terminal sequence analysis is shown in table 4.3.

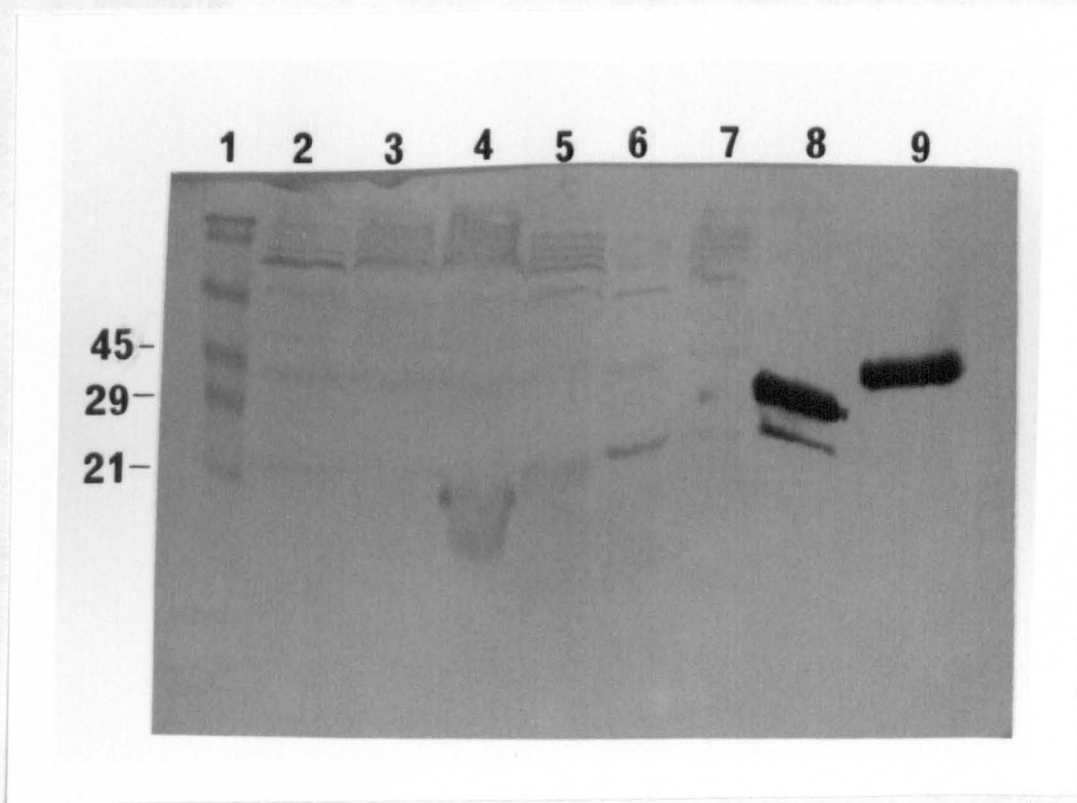


Figure 4-12. Western Blot (stained using alkaline phosphatase system) to Screen for Δ TIMP-1 producing pASK60 clones.

Lane 1: Molecular weight markers. Lane 2: Clone Δ 10. Lane 3: Clone Δ 11. Lane 4: Clone Δ 2a. Lane 5: Clone Δ 3a. Lane 6: Clone Δ 6a. Lane 7: Clone Δ 9a. Lane 8: Deglycosylated TIMP-1. Lane 9: Wild type TIMP-1.

Sample	Inhibitory activity units/litre	Protein Yield mg/litre	Specific activity units/mg
clone 5 periplasm	15	0.00078	19230
clone 5 cytoplasm	43.2	0.002	21600
clone 8 periplasm	16.5	0.043	384
clone 8 cytoplasm	33.9	0.0003	113000

Table 4.2. Analysis of specific activities of protein extracted from clones 5 and 8.

The material from clone 5 has a specific activity close to what would be expected from conventional purifications. The periplasm from clone 8 has a low specific activity, which might be attributable to a low purity. The activity of the cytoplasm of clone 8 is unusually high, and may be due to other factors than the presence of TIMP-1.

Sequence position	1	2	3	4	5	6
Sequencing Result	Ile	Thr	Gln	Gly	Pro	Pro
		Glu	Val	Val		
Possible identity	X	Thr	X	Val	Pro	Pro

Table 4.3. N-terminal sequence analysis of clone $\Delta 2a$. The sequencing results are shown with residues that agree with the expected TIMP-1 sequence shown on the bottom line (cysteine does not appear in the result since it cannot be detected by the sequencing methodology). The sequence is almost certainly that of TIMP-1, showing that the *ompA* peptide was cleaved correctly.

4.4. Discussion.

The initial attempt to produce an expression system for TIMP-1 and Δ TIMP-1 was not successful. Sequence analysis of the vector inserts showed that the cDNA, fusion protein and engineered factor Xa cleavage site were all correct. Western blotting found that several proteins were being produced that could be detected by a polyclonal anti-TIMP-1 antibody. The crude media and to a lesser extent the partially purified material was sensitive to *E.coli* proteinases. This was avoided by the addition of inhibitors, carefully chosen to avoid inhibiting the factor Xa.

The purification methods used did increase the homogeneity of the samples. Interestingly a greater yield was obtained for the Δ TIMP-1, purified on IgG Sepharose than was obtained for TIMP-1 purified by CNBr-activated Sepharose-P3G6 (see chapter 3). The difference in yield between these two samples may be due to a simple difference in the levels of expression in each vector. Alternatively the IgG binding domains might reduce the affinity of the recombinant TIMP-1 for the CNBr-activated Sepharose-P3G6, IgG Sepharose was binding other proteins or the antibody was being removed from the matrix in the elution process.

Some slight inhibitory activity was seen in cytoplasmic material from all of the cultures studied, but was absent from the affinity purified material. Since the inhibitory activity is lost after affinity purification of TIMP-1, or Δ TIMP-1 from the cytoplasmic extracts it is unlikely to be due to the action of active TIMP-1 or Δ TIMP-1. This activity was also seen in preparations of cytoplasm from cells containing the vector only, and so could be due to the action of *E.coli* proteinases degrading the collagenase used in the assay.

The increased purity of the material could be detected by SDS PAGE and Western blots, but on no occasion was a single clear band produced. However bands of the expected molecular weight were seen for both the ZZ-TIMP-1 (~45 kDa) and ZZ- Δ TIMP-1 (~30 kDa) suggesting that the desired fusion product was being expressed.

The presence of the IgG binding domains made accurate assessments of the presence of TIMP-1/ Δ TIMP-1 particularly difficult. ELISA assays were not reproducible and it is possible that false positives or negatives would be found as a result of interference by the fusion protein.

Attempts to remove the fusion protein using factor Xa were not successful. No inhibitory activity was generated in treated samples and in only one preparation was any change in molecular weight observed where the band assumed to be the correct fusion product for the Δ TIMP-1 system, decreased in size by close to the expected amount (14 kDa). By using the second antibody alone as a control for IgG binding domains in a Western blot, no band was identified that could correspond to free Δ TIMP-1. Urea was used in an attempt to unfold the protein sufficiently, to allow access to the cleavage site. Thrombin, which does not cleave TIMP-1, was also used to try and partially degrade the fusion protein to increase access to the Xa site. Neither strategy appeared to aid the successful release of the fusion protein from TIMP-1. At no point was inhibitory activity seen for any of the samples of media or periplasm.

This vector system is not suitable for the production of TIMP-1 or Δ TIMP-1. Although the overall protein yields are not acceptable, under fermentation conditions, with further work, the growth conditions could have been optimised to improve the yield. The greatest difficulty lay with cleaving the fusion protein. It is possible that the N-terminus of TIMP-1 is sufficiently buried to prevent access by the factor Xa. The structure of the N-terminal fragment of TIMP-2 published recently [141] suggests that the N-terminus is at least partially buried and the same may be true for TIMP-1. Another possibility is that the presence of the fusion protein prevents the correct folding of TIMP-1 and Δ TIMP-1 molecules. In particular Cys-1, and the formation of its correct disulphide bond with Cys-99 could be affected by the presence of N-terminal protein. If the cleavage did occur correctly as it may have done for the Δ TIMP-1 sample, the resulting protein may have still been incorrectly folded, hence the lack of activity.

For the second expression system tried, the factor Xa cleavage site was not included. For both the full length and the truncated TIMP-1 there were a greater number of clones available for assessment than for the pEZZ18 system. The two most promising clones for the full length TIMP-1 were assessed in detail.

The material produced could be recognised on a Western blot, appeared to be the correct molecular weight (21 kDa), and was recognised in a TIMP-1 ELISA. Low levels of inhibitory activity were detected in both the periplasm and the cytoplasm. Interestingly, more inhibition was seen in the cytoplasm than in the periplasm, in particular for clone 8. Although TIMP-1 was detected in the cytoplasm (by ELISA) it would not be expected to be folded, or active under the reducing conditions present. The activity detected was most probably due to the proteinase activity described in the pEZZ18 vector tests.

The protein produced appears to be non-glycosylated recombinant TIMP-1. The product from clone 8 is the correct molecular weight (~21 kDa). Although the N-terminal sequence could not be clearly defined due to the presence of contaminating bands on the PVDF blot, it contains elements that indicate it may be correct (in particular Pro-5 and Pro-6). The protein binds to a CNBr-activated Sepharose-P3G6 column, is detected by a specific TIMP-1 ELISA and shows inhibitory activity against collagenase. From these results it can be said that TIMP-1 has been expressed successfully in the periplasm of *E.coli*. However the yields obtained were very low. Were the cells to be grown under fermentation conditions a higher yield would be expected. For this expression system to be viable for the production of large quantities of TIMP-1 for structural studies, a yield in the order of 20 mg /L would be an acceptable minimum. To reach this level of expression an increase in yield of 500-1000 fold is required. This would be exceptionally difficult to achieve.

Truncated TIMP-1 was also produced in the same system. Again, a gene product of the expected molecular weight and with the correct N-terminal sequence was

produced. However, as for the full length molecule the protein yield was exceptionally low. Although not assayed (an ELISA using monoclonal antibodies to the full length protein will not necessarily be reliable for a truncated protein) the appearance of the bands on SDS PAGE and Western blots indicated a similar yield to that obtained for the full length molecule.

This yield is similar to that obtained by Cocuzzi et al [285] using a similar method of refolding the protein from inclusion bodies as that described by Kohno et al [287] (indicating that the overall yield obtained by both groups was probably low). The most successful method published to date also uses a cytoplasmic expression system and a different refolding process [286]. The yields quoted are up to 10 mg/L which is an encouraging sign that it should be possible to produce large enough amounts of TIMP-1 using relatively low volumes of media.

4.4.1. Alternative strategies

Obviously it is necessary to try an alternative approach to the production of large quantities of whole or truncated TIMP-1 in *E.coli*. Although periplasmic expression did result in the expression of the correct protein, none of the available vectors have the strong promoters and subsequent high levels of expression that are seen for conventional cytoplasmic expression systems. Since the most successful approaches have used cytoplasmic expression followed by denaturation/renaturation, it is probable that a similar method will be the most productive. By varying the refolding conditions, and including different agents to aid the correct formation of disulphide bonds, it should be possible to obtain acceptable yields from a cytoplasmic expression of TIMP-1.

Chapter 5.

Secondary Structure and Thermostability of TIMP-1.

5.1. Introduction.

The secondary structure content of a protein is a measure of the relative quantities of sheet, helix, turn and coil that are present. This information provides a useful indication of the structure that could be expected from more detailed studies. For TIMP-1 in particular the secondary structure content gives an idea of how difficult assigning the structure by NMR might be. A protein with a high alpha helical content tends to be more difficult to analyse because the signals arising from alpha protons are less dispersed. In beta sheet structures the chemical shifts of these protons are often further downfield, away from resonances of β -, and other protons. This increases the dispersion in a potentially very crowded region of the spectrum.

Spectroscopic techniques such as Fourier transform Infra-red spectroscopy (FTIR) and Circular dichroism spectroscopy (CD) can be used to study the secondary structure of proteins. The recorded spectra from a sample can be compared to spectra from control samples with a known secondary structure content. From this a reliable approximation of the secondary structure can be made.

These techniques are particularly sensitive to changes in the secondary structure of a protein, allowing analysis of the changes that occur during temperature variations or under different concentrations of denaturants such as guanadinium chloride and urea. Subsequently they can be used to study folding pathways and thermally induced structural changes. Studying the thermal stability of a sample under these conditions gives a useful indicator of how the protein will behave under the more demanding

conditions required for NMR (higher temperatures, higher concentrations, low pH and long experiments). In particular, for studies by FTIR, the protein concentration required is similar to that for NMR, although the sample volume is much smaller. Consequently an unstable protein can be identified before large quantities of precious material are committed.

There are now large numbers of algorithms that attempt to predict the secondary structure of proteins using a range of methods. Some use the probability of a residue being in any particular secondary structural feature based on analysis of a database of known structures [294]. Another uses the context of an individual residue to characterise its most probable environment [295]. The most recent advance in structure prediction has been the development of neural networks that claim to have a much greater accuracy than other methods. As we learn more about the structures of proteins and the way in which sequence influences structure it is possible such programs will become more accurate.

This chapter discusses the secondary structure content of TIMP-1 and compares the results to those obtained using structure prediction programs. The thermal stability of TIMP-1 and the effects of temperature on its secondary structure are also discussed.

5.2. Methods.

5.2.1. Materials.

Wild type TIMP-1 was purified as described in chapter 3. Infra-red spectra were recorded on a Perkin-Elmer 1760X FTIR spectrometer. The sample cell was a Specac 20500 cell fitted with a CaF₂ window and a 50 μm Teflon spacer for experiments in D₂O, and a 6 μm tin spacer for H₂O experiments. D₂O was 99.9 atom %D from Aldrich Chemical Company. CD spectra were recorded on a Jasco J-600 spectropolarimeter.

5.2.2. Experimental Details.

The differential binding of TIMP-1 to Concanavalin A (see chapter 3) implies that there is more than one glycosylation pattern. One or more of these forms is unable to bind strongly to the Concanavalin A lectin. This may be due either to composition or structure. To increase the homogeneity of samples used for spectroscopy the Concanavalin A binding form(s) of wild type TIMP-1 was used for this study.

Fourier-Transform Infra-Red (FTIR) Spectroscopy.

Samples were prepared in 100 mM KH₂PO₄ buffer (pH 7.0), using either H₂O or D₂O at 9.8 mg/ml and 7.5 mg/ml respectively. Sample temperature was maintained at 20 °C \pm 0.1 °C using a cell jacket of circulating water. The spectrometer was continuously purged with dry air to eliminate water vapour. A sample shuttle was used to allow the background spectrum to be signal-averaged over the same time period as the sample spectrum. In all cases, 256 scans were co-added, apodised with a Norton-Beer function and Fourier transformed to give a resolution of 2 cm⁻¹.

Spectra of the appropriate buffers were recorded in the same cell and under the same instrument conditions as the sample spectra. Difference spectra were generated by an interactive difference routine to subtract the appropriate solvent spectrum from the spectrum of each protein solution. Proper subtraction of water should yield an

approximately flat baseline from 1900 to 1720 cm^{-1} , avoiding negative side lobes and the removal of the water band near 2130 cm^{-1} . When required, an infrared spectrum of water vapour was also interactively subtracted from the difference spectra. Subtraction of D_2O was adjusted to optimise the removal of the D-O-D bending absorption near 1220 cm^{-1} . Second derivative spectra were generated from the difference spectra using the Perkin-Elmer DERIV routine. 13 or 19-data point (13 cm^{-1} or 19 cm^{-1}) windows were selected.

For the thermal denaturation study, the temperature was raised in 10°C increments, allowing approximately 15 minutes for equilibration before recording the spectra. Secondary structure calculation was carried out using the Perkin-Elmer CIRCOM program, which is based on factor analysis of a data set of the spectra of known structures [296].

Circular Dichroism (CD) Spectroscopy.

Solutions of TIMP-1 of known concentration, in the range 0.3 - 0.5 mg/ml, were prepared in 100 mM KH_2PO_4 buffer (pH 7.0) in H_2O . CD spectra of the solutions were recorded in both the near-UV (340-240 nm) and the far-UV (260-180 nm) regions using cylindrical cells of pathlengths 1.0 cm and 0.02 cm respectively. A temperature of 20°C was maintained for the secondary structure determination using a circulating water bath. For the thermal denaturation study, the temperature was raised in 10°C increments, with an equilibration time of approximately 15 minutes, before recording spectra. Solvent baselines were recorded at 20°C using the same cells. These were subtracted from the spectra, which were then converted to ϵ based on the molar concentration of residues (mean residue weight of TIMP-1 = 155). Secondary structure content was calculated using the method of Provencher and Glöckner by analysis of the far-UV CD spectra using the CONTIN program (version 2DP) [297].

NMR results

All experiments and subsequent processing were performed on a Bruker AMX 500 spectrometer running standard Bruker UXNMR software. Samples were prepared at 40 mg/ml, equivalent to 1.4 mM, in 500 μ l of D₂O. The sample is self-buffering at pH 4.2. All spectra were acquired at a probe temperature of 32 °C. For the 1D spectrum, 1024 FIDs were acquired into 16 K data blocks with a 60 degree excitation pulse of 6 μ s, a spectral width of 7042 Hz, an acquisition time of 1.16 s and a relaxation delay of 1.5 s. The phase-sensitive, double-quantum-filtered (DQF) COSY spectrum [298, 299, 300, 301] was acquired by accumulating 512 FIDs into 2 K data blocks using the same spectral width as for the 1D accumulations. 2D data were zero-filled once in F1 and Fourier transformed with the application of a $\pi/3$ shifted sine bell function in both dimensions. In all experiments the solvent peak was suppressed using a low power pre-irradiation pulse of 1.5 s, corresponding to the relaxation delay.

Secondary Structure Prediction.

The secondary structure content of TIMP-1 was predicted using Protein Predict [302], SOPM [303] and nnpredict [304] programs via the MSU mail server facility [305]. The Robson-Garnier and Chou-Fasman structure predictions used the peptide structure program (part of the GCG package, Genetics Computer Group, University of Wisconsin).

5.3. Results.

5.3.1. Secondary Structure Determination

Fourier-Transform Infra-Red (FTIR) Spectroscopy.

Difference and second derivative FTIR spectra of both the H₂O and the D₂O samples are shown as figures 5·1, 5·2, 5·3 and 5·4. The difference spectrum of TIMP-1 in H₂O (figure 5·1) shows the amide I band at 1643 cm⁻¹ and the amide II band at 1550 cm⁻¹. The amide I band is assigned principally to C=O stretching and the amide II band principally to N-H bending of the peptide bonds. When dissolved in D₂O buffer, the amide II band shifts to lower wavenumbers as a result of isotopic exchange of N-H to N-D. This exchange was complete after 48 hours to give bands at 1637 cm⁻¹ and 1456 cm⁻¹ respectively (figure 5·2). In all cases, the amide bands are broad and composed of several overlapping components; these are revealed in the second-derivative spectra. In H₂O (Figure 5·3), the major components in the amide I region are assigned to β -sheet at 1637 cm⁻¹, α -helix and/or turns at 1659 cm⁻¹ and anti-parallel β -sheet and, or turns at 1684 cm⁻¹.

In D₂O (Figure 5·4), the major amide I components are assigned to β -sheet at 1638 cm⁻¹, α -helix at 1656 cm⁻¹ and anti-parallel β -sheet and, or turns at 1685 cm⁻¹. The absorptions of several amino-acid side chains are also revealed in the second derivative. These are aspartate at 1585 cm⁻¹, glutamate at 1562 cm⁻¹ and tyrosine at 1515 cm⁻¹.

Quantitative analysis of the secondary structure content was made by factor analysis of the difference spectrum of TIMP-1 in H₂O [296]. This gave 42% β -sheet, 24% α -helix and 22% turns. The Mahalanobis' statistic [296] was 0·83, indicating that the spectrum of TIMP-1 is within the range of variation of the reference spectra in the data set.

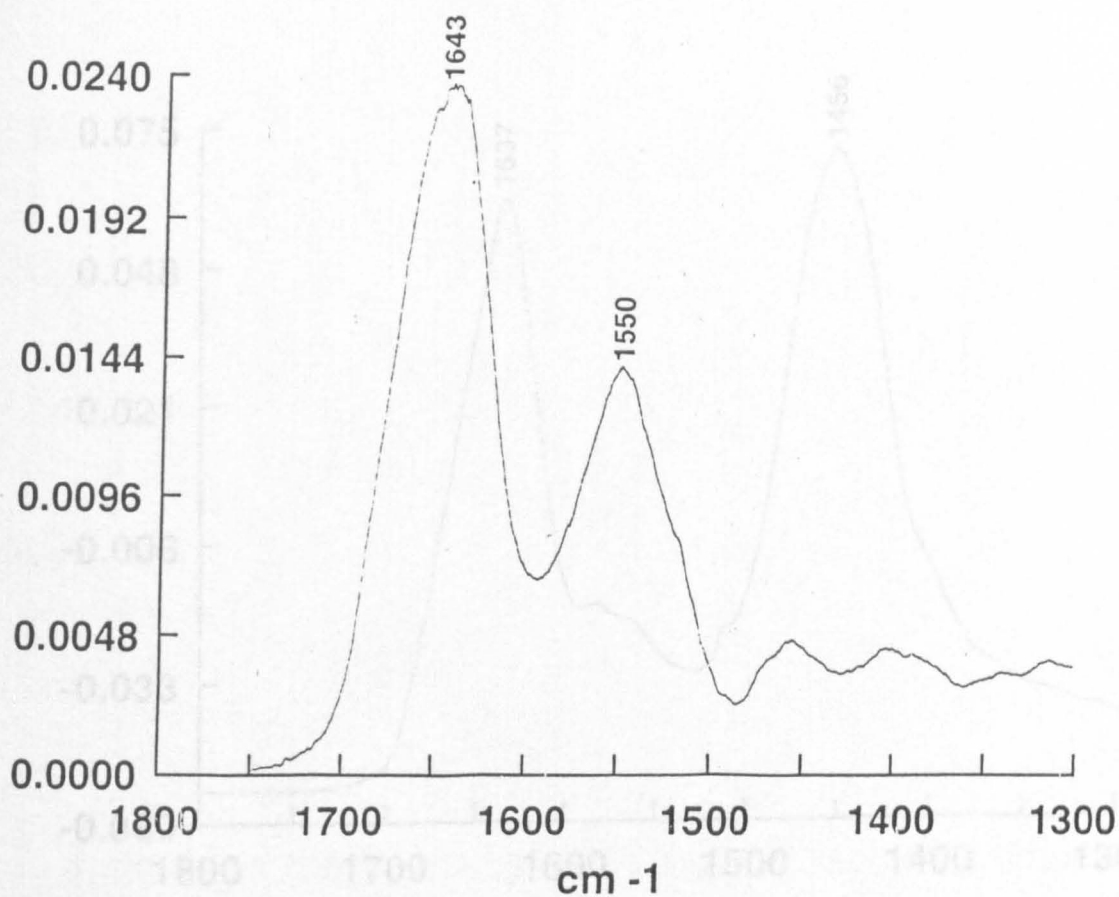


Figure 5-1. FTIR difference spectrum of TIMP-1 in H₂O. The protein concentration was 9.8 mg/ml in 100 mM KH₂PO₄ buffer (pH 7.0). 256 scans were recorded at a resolution of 2 cm⁻¹. The characteristic amide I and amide II bands are seen at 1643 and 1550 cm⁻¹ respectively.

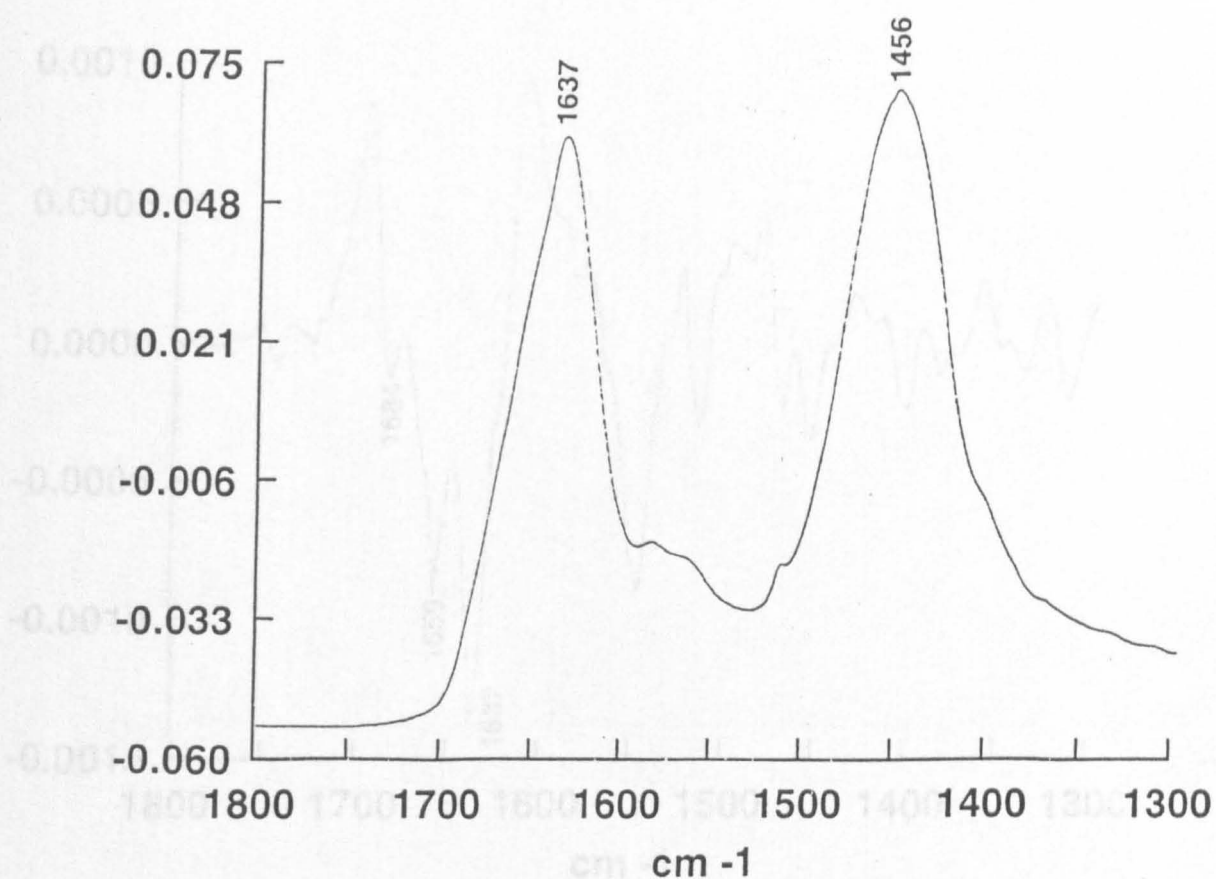


Figure 5-2. FTIR difference spectrum of TIMP-1 in D₂O. The protein concentration was 7.5 mg/ml in 100 mM KH₂PO₄ buffer (pD 7.0). 256 scans were recorded at a resolution of 2 cm⁻¹. The amide bands have shifted to 1637 cm⁻¹ and 1456 cm⁻¹. The shoulder around 1575 cm⁻¹ may reflect a population of non-exchangeable amide protons.

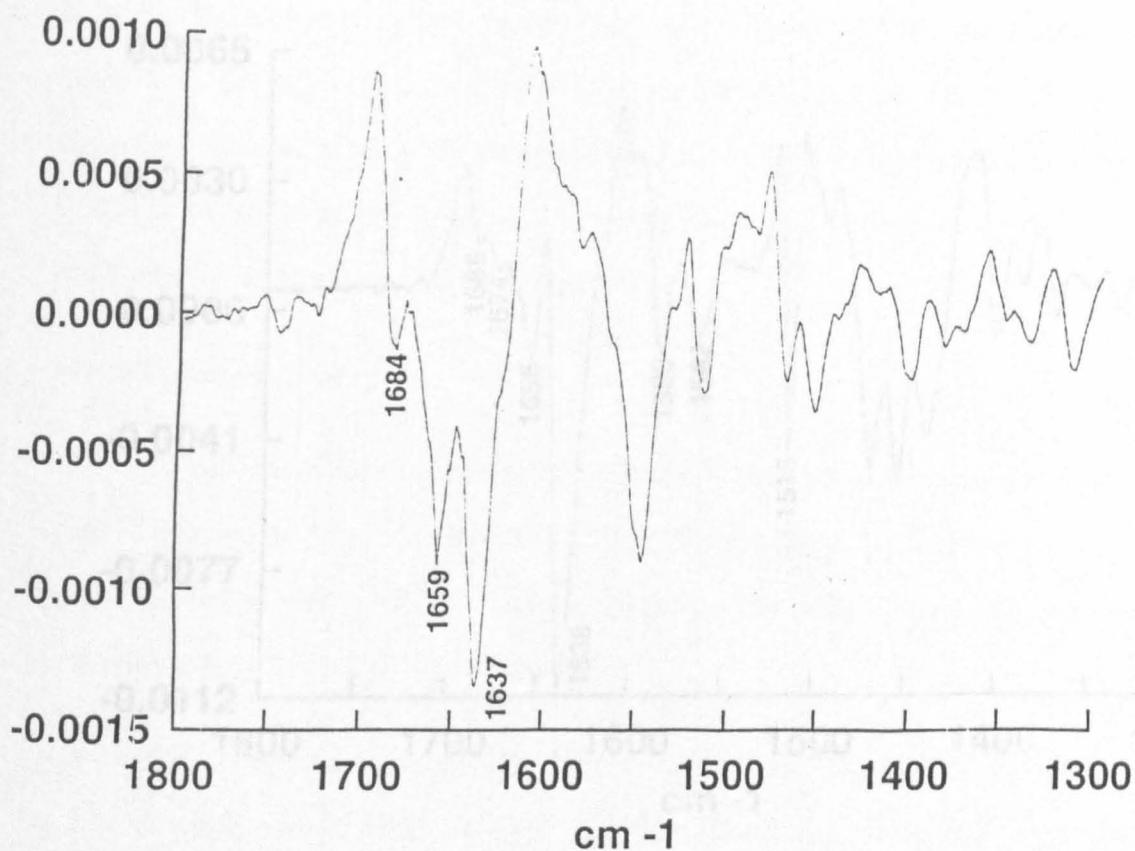


Figure 5-3. Second-derivative spectrum of TIMP-1 in H₂O using a 19 data point window. The major peaks of interest in the spectrum are marked and have been identified as: 1637 cm⁻¹ - sheet, 1659 cm⁻¹ - α -helix and/or turns and 1684 cm⁻¹ - anti-parallel β -sheet and/or turns.

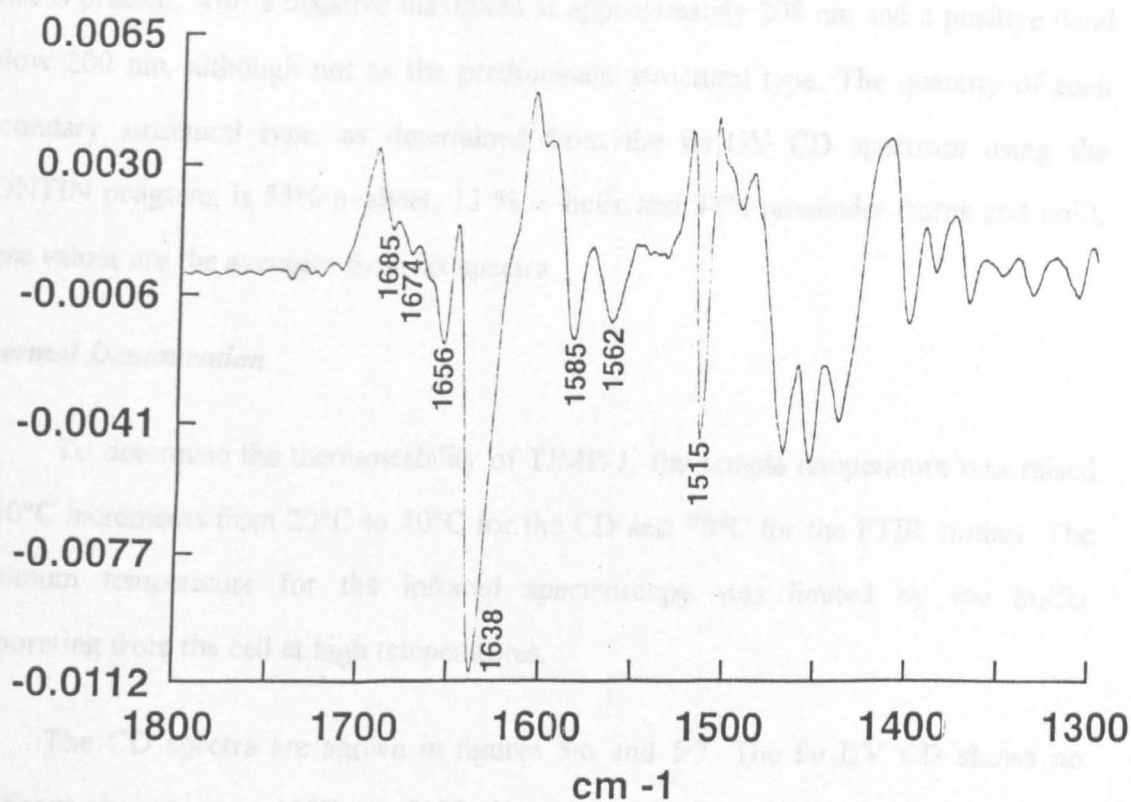


Figure 5-4. Second-derivative spectrum of TIMP-1 in D₂O using a 13 data point window. Again the major peaks have been marked, along with others that derive from individual amino acids which absorb in this region. These are aspartate at 1585 cm⁻¹, glutamate at 1562 cm⁻¹ and tyrosine at 1515 cm⁻¹. The amide peaks have been assigned as 1638 cm⁻¹ - β -sheet, 1656 cm⁻¹ - α -helix and 1685 cm⁻¹ - anti-parallel β -sheet and/or turns.

Circular Dichroism (CD) Spectroscopy.

The overall shape of the far-UV CD spectrum (figure 5-5) would indicate that α -helix is present, with a negative maximum at approximately 208 nm and a positive band below 200 nm, although not as the predominant structural type. The quantity of each secondary structural type, as determined from the far-UV CD spectrum using the CONTIN program, is 53% β -sheet, 13 % α -helix and 34% remainder (turns and coil); these values are the averages from six spectra.

Thermal Denaturation

To determine the thermostability of TIMP-1, the sample temperature was raised in 10°C increments from 20°C to 80°C for the CD and 70°C for the FTIR studies. The maximum temperature for the infrared spectroscopy was limited by the buffer evaporating from the cell at high temperatures.

The CD spectra are shown in figures 5-6 and 5-7. The far-UV CD shows no significant change up to 60°C. At 80°C, however, the height of the maximum around 190-195 nm decreased noticeably compared to the same peak at 20°C (figure 5-6). Maintaining the temperature at 80°C for a total of 4 hours caused the spectrum to change markedly. The broad negative band between 200 nm and 230 nm decreased sharply and the overall shape of the spectrum changed significantly. This effect was not reversed on cooling to 20°C, suggesting that the protein had denatured or precipitated.

An identical sample studied in the near-UV region (figure 5-7) shows some small changes. The intensity of the positive maximum at 290 nm (which is due to tryptophan side chains) varies with temperature, decreasing as the temperature increases (by approximately 50% at 60°C). This can be explained as a result of the protein structure becoming less tightly packed, allowing the tryptophans greater freedom of rotation (mobile tryptophans have a much weaker signal in CD than those that are spatially confined).

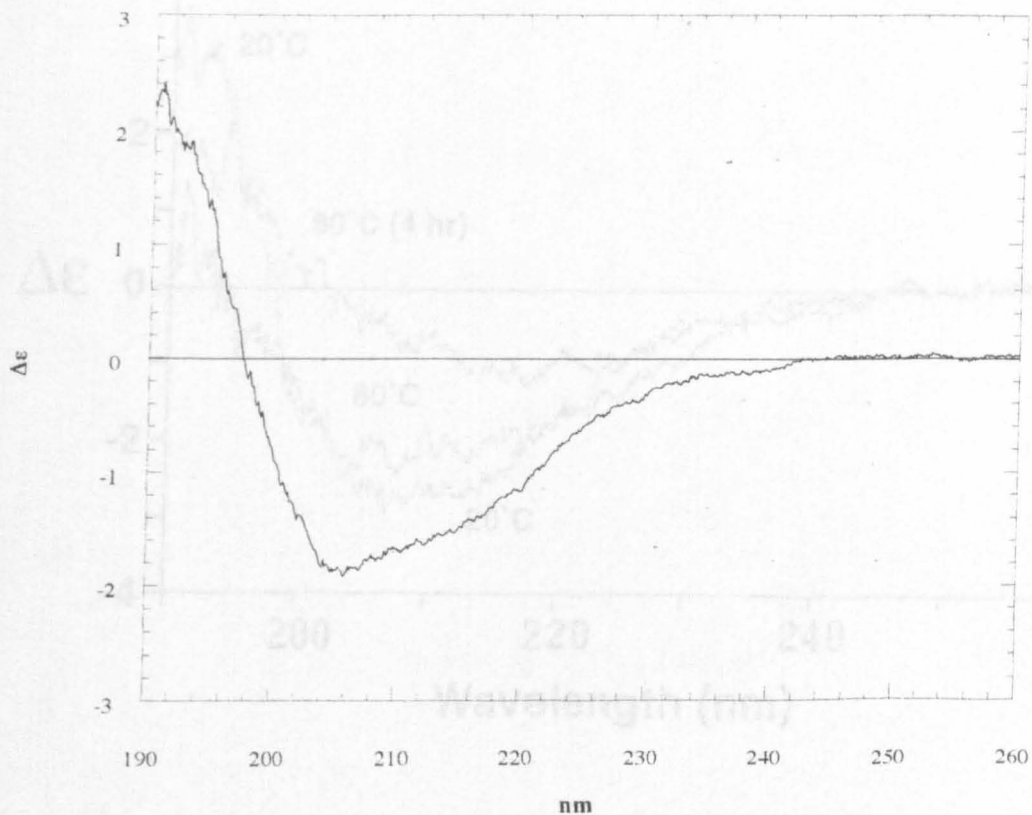


Figure 5-5. Mean of Four Far UV CD Spectra of TIMP-1 in H₂O.

All spectra were recorded at 20°C, with a sample concentration of 0.3 - 0.5 mg/ml in 100 mM KH₂PO₄ (pH 7.0) buffer, with a scan speed of 10 nm/min and a time constant of 4s. A cell pathlength of 1 cm and a bandwidth of 1 nm were used for the acquisition.

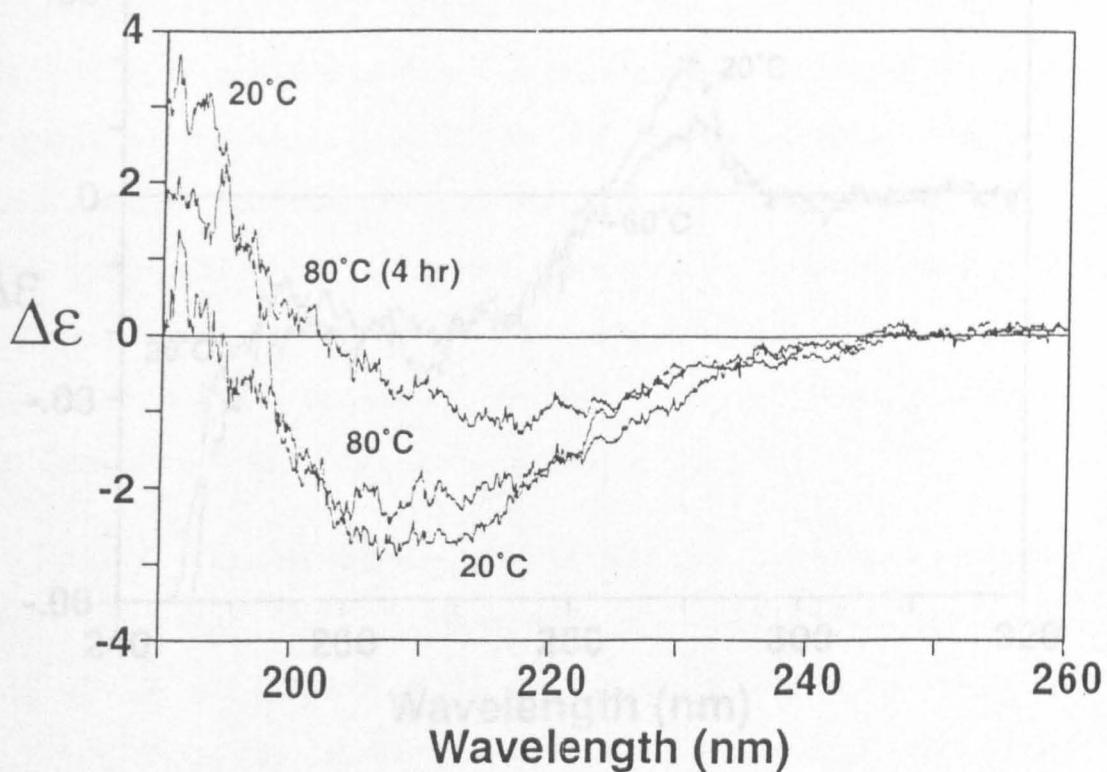


Figure 5-6. Far UV CD spectra of TIMP-1 showing the changes occurring through a temperature variation. Spectra were acquired for the same sample using a 0.02 cm pathlength cell and a 2 nm bandwidth. No significant changes were observed in spectra recorded at temperatures between 20°C and 80°C.

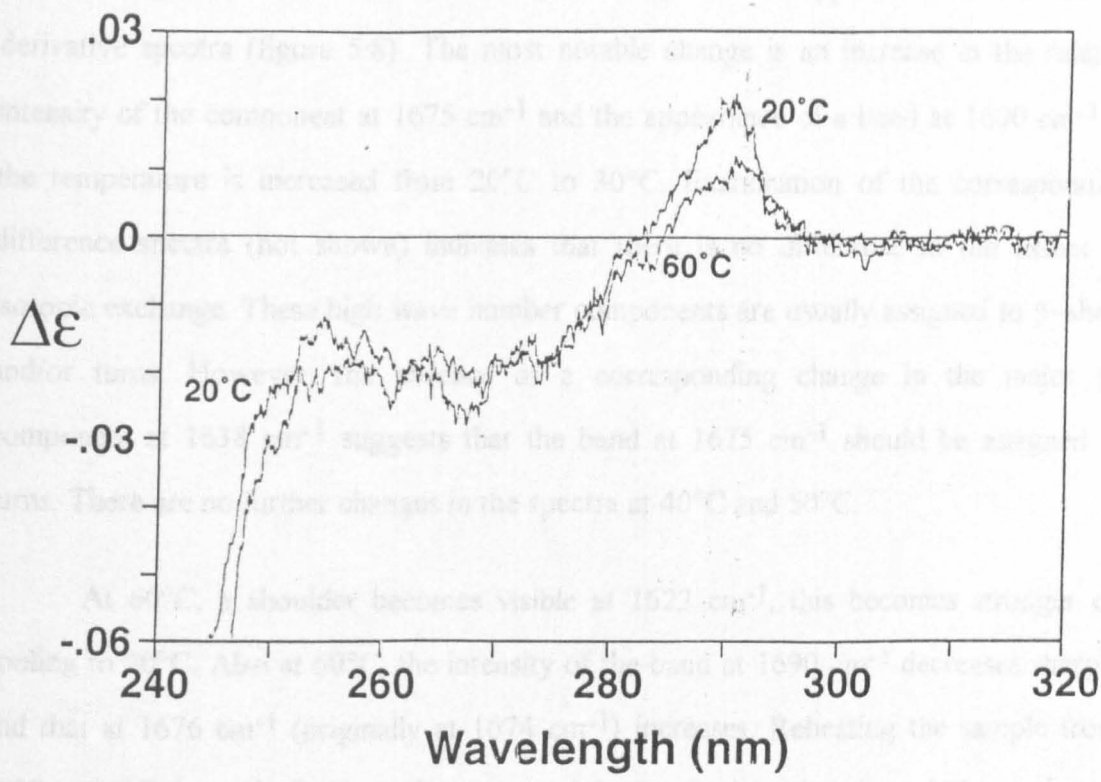


Figure 5-7. Near UV CD spectrum of TIMP-1 at 20°C and 60°C. These spectra were acquired for the same sample, during the same temperature study as in figure 5-6. The effect of increased temperature is observed in the absorbance of the tryptophan side chain before any change is observed in the overall structure.

The same procedure using FTIR shows broadly the same effects. There are very minor changes up to 50°C, with no major changes in the appearance of the second derivative spectra (figure 5-8). The most notable change is an increase in the relative intensity of the component at 1675 cm⁻¹ and the appearance of a band at 1690 cm⁻¹ as the temperature is increased from 20°C to 30°C. Examination of the corresponding difference spectra (not shown) indicates that there is no difference in the extent of isotopic exchange. These high wave number components are usually assigned to β -sheet and/or turns. However, the absence of a corresponding change in the major β -component at 1638 cm⁻¹ suggests that the band at 1675 cm⁻¹ should be assigned to turns. There are no further changes in the spectra at 40°C and 50°C.

At 60°C, a shoulder becomes visible at 1623 cm⁻¹, this becomes stronger on cooling to 20°C. Also at 60°C, the intensity of the band at 1690 cm⁻¹ decreases sharply and that at 1676 cm⁻¹ (originally at 1674 cm⁻¹) increases. Reheating the sample from 20°C to 70°C dramatically alters the spectrum. An intense band is seen at 1616 cm⁻¹, and many of the bands in the spectrum of the unheated protein are lost entirely, being replaced with bands at 1682 cm⁻¹, 1659 cm⁻¹, 1647 cm⁻¹ (shoulder) and a greatly reduced band at 1639 cm⁻¹. This effect was also seen at 50°C in a sample that was heated to 40°C and then cooled to 20°C for 48 hours before continuing the temperature variation study (data not shown).

NMR Analysis

The aromatic region of a DQF-COSY and accompanying one-dimensional spectrum is shown in figure 5-9. It is possible to identify a number of through bond connectivities in this region. There are a number of downfield shifted α -proton signals between 5 and 6.2 ppm, which are clearly devoid of COSY connectivities to aromatic protons, and which are characteristic of β -sheet regions [306].

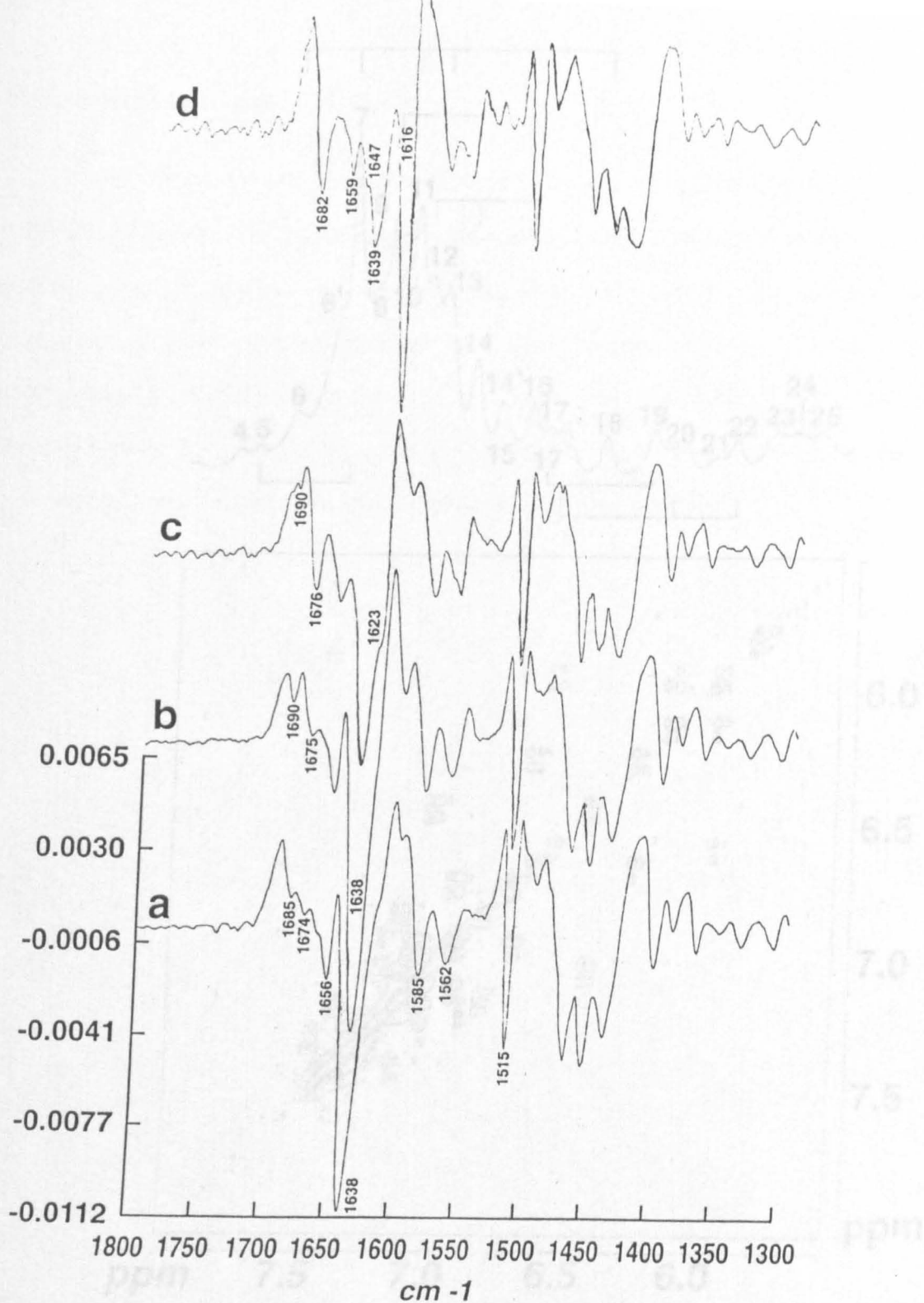


Figure 5.8. IR FTIR spectra of TIMP-1. Arrows indicate the peaks in the aromatic region with a few

Figure 5.8. The effect of temperature on the second-derivative FTIR spectrum of TIMP-1. All spectra were recorded under the same conditions as for the structure determination and calculated using a 13 data point window. The temperature was raised in 10°C increments allowing sufficient time for equilibration before recording the spectra. (a) FTIR spectrum of TIMP-1 at 20°C as used for structure determination. (b) Spectrum at 30°C. (c) Spectrum at 60°C. (d) Spectrum at 70°C.

5.3.2. Secondary structure Prediction

The 1H NMR proton spectrum of TIMP-1 was analysed using a range of different structure prediction programs. The predicted secondary structure is shown in table 5.1. The relative quantity of each secondary structure element is also listed. The program output or calculated 1D proton spectrum is shown in figure 5.9. The peaks in the 1D spectrum are numbered 1-25. The peaks are numbered in the order of their chemical shift from highest to lowest. The peaks are numbered in the order of their chemical shift from highest to lowest. The peaks are numbered in the order of their chemical shift from highest to lowest.

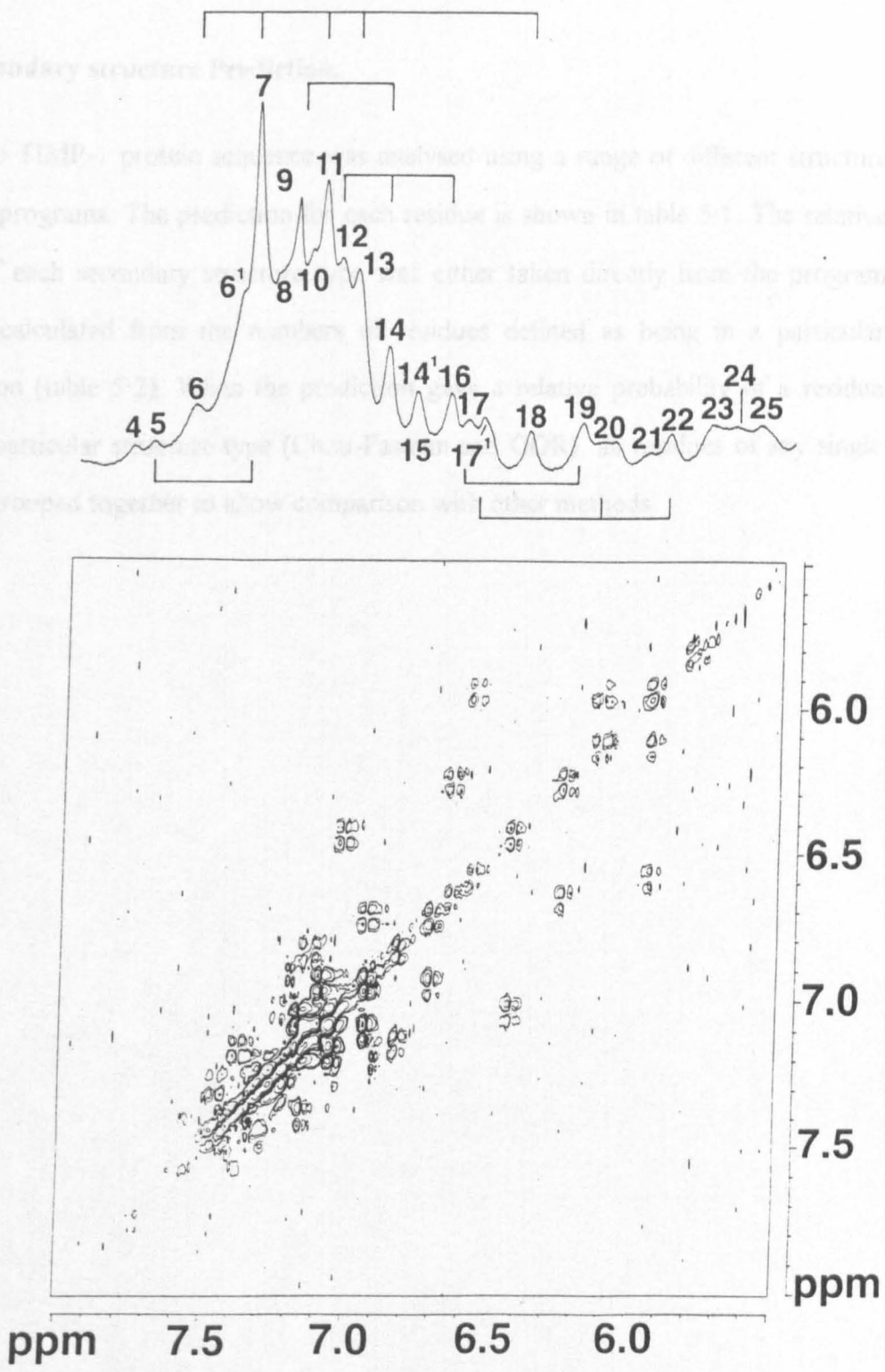


Figure 5-9. DQF COSY spectrum of TIMP-1. Aromatic region with a few characterised spin-spin coupling systems traced out in the accompanying one dimensional spectrum. A number of peaks in the 1D spectrum do not show any cross peaks indicating that they may be downfield shifted N-H protons.

	CTCVP	PHPQT	AFCNS	DLVIR	AKFVG	TPEVN
C+F	tt.EE	eeetT	Thhhh	hhhh.	...EE
GOR	TTT..	..TTT	TTTTT	T..TT	T....T
SOPM	EEEC	CCCCH	HHHCC	CEEEE	EEEEC	CCCC
NNHEEE	E....
PPE	SE...	.EEEE	EEEE.	.EEE.
	QTTLY	QRYEI	KMTRM	YKGFQ	ALGDA	ADIRF
C+F	EEEE	E..HH	HHHH	...ah	hhhhh	hhEEE
GOR	T...H	HHHH	HHHH	HHHH	HHHH	HHEEE
SOP	CCCH	HHHE	EEEE	CCHH	HCCCH	HHHH
NNHHH	HHHH	HHHH	HH...	..EEE
PP	EEEE	..E.EEEE
	VYTPA	MESVC	GYFHR	SHNRS	EEFLI	AGKLQ
C+F	EEHh	hhhhht	ttttt	HHHH	HHHHT
GOR	EE...	.TTTT	TTTTT	HHHH	HHHH
SOPM	EECH	HHHH	HHEH	CCCC	HHEE	ECCC
NN	E....	..HH.	.HHE.	HHHH	H..HH
PP	EE...	.EEEE	EEEE	E....	EEEE	EE...
	DGLLH	ITTCS	FVAPW	NSLSL	AQRRG	FTKTY
C+F	TtEEE	EEEE	EEtt	.tthh	hhhh.	EEEE
GOR	TTEEE	EEEE	EE.TTTTT	TTTTT
SOPM	CCEEE	EEHH	EECC	CHHH	HCCC	CEEE
NN	H..EE	EE...HHH	HH...E
PP	...EE	EEEE	EE..	.HHH	HHHH	H...
	TVGCE	ECTVF	PCLSI	PCKLQ	SGTHC	LWTDQ
C+F	EE.hh	hhhhh	tt..t	TTe	eeee
GOR	T.TTT	TTTT	TTTT.	TTTT	TTTT	TT...
SOPM	EEEC	CCEE	EEEE	CCCC	CCCE	EEEE
NNHH
PP	EEEEEE..	...EE	EEEE.
	LLQGS	EKGFQ	SRHLA	CLPRE	PGLCT	WQSLR
C+F	eee.h	hhhhh	hhhh	hh...	TTEE	EEEE.
GORTTTT	TTTTT	T.TT.	TTTT	T...T
SOP	EECC	CCCC	CCEC	CCCC	CCEE	EHHHC
NN	HHH..E
PPEEE	EE...H	HHHH
	SQIA					
C+F					
GOR	TT..					
SOPM	CCCE					
NN					
PP	HHH.					

Table 5-1. Secondary structure prediction from five different programs. Helix is indicated by H, sheet by E, turn by T and coil or loop by C. Less certain predictions for some programs are in lower case and residues for which a structural type was not assigned are marked as a point.

	α -helix %	β -sheet %	other %	turn %
Chou + Fasman	35.9	29.9	22.8	11.4
GOR	12.5	8.2	33.6	45.7
SOPM	21.74	33.7	44.57	nd
nnpredict	21.7	8.2	70.1	nd
protein predict	10.3	38.6	51.1	nd

Table 5.2. Results drawn from the structure prediction of TIMP-1 by five different algorithms; the methods of Chou and Fasman [294], Gibrat et al [295] (GOR), the self optimised prediction method (SOPM) [303], the nnpredict [304] and protein predict [302] neural network programs. Where a program could not assign an individual residue, or assigned it as coil it has been included as 'other' structural types. Some programs do not produce figures for turn structures, so for the neural network predictions the 'other' category includes turns.

5.4. Discussion.

This work (with the exception of the structure prediction) is the first study to provide data on the structural content of TIMP-1 [307].

The secondary structure content of TIMP-1 has been determined by two complementary methods: circular dichroism and Fourier transform infrared spectroscopy. The far-UV CD spectrum identifies a structure containing 53% β -sheet, 13% α -helix and 34% as remainder (turns and coil). The FTIR spectrum of TIMP-1 in H₂O gives a result of 42% β -sheet, 24% α -helix and 22% turns. This quantitative analysis is supported by the assignment of the bands in the second-derivative FTIR spectrum. The CD and FTIR analyses are in reasonable agreement. FTIR generally gives a more accurate determination of the β -sheet content than does CD.

Previous studies of TIMP-1 have indicated that it has a high thermal stability [308], which is consistent with the high number of disulphide bonds in relation to its size. However, to follow the stability using biological assays, the samples had to be cooled, precluding any analysis of possible reversible changes at higher temperatures. For the current experiments, the temperature was limited by the constraints of the equipment to a maximum of 60-80°C. The effects of temperature on the secondary structure are not extensive up to 60°C. FTIR spectra indicate that there are changes in turn structures at lower temperatures. The β -sheet structure is unaffected until a threshold temperature of 60°C is reached. The appearance of the band at 1616 cm⁻¹ has been associated with the aggregation of anti-parallel β -sheets in other proteins [309]. The native β -sheet structure is lost at higher temperatures (greater than 60°C) and the denatured protein interacts irreversibly to form multimeric complexes. Aggregation also occurs on heating to lower temperatures, followed by long periods at room temperature.

There was no significant change in the far-UV CD spectrum up to 60°C. When the sample is held at 80°C, irreversible changes occur as described above. By comparison with the FTIR experiment, the change is probably not due to structural alterations but is

caused by sample aggregation. Although aggregation occurs at different temperatures in the two techniques, this is probably due to the higher sample concentration that had to be used for the FTIR technique.

The near-UV CD spectrum of TIMP-1 shows an increase in the mobility of the tryptophan residues as the temperature is increased. These changes could imply that the tertiary structure surrounding the tryptophan rings becomes less closely packed as the temperature increases, which is in agreement with the FTIR and far-UV CD results. The results of the secondary structural analysis, combined with the thermal stability study, suggest that TIMP-1 could be similar to many other inhibitors in having a generally stable structure based around an exceptionally stable core of anti-parallel β -sheet.

NMR experiments were carried out as part of a general assessment of the suitability of TIMP-1 for further structural analysis. The presence of several downfield shifted α -proton signals supports the conclusions drawn from the CD and FTIR studies. From the DQF-COSY experiment, it was possible to identify a number of scalar connectivities through several very clear cross peaks in the aromatic region.

Secondary Structure Prediction.

Of the five structure prediction methods tried, none predicted a secondary structure content that agreed entirely with the experimental evidence. The Chou and Fasman method significantly overpredicted the α -helical content of TIMP-1. All of the other methods gave helical predictions that were in line with the results obtained from CD and FTIR. In all the predictions the β -sheet content was underestimated. The GOR and nnpredict programs both predicted a sheet content of 8.2 %. These values are entirely different to the experimental ones and indicate that although structure prediction methods have improved they are by no means reliable in all cases. The GOR prediction in particular has designated almost half of the protein as being in a turn conformation, which would be very unusual.

Table 5.1 shows the predictions by the different programs for each residue in the TIMP-1 sequence. For the first fifteen residues there is no agreement between the different methods. The next block of ten shows some consensus towards sheet. The next section where the results are in general agreement is between Gln-36 and Asp-57, where the prediction is mostly helix. Residues Glu-81 - Ala-86 are also predicted as being helical. The section, Lys-93 - Ala-103 was predicted as being in a β -sheet conformation. There are no other long regions where all five predictions are in good agreement. Some individual residues were given the same assignment by all five methods such as Ile-96 (sheet). There are also some where four have given the same assignment and the fifth not given a prediction such as Gln-50 (helix). Overall there is not a great deal of agreement between the different methods

These methods can give accurate predictions of secondary structure. The protein predict algorithm claims an accuracy of greater than 70 %, whilst the nn predict program has been accurate to 79 %. SOPM claims an overall accuracy of 69 %, with the most accurate predictions being for loop or coil (74 %), α -helix is predicted to 66.3 % accuracy and β -sheet to only 60.9 % accuracy. For structure prediction in general it appears that accurately estimating the quantity of β -sheet is much less reliable than any other structural class. For a protein with a high β -sheet content, such as TIMP-1, it is not surprising that the predictions do not tie in with the experimental evidence. The best overall predictions were from the protein predict and SOPM programs, both of which are more recent developments. Future programs may be more accurate but extreme caution should be exercised when interpreting the results.

Comparison between Secondary Structure of TIMP-1 and the Structure of the N-terminal Domain of TIMP-2 [141].

Although TIMP-1 and TIMP-2 do not have an extremely high sequence homology, from the complete conservation of the cysteine residues and their similar function it is probable that the two molecules share the same overall topology. According

to the NMR data, the N-terminal domain of TIMP-2 contains 40 % β -sheet, most of which is anti-parallel. This is very similar to the high quantity of β -sheet and the indication that much of it is anti-parallel obtained by CD and FTIR for TIMP-1. The relatively low helical content also appears to be similar. However it is neither easy, nor valid to draw conclusions from this comparison, since the C-terminus of TIMP-2 was not studied and further data may alter the picture entirely. The general impression given by the data is one of a protein with a large amount of antiparallel β -sheet.

6.1. Introduction.

Although the interior of a protein is considered to be a hydrophobic environment, it is the surface that is most important in its solubility and activity, as well as its interactions. Studying the conformation of the surface, in particular the way charged residues, such as exposed hydrophobic patches and charged residues, has an effect on the way the protein fits into the mechanism of inhibition with its substrate is an important area of research.

It is known that TIMP-1 is known to be glycosylated at two sites, Asn208 and Asn214, which do not appear to have any function in terms of its specific activity (1,2). However, they may have a role in the behaviour of TIMP-1 in vivo, possibly through the availability to particular regions of the tissue and its stability. It would be interesting to know whether the glycosylation of TIMP-1 is important in its biological activity. This is an area that needs to be investigated. There has been a suggestion that the glycosylation of TIMP-1 is important in its biological activity (3). It is also known that TIMP-1 is glycosylated at two sites, Asn208 and Asn214, which do not appear to have any function in terms of its specific activity (1,2). However, they may have a role in the behaviour of TIMP-1 in vivo, possibly through the availability to particular regions of the tissue and its stability. It would be interesting to know whether the glycosylation of TIMP-1 is important in its biological activity. This is an area that needs to be investigated.

In TIMP-1, the majority of residues that are exposed to the solvent are in the N-terminal domain, which are conserved with TIMP-2. The C-terminal domain is more conserved with TIMP-2. However, there are some differences in the sequence of the N-terminal domain between TIMP-1 and TIMP-2. The N-terminal domain of TIMP-1 is more hydrophobic than that of TIMP-2. This is reflected in the higher content of β -sheet in TIMP-1 compared to TIMP-2. The N-terminal domain of TIMP-1 is also more hydrophobic than that of TIMP-2. This is reflected in the higher content of β -sheet in TIMP-1 compared to TIMP-2.

Chapter 6.

Some Surface Features of TIMP-1.

6.1. Introduction.

Although the interior of a protein is essential to its overall structure, it is the surface that is most important in its solubility and interactions with other molecules. Studying the composition of the surface, in particular for any unusual residues, such as exposed hydrophobic patches and charged residues lost on interaction can give an insight into the mechanism of inhibition when no structural data is available.

Wild type TIMP-1 is known to be glycosylated at two sites, Asn-30 and Asn-78 which do not appear to have any function in terms of biological activity [141]. However they may have a role in the behaviour of TIMP-1 *in vivo*, possibly determining the accessibility to particular regions of the tissue and its stability in the blood. *In vitro*, the glycosylation may affect the solubility of TIMP-1 in concentrated solutions which will have implications for the study of recombinant protein. There are also other points at which a protein may be glycosylated. There can be O-linked glycosylations at serine and threonine residues which can not be predicted directly from the sequence. These might also not be detected after removal of the N-linked carbohydrate, particularly if the modification is not very large.

In NMR spectra the majority of protons from the sugar residues have proton resonances which are overlapped with those of the protein side chains (between 2 and 4 ppm). However, cross-peaks from the anomeric protons of the sugars are often found in a relatively uncrowded region of a COSY spectrum. Studies of carbohydrates have identified characteristic chemical shifts for different sugar residues in particular

oligosaccharide environments [310, 311]. The chemical shifts of cross-peaks between anomeric, and vicinal C2 sugar protons can be compared with published data. It is then possible to make a tentative identification of the sugar type and position in the carbohydrate chain.

There are a number of paramagnetic molecules, which have a large (electronic) magnetic moment and can bind to various groups on the surface of proteins. The result of this binding is that the relaxation rate of any nuclei close to the introduced paramagnetic molecule is increased. This increases the linewidth of signals seen from the surface groups in NMR spectra. This is observed as the broadening of peaks in a 1D spectrum and the reduction or cancellation of cross-peaks in a 2D COSY spectrum [312]. The COSY experiment is particularly sensitive to line broadening. This is because the cross peak lobes are antiphase and if they become broader, will cancel themselves out as well as dropping down to the level of the noise.

Careful choice of the compounds used will allow the composition of a proteins surface to be probed. Unusual surface residues can be identified, as can residues that become protected in protein-protein interactions. One of the most widely used probes is 4-hydroxy-2,2,6,6-tetramethylpiperidinyl-N-oxyl (OH-TEMPO). This is an organic free radical with an unpaired electron which does not cause a substantial change in the chemical shift of protein side chains on binding. OH-TEMPO interacts with hydrophobic side chains such as tryptophan, valine, leucine and isoleucine. Identifying exposed hydrophobic residues can be important in identifying and mapping protein-protein and protein-ligand interactions [313].

8-anilino-1-naphthalene sulphonate (ANS), is a fluorescent probe that binds non-covalently to hydrophobic regions of proteins. When this probe binds to proteins its fluorescence alters. The total fluorescence will increase and the wavelength of the emission can shift towards a lower wavelength. By titrating against ANS and calibrating the titration using a factor derived from a protein titration it is possible to determine the

number of ANS binding sites and their affinity [314]. As with the NMR probes, ANS can be used in studying protein-protein interactions when changes in conformation, or hydrophobic exposure occur.

Characterisation

This chapter describes three analyses of surface features of TIMP-1 using these techniques.

Carboxypeptidase Y (CPY) and *Neutrophil elastase* was from Boehringer Mannheim UK, Lewes, Sussex. Biotin-conjugated Concanavalin A was from Sigma Chemical Company, Poole, Dorset UK. Isogel-agarose plates for SDS-PAGE analysis were from Biorad, Radcliffe, Denmark. BioPhoresis horizontal electrophoresis cell was from Dr. Rad Laboratories Ltd, Hemel-Hempstead, Herts, UK. Western blots were prepared using a 1.5-4.0 trans-bleb cell and Kodak EZE Imager Screen 1 (0.0.5 M Tris-HCl, 0.1% 2-mercaptoethanol, pH 8.3, 20% ethanol). IEF markers were from Pharmacia Fine Chemicals, Uppsala, Sweden. Analysis of sugars was carried out on a Dionex D500 HPLC system with a PA1-4x250mm CARBOPAK. Data was processed using Dionex Peaking software.

ANS Probe

All experiments were carried out on a Bruker AMX 300 spectrometer. 4-hydroxy-2,2,6,6-tetramethylpiperidine-1-oxyl radical (OH-TEMPO) and $MnCl_2 \cdot 4H_2O$ were from the Sigma Chemical Co., Poole, Dorset, U.K.

ANS Binding Study

ANS was purchased from Molecular Probes Inc. NCAR TIMP-1 was prepared as described in chapter 3. The N-terminal fragment of porcine fibroblast collagenase was prepared as described by O'Hate *et al.* [315]. Fluorimetry was carried out on a Perkin-Elmer LS2 Laser fluorimeter.

6.2. Methods.

6.2.1. Materials.

Carbohydrate Analysis.

Glycopeptidase F (PNGaseF) and Neuraminidase was from Boehringer Mannheim UK, Lewes, Sussex. Biotin-conjugated Concanavalin A was from Sigma Chemical Company, Poole, Dorset UK. Isogel- agarose plates for iso-electric focusing were from FMC BioProducts, Denmark. Biophoresis horizontal electrophoresis cell was from Bio-Rad Laboratories Ltd, Hemel-Hempsted, Herts, UK. Western blots were prepared using a Bio-Rad trans blot cell and Kodak EZE buffer formula 1 (0.025 M Tris-HCl, 0.192 M glycine pH 8.3, 20% methanol). IEF markers were from Pharmacia Fine Chemicals, Uppsala, Sweden. Analysis of sugars was carried out on a Dionex Dx500 HPLC system with a PA1-4x250mm CARBOPAK. Data was processed using Dionex Peaknet software.

NMR Probes.

All experiments were carried out on a Bruker AMX 500 spectrometer. 4-hydroxy-2,2,6,6-tetramethylpiperidinyloxy, free radical (OH-TEMPO) and $MnCl_2 \cdot 4H_2O$ were from the Sigma Chemical Co., Poole, Dorset, U. K.

ANS Binding Study.

ANS was purchased from Molecular Probes Inc. NCAB TIMP-1 was purified as described in chapter 3. The N-terminal fragment of porcine fibroblast collagenase was purified as described by O'Hare et al [315]. Fluorimetry was carried out on a Perkin-Elmer LS2 filter fluorimeter.

6.2.2. Methods.

Carbohydrate Analysis.

0.1 mg of NCAB TIMP-1 at 0.06 mg/ml was incubated at 37°C for a minimum of 7 hours with 1 unit of PNGase F in 0.2M phosphate, 1 mM EDTA buffer, pH 8.6, to remove N-linked sugars. SDS PAGE was as described. Western blotting was carried out essentially as described in chapter 2. Molecular weight markers (both pre-stained and unstained), and untreated TIMP-1 were included as controls. After the transfer procedure, the nitrocellulose was blocked with a solution of 1% BSA in TBS-TWEEN for 1 hour. The blot was given a first incubation of 16 hours with biotinylated Concanavalin A at 2mg/ml in TBS-TWEEN, then washed as described. The second incubation was for 2 hours with horse-radish peroxidase linked streptavidin at 1.6 mg/ml followed by extensive washing with TBS-TWEEN. The blots were developed using 4-chloro-naphthol (chapter 2).

Iso-electric focusing was carried out according to the manufacturers' instructions using 10-100 µg of protein per lane. Gels were run at 20 mA until the current dropped towards 10 mA. Standards of known pI were included. Gels were stained in 0.1 % Coomassie and destained in 25 % ethanol, 9 % acetic acid. Alternatively they were silver stained according the manufacturers' instructions.

Neuraminidase was used to remove the free sialic acid residues from the carbohydrates. Both CAB and NCAB TIMP-1 were at approximately 1 mg/ml. The buffer was adjusted to 50 mM acetate pH 5.0, neuraminidase added and samples incubated overnight at 37°C.

CAB and NCAB TIMP-1 were prepared for monosaccharide analysis by preparative SDS-PAGE and Western blotting. 1mg of CAB and 0.65 mg of NCAB TIMP-1 were loaded across the top of large (3mm thick) SDS PAGE gels and run at 300 V for 3-4 hours, then blotted onto nitrocellulose using a 30 mA current overnight.

Acid hydrolysis of attached carbohydrates was carried out on strips, up to 3mm wide, cut from the western blots of both CAB and NCAB TIMP-1. Strips from each were immersed in 200 μ l of either 6M HCl or 2M trifluoroacetic acid (TFA). Control strips from regions of the blots containing no protein were also included. These samples were incubated at 105°C for 4 hours, the strips removed and the remaining material dried in a rotavap.

The hydrolysis products were resuspended in 20 μ l of H₂O and centrifuged to remove residual Coomassie stain and precipitated material. PNGase F treated samples and controls were also centrifuged to remove precipitates and analysed without further treatment. 5 μ l of each sample were loaded onto the HPLC, pre-equilibrated, and run with 25 mM NaOH. Detection of monosaccharides was with an electrochemical detector sampling at a rate of 1s⁻¹. To identify the peaks and give a quantitative measure of the monosaccharides present, standards of a known concentration were used to calibrate the results.

Glycosylated samples for analysis by NMR were prepared at 40 mg/ml, equivalent to 1.4 mM in 500 μ l of 100 % D₂O. The sample is self buffering at pH 4.2. The experimental details for the acquisition of DQF-COSY spectra are as described in chapter 5 (methods).

NMR Paramagnetic Probe-Experiments.

The same TIMP-1 sample was used for the OH-TEMPO experiments and for the sugar analysis. 20.1 mg of OH-TEMPO were dissolved in 500 μl of D_2O and the pH adjusted to 4.4 using DCl. One-dimensional spectra were recorded as described above for samples containing 0, 0.75, 1.5, 6, 9.75, and 13.5 mM OH-TEMPO. A DQF-COSY spectrum was recorded for the final sample under the conditions described above using a 9 μs , 90° pulse.

For experiments using MnCl_2 , a fresh sample was made up at 24 mg/ml (0.85 mM) in D_2O . MnCl_2 was dissolved in D_2O to a final stock concentration of 1 mM. One dimensional spectra were recorded as described above for samples containing 0, 2.5 μM , 5 μM , 12.5 μM , 25 μM , 37.5 μM , 87.5 μM , 330 μM , 2.83 mM, 5.33 mM and 7.83 mM. Again a DQF-COSY spectrum was recorded for the final sample.

ANS Binding Experiments.

ANS was dissolved in H_2O to give a 10 mM stock solution. This was diluted as necessary and the actual concentration determined from the absorbance of solutions at 350 nm (a 0.1 mM solution has an A_{350} of 0.5). All experiments were carried out in a buffer of 0.1 M Tris-HCl, 0.1 M NaCl, 2 mM CaCl_2 , pH 8.0. Sample tubes were foil wrapped and exposure to light minimised. All samples were incubated with ANS in the dark at room temperature for two hours prior to recording the fluorescence. When TIMP and collagenase fragments were used together an additional two hour incubation was used prior to the addition of ANS. An excitation wavelength of 340 nm was used and emission spectra recorded between 390 and 560 nm. Wavelength scans were run automatically, other readings were made individually. After each reading, the fluorimeter was washed with buffer until the emission returned to zero.

Samples prepared for wavelength scans were 3 μM TIMP-1, 100 mM ANS; 2.5 μM each of TIMP-1 and collagenase fragment, 100 mM ANS; 0.5 mM collagenase

fragment, 200 mM ANS and 200 mM ANS only. Samples for the more accurate assessment of λ max used 2 mM protein and 200 mM ANS. Samples for titrations used protein concentrations of 0 - 3 mM and 0 - 500 mM ANS. For the protein titrations ANS was kept constant at 100 mM and for the ANS titrations the protein concentrations were kept constant at 1 mM.

Concanavalin A Western blotting. The gel and blot are shown as figures 6-1 and 6-2 respectively. SDS PAGE (figure 6-1) shows that the PNGase F treatment has reduced the molecular weight of the TIMP-1. Two bands are present in lane 2 of this figure, the higher is at approximately 26 kDa and the lower is at 21 kDa. Western blotting (figure 6-2) using a Concanavalin A based detection system, picked out the glycosylated molecular weight markers (lane 1) and the untreated TIMP-1 control (lane 2). A similar quantity of TIMP-1 was loaded into lane 3 resulting in the first band observed. The same pair of bands seen in the SDS PAGE analysis of the treated sample is also seen on the western blot (lane 3). This shows that in both cases a Concanavalin A binding capacity has been retained after PNGase F cleavage of the N-linked carbohydrate.

IEF Analysis of CAB and NCAB TIMP-1.

Figure 6-3 shows the IEF profile of CAB TIMP-1. A range of sample loadings has been used in lanes 1 to 6. A large number of different pI are present. The major bands have pI of approximately 9.2, 9.0, 8.9, 7.9, 6.7, 5.9 and 5.6. Figure 6-4 shows the IEF profile of NCAB TIMP-1 (lane 6) and both CAB (lane 3) and NCAB TIMP-1 (lane 5) after treatment with neuraminidase. The CAB and NCAB forms of TIMP-1 have different profiles that can be clearly distinguished on the IEF gel. The NCAB TIMP-1 (lane 6) has pI of 8.4, 8.2, 7.3, 6.3, 5.6, 5.3 and 5.0.

After treatment with neuraminidase, the large number of widely distributed bands is reduced to one or more bands with a narrow range of pI (figure 6-4, lanes 3 and 5). Even after neuraminidase treatment, some differences are apparent between the CAB and NCAB forms. The NCAB form of TIMP-1 (lane 5) shows at least five different pI between 8.2 and 9.2, while the CAB form (lane 3) has reduced to a single band with a pI of approximately 9.0.

6.3. Results.

6.3.1. Carbohydrate Analysis.

Analysis of Endoglycosidase Treated TIMP-1.

NCAB TIMP-1 treated with PNGase F was analysed by SDS PAGE and Concanavalin A Western blotting. The gel and blot are shown as figures 6.1 and 6.2 respectively. SDS PAGE (figure 6.1) shows that the PNGase F treatment has reduced the molecular weight of the TIMP-1. Two bands are present in lane 2 of this figure, the higher is at approximately 26 kDa and the lower is at 21 kDa. Western blotting (figure 6.2) using a Concanavalin A based detection system, picked out the glycosylated molecular weight markers (lane 1) and the untreated TIMP-1 controls (lane 3). A smaller quantity of TIMP-1 was loaded into lane 3 resulting in the faint band observed. The same pair of bands seen in the SDS PAGE analysis of the treated sample is also seen on this western blot (lane 2). This shows that in both forms a Concanavalin A binding capacity has been retained after PNGase F cleavage of the N-linked carbohydrate.

IEF Analysis of CAB and NCAB TIMP-1.

Figure 6.3 shows the IEF profile of CAB TIMP-1. A range of sample loadings has been used in lanes 2 to 6. A large number of different pIs are present. The major forms have pIs of approximately 9.2, 9.0, 8.9, 7.9, 6.7, 5.9 and 5.6. Figure 6.4 shows the IEF profile of NCAB TIMP-1 (lane 6) and both CAB (lane 3) and NCAB TIMP-1 (lane 5) after treatment with neuraminidase. The CAB and NCAB forms of TIMP-1 have different profiles that can be clearly distinguished on the IEF gel. The NCAB TIMP-1 (lane 6) has pIs of 8.4, 8.2, 7.3, 6.5, 5.6, 5.3 and 5.0.

After treatment with neuraminidase, the large number of widely distributed bands is reduced to one or more bands with a narrow range of pIs (figure 6.4, lanes 3 and 5). Even after neuraminidase treatment some differences are apparent between the CAB and NCAB forms. The NCAB form of TIMP-1 (lane 5) shows at least five different pIs between 8.2 and 9.2, whilst the CAB form (lane 3) has reduced to a single band with a pI of approximately 9.0.

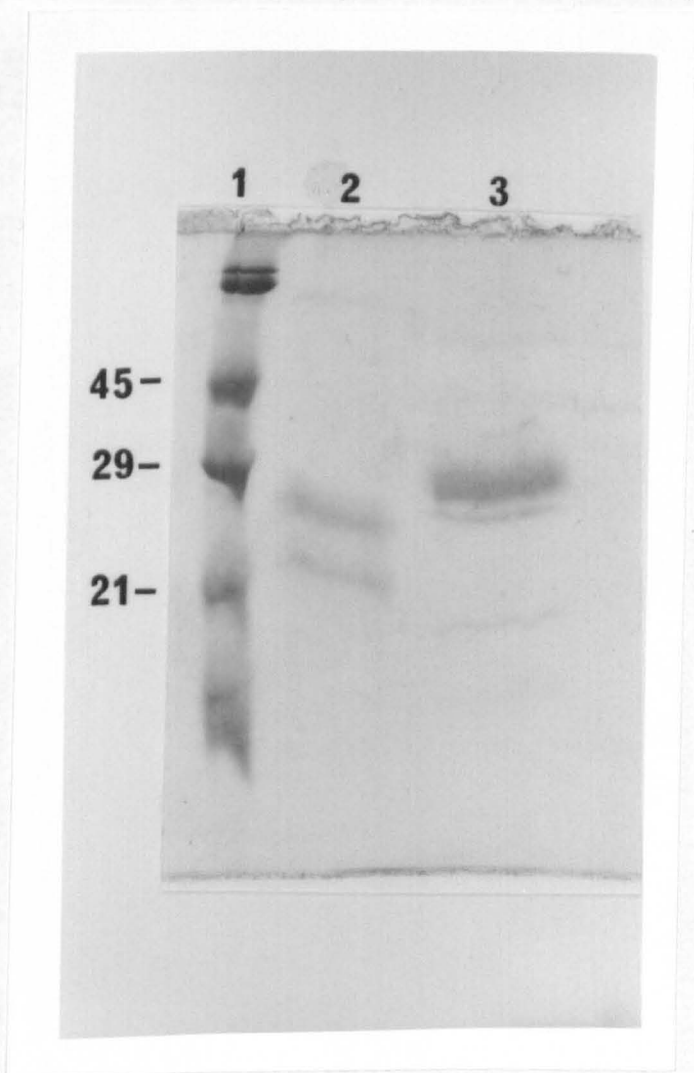


Figure 6.1. SDS PAGE of PNGase-F treated TIMP-1. Lane 1: molecular weight markers, Lane 2: PNGase-F treated TIMP-1, Lane 3: wild type TIMP-1. The molecular weight of the lower band in lane 2 is approximately 21 kDa showing that all N-linked sugars have been removed. The upper band of approximately 25 kDa is partially deglycosylated.

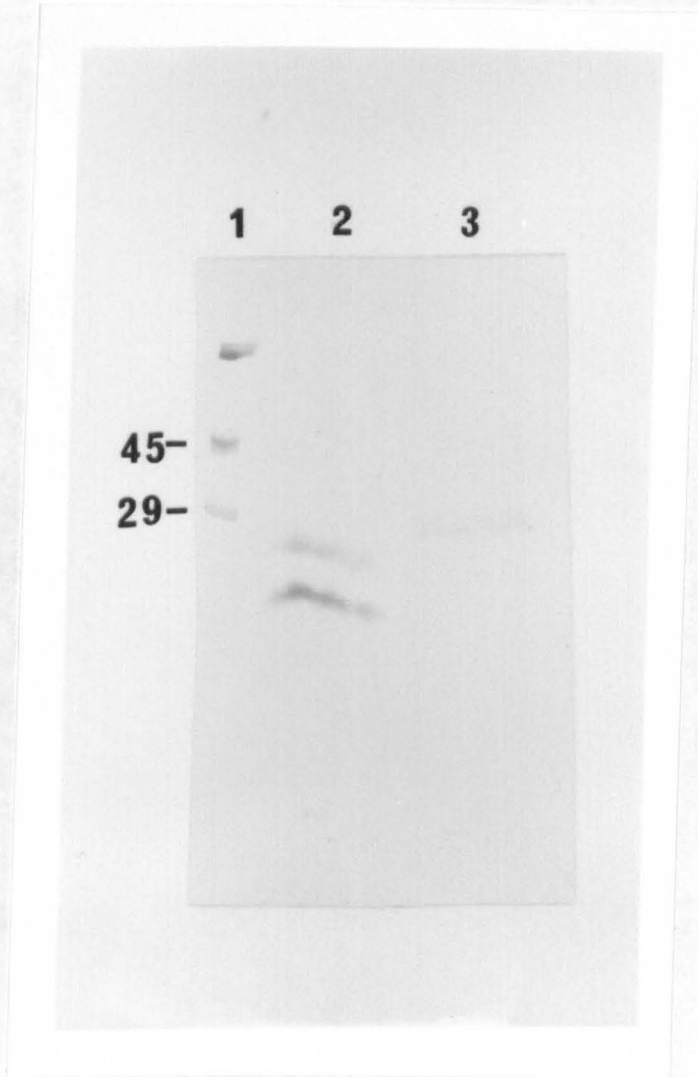


Figure 6.2. Western blot of PNGase F treated TIMP-1. Biotinylated Concanavalin A is used to detect proteins with bound sugars. Lane 1: molecular weight markers, Lane 2: PNGase F treated TIMP-1, Lane 3: wild type TIMP-1. The Concanavalin A detection system has picked out some of the molecular weight markers, the untreated TIMP-1 and both bands of the treated sample. This suggests that other forms of glycosylation may be present.

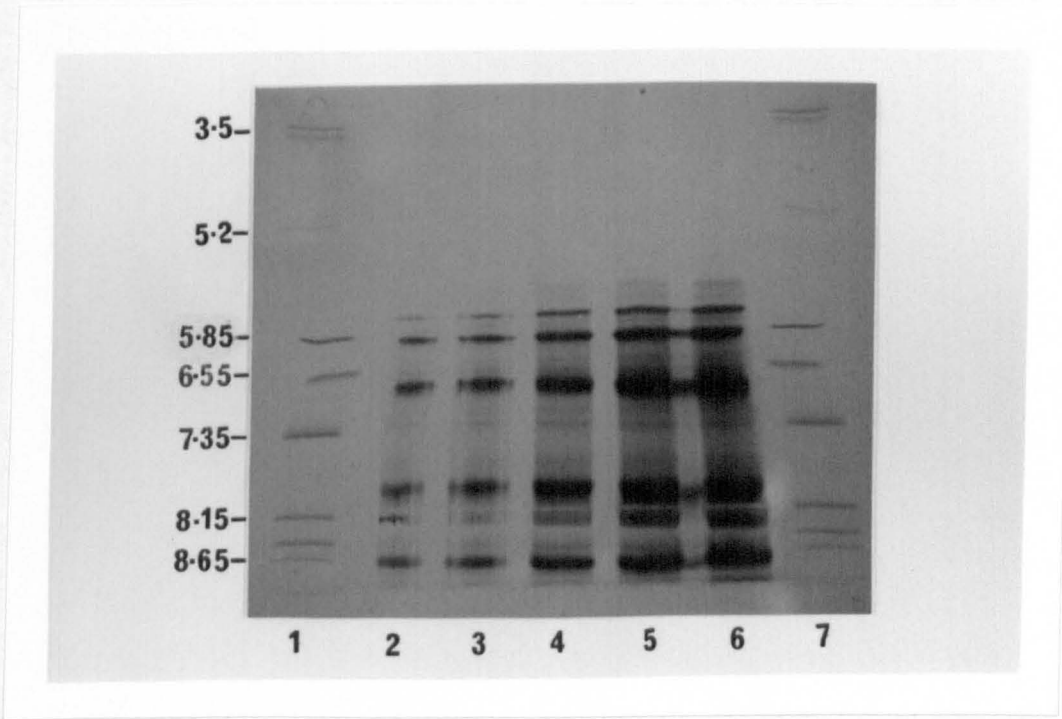


Figure 6-3. IEF gel of CAB TIMP-1. Lanes 1 and 7 contain markers of known pI. Lanes 2 through 6 contain a range of protein quantities (10 μ g - 100 μ g). The IEF profile shows that wild type TIMP-1 has an extremely complex mixture of pIs.

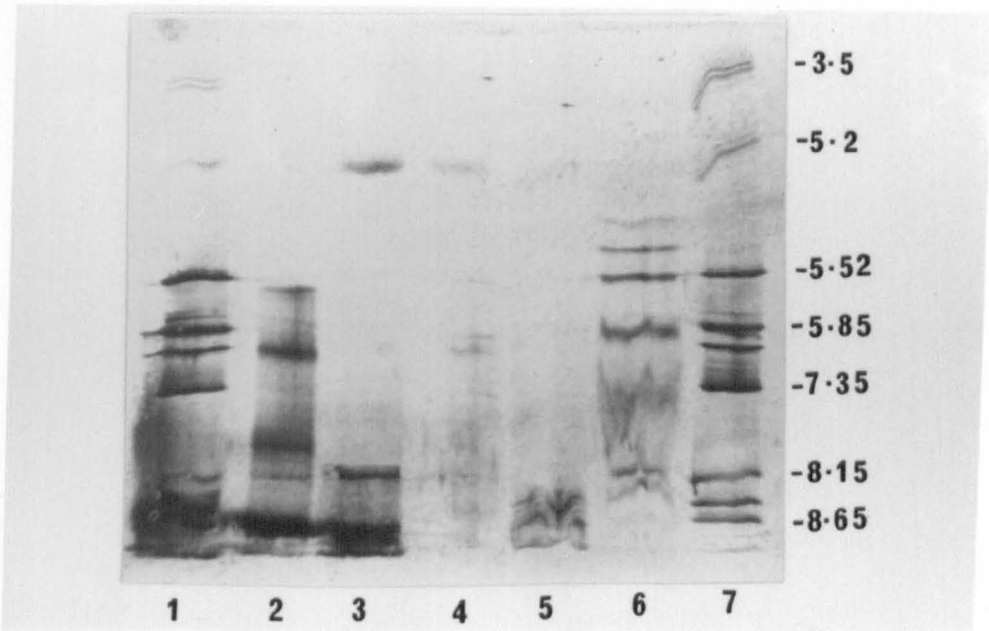


Figure 6-4. IEF gel showing CAB and NCAB TIMP-1 before and after treatment with neuraminidase. Lane 1: pI markers, Lane 2 CAB TIMP, Lane 3: CAB TIMP treated with neuraminidase, Lane 4: neuraminidase, Lane 5: NCAB TIMP treated with neuraminidase, Lane 6: NCAB TIMP, Lane 7: pI markers. NCAB TIMP-1 has a different pattern of pIs to CAB TIMP-1, both before and after neuraminidase treatment.

Monosaccharide Composition.

Data from the HPLC chromatograms was converted into relative percentage composition using the calibration from the set of known standards. This data is shown in tables 6·1, 6·2, 6·3 and 6·4. The results from both the TFA and HCl hydrolysis of the monosaccharides are shown for CAB TIMP-1 and NCAB TIMP-1.

Monosaccharide	Concentration/mM	Relative %
fucose	0·039	4·1
galactosamine	0·021	2
glucosamine	0·552	59
galactose	0·238	25
mannose	0·08	8·5

Table 6·1. Monosaccharide composition of CAB TIMP-1 (HCl hydrolysis).

Monosaccharide	Concentration/mM	Relative %
fucose	0·12	8
galactosamine	0·002	0·2
glucosamine	0·609	40
galactose	0·576	38
mannose	0·199	13

Table 6·2. Monosaccharide composition of CAB TIMP-1 (TFA hydrolysis).

Monosaccharide	Concentration/mM	Relative %
fucose	-	-
galactosamine	-	-
glucosamine	1.081	79.68
galactose	0.277	20.4
mannose	-	-

Table 6.3. Monosaccharide composition of NCAB TIMP-1 (HCl hydrolysis). Very small peaks could be observed at retention times indicative of fucose galactosamine and mannose (slightly larger peak). However, these were not identified as peaks by the software and their concentration was not determined.

Monosaccharide	Concentration/mM	Relative %
fucose	0.121	8.67
galactosamine	-	-
glucosamine	0.676	48.64
galactose	0.371	25.59
mannose	0.227	16.72

Table 6.4. Monosaccharide composition of NCAB TIMP-1 (TFA hydrolysis). No significant peak was observed for galactosamine.

Both HCl and TFA were used for chemical deglycosylation because slightly different results are obtained using the different acids (as can be seen in the tables above). However, the differences between the two acid hydrolyses are not large and the overall picture for each TIMP-1 form (CAB and NCAB) is very similar. For all four analyses the chromatograms recorded for the blank controls showed only glucose at higher concentrations than in the samples. From this it was concluded that glucose was not present in the samples. The composition of both glycoforms is very similar. Galactosamine is present at trace quantities (< 2%) and fucose makes up 4-8% of the total. Although complete data was not obtained for mannose it appears to be very similar for both glycoforms and is present at slightly greater than 10% of the total. The primary difference is the relative quantities of galactose and glucosamine. In the NCAB form there is more glucosamine and less galactose (by percentage) than the CAB form. Since the material for these analyses was obtained from Western blots it was not possible to quantify the amount of each sugar, only the relative proportions.

NMR Analysis

The one-dimensional spectrum of CAB TIMP-1 in D₂O is shown as figure 6.5. Some of peaks in the amide N-H region (downfield of approximately 7 ppm), may be due to signals from N-acetylated sugars. A dominant feature of the spectrum is a number of sharp peaks due to mobile sugar residues, the majority being found in the region between 3.5 and 4.5 ppm. These are due to the sugar ring protons, with the exception of the anomeric proton signals which are shifted to the region between 4.5 and 5.5 ppm. At higher field (about 2 ppm), resonances from the methyl group of N-acetylated sugar residues such as N-acetylglucosamine and sialic acid are evident.

The region containing the majority of the sugar signals of a DQF-COSY is shown in figure 6.6. Cross peaks due to the anomeric protons of different sugars have strongly characteristic chemical shift coordinates in a 2D spectrum. These have been recorded for synthetic polysaccharides in D₂O and H₂O, and, although these could differ slightly in a

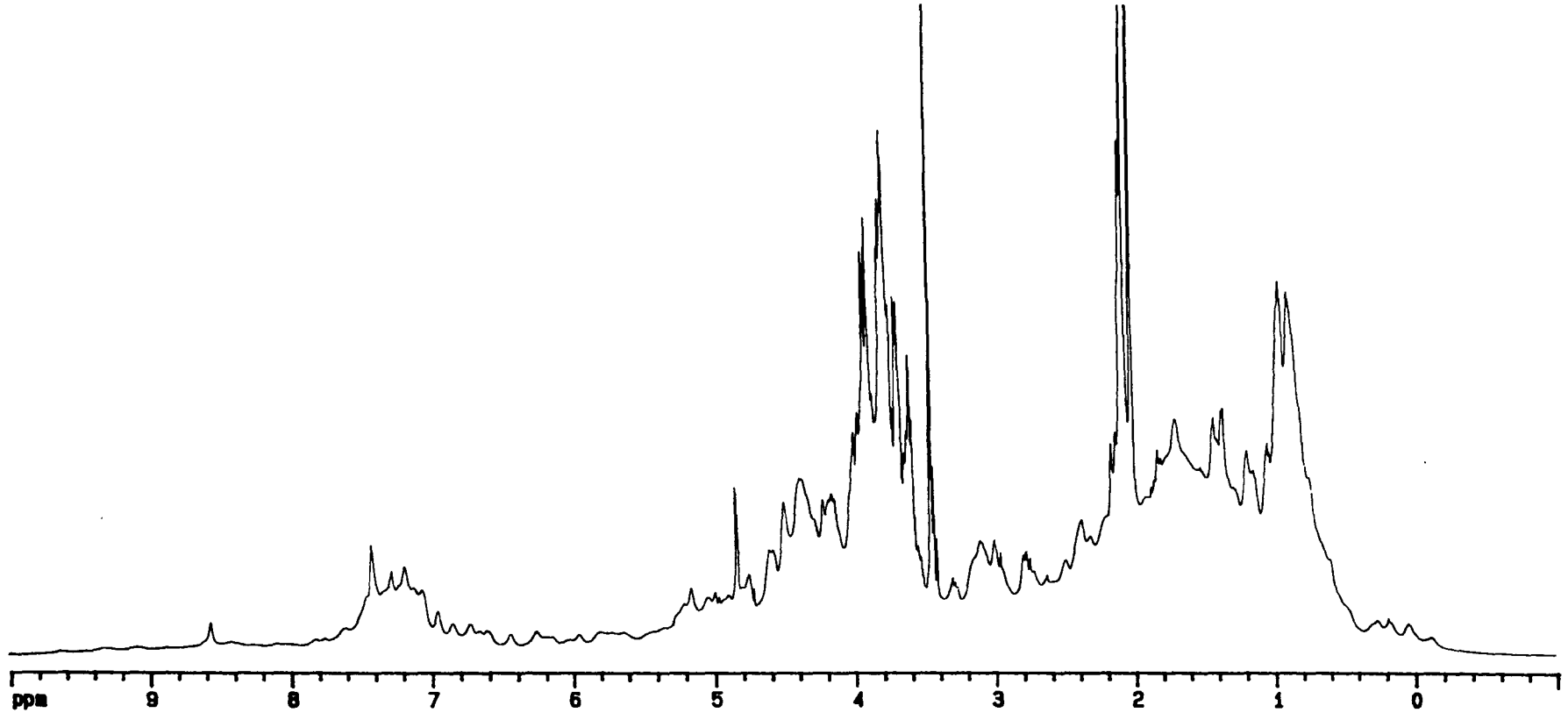


Figure 6-5 1D NMR spectrum of TIMP-1 in D₂O. The sharp peaks indicated are from the sugars which are both very abundant and have greater mobility. The result of this is that much of the protein spectrum is obscured.

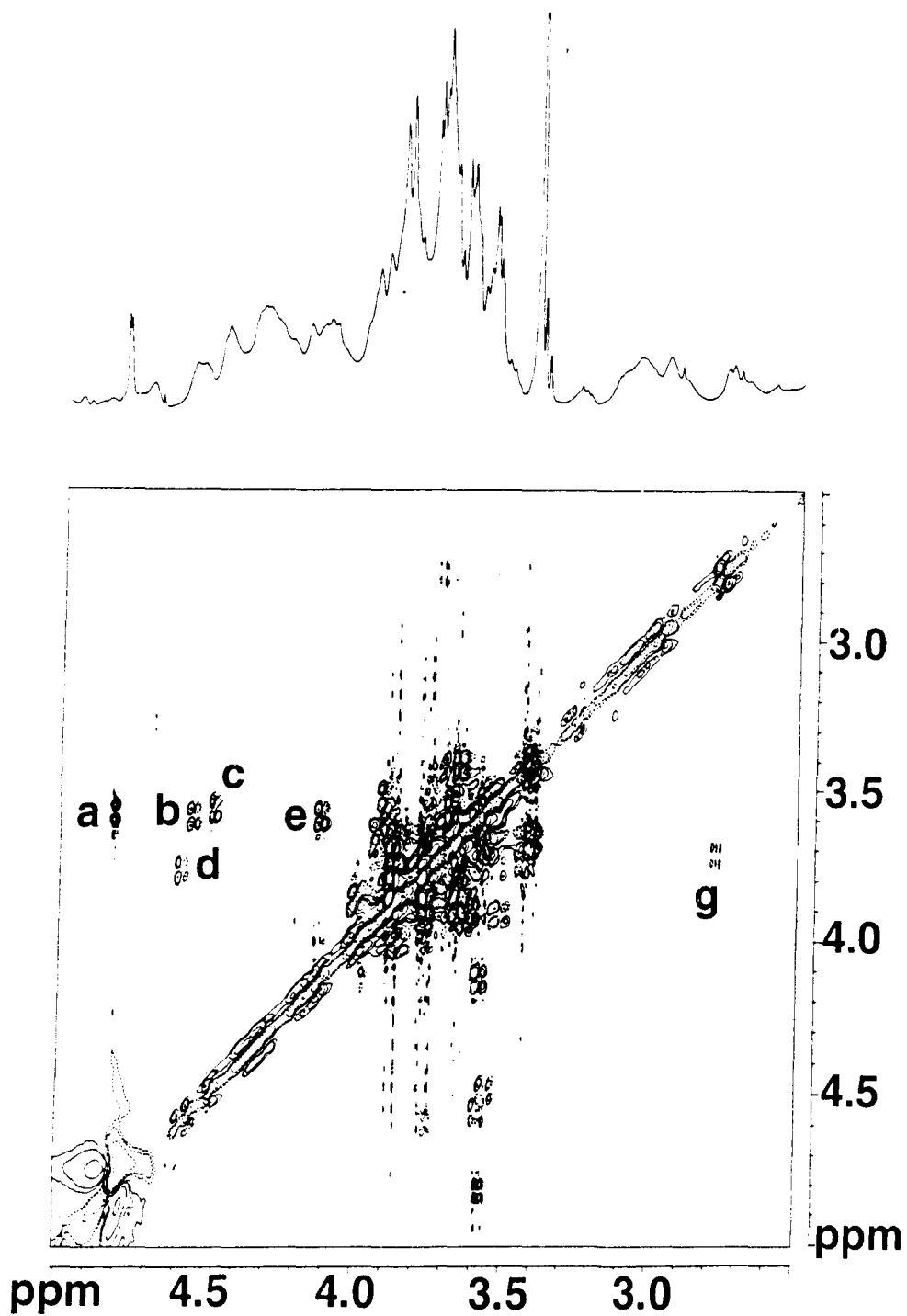


Figure 6-6. Section of COSY spectrum of TIMP-1. Non-methyl sugar region, with assigned cross peaks labelled as referred to in the text, except peak f, which is only apparent at a much higher plot gain.

glycoprotein spectrum, the difference in most cases will be only a few hundredths of a ppm. By referring to the published resonance frequencies, it was possible to identify some of the monosaccharide types in TIMP-1. The cross peaks of interest in figure 6-6 are labelled a to g. Cross-peak (a) is ambiguous: it may be from mannose, although it does not fit any of the tabulated shifts closely. The appearance of the cross-peak suggests a small J_{H1-H2} consistent with the axial-equatorial interaction expected in a β -linked mannose residue. However, it may also be α -linked fucose. Cross-peak (b) may reflect the $H1\beta$ - $H2$ connectivity of galactose at the non-reducing end of an oligosaccharide chain. Cross peak (c) is also due to the $H1\beta$ - $H2$ protons of galactose, which in this case is located in the backbone. Cross-peak (d) is consistent with connectivities between the $H1\beta$ and $H2$ protons of glucosamine or glucose. Cross-peak (e) could be due to the connection between the $H4$ and $H5$ protons of galactose, this time at the reducing end of the oligosaccharide. Cross-peak (f) between resonances at 4.716 and 3.812 ppm is much weaker than the others. It may be a connectivity between the $H1\beta$ and $H2$ protons of a backbone glucosamine at a branch point in the oligosaccharide. Cross-peak (g) corresponds exactly to the connectivity between the $H3$ equatorial and $H4$ protons of sialic acid. Further cross-peaks would have been expected for the $H3_{ax}$ - $H4$ and $H3_{ax}$ - $H3_{eq}$ connectivities, but they occur in regions of the spectrum that are extremely crowded, thus preventing unambiguous assignment.

6.3.2. NMR Paramagnetic Probe Experiments.

The series of 1-D spectra recorded for the OH-TEMPO study is shown in figure 6-7. In these spectra line broadening can be seen as the concentration of the paramagnetic probe is increased. Certain signals were particularly affected by the presence of the probe. A large number of signals between 0 and 3.5 ppm show evidence of line broadening, in particular, those between 0 and 2 ppm. The highfield signals between 0 ppm and 0.5 ppm are usually associated with methyl groups located above the plane of aromatic rings in a folded protein structure. Further downfield, signals between 6 and 7 ppm also broaden in response to the probe. Sections of a COSY

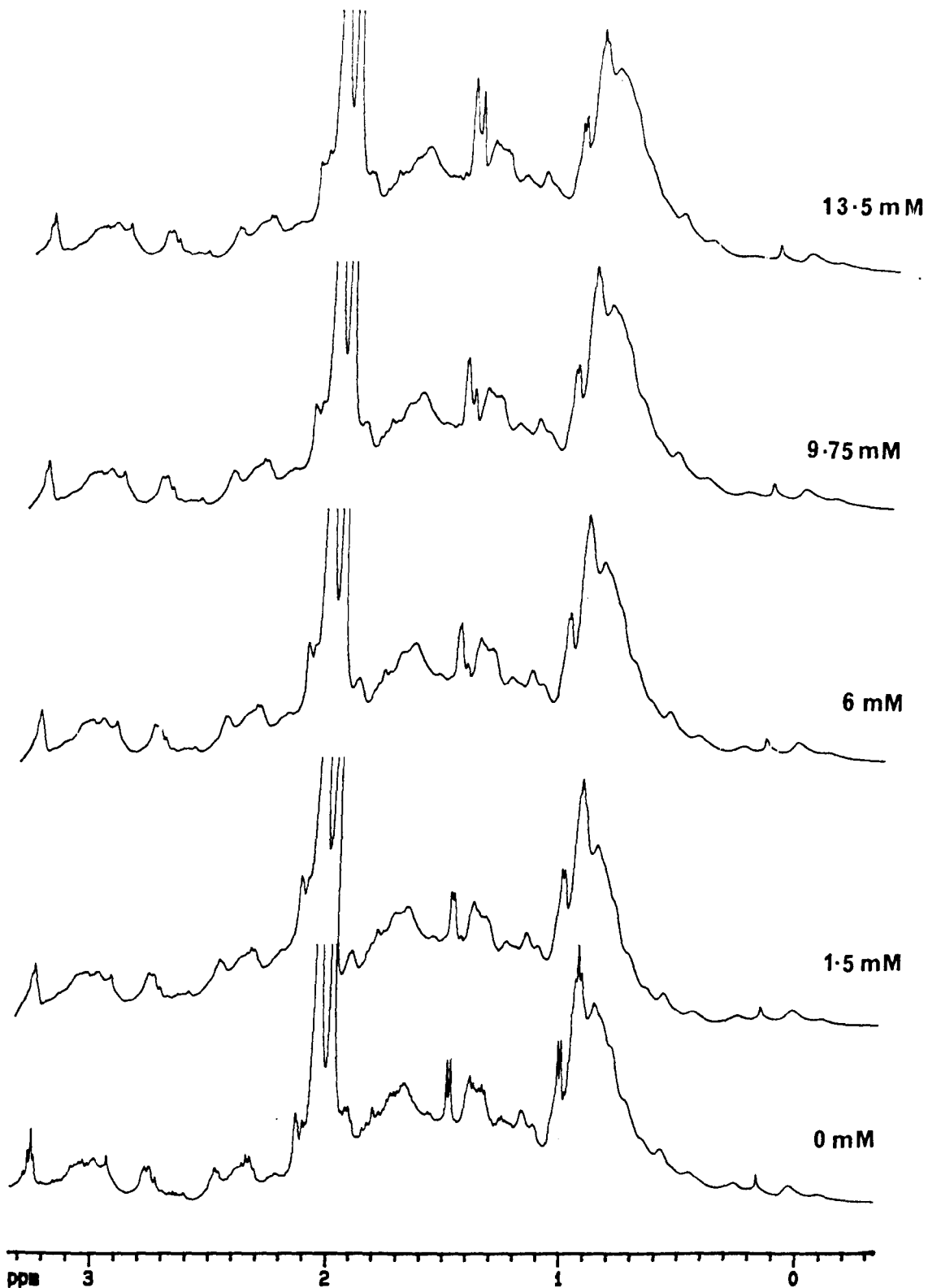


Figure 6.7. Series of 1D spectra of TIMP-1 showing the effect of the spin probe, OH-TEMPO. The concentration of OH-TEMPO is marked next to each spectrum. A number of peaks show clear line broadening as the concentration of OH-TEMPO is increased. Those at highfield could be attributed to the side chains of residues such as Val, Leu or Ile. The downfield peaks may be associated with tryptophan side chains.

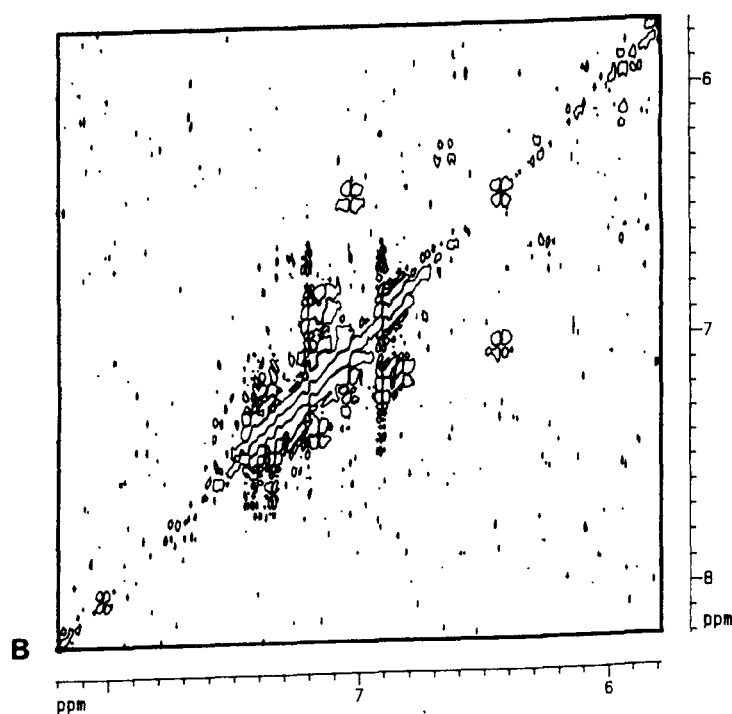
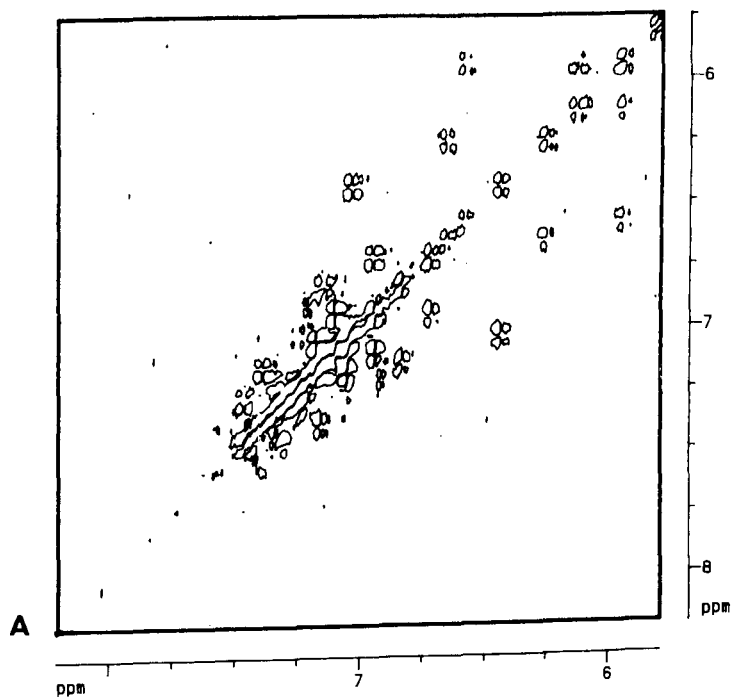


Figure 6·8. COSY spectra of TIMP-1, without (A) and with (B) 13.5 mM OH-TEMPO. The section shown is part of the aromatic region. A number of cross peaks are absent from spectrum B. These may be due to Tyr, Phe or Trp.

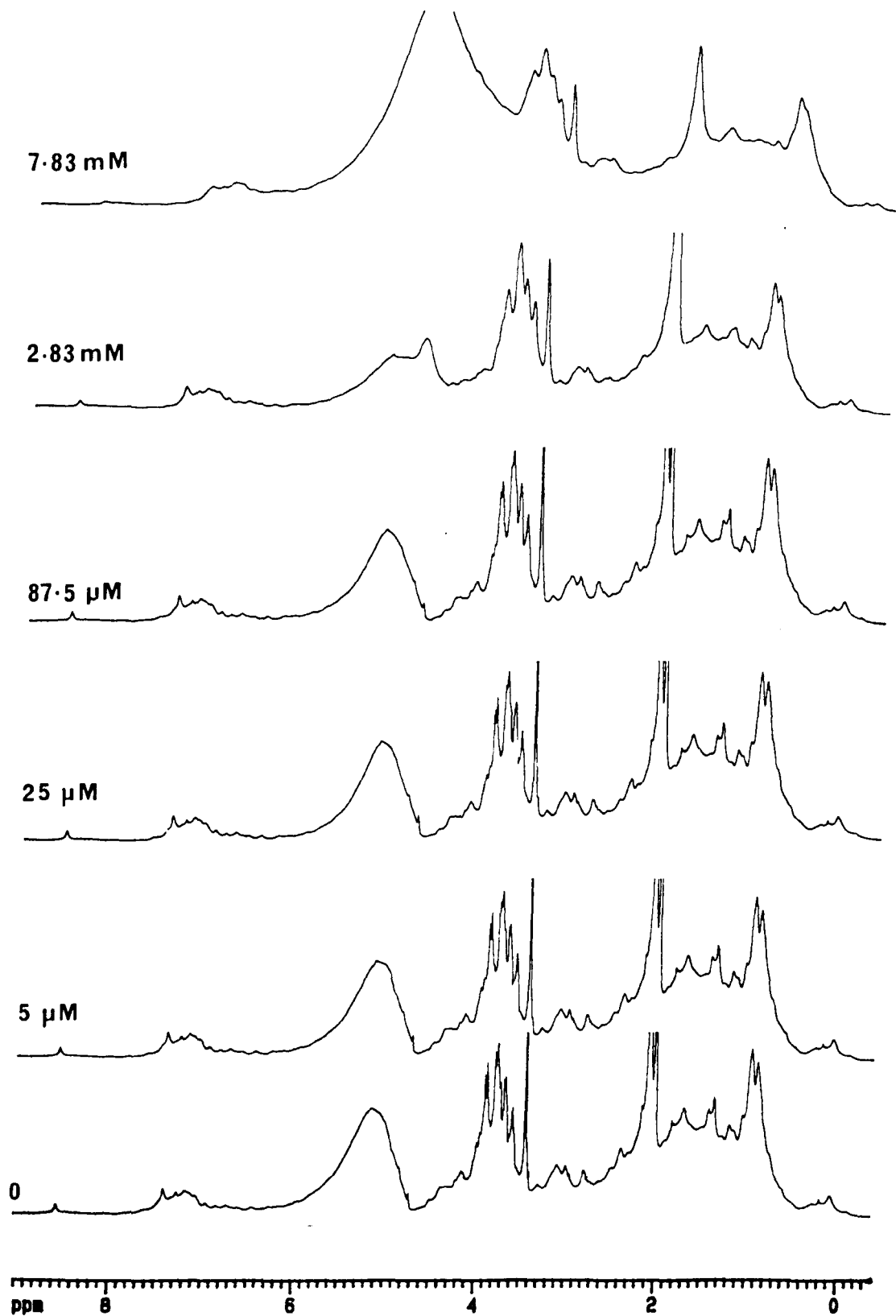


Figure 6.9. Series of 1D spectra of TIMP-1 showing the effect of the spin probe, MnCl_2 . A large number of peaks in the spectrum exhibit line broadening as the concentration of MnCl_2 is increased.

spectrum recorded with the highest OH-TEMPO concentration are shown alongside COSY spectra recorded for the sample prior to the addition of the probe (figure 6·8). These clearly show where line broadening has occurred in the aromatic region. Cross peaks associated with two separate spin systems have been broadened such that they have effectively been removed from the spectrum. One spin system has observable peaks at 6·24 and 6·67 ppm. From these chemical shift co-ordinates, these resonances are tentatively assigned as being from the aromatic ring of a tyrosine residue. The other spin system has peaks at 5·94, 6·12 and 6·58 ppm. These may be from the aromatic ring of either tryptophan (with some resonances overlapped) or phenylalanine. Alternatively they may also be due to a tyrosine ring which is flipping slowly.

A similar series of 1D spectra is shown in figure 6·9, for the experiments using increasing concentrations of MnCl₂. Here, extensive line broadening can be seen for many signals as would be expected from the binding of Mn ions to charged surface groups (Asp and Glu).

6.3.3. ANS Binding Study.

Preliminary wavelength scans of the emission spectra were recorded for each sample and an ANS only control to approximate the wavelength where emission was the greatest (λ max). This was found to be close to 520 nm for all samples. Table 6·5 shows fluorescence measurements made at 510, 520 and 530 nm for ANS, TIMP, porcine collagenase fragment and TIMP + porcine collagenase fragment.

From the evidence in table 6·5, it would appear that the N-terminal fragment of collagenase does not have any binding sites for ANS and no further study was made of it.

For TIMP-1 two titrations were performed in an attempt to determine the number and affinity of the ANS binding sites that are present. The first used a varying concentration of protein and a fixed concentration of ANS, in the second, the protein concentration was kept fixed and the ANS concentration varied.

	510 nm	520 nm	530 nm
ANS	37.3	39.85	38.0
TIMP-1	0.5	0.4	0.3
Collagenase Fragment	0.3	0.3	0.2
ANS/TIMP	43.65	45.9	42.1
ANS/Collagenase Fragment	38.05	40.05	38.3
TIMP/Collagenase Fragment	0.7	0.6	0.45
ANS/TIMP/Collagenase Fragment	47.05	48.2	44.65

Table 6.5. Fluorescence of TIMP-1, Porcine Collagenase N-terminal fragment and ANS in combination. The figures given are in arbitrary units. The protein alone makes little contribution to the total fluorescence of samples and the increase on the addition of ANS is small for TIMP containing samples. There is effectively no change in the fluorescence when ANS is added to collagenase fragment alone. When TIMP and collagenase fragment are present (with ANS) the fluorescence is higher than that of either component alone.

The protein titration was used to generate a calibration factor giving the units of fluorescence change per micromole of ANS bound. This figure was obtained from the y intercept of a plot of $1/\text{fluorescence}$ against $1/[\text{protein}]$ (figure 6.10). For TIMP-1 the calibration factor is 10.3. The ANS titration was used to find the difference in fluorescence (ΔF) between the sample + ANS and ANS alone (figure 6.11). The calibration factor and ΔF were used to create binding isotherms for the sample (figure

Figures 6·10 to 6·14 show the stages involved in analysing the protein and ANS titration data to give final Klotz and Scatchard plots. Values are derived from these plots for the number and average affinity of any ANS binding sites present on TIMP-1. Curve fitting was carried out using the Kaleidagraph analysis package for Apple Macintosh. Data for figure 6·10 was fitted to a curve with the equation $y=m1-(m2/(m3+m0))$, all other data could be fitted to conventional formats (i.e. smooth, exponential or linear). $m0$ represents the x values.

Figure 6·10 is used to calibrate the experiment by determining the maximum increase in fluorescence/ μ M ANS bound. This is taken from the y intercept of the plot (at infinite protein concentration, where no ANS is free in solution). Figure 6·11 shows the titration of ANS alone, ANS plus protein and the third curve, and the difference between them (ΔF , the change in fluorescence caused by ANS binding). This set of values (ΔF at different ANS concentrations) is converted into moles of ANS bound per mole of TIMP-1 by multiplication with the calibration factor (10^{-3}) derived from figure 6·10. Figure 6·12 shows the amount of ANS bound (v) plotted against the concentration of free ANS. The concentration of free ANS is derived by calculating the total amount of ANS bound to the TIMP-1 (from v and the protein concentration) and subtraction from the total amount of ANS in the sample. This plot shows the equilibrium between free and bound ANS. The data was fitted to an exponential curve with an R factor of 0·95. However the majority of the data would also fit linearly in the absence of the point at 0 moles of ANS bound. This point was included to represent zero ANS binding and was not used in subsequent calculations.

To calculate the number and affinity of ANS binding sites on TIMP-1, the amount of ANS bound (v) and the amount of free ANS are presented as a linear Scatchard plot in figure 6·13. The x intercept indicates the presence of one, and one partial binding site and the gradient shows an average K_d of 2.6×10^4 M. Although linear, the fit to the data is not good (the R factor of 0·8 where an R factor of 1 indicates a perfect fit). A better fit was obtained from a Klotz analysis of the data (figure 6·14). Here the data is presented as a double reciprocal plot of $1/v$ (moles of ANS bound per mole of TIMP-1) against $1/\text{the concentration of free ANS}$. In this case the linear fit had an R factor of 0·98. The value at the y intercept shows that one binding site is present with a K_d of $3.3 \times 10^4\text{M}^{-1}$ (from the gradient).

6.12). This was achieved by multiplying the values for ΔF by the calibration factor to give v . The resulting curve shows the number of moles of ANS bound per mole of protein. This can then be used to generate either Scatchard [316] or Klotz [317] plots for the data (figures 6.13 and 6.14) from which the number of binding sites and an average Ka can be calculated.

From the linear Scatchard plot, one complete and one partial binding site was indicated with an average Ka of $2.6 \times 10^4 \text{ M}^{-1}$. The R factor of 0.8 indicates that the results drawn from this plot are not very accurate. When a Klotz plot was used it was found that a single binding site was present with a Ka of $3.3 \times 10^4 \text{ M}^{-1}$. In this case the R factor was close to 1, (0.98) indicating an excellent fit to the data.

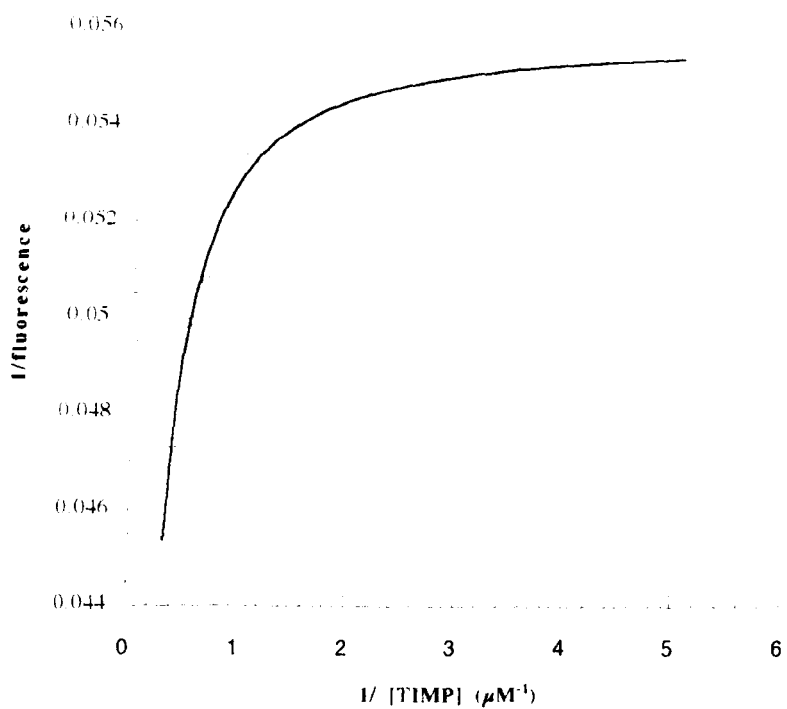


Figure 6.10. Calibration Plot for TIMP-ANS Binding.

The y intercept (infinite protein concentration) of this double reciprocal plot represents the maximum increase in ANS fluorescence per μM ANS bound.

The y intercept is taken from the equation describing the curve.

This value is found to be 10.3 units/ μM (of ANS bound).

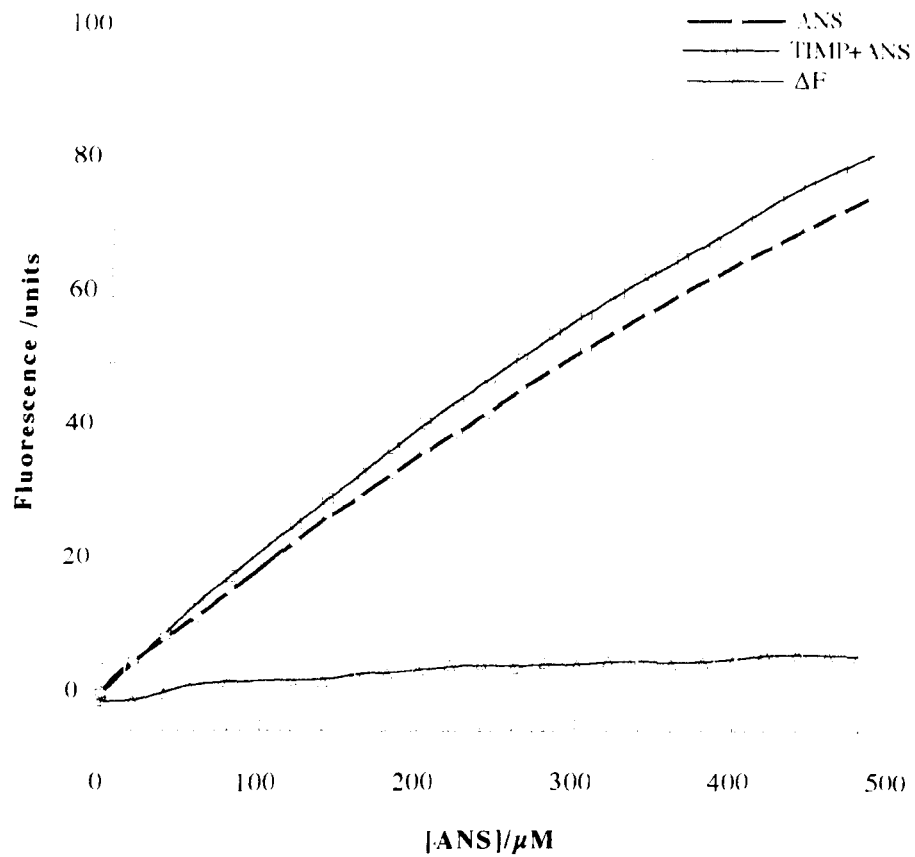


Figure 6-11. ANS Titration for TIMP-1.

Protein concentration is kept fixed at $1\mu\text{M}$. The fluorescence of ANS alone and the small inherent protein fluorescence is subtracted to give ΔF .

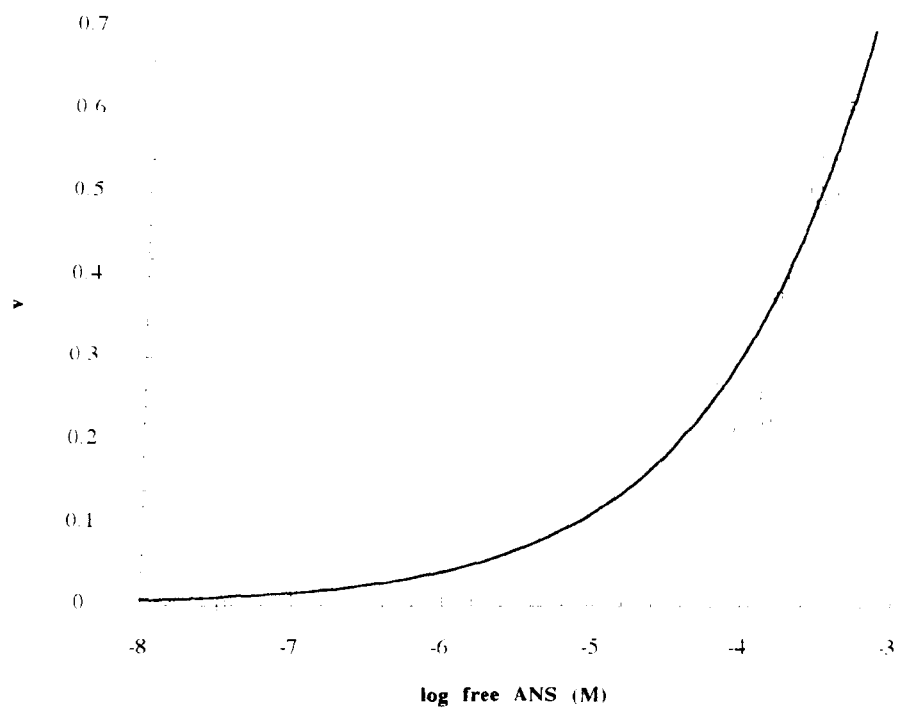


Figure 6-12. Binding Isotherm for TIMP-1-ANS.

Where v is the number of moles of ANS bound per mole of protein, calculated from ΔF and the calibration factor.

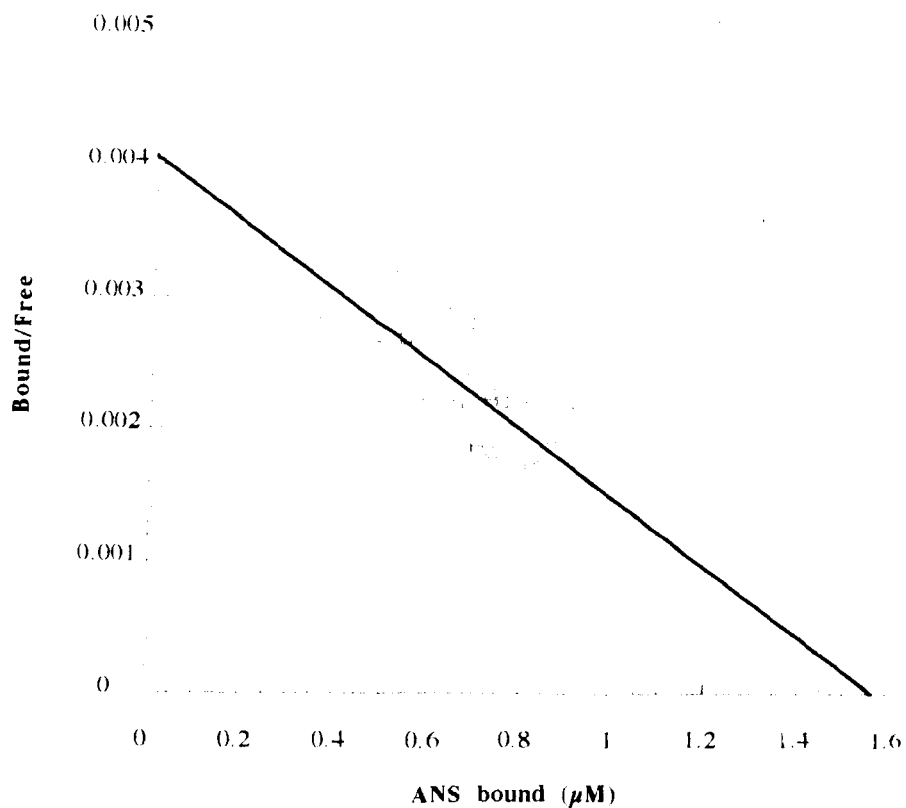


Figure 6-13. Scatchard Analysis of ANS Binding to TIMP-1.

The plot is linear indicating that the binding is non-cooperative. The x intercept shows one complete and one partial binding site present. The K_a (- gradient) is $2.6 \times 10^4 \text{ M}^{-1}$. The R factor is 0.8.

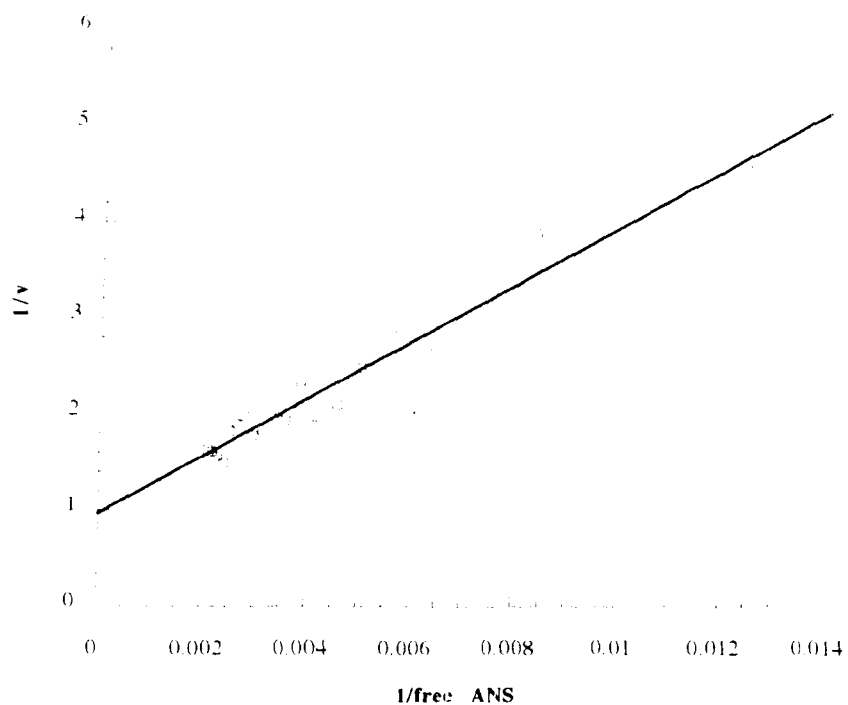


Figure 6.14. Klotz-Plot Analysis of TIMP-ANS Binding.

The number of binding sites is taken from $1/y$ intercept. The K_a is derived from $1/\text{gradient}$. From this plot, there is a single binding site with a K_a of $3.3 \times 10^4 \text{ M}^{-1}$. The R factor for this curve fit is 0.98.

6.4. Discussion

In this chapter a number of different techniques have been used to study some of the surface features of TIMP-1. A short study has also been made of the N-terminus of collagenase, and how it might interact with TIMP-1.

To date there has been no detailed analysis of the carbohydrate present on the human form of TIMP-1. Two sites for N-linked glycosylation are apparent from the amino acid sequence and treatment with endoglycosidases gives a two stage deglycosylation showing that both available sites are occupied [129]. Previous studies have also been made of the charge of the sugars. TIMP-1 has a large number of pIs which generally reduce to a single band on removal of sialic acid residues using neuraminidase [134]. Other than an estimate of the number of sugar residues present and evidence from the lectin binding behaviour, no analysis has been made of the carbohydrate composition.

A detection method for use on Western blots has been devised to identify glycoproteins. Biotinylated Concanavalin A was chosen as the detecting agent because it has an affinity for the type of sugars likely to be found at an O-linked site. The biotinylated form was used to detect and amplify the signal. The results show that even after treatment of wild type TIMP-1 with PNGase F, a band is still present at 21 kDa on the blot after staining for carbohydrates. This band is also seen in Western blots using the TIMP-1 polyclonal detection method (chapter 4). This result indicates that TIMP-1 may have more glycosylation sites than have previously been identified. Since these additional sugars are not removed after extended treatment with PNGaseF, it is likely that they are not N-linked. The next most common type of glycosylation is at an O-linked site, where the initial sugar is attached to an amino acid with a free hydroxyl group (i.e. serine or threonine).

It is also possible that the bands seen in this experiment are an artifact. There may be a non-specific interaction occurring between the proteins present and the lectin,

possibly as a result of using an excess of Concanavalin A. Since only a few of the proteins in the marker lane, and none of the BSA used in the blocking step responded, it is unlikely to be a general protein-lectin binding.

However, the nature of this additional glycosylation remains to be determined. Since recombinant TIMP-1 is known to have normal inhibitory activity against the MMPs, it is unlikely to be important for function. It is possible that this additional glycosylation is a spurious feature of TIMP-1 produced by cultured cells. A similar study of TIMP-1 purified from human tissues would be required to confirm whether this is the case.

Human TIMP-1 is known to have heterogeneous glycosylation. Multiple pIs and differential binding to Concanavalin A-Sepharose have been observed. Both CAB and NCAB TIMP-1 were purified and studied by IEF. The patterns of bands seen on these gels confirm that TIMP-1 has a heterogeneous mix of carbohydrates present. The CAB and NCAB forms show different IEF patterns, which collapse to patterns which still differ after treatment with neuraminidase. This shows that there is heterogeneity in both the composition and charge of the carbohydrates, and that the apparent separation of glycoforms by Concanavalin A-Sepharose is genuinely separating two different pools of material.

HPLC analysis of monosaccharides removed from both CAB and NCAB TIMP-1 by acid hydrolysis confirms the heterogeneity seen in IEF. CAB TIMP-1 has relatively less glucosamine and relatively more galactose than NCAB TIMP-1. This differs from the composition of the bovine TIMP-1 [132], which has a much greater mannose (25% of the total compared with 8% for human TIMP-1) content. The glucosamine content of bovine TIMP-1 is similar to CAB TIMP-1 whilst the galactose content is similar to NCAB TIMP-1.

A similar picture was obtained in the NMR study of the carbohydrates. It was possible to identify certain individual sugar residues from the chemical shifts of the

anomeric and H2 protons of the carbohydrate groups. Galactose has been identified in the backbone and at both the reducing and non-reducing ends of the carbohydrate chains, while glucose or glucosamine (more probable in view of the HPLC analysis) may be present at a branch-point in a chain. Sialic acid is present, but no other sugar type was specifically identified. Mannose was not unambiguously identified, with no clear resonances from mannose protons in the 2D spectra. Unfortunately it is not possible to quantify the sugars from the intensities of the COSY cross-peaks.

Since sialic acid does not participate in the binding to Concanavalin A, one explanation for the differential binding to this lectin lies in the different proportions of galactose and glucosamine. This might be due to the loss of galactose or addition of glucosamine residues in NCAB TIMP. Concanavalin A binds α -mannose, α -glucose and sterically related residues. Subsequently the differential binding may reflect a different spatial arrangement of sugars that does not expose sufficient sterically correct hydroxyl groups for a strong interaction with Concanavalin A.

NMR was also used to study another aspect of the surface of TIMP-1. In this study spin probes were used to identify signals from charged, or hydrophobic surface residues. As would be expected, the MnCl probe caused a large number of signals to broaden. Most of these were in the region where signals from acidic side chains would normally be seen.

When the hydrophobic spin probe, OH-TEMPO was added to the TIMP-1 sample, a number of peaks in the aromatic and highfield (above 1 ppm) regions of the spectrum broadened. This indicates that one or more hydrophobic residues are exposed on the surface of the protein. From the chemical shift of the aromatic signals it is possible that at least one of these residues is a tyrosine. The identity of the second susceptible spin system is less clear. The signals are more dispersed than those expected from the aromatic ring of Phe, but a complete tryptophan ring system is not observed. It is possible that the additional tryptophan peaks are very weak or overlapped with others.

Both of these spin systems are found at a low chemical shift. This may indicate that each lies close to another aromatic ring in an unusual (possibly exposed) environment.

The broadening effect seen with the high field signals may be related to the exposed aromatic residue(s). These highfield signals are probably from methyl groups on side chains that lie close to an aromatic ring. Since they are affected by the OH-TEMPO they may be close to an exposed hydrophobic residue. Interestingly, in another experiment [131] TIMP-1 was treated with the reagent, 2-nitrophenylsulphenylchloride (2-NPSCI) which modifies tryptophan residues. It was found that the use of a 5.6 fold excess of 2-NPSCI resulted in a 55% decrease in inhibitory activity of TIMP-1.

Data from the solution structure of the N-terminus of TIMP-2 [141] shows that several hydrophobic residues are exposed on the surface of the molecule. These are Phe-103, Leu-85, Trp-107, Leu-118 and Tyr-122. They form part of a concave face that also includes His-7. The evidence presented here suggests that TIMP-1 also has a number of exposed hydrophobic residues. In TIMP-1 all but one of these residues is homologous to TIMP-2 (Leu-118 is substituted by Phe-116). It is possible that this concave site will also be found on TIMP-1.

Experiments studying the effects of ANS binding on TIMP-1 also indicate that one or more hydrophobic groups may be exposed on the surface. The increase in fluorescence on the addition of ANS to TIMP-1 shows that the ANS molecule is binding to the protein surface. The titration against ANS indicates that there is probably only a single low affinity binding site present. An additional study with the N-terminal fragment of recombinant porcine collagenase found that no ANS binding sites were present on the enzyme. When the collagenase fragment, and TIMP-1 were incubated together prior to the addition of ANS, the fluorescence seen was greater than for TIMP-1 alone. This suggests that an interaction between the two molecules had altered the hydrophobic surface of one, or both proteins.

Although a titration analysis was carried out using a 1:1 ratio of TIMP and collagenase fragment, the analysis is complicated by the fact that a large excess of TIMP-1 (50 fold) is required to inhibit the N-terminal fragment of collagenase [28]. Such large quantities of TIMP-1 (in the order of 15 mg per sample) are not available.

The increased fluorescence in the presence of collagenase fragment could suggest that a conformational change has occurred on binding, increasing the accessibility of the ANS binding site. It cannot be assumed that the ANS binding site on TIMP-1 is the same one that is present in the TIMP-1-collagenase fragment complex. It is possible that the first site is blocked by the interaction with the collagenase fragment and a second site becomes available as a result of conformational changes. Another explanation is that additional sites have been exposed on one or both proteins. To fully investigate this phenomenon it will be necessary to determine the proportion of protein found as a complex in the mixture. Also the rate at which the complex forms and dissociates may affect the results seen. If an ANS binding site is buried on interaction and additional sites exposed the data will be further complicated by a heterogeneous mix of the two species.

A simpler, and more biologically relevant study would be made using intact porcine collagenase, adding the ANS both before and after the TIMP-1. Sufficient quantities of full length enzyme have been made available and these studies are now in progress.

Chapter 7.

Study of a Peptide Derived From the N-terminus of TIMP-1.

7.1. Introduction.

The inhibitory activity of TIMP-1 has been shown to be primarily in the N-terminus [230]. Consequently a great deal of attention has been focused on this region, to identify residues that are important for inhibition of the MMPs. Of particular interest are the first 23 residues, which show a high degree of conservation throughout the TIMPs. As discussed in the introduction, a high degree of homology may be an indication of either a structurally, or a functionally important feature. Deletion of the VIRAK (residues 18-22) sequence results in virtually no protein production [244] suggesting it has a structural role (confirmed on the publication of the TIMP-2 N-terminal structure). The region between Cys-3 and Cys-13 has been implicated in the inhibition of the MMPs. Mutants where His-7 and Gln-9 were substituted have reduced inhibitory activity [244]. Also modification with DEPC indicated that a histidine residue was involved in the inhibition of the MMPs. However, the evidence pointed more to His-95, rather than His-7 in this experiment.

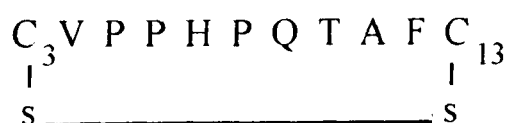
By analysing the N-terminal sequences of all the known TIMP sequences a clear consensus is seen for the first thirteen N-terminal residues. This consensus is CXCXHPQX AFC. A search of the EMBL database using this consensus sequence identified all the TIMP sequences, as would be expected. Interestingly another family of proteins was also shown to have a strong homology to this consensus sequence. This was the Bowman-Birk family of proteinase inhibitors. These are a group of small serine proteinase inhibitors found in plants (i.e. soybean, adzuki bean and cowpea). They are able to inhibit both trypsin and chymotrypsin, using different regions of the molecule.

This type of inhibitor is known as "double headed". The region of homology between the soy bean inhibitor and the TIMP consensus sequence is shown below.

	10
TIMP consensus	CXCXPHHPQXAFC
	: : : : :
Soybean BBI homologous sequence	CICALSYPAQCFC
	40 50

This homologous region includes the residues that are involved in the inhibition of chymotrypsin (Tyr-44 and Ser-43). The solution structure of this protein has been determined [318]. This region is found as a loop, disulphide bonded at the base (Cys-41 Cys-49), which exposes the inhibitory residues. When this loop was isolated from the rest of the protein it retained inhibitory activity, although the *K_i* was reduced [319]. It was postulated that, although these are two very different families of inhibitors, they may be using a similar structure to expose crucial residues for the inhibition of their respective enzyme.

The high conservation of the N-terminal sequence of the TIMPs, the sensitivity of His-7 and Gln-9 to mutation, and the intriguing similarity to the Bowman-Birk inhibitors suggested it may be possible for a peptide based on the N-terminal sequence of a TIMP to show inhibitory activity. A peptide was produced, based on human TIMP-1, with the sequence:



The residues are numbered according to their position in the original TIMP-1 sequence for clarity. The peptide was initially obtained with the two cysteines joined by a disulphide bond, creating a cyclised molecule. This was to ensure that no free sulphhydryl groups were available to interact with the active site of the enzymes assayed. Any interaction between the enzymes and free thiol groups may have given a false impression of inhibitory activity.

In this chapter the peptide Cys-3 - Cys-13 is assayed for activity against a number of different enzymes in both cyclised and linear (reduced and methylated) form. The cyclised form was also studied by NMR in both H₂O and the structure stabilising solvent TFE-d₂.

7.2. Methods.

7.2.1. Materials.

The 11-mer peptide CVPPHPQTAFC was purchased in oxidised form from Bachem Ltd, California. TFE-d₂ was from Fluorochem, Glossop, Derbyshire UK. Methyl iodide (MeI), DFP and DTT were from Sigma Chemical company, Poole, Dorset UK. Enzymes for assays were either purified in the Rheumatology Research Unit or purchased from Sigma.

7.2.2. Experimental Details.

Preparation and storage.

The freeze dried peptide was made up to 1 mM in H₂O for assays and stored in 200 µl aliquots at -20°C. Samples for NMR were made up in either 90% H₂O/10% D₂O or 100% TFE-d₂ at 31.4 mg/ml and stored at -20°C.

To reduce and methylate the peptide, 5 µl of 2M Tris buffer pH 8.0, and 5 µl 3M DTT were added to a 200 µl aliquot of the peptide (1 mM) and incubated for a minimum of 3hrs at 37°C. The MeI stock solution was diluted to 1M (1/16 dilution) in sterile H₂O and both the sample and MeI were chilled on ice. 5 µl of MeI (1M) was added and the mixture incubated at 4°C for 1 hour. To remove residual reagents, the samples were passed down a PD-10 desalting column using H₂O as the eluting buffer. Fractions of 200-250 µl were assayed for the presence of the peptide using the BCA assay and also assayed for inhibitory activity.

Assays.

Inhibitory activity against collagenase was assayed using the diffuse collagen fibril assay (chapter 2). Inhibitory activity against gelatinase was assayed using a similar method. ³H-gelatin was prepared by denaturing ³H collagen for a minimum of 30 minutes at 56°C in the presence of 2 mM DFP. 72 kDa gelatinase was used as the

equivalent of the active enzyme in the collagenase assay. Trypsin (10 μ l at 1mg/ml) is used as a control for total degradation of the gelatin. The assay tubes contain 100 μ l of Tris buffer (as for collagenase), 100 μ l of 3 H gelatin, 10 μ l of gelatinase, up to 40 μ l of sample and sufficient cacodylate buffer (as for collagenase) to make the volume up to 250 μ l. Samples are incubated for 20 hours at 37°C, then 50 μ l of 90% TCA is added. Samples are incubated on ice for 30 minutes, centrifuged at 37000 rpm for 10 minutes then counted. The assay for inhibitory activity against bacterial collagenase was adapted from the collagenase assay, using sufficient bacterial collagenase to give 70-80% lysis of the 'active enzyme control'. The assay for inhibitory activity against trypsin was a similar modification of the gelatinase assay.

NMR Studies.

All NMR experiments were carried out on either a Bruker AMX 360 or a Bruker AMX 500 spectrometer. The sample was prepared at a concentration of 30 mM in 90% H₂O/10% D₂O, and the pH adjusted to 5.32 with HCl. On completion of the H₂O experiments, the sample was lyophilised and re-dissolved in 100% TFE-d₂. All spectra for the H₂O sample were recorded at a temperature of 300K. One dimensional (1D) spectra were recorded for the TFE-d₂ sample over a range of temperatures and 2D spectra were recorded at either 273K or 283K. 2D spectra were acquired with 512 t₁ increments and 2048 t₂ data points. For TOCSY spectra [320] a total mixing time of 60 ms was used for the sample in H₂O and 63 ms for the sample in TFE-d₂. A DIPSI-2 spin lock [321] was found to give the best quality spectra. ROESY spectra [322] were acquired with a mixing time of 200 ms. Most NOESY [323, 324] spectra were acquired with a mixing time of 25 ms. Solvent suppression was achieved by a 1.5s saturation pulse. 2-D data were zero-filled once in F1 and Fourier transformed with the application of a $\pi/3$ shifted sine bell function in both dimensions.

7.3. Results.

7.3.1. Inhibitory Activity.

No inhibitory activity was seen against porcine fibroblast collagenase, trypsin or bacterial collagenase (data not shown). 72 kDa gelatinase however, was inhibited, although the effect was only seen at relatively high peptide concentrations. A thousand-fold excess is required to give a 10% reduction in the activity of gelatinase in a bioassay (sample activity of 13800 dpm compared to 15270 for the enzyme alone). The reduced, methylated form of the peptide does not show any activity against any of the enzymes assayed.

7.3.2. NMR studies of the Cyclised form of Cys-3 - Cys-13.

Since the cyclised form of the peptide showed a weak inhibitory activity against 72 kDa gelatinase a series of NMR experiments were performed to determine its structure.

Cys-3 - Cys-13 is a stable monomer under the conditions used. No evidence of aggregation or deterioration of the sample was observed in either solvent, even after extended periods at room temperature.

Cys-3 - Cys-13 in H₂O.

The 1D spectrum of this sample is shown in figure 7-1. Figures 7-2, 7-3, 7-4 and 7-5 show the TOCSY and ROESY spectra of Cys-3 - Cys-13 with the assigned cross peaks marked. The number of cross-peaks was far greater than would have been expected from a peptide of this size. The 1D spectrum shows a large number of relatively broad, low intensity peaks in the NH region, which correspond with the TOCSY cross-peaks. This indicates that there may be large number of conformers present. The spin systems were assigned primarily from the TOCSY experiment shown in figures 7-2 and 7-3. Where it was not possible to uniquely assign a particular spin system (i.e.

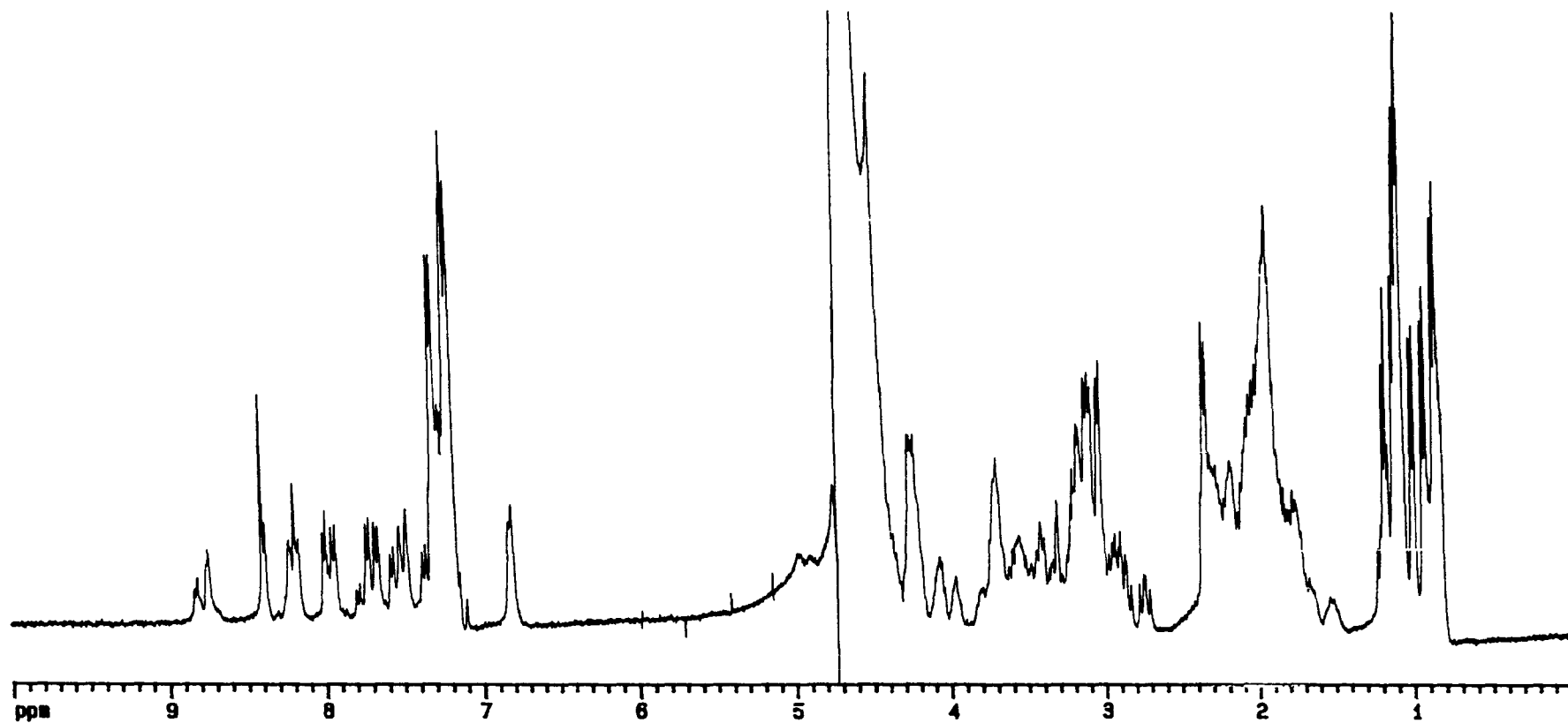


Figure 7-1. 1D spectrum of C_3-C_{13} in H_2O . The spectrum was recorded on a 360 MHz spectrometer at 300K on a 30mM sample. The high sample concentration and small molecular weight produce sharp lines and good resolution. The amide region shows a large number of peaks, an indication of multiple conformers.

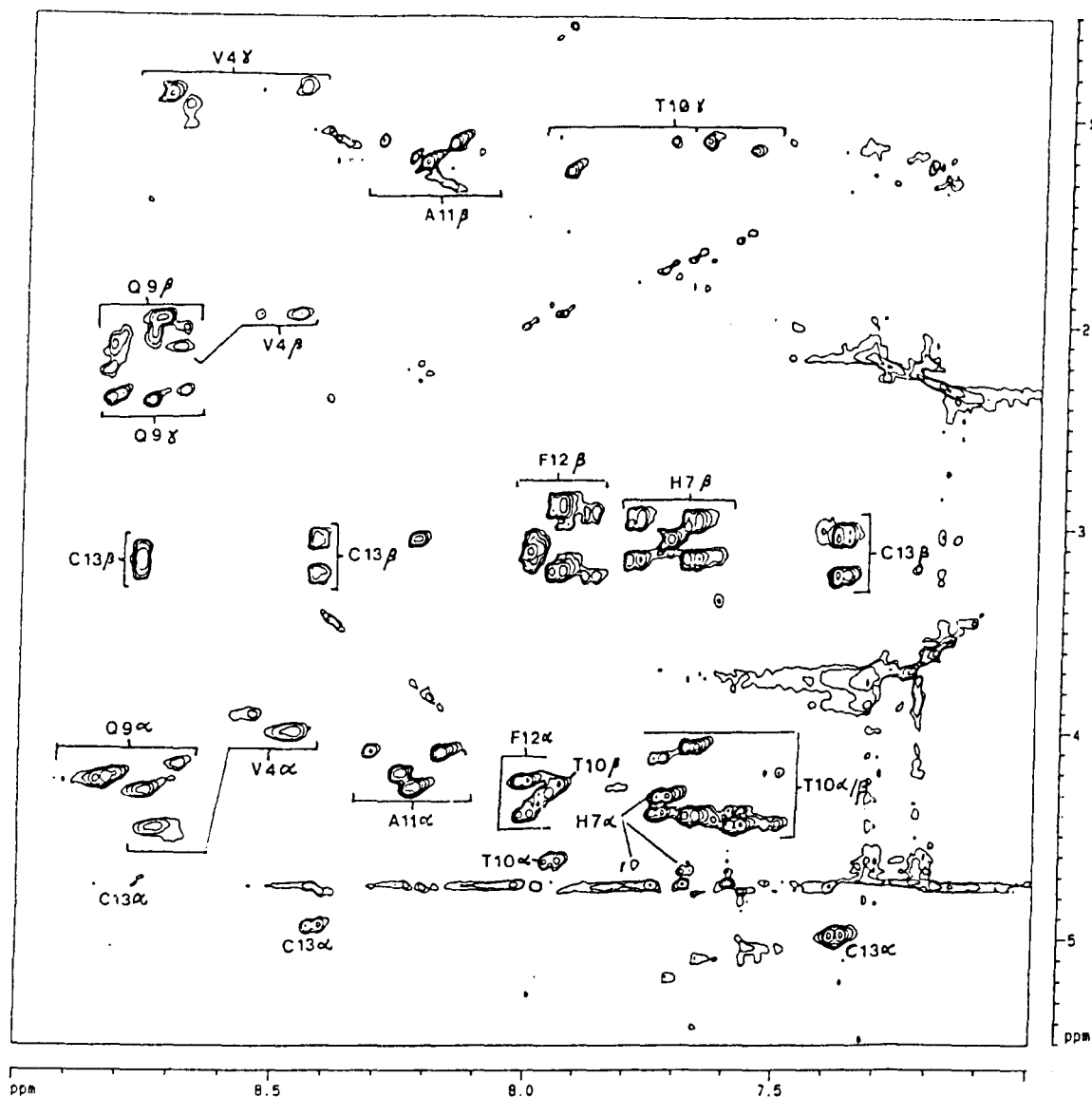


Figure 7-2. TOCSY of Cys-3-Cys-13 in H₂O. Off diagonal showing assignments for all residues except for prolines and C₃. Multiple conformers are grouped within brackets.

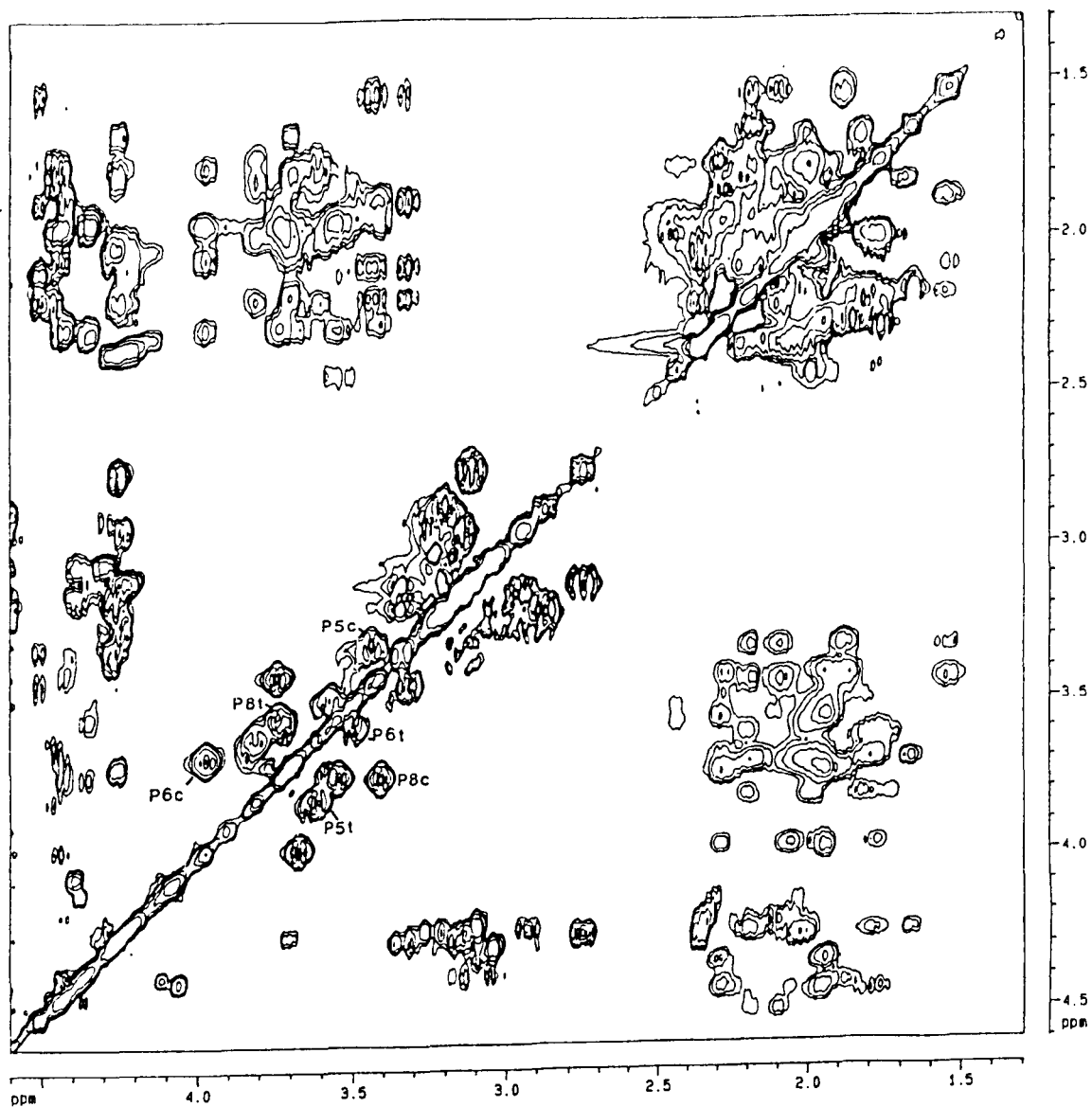


Figure 7-3. TOCSY of C_3-C_{13} in H_2O . Region taken from the diagonal to show the proline δ - δ cross peaks and demonstrate the isomerisation occurring (*t-trans*, *c-cis*). The intensities of all of these cross peaks are very similar indicating increased stability of the *cis* form.

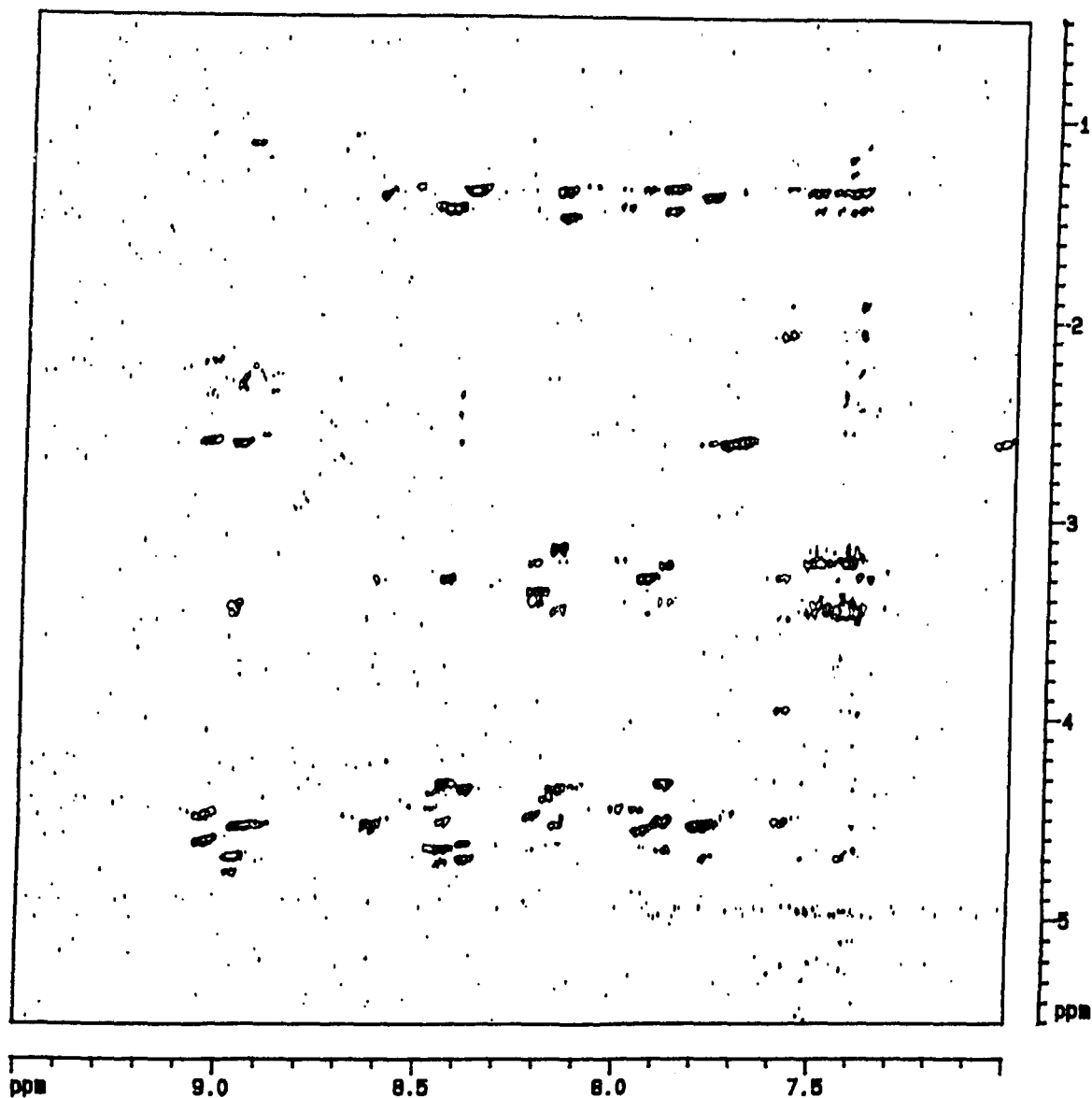


Figure 7-4. ROESY of C₃-C₁₃ in H₂O. Equivalent region to figure 7-2. The number of conformers at closely similar chemical shifts has resulted in a large number of very close ROEs. The total number of ROEs is not sufficient to uniquely identify any single conformer.

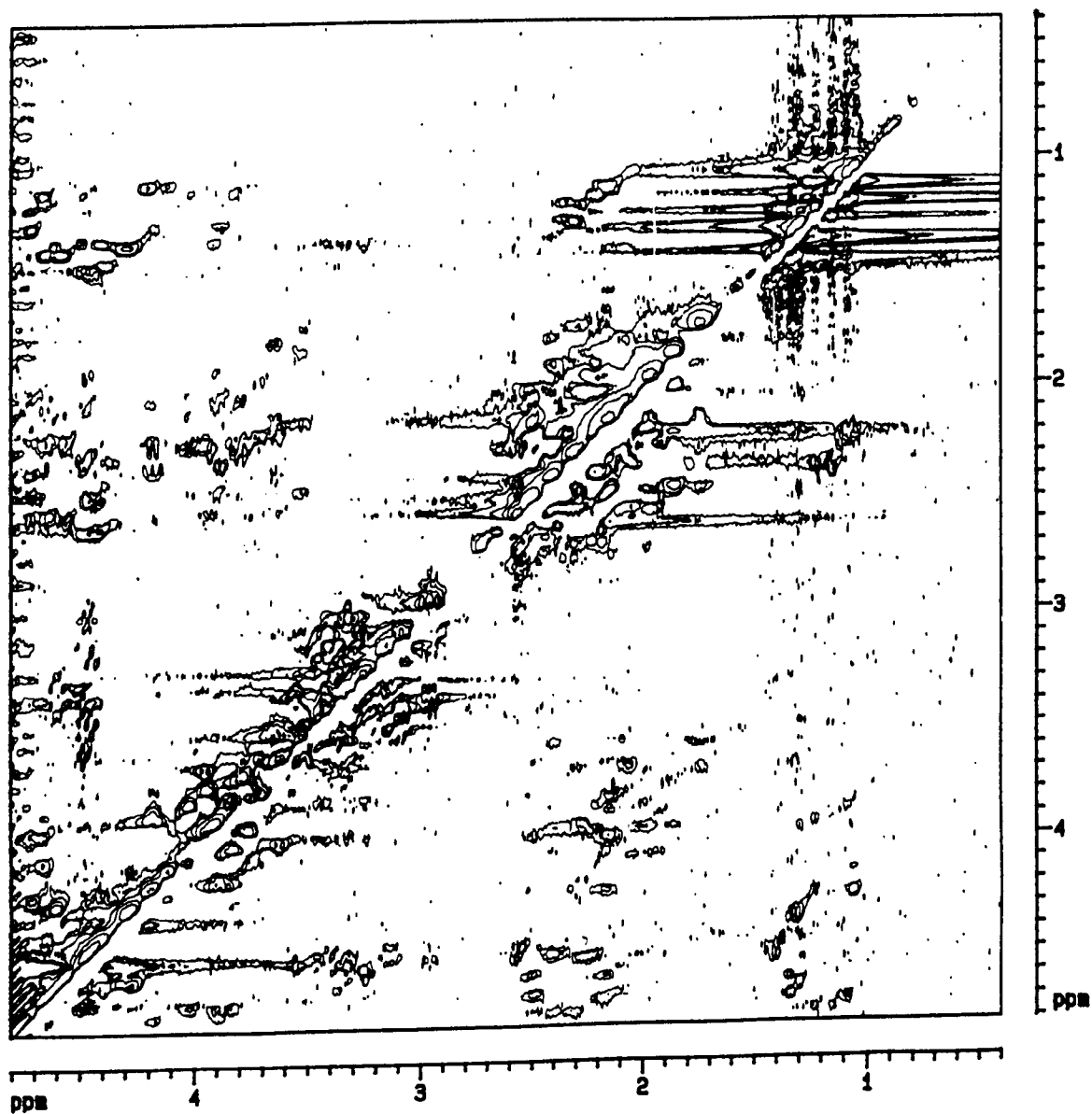


Figure 7.5. ROESY of C₃-C₁₃ in H₂O. Upfield region of the same spectrum as 7.4.

differentiating the His, Phe and Cys residues) from the TOCSY, the ROESY spectrum was used to find NH-H α NOEs from adjacent residues and thus give a sequence specific assignment [320].

The large number of cross-peaks provides evidence that the peptide, Cys-3 - Cys-13 adopts a large number of conformers which are in slow exchange on the proton NMR timescale. In most cases the cross-peaks from each residue are clustered around similar chemical shift co-ordinates. A few are shifted away from the main cluster, such as the cluster of signals from the alanine β -protons which has one or two shifted strongly downfield. With the exception of Ala-11 and Thr-12, most of the residues show evidence for only three or four conformers (every residue has at least two distinguishable conformers) which can be subdivided into two sets on the basis of their chemical shift. Two conformers are very similar, with shifts not far removed from the random coil values, the third shows a strong shift away from random coil (appendix 5 shows random coil values for the amino acids). Other conformers coincide with either of these groups. This could imply that there are three dominant conformations.

Figure 7.3 shows the region of a TOCSY spectrum showing cross-peaks associated with the proline residues. For the three proline residues in the peptide there are a total of six δ - δ cross-peaks. This shows that each of the proline residues is present in both *cis*, and *trans* form. These conformers do not adhere to the statistical distribution of approximately 80% *trans* - 20% *cis* [325]; most of the proline δ - δ cross peaks are of equivalent intensity. In particular the ratio is reversed for Pro-6, where the *cis* conformation is dominant. An exact quantification of the relative abundance of each isomer is not possible since cross peak intensity is a function of many factors including relaxation times. However the dominance of the *cis* form of Pro-6 is clearly seen in the data.

Assignments of these spin systems were made on the basis of NOEs from adjacent residues. The conformation of each isomer was deduced from the presence of

NOEs that would be unique to that conformation. NOEs between proline δ and the HN or H α of the preceding residue indicate the *trans* conformation. NOEs between a proline α -carbon proton and the α -carbon proton of the preceding residue indicate a *cis* conformation. The assignments are shown in table 7-1.

NOE data was collected to obtain structural information for this peptide. However, it was not possible to distinguish between individual conformers, nor could sufficient data be obtained for a single conformer to calculate a structure. There are inter-residue NOEs between the His-7NH proton in all conformations, and the methyl protons of Ala-11 and Phe-12. There are also weak or ambiguous NOEs suggesting that the His-7NH proton may also be close to the side chain of Thr-10. In addition there are NOEs seen from the Phe-12NH to either the H α or H β protons of His-7. It is unfeasible that all of these conditions would be found in a single conformation. There are no NOEs to the side chain of Gln-9 suggesting that in all conformations this residue is exposed. A similar situation is found for the histidine ring protons. The C-terminal cysteine (Cys-13) NH shows NOEs to the His-7 alpha proton and Thr-10 methyl protons in both conformations. Pro δ also shows NOEs to Thr-10 or Ala-11 dependent on conformation. Figure 7-6 summarises of the NOE data (NOEs are tabulated in appendix 6).

Residue	NH	C α H	C β H	Others
C3		4.907	3.217, 3.040	
V4a	8.545	3.901	1.940	0.806, 0.851
V4b	3.464	3.989	1.936	0.819, 0.865
V4c	8.693	4.498	2.102	0.920, 1.023
V4d	8.727	4.461	1.949	0.863
P5t		4.448	2.200	1.987, 1.810, 3.609, 3.810
P5c		4.507	2.184	2.094, 3.486, 3.574
P6t		4.507	2.191, 2.093	1.875, 3.311, 3.438
P6c		4.427	2.288, 2.052	1.770, 3.670, 3.973
H7a	7.728	4.298	3.041	
H7b	7.791	4.644	2.932, 3.138	
H7c	7.683	4.660	2.9533.138	
P8t		4.353	2.287	1.951, 3.553, 3.739
P8c		4.419	2.273	1.933, 1.879, 3.408, 3.744
Q9a	8.828	4.212	2.092, 2.200	2.349
Q9b	8.809	4.200	2.051, 2.142	2.327
Q9c	8.7570	4.275	1.961, 2.030	2.359
Q9d	8.689	4.147	2.004, 2.094	2.311
T10a	7.731	4.835	4.114	1.093
T10b	7.664	4.400	4.060	1.088
T10c	7.983	4.602	4.239	1.223
T10d	7.569	4.447		1.134
A11a	8.314	4.081	1.085	
A11b	8.254	4.192	1.168	

A11c	8.237	4.255	1.200	
A11d	8.225	4.255	1.192	
A11e	8.176	4.085	1.104	
A11f	8.235	3.752		
A11g	8.203	3.812		
A11h	8.179	3.864		
F12a	7.952	4.612	3.192, 2.868	
F12b	7.888	4.750	2.907, 3.222	
F12c	8.000	4.612	3.096,	
C13a	7.375	4.981	3.224, 3.015	
C13b	8.428	4.933	3.224, 3.044	
C13c	8.770		3.130	

Table 7.1. Assignments for the peptide, C₃-C₁₃ in H₂O. Complete assignments have been made for the majority of spin systems identified. Different conformers of the same residue are distinguished by letter. Where a system is not completely assigned it is because it is a very minor conformer and TOCSY or ROESY cross peaks were too weak to be observed. Chemical shifts were measured to ± 0.001 ppm. This level of accuracy was used in an attempt to distinguish some closely overlapped signals.

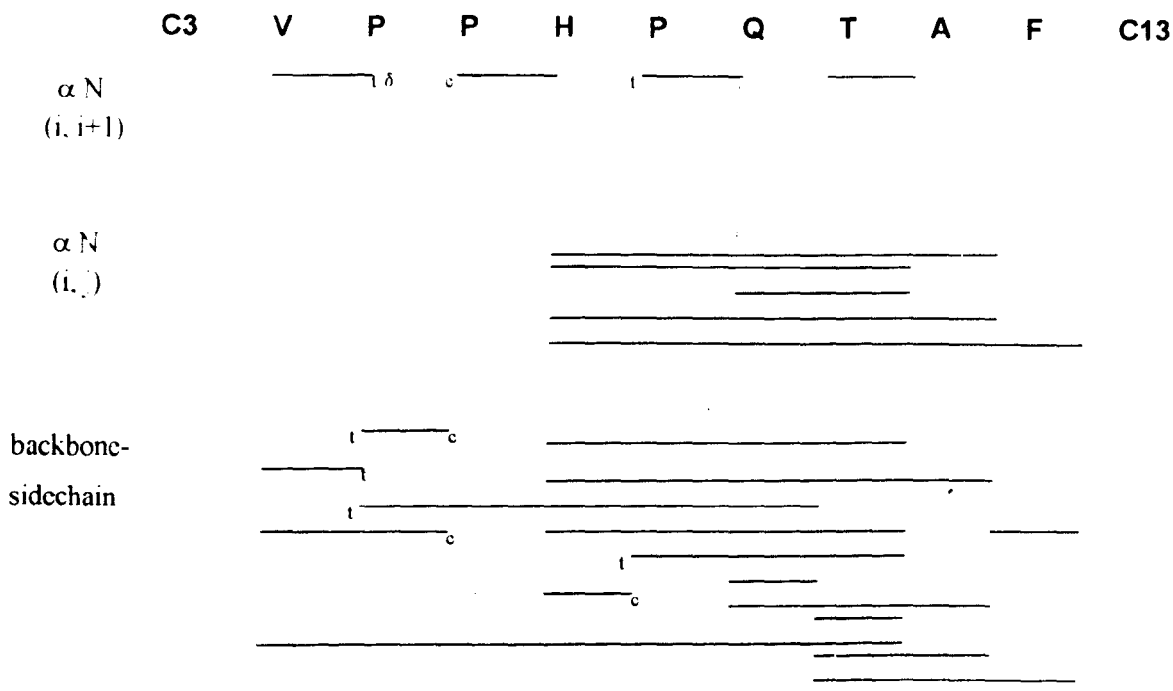


Figure 7-6. Representative diagram showing NOE contacts found in the family of conformers adopted by Cys-3 - Cys-13 in H₂O. NOEs are represented as a line beginning and ending beneath the relevant residues. The protons involved are shown on the left of the figure. *Cis/trans* isomers are designated as t or c. Some NOEs are duplicated where they were observed for more than one conformer.

Cys-3 - Cys-13 in TFE-d₂.

The 1D spectrum of Cys-3 - Cys-13 in TFE-d₂ is shown in figure 7-7. There is less dispersion when compared with the spectra in H₂O. Figures 7-8, 7-9, 7-10 and 7-11 show selected regions of a TOCSY spectrum and a NOESY spectrum of Cys-3 - Cys-13 in TFE-d₂. These spectra are much less complex than for the sample in H₂O, with only two residues showing evidence of any conformational heterogeneity (figure 7-8). There are only three clearly observable proline spin systems (figure 7-9), indicating that the TFE-d₂ has reduced the extent of the *cis-trans* isomerisation. One dominant form is observed, although two sets of signals from Val and Thr are seen. This has made for a more straightforward assignment.

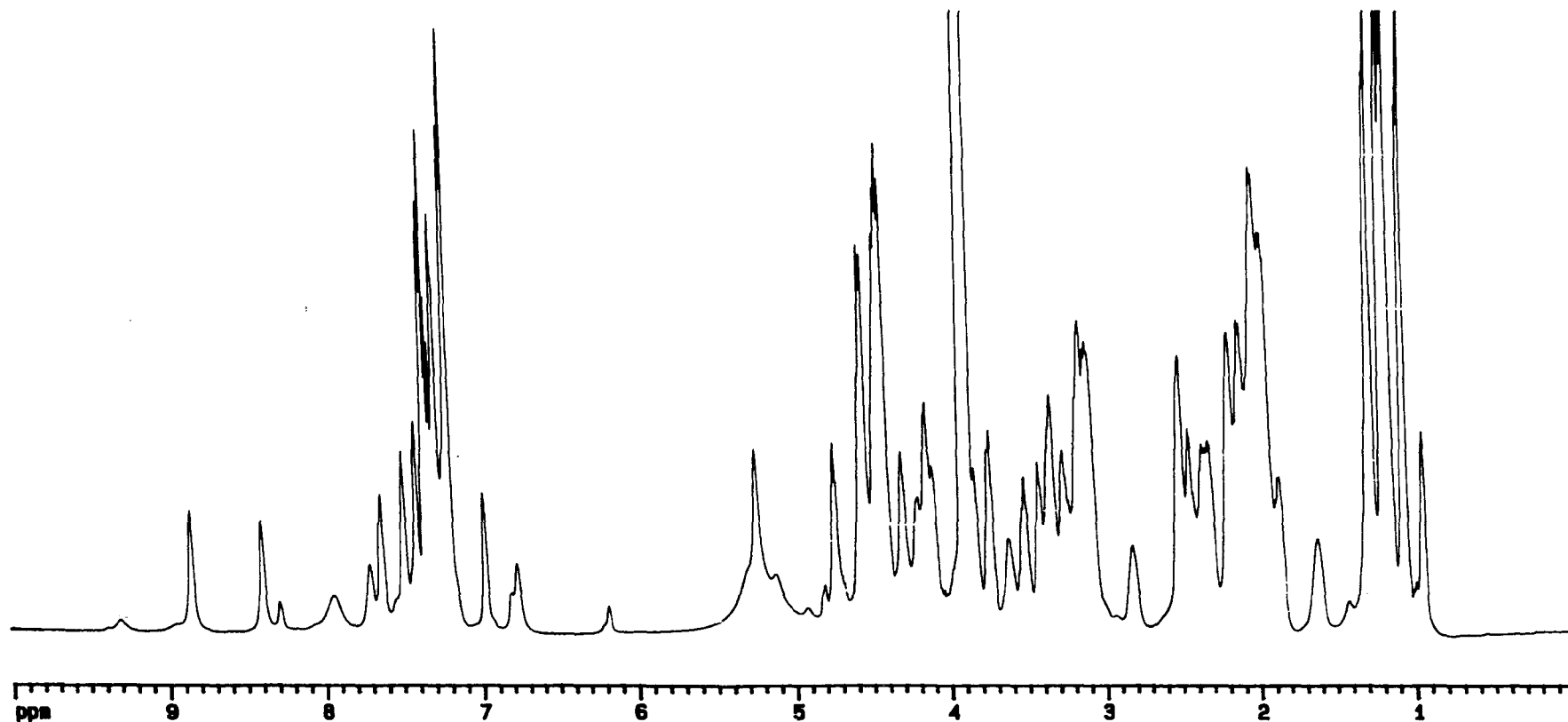


Figure 7-7. 1D spectrum of C_3-C_{13} in TFE- d_2 . The spectrum was recorded on a 500 MHz magnet at 300K. Sample is at 30mM. This spectrum shows less dispersion and less complexity than when the sample was in H_2O (figure 7-1).

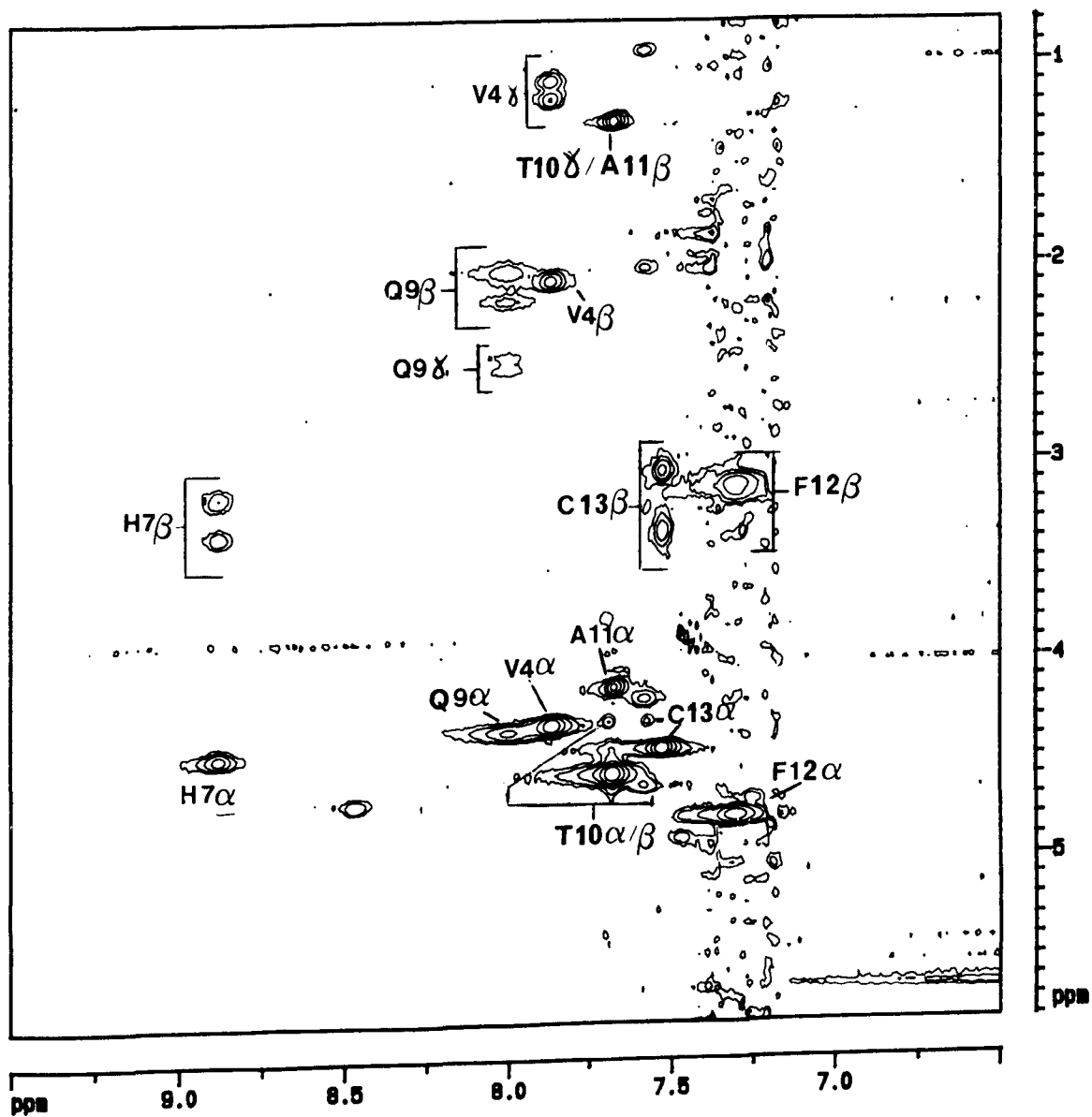


Figure 7-8. TOCSY of C₃-C₁₃ in TFE-d₂. Off diagonal region showing assigned spin systems.

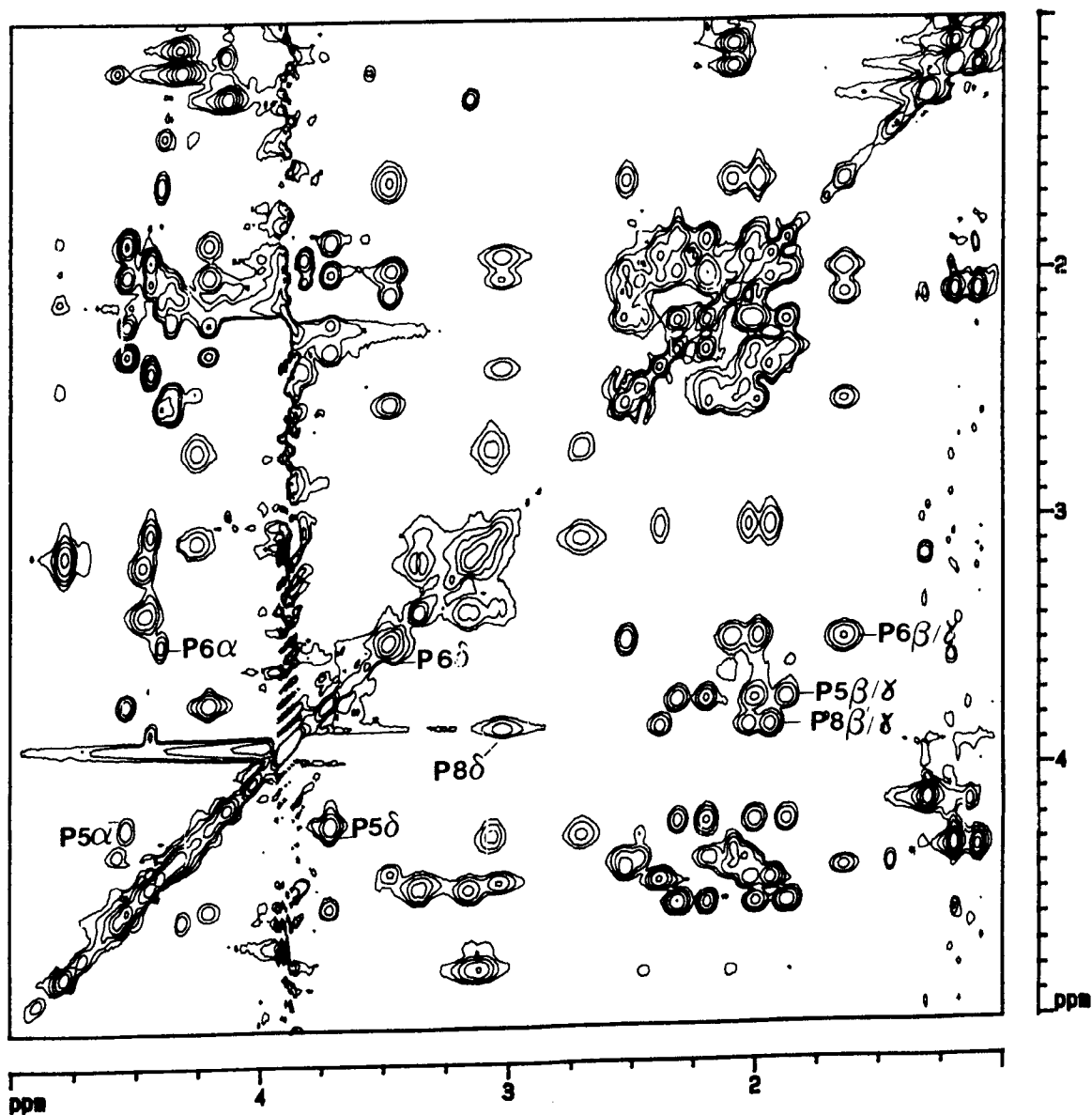


Figure 7.9. TOCSY of C_3 - C_{13} in TFE- d_2 . Upfield region showing the proline spin systems.

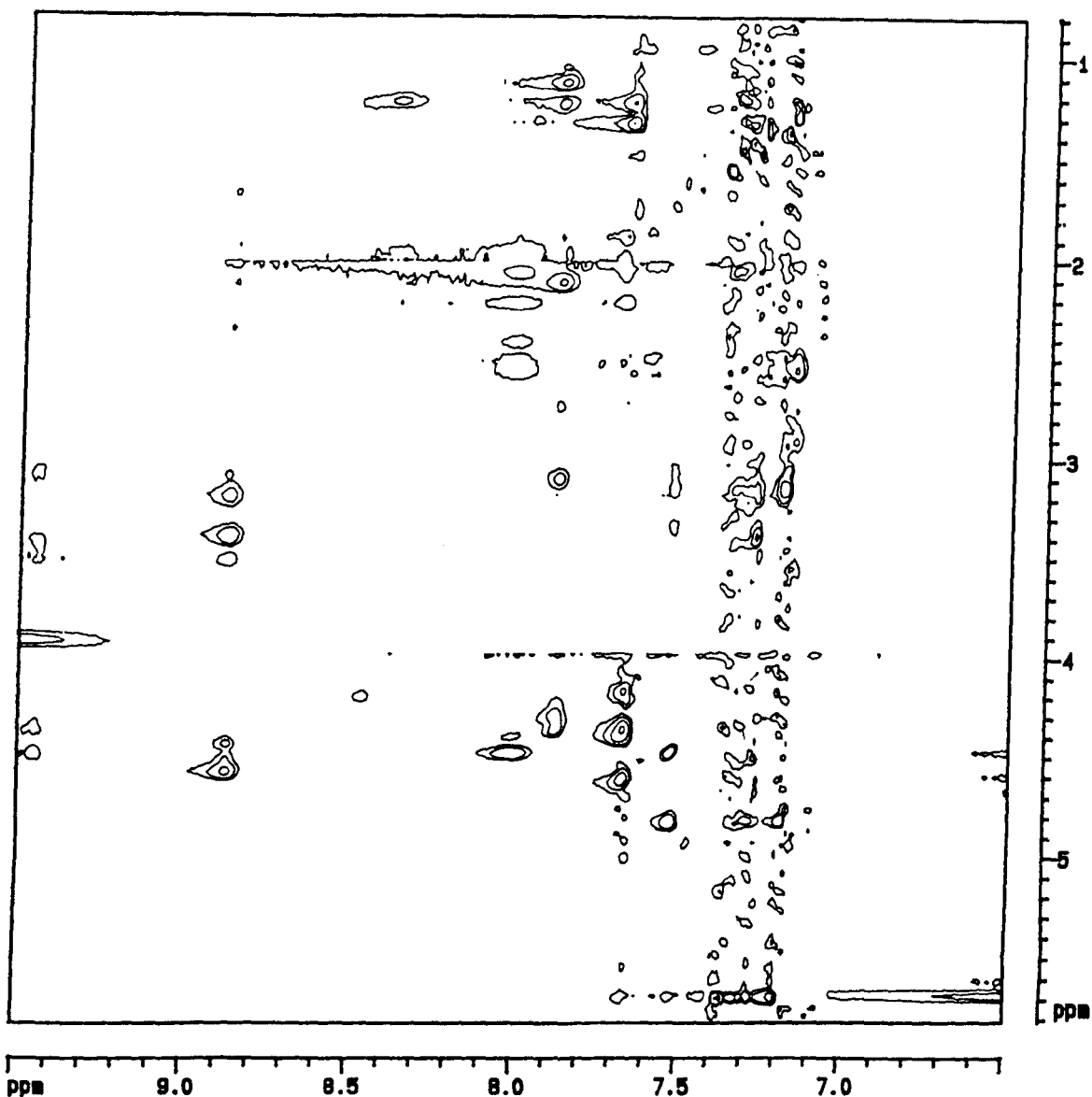


Figure 7-10. NOESY spectrum C₃-C₁₃ in TFE-d₂. A number of NOEs are observed. However these spectra were interpreted cautiously since TFE can aid solvent mediated magnetisation transfer. The clearest examples of this are provided by the downfield shifted histidine which has a string of NOEs over a large range of chemical shifts, and the phenylalanine, which is almost entirely obscured by noise.

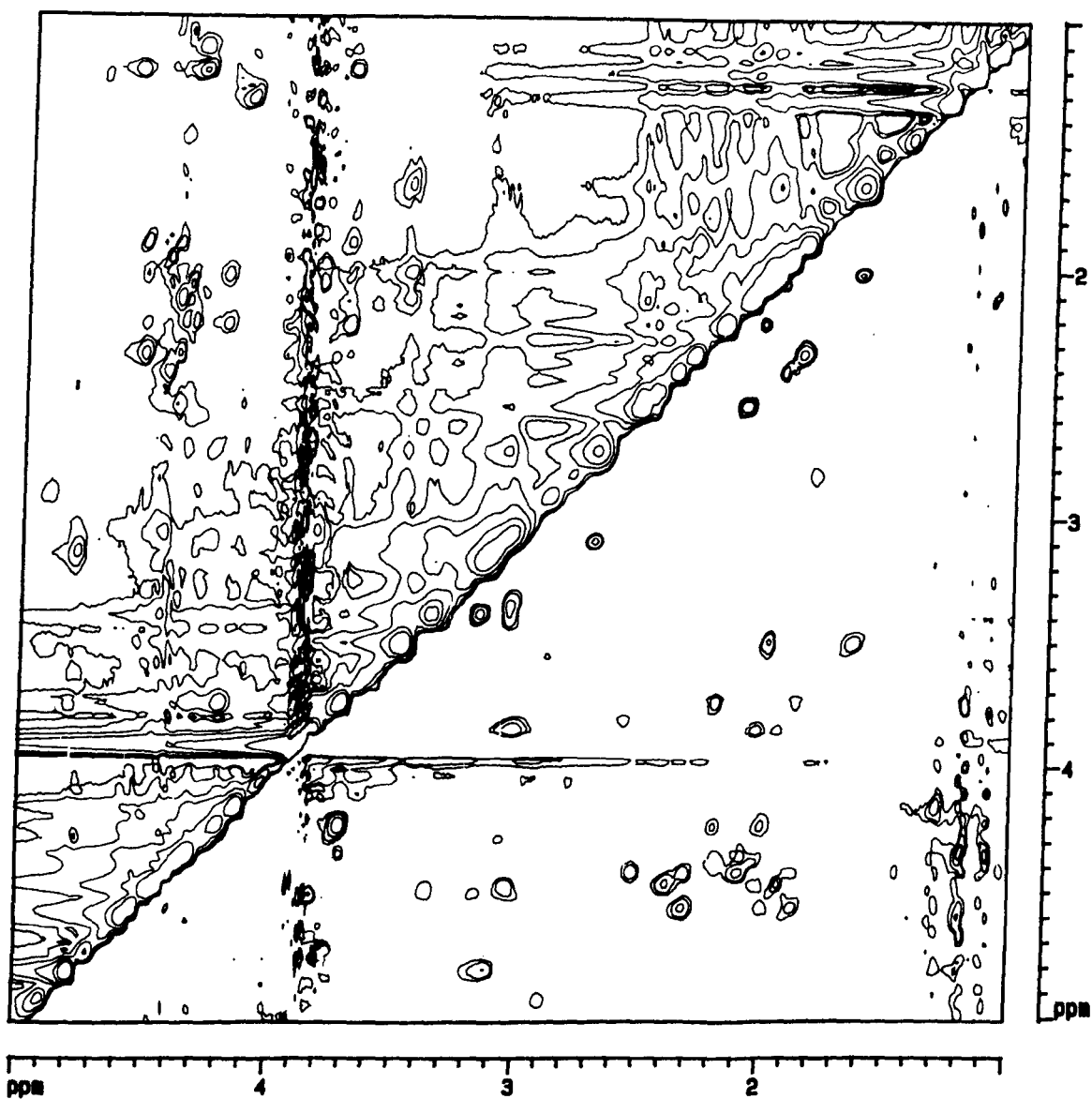


Figure 7-11. NOESY spectrum C_3-C_{13} in TFE-d₂. The same spectral region as 7-9, showing the proline systems. The spectral quality is not ideal; a lot of noise is present making interpretation complex.

Residue	NH	C α H	C β H	Others
V4a	7.859	4.315	2.072	1.173, 1.084
V4b	7.576	4.181	2.008	0.928
P5a		4.535	2.304, 1.985	2.132, 4.210, 3.719
P6		4.392	2.515, 1.627	2.080, 3.476
H7	8.877	4.458	3.352, 3.149	
P8		4.433	2.322, 1.928	2.013, 3.826, 3.036
Q9	7.998	4.344	2.171, 2.025	2.524, 2.457
T10a	7.686	4.570	4.302	1.289
T10b	7.584	4.622	4.295	
A11	7.669	4.122	1.285	
F12	7.301	4.775	3.357, 3.115	
C13	7.521	4.434		

Table 7.2. Assignments for the peptide C₃-C₁₃ in TFE-d₂. Assignments have been made for all residues other than C₃ which was not assignable due to the absence of an N-H - α H TOCSY connectivity. Where a chemical shift is not recorded for an individual proton it may be due to overlap, or its signal may not have been observable in the spectra. Different conformers of the same residue are distinguished by letter (a,b).

The same assignment procedure was used as for Cys-3 - Cys-13 in H₂O. Cross peaks are shown labelled in figures 7·8 and 7·9 and the full assignment list is shown in table 7·2.

Analysis of NOESY spectra was approached with caution. Given the high concentration of TFE-d₂, it is possible for magnetisation transfer to occur via the solvent, giving spurious NOEs. Consequently relatively few NOEs were recorded. The NOE data are summarised in a representative diagram (figure 7·12) and tabulated in appendix 7.

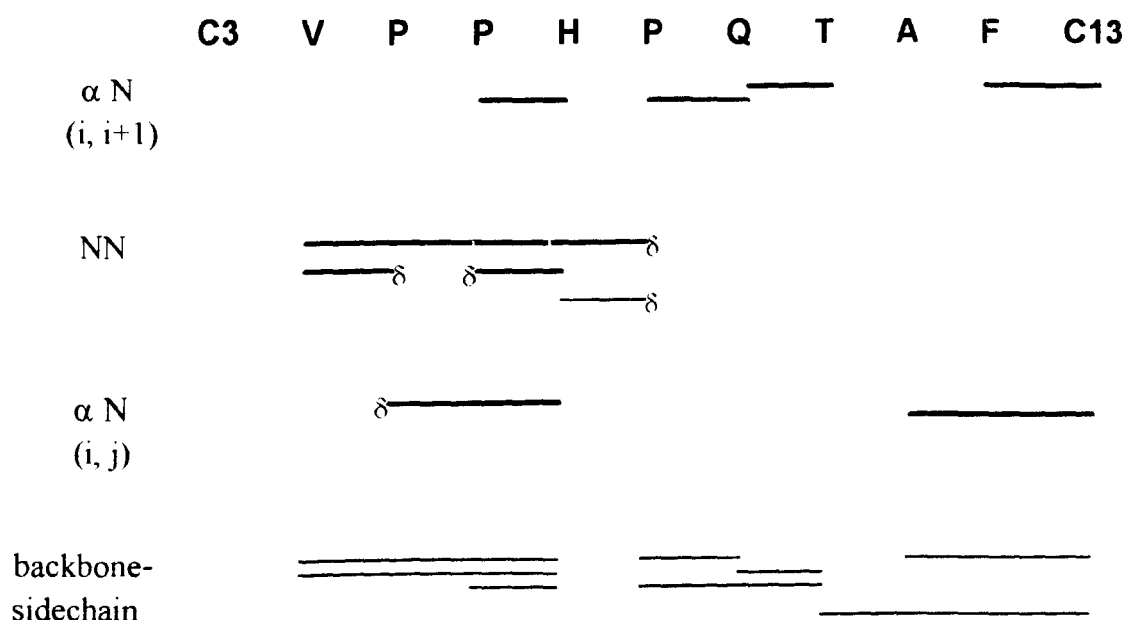


Figure 7·12. Representative diagram showing NOE contact for Cys-3 - Cys-13 in TFE-d₂.

The pattern of NOEs seen here is very different to that seen for the sample in H₂O. There are no contacts seen between His-7 and Thr-10, Ala-1 or Phe-12. Instead, NOEs between His-7HN and Val-4 methyls indicate a sharp turn around the two prolines (Pro-5 and Pro-6). Also seen is a contact between the NH proton of Val-4 and the δ

protons of Pro-8 which might be expected were there to be a tight turn as described. The absence of Pro-5 α -Pro-6 δ NOEs may indicate that Pro-6 is again in a *cis* conformation. Weak NOEs between the NH proton of Thr-10 and β -protons of Pro-8 suggest that the chain turns back on itself around Gln-9. There are also contacts between the Cys-13 NH proton and the α , and methyl/methylene protons of Ala-11 and Phe-12.

7.4. Discussion.

The peptide, Cys-3 - Cys-13 was found to be a weak inhibitor of 92 kDa gelatinase, but not of any other enzyme tested. This activity was not seen in the reduced, methylated form of the peptide, suggesting that the inhibitory activity may be associated with the cyclised conformation. An attempt was made to determine the solution structure of this peptide and subsequently to explain its mechanism if possible.

However, it has proved very difficult to determine the structure of Cys-3 - Cys-13 in H₂O. Were the peptide to be linear, only a single apparent conformer, with chemical shifts close to random coil, might be expected as a result of conformational averaging. Alternatively a (small) number of slowly interconverting structures might be seen due to local effects from proline isomerisation. Since no study was made of the reduced form of the peptide, this assumption cannot be confirmed. The presence of the disulphide bond would be expected to reduce the number of accessible conformations by reducing the overall flexibility. However the peptide remains sufficiently flexible for proline isomerisation to occur resulting in a large number of observable conformers in slow exchange. Because of the presence of multiple conformers a detailed structural analysis was not attempted. Consequently it is not possible to infer the presence of any elements of stable secondary structure.

It was found that all three of the proline residues were exhibiting *cis-trans* isomerisation. The rarer *cis* form (*cis:trans* ratio is normally 20:80) had an increased stability as shown by the similar intensities of all the cross-peaks in a TOCSY experiment. The permutations of all three proline residues being in either the *cis* or *trans* form is at least in part responsible for the large number of different peptide conformations. Since the peptide is cyclised via a disulphide bond, either the local, or the overall structure will have to alter to accommodate the isomerisation, giving rise to the different conformations. It is noteworthy that His-7, which is flanked by proline residues, only shows evidence of three different environments. This may be an indication that the

proline isomerisation only results in a small amount of conformational variation and the remainder is due to larger structural flexibility.

Ideally the structure of each conformer would be determined. However in ROESY spectra only intra-residue NOEs could be found for many of the residue conformers. Unfortunately, the few sequential inter-residue NOEs identified only extended over two residues. Also very few NOEs were found for either Cys-3 or Val-4, making analysis of the N-terminus of the peptide very difficult.

The overall picture of Cys-3 - Cys-13 in H₂O is of families of structures that although constrained by the presence of a disulphide bond, are able to adopt a large number of rapidly interconverting conformations in solution. These conformations are such that the *cis* form of the proline residues is stabilised, in particular at Pro-6. Another peptide study involving a Pro-Pro unit in a short, disulphide bonded peptide also shows the second Pro is in a *cis* conformation [326].

Some of the of the hydrophobic residues (Ala-11 and Phe-12, possibly Thr-10) in Cys-3 - Cys-13 appear to cluster around the histidine NH or C α protons, although there is no single, clearly defined arrangement. The side chains of both His-7 and Gln-9 are solvent exposed. The small number of NOEs from the N-terminus of the peptide could suggest that in the majority of conformers, this region has very few contacts with the remainder of the molecule. The presence of backbone-sidechain NOEs between Val-4 and Pro-5/Pro-6, and the dearth of NOEs to other residues, implies that these residues may be forming a small cluster, remote from the rest of the structure. The schematic diagram (figure 7.13) attempts to summarise the general features observed in the NOE data.

On transfer to TFE-d₂, Cys-3 - Cys-13 is found to adopt an entirely different conformation to that seen in H₂O. The overall impression is of an elongated molecule with a sharp turn at one end (Pro-Pro turn) and a more open turn at the other. Residues that were distant from each other in H₂O, are close together when in TFE-d₂.

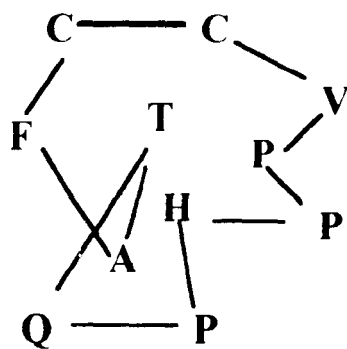


Figure 7-13. Representative figure indicating the possible general arrangement of C_3-C_{13} in H_2O . This diagram is intended only to create an impression of the spatial arrangement of the residues and for comparison with its equivalent for C_3-C_{13} in TFE-d₂. Some key longer range NOEs are marked as dotted lines.

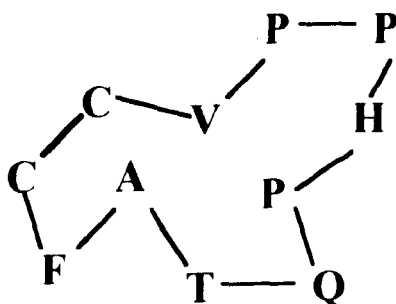


Figure 7-14. Simplified Schematic diagram showing the general arrangement of C_3-C_{13} in TFE-d₂. The presence of TFE-d₂ has allowed greater exposure of the hydrophobic residues than in H_2O , and the overall structure is more open. Some key longer range NOEs are marked as dotted lines.

Although there is no direct observation of proline isomerisation (only three proline δ - δ cross peaks are seen), there is other evidence of isomerisation. Minor conformers are observed for Val-4 and Thr-10 suggesting that some isomerisation is occurring for at least one Pro residue. An interesting feature is that the peptide bond of Pro-6 remains in the *cis* conformation. It is possible that in certain proteins and peptides, the *cis* form of the Pro-Pro amide bond is favoured over the *trans* form. The schematic diagram shown in figure 7-14 summarises the main points drawn from the NOE data. Although using TFE-d₂ as a solvent for the peptide has allowed for a simple assignment it is unlikely that this structure has any biological relevance since the same solvent cannot be used for assays.

Examples have been published where a peptide based on the parent protein exhibits inhibitory activity. This was found for soybean Bowman-Birk inhibitor and for chymotrypsin inhibitor-2 (CI2) [327]. In this case the inhibitory residues are sequentially close, and exposed on a long flexible loop that was produced as a disulphide bonded peptide. Other inhibitors have a more complex mechanism, using sequentially distant residues, and large regions of the molecule.

Recent data from structural, and antibody/peptide competition studies of TIMP-1 and TIMP-2 indicate that large regions of the protein are involved in the inhibition of the MMPs. The N-terminus of TIMP-2 has been shown to be an extended loop, finishing in a single turn helix (TIMP-1 is likely to be very similar). Although no detailed structures were obtained for the peptide, Cys-3 - Cys-13, the structures suggested by the NMR analysis are entirely unlike those seen in the intact protein. This is not surprising since the disulphide bond in the peptide draws residues which are normally distant, close together. Were this peptide not to have been disulphide bonded it would not necessarily have adopted a similar conformation to the same sequence in the context of its parent protein. Higher order interactions are often essential to function. This may well explain the complete absence of activity seen for the reduced form of Cys-3 - Cys-13.

The very weak inhibition seen in the cyclised form is almost certainly due to a property unique to the peptide. It may be due either to a weak property of many conformers, or a stronger effect restricted to a minor conformer. This inhibition may be due to the histidine being able to co-ordinate with the active site zinc atom, or a weak interaction with the active site cleft that reduces substrate access.

Chapter 8.

The Suitability of TIMP-1 for Further NMR Studies.

8.1. Introduction.

The overall aim of this research project is to obtain as much structural information about TIMP-1 as possible. Previous work in the Rheumatology Research Unit had found that although wild type TIMP-1 did form crystals on one occasion, they were very small and the crystallisation could not be reproduced. A recent publication has shown that TIMP-1 which has had the glycosylation sites removed by site directed mutagenesis does form crystals of a quality suitable for X-ray crystallography [278]. Although NMR studies have been made of many proteins, full structural determination has been limited to relatively small proteins (up to ~30 kDa [328]). As the size of the protein increases, the spectra become increasingly complex, making them harder to assign. In addition, larger molecules tumble more slowly in solution which increases transverse, or spin-spin relaxation rates and hence the line widths, decreasing the resolution of the spectra [329]. One of the most effective ways of increasing the resolution of complex spectra is to incorporate stable isotopes (commonly ^{13}C and ^{15}N , although deuterium and fluorine may also be used) into the protein during expression. These isotopes can be detected by NMR and allow the use of more complex, multi-dimensional experiments which distribute the data and provide information on the spatial arrangement of all atoms within the protein. At 184 residues, TIMP-1 is close to the maximum desirable size for NMR studies. The combination of higher field strength spectrometers and more versatile software should allow the structure of isotopically labelled TIMP-1 to be determined.

This chapter presents preliminary data from experiments carried out using the wild type protein. This work was done to assess the suitability of TIMP-1 for further

NMR studies and complements the NMR data that has been described in previous chapters. Before embarking on a potentially costly project to produce tens of milligrams of isotopically labelled protein it is important to assess how the protein will behave under the conditions used for NMR studies. Although TIMP-1 is known to be exceptionally stable, NMR experiments are typically performed at room temperature or above, using protein concentrations of greater than 1 mM in a low pH solution. These conditions are necessary to obtain spectra of sufficient quality for structural analysis. Thus it is important to have data on solubility, sensitivities to temperature and pH and how the protein withstands extended periods under these conditions.

8.2. Methods.

8.2.1. Materials.

Wild type TIMP-1 was purified as described in chapter 3. NaOD, DCl and D₂O were from the Sigma Chemical Co. (Poole, Dorset, UK).

8.2.2. Experimental Procedures.

All NMR spectra were recorded on either a Bruker AMX 360 or a Bruker AMX 500 spectrometer. Lyophilised wild type TIMP-1 was dissolved in H₂O at a concentration of 40.2 mg/ml (1.4 mM). The sample was lyophilised again, and resuspended in D₂O for some experiments. Samples have been kept for over a year stored at 4°C in the absence of bacteriostatic agents. Before any experiment, a 1D spectrum is acquired to determine the condition of the sample. For 1D spectra at 500 MHz, 1024 FIDs were acquired into 16 K data blocks with a 60 degree excitation pulse of 6 µs, a spectral width of 7042 Hz, an acquisition time of 1.16 s and a relaxation delay of 1.5 s. The temperature is the same as subsequent experiments.

For the pH titration, NaOD was added in small quantities (up to 10 µl), and the sample mixed by inversion of the tube. The pH was recorded inside the 5mm NMR tube using a 3.7mm outer diameter Russel (Auchtermuchty, Scotland) glass electrode and 1D spectra acquired at 305K.

For NOESY spectra TIMP-1 was dissolved to 30 mg/ml in 90% H₂O/10% D₂O at pH 3.8. Sample temperature was 305K. A total mixing time of 100 ms was used. 2D data were zero-filled once in F1 and Fourier transformed with the application of a $\pi/3$ shifted sine bell function in both dimensions. The solvent peak was suppressed using a low power pre-irradiation pulse of 1.5s.

8.3. Results.

8.3.1. Solubility, Stability and 1D Spectra.

Wild type TIMP-1 is readily soluble, with protein solutions of over 40 mg/ml showing no visible sign of degradation over long periods of time. Figure 8.1 shows a 1D spectrum of TIMP-1 in H₂O. As would be expected, the spectrum in H₂O shows a large number of peaks in the amide N-H region (downfield of approximately 7 ppm), some of which may be due to signals from N-acetylated sugars. There is no evidence of significant aggregation in solution over several months at 4°C, with the linewidths remaining unchanged. In addition there are no changes seen over the course of 48 hour experiments at higher temperatures. There are five well resolved peaks between 0.6 and 0.0 ppm that are only usually observed as a consequence of methyl or methylene groups being located above the plane of aromatic rings. This feature is usually indicative of a folded protein structure.

A dominant feature of the spectrum is a number of sharp peaks due to mobile sugar residues, the majority being found in the region between 3.5 and 4.5 ppm. These are due to the ring protons, with the exception of the anomeric protons which are shifted to the region between 4.5 and 5.5 ppm. At higher field (about 2 ppm), resonances from the methyl groups of N-acetylated sugar residues such as N-acetylglucosamine and sialic acid are evident.

On transfer to D₂O, most exchangeable proton signals disappeared very rapidly, within one hour, although some amide signals remained for longer periods (see figure 6.5 for 1D spectrum in D₂O). This is an indication that these protons are buried within the protein, protected from exchange with the solvent. The H₂ protons from the six histidine residues coincide to give a sharp, well-resolved signal at 8.53 ppm.

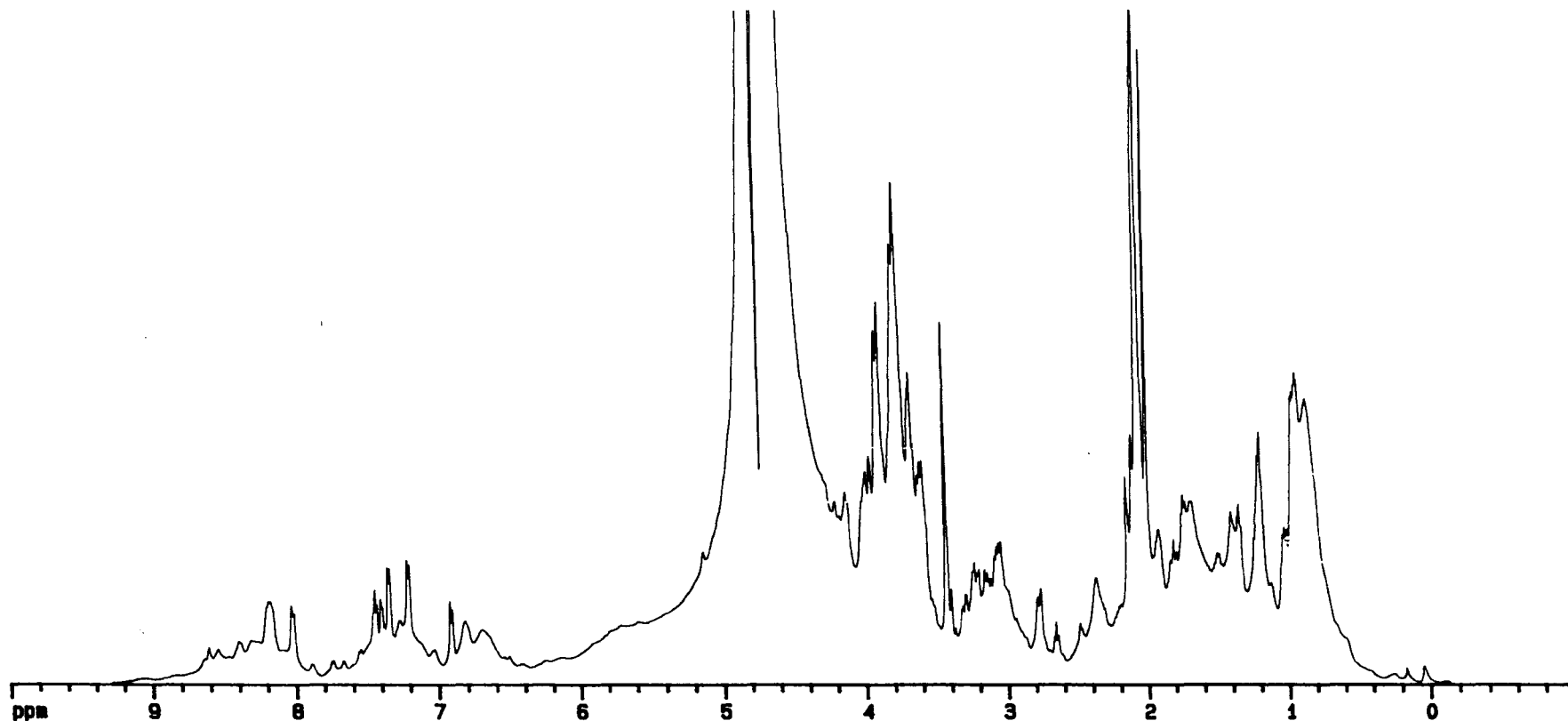


Figure 8-1. 1D Spectrum of Wild Type TIMP-1 in H₂O. Sample conditions are 1.4 mM, pH 4.3, 305K. The signals from the protein portion are dwarfed by the sharp, intense signals from the sugars. Highfield signals (between 0 and 1 ppm) indicate that the protein is folded in solution.

8.3.2. pH Stability.

A pH titration experiment was carried out to assess the stability of TIMP-1 under differing conditions. This experiment was also intended to identify a pH at which the histidine signals could be resolved from each other. Figure 8.2 shows a series of 1D spectra recorded at different pH values. The peak of the histidine H2 protons moves upfield from 8.53 to 8.0 without resolving any individual peaks. As the pH is raised from 5.78 to 6.15, extensive line broadening is seen as the protein precipitates. This process is reversible on returning the sample to a more acid pH.

8.3.3. 2D Spectra.

Some 2D COSY data has already been presented in chapter 5 and is not included here. Figure 8.3 shows selected regions of a NOESY spectrum of TIMP-1 in H₂O. Although the sample concentration used was low in comparison with that typically used for studies of other proteins, a large number of NOEs are seen.

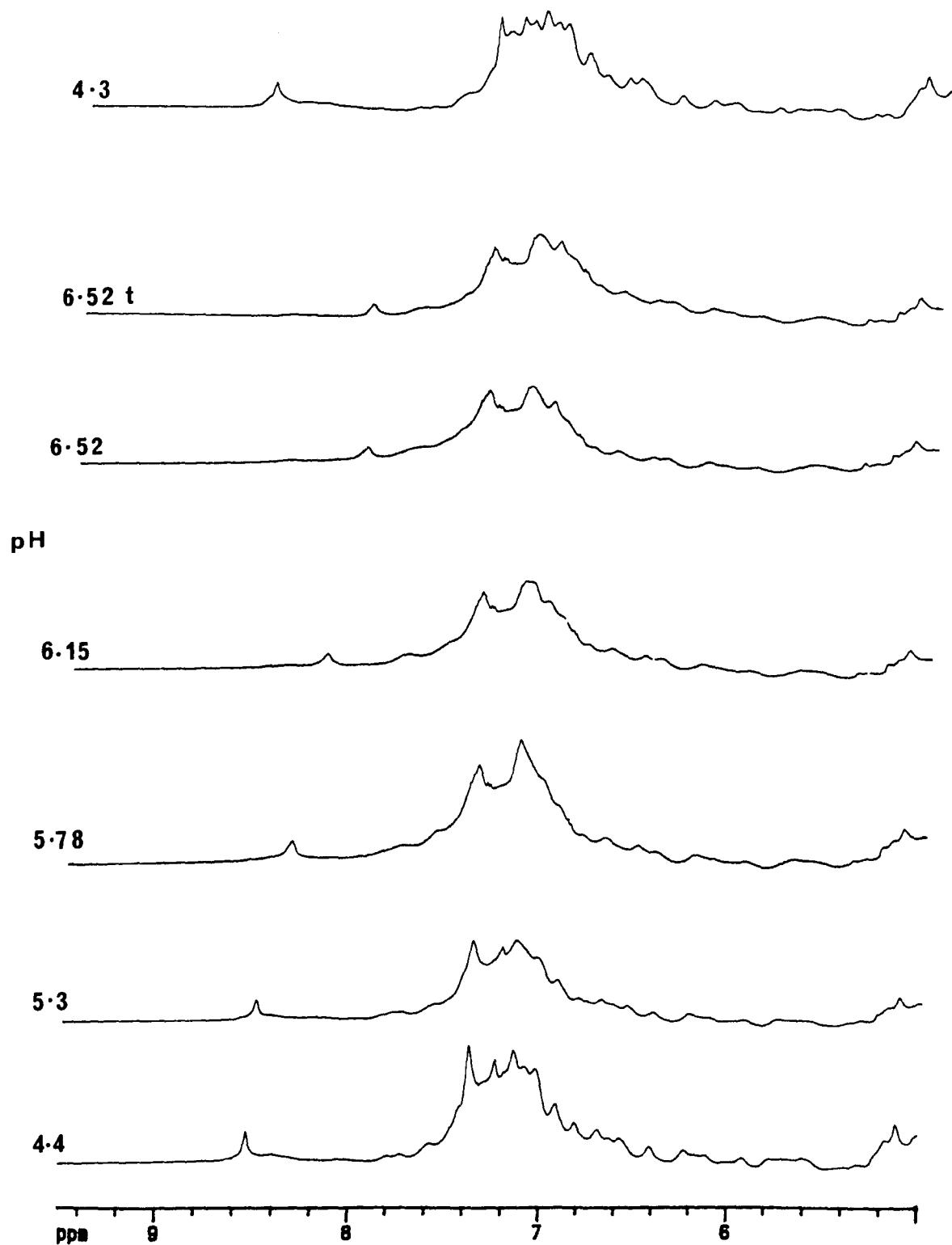


Figure 8-2. The aromatic region of the TIMP-1, 1D spectrum recorded at differing pH. The histidine H2 proton signals are moving upfield with increasing pH. As the sample approaches pH 6 the spectra give evidence of protein aggregation (broad lines and decreased resolution). pH 6.52 t was recorded after 16 hours at this pH. The uppermost spectrum is of the sample on return to pH 4.3 showing complete recovery.

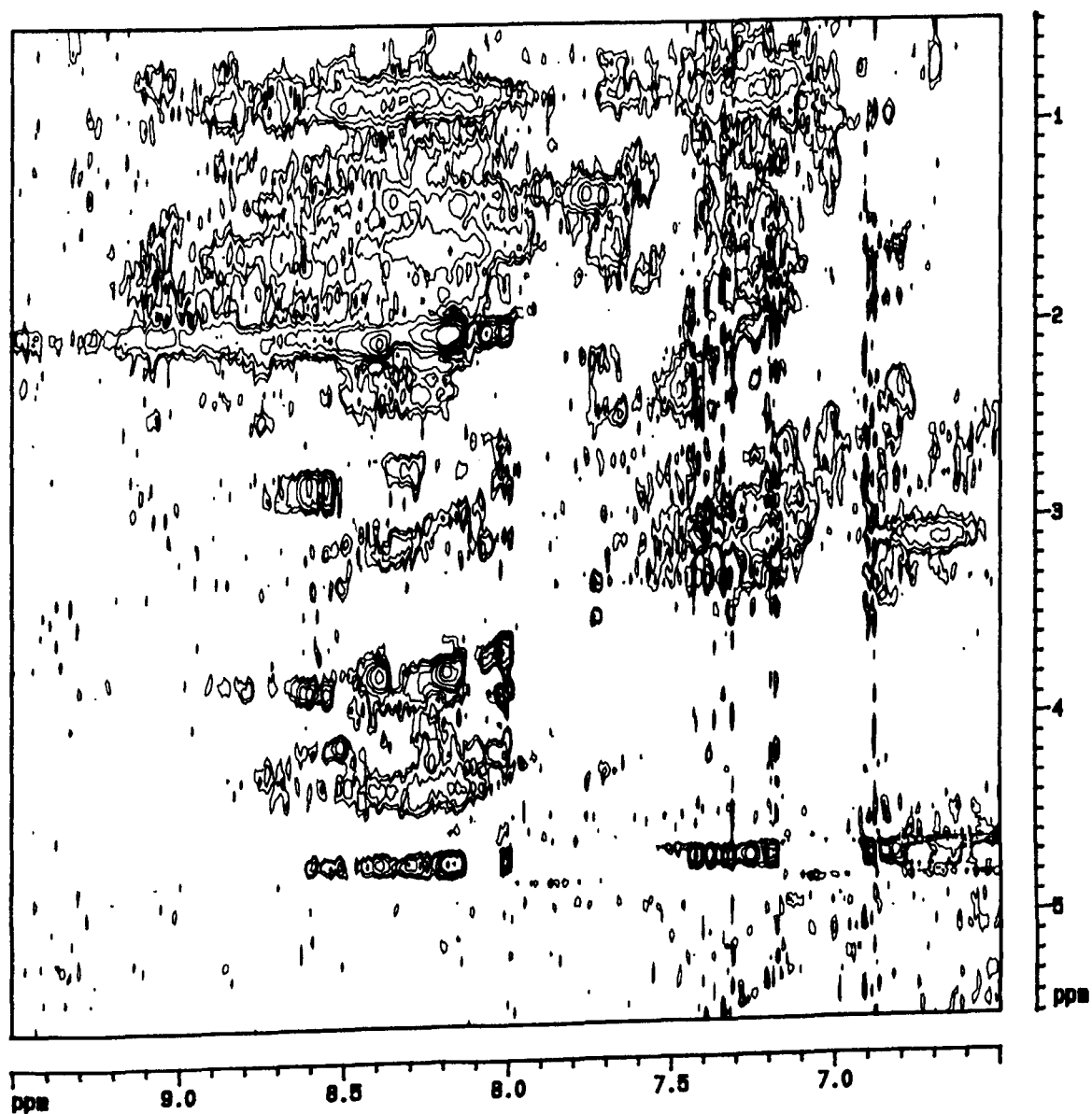


Figure 8.3. NOESY spectrum of wild type TIMP-1 at 0.8 mM. This spectrum contains too much data to attempt any analysis. This region does show that the data is well dispersed, and the spectrum is of good quality. This is a good indication for future studies.

8.4. Discussion.

Preliminary spectra of wild type TIMP-1 show that it is very suitable for further NMR studies. It is soluble to a desirable concentration (greater than 1 mM), and may be soluble to higher concentrations, although this was not determined. Samples of TIMP-1 have remained stable in solution for many months at 4°C. The solubility of TIMP-1 may be affected by the glycosylation. It is possible that the solubility and long term stability may differ in a recombinant protein. One possibility is that the sugars are masking a hydrophobic or charged part of the surface that may enhance aggregation when exposed. Reports of the formation of crystals of non glycosylated mutants of TIMP-1 suggest that this may not be a problem. In H₂O the pH of the prepared sample is low (4.3) which slows the exchange rate of the amide protons with water, improving the quality of the spectra. It is not yet known whether recombinant, non-glycosylated TIMP-1 can withstand low pH at high protein concentrations.

It is not unsurprising that the pH titration did not resolve the histidine H2 protons since they do not normally separate until a more basic pH (up to pH 9). The aggregation between pH 5.78 and pH 6.15 may be due to the protein reaching its pI. Recorded pIs for bovine and rabbit TIMP-1 are between 5.5 and 6.5, whilst pIs determined for human TIMP-1 include 6.7, 5.9 and 5.6. Computer prediction of the pI gives a result close to 7, but is not necessarily reliable. It is possible that in this case, the aggregation was mediated by the charged sugar residues and the situation may differ in a recombinant sample. Fortunately this process appears to be reversible, unlike the aggregation that occurs at high temperatures.

The spectra obtained of TIMP-1 are of good quality, with good dispersion in two dimensions. Triple resonance techniques and high field magnets allow assignment of proteins with a molecular weight of up to 30 kDa, with structural determination of proteins with molecular weights approaching 20 kDa. A full assignment and subsequent structure determination of a 184 residue (20.5 kDa) protein should be feasible if the

quality of spectra and dispersion in heteronuclear dimensions is good [320, 329]. Techniques such as automated spectral assignment, improved structure calculation protocols and low level isotopic labelling (i.e. 10% ^{13}C for stereo-assignment of Val/Leu methyls) will also aid the analysis.

Since the partial structure of TIMP-2 was published a useful model has been obtained to aid in the assignment of TIMP-1. Homology modelling, and comparison with published data will assist in the identification of NOEs and may lead to a high quality three dimensional structure.

Chapter 9.

Concluding Discussion.

The extracellular, connective tissue matrix forms the scaffolding for all other tissues and it is essential that it is maintained correctly. Connective tissue turnover is an ongoing process which begins during foetal development and continues throughout life. The primary agents of connective tissue breakdown are the MMPs, which are tightly regulated at many levels. Too little activity leads to a build up of tissue as in fibrotic conditions. Too much or inappropriate activity is associated with a host of common diseases such as arthritis, cancer and osteoporosis.

The TIMP family is an extremely important group of MMP inhibitors. They have been found in many species and a strong conservation of key residues has been seen. Particularly notable are the 12 cysteines, forming the disulphide bonds that contribute to the high stability of these proteins. TIMPs have been identified as products of a great number of cell lines and appear in many tissues. TIMP-1 in particular seems quite ubiquitous, whereas to date TIMP-3 has only been found in stromal tissue.

The TIMPs may provide an important key for regaining control of the MMPs in disease states. By understanding how the inhibition process works it may be possible to design compounds to mimic this activity. The aim of this project is to obtain structural data on TIMP-1, which will contribute to our understanding of the TIMP-MMP interactions.

The work presented here forms part of a continuing project of structural and functional studies of human TIMP-1. Obviously this type of work requires a reliable supply of protein. The source used for the majority of the work so far has been wild type, human TIMP-1 purified from bulk cultures of foetal lung fibroblasts (WI-38 cells). Producing and processing this volume of media is costly and time consuming. The

conventional purification scheme has been used successfully for many years, giving very acceptable yields. However, it does require a large amount of processing, utilising several column chromatography steps, with the accompanying need for concentration and dialysis between stages. This makes the purification of bulk quantities of protein a very slow process. Given that recombinant TIMP-1 produced in *E.coli* will have a different molecular weight, no glycosylation, and possibly a different surface charge, it is unlikely that the accepted protocol would be as suitable as for wild type protein.

Affinity purification of proteins using monoclonal antibodies attached to a support matrix is a very effective method of purification, which has already been used successfully for TIMP-1 by other workers. A number of monoclonal antibodies have been produced in the Rheumatology Research Unit which had previously been assayed for their ability to bind TIMP-1 when bound to a Sepharose matrix. One of these, P3G6, was selected for further tests, having been the most effective in preliminary columns. P3G6 was bound to different types of Sepharose matrix and tested for its ability to bind TIMP-1. The most effective of these was found to be CNBr-activated Sepharose-P3G6. The original elution protocol using low pH buffer was only effective for small column volumes. 3M NaI was found to be a suitable alternative for larger column volumes (up to 760 ml). This affinity column was used to rapidly purify most of the TIMP-1 used for the experiments described.

The monoclonal affinity column is now used for all purifications of wild type TIMP-1 in the Rheumatology Research Unit. It is hoped that it will also be suitable for the large scale purification of recombinant TIMP-1. This matrix can also be used to remove TIMP-1 from samples where it is not required (i.e. to remove traces that may contaminate an MMP preparation).

Since it is intended to carry out NMR studies of TIMP-1, production in human cell culture is completely unsuitable. To a spectroscopist, glycosylated material is an undesirable product of expression in human cells. In addition, isotopic labelling is not

feasible in this system, since to ensure homogenous labelling all nitrogen or carbon sources must be labelled. This is only realistic in organisms that can flourish on a simple single source of nutrient. Thus it was necessary to develop a bacterial expression system to meet the demands of this project.

The disulphide bonds in TIMP-1 make expression in *E.coli* a non trivial task. The reducing environment of the cytoplasm causes the protein to be produced as unfolded, insoluble aggregates in the cytoplasm. To retrieve the protein it must be solubilised and denatured, then refolded. Whilst this is a successful approach for many proteins, the need to reform all six disulphide bonds correctly makes this procedure exceptionally difficult in this case. Early reports in the literature indicated that this approach was not very successful, with very low yields of under 1mg/L. To avoid the pitfalls of refolding TIMP-1 from cytoplasmic inclusion bodies, two alternative *E.coli* expression systems were assessed.

Expression vectors were tested that directed the protein to either the medium or the periplasm. Both of these environments allow the formation of disulphide bonds. The extracellular matrix is not a reducing environment, whilst the periplasmic space contains a disulphide isomerase which aids the correct formation of disulphides by shuffling disulphide pairs until a stable (hopefully correctly folded) conformation is obtained.

The first vector used, directed the protein out into the medium. This was pEZZ18 which included a pair of IgG binding domains at the N-terminus of the protein. An engineered factor Xa site should have allowed the TIMP-1 to be cleaved from the fusion protein. However this proved not to be possible, even under mildly denaturing conditions. Analysis of the sequence, taking into account the positions of the disulphide bonds, suggested that the N-terminus might not be very accessible. The regions around Cys-1 and Cys-99 contain a large number of hydrophobic residues and prediction of the surface accessibility indicated that this site may be partially buried in the protein. In the partial TIMP-2 structure [141] the N-terminus does not appear to be significantly buried.

However, the exact positions of some of the loops (i.e. Cys-72 - Cys-101) remain undetermined, and these may prevent access to the N-terminus.

Although active TIMP-1 with the correct N-terminal sequence was produced using the second vector system a problem was encountered. pASK-60 uses an ompA signal sequence to direct the protein to the periplasm, where disulphide bond formation can occur. Unfortunately the yields were very low, in spite of attempts to reduce premature expression and using a rich medium. In order to achieve a reasonable level of expression (20 mg/L or greater) the yield would have to increase by at least 500-fold. The few periplasmic expression vectors produced so far do not have a very strong promoter (such as T7). This suggests that although high yields are reported by the manufacturers for some proteins, it is not necessarily true for all proteins.

It appears that the most effective way to obtain sufficient recombinant protein may be to design an improved protocol for refolding TIMP-1 from cytoplasmic aggregates. To do this will require a careful assay of protocol for removing the denaturant, different redox buffer systems and folding catalysts (such as chaperones and protein disulphide isomerase). Further studies are being made of *E.coli* expression systems and refolding protocols.

Although the absence of a bacterial expression system meant that it was not possible to carry out a full NMR study of TIMP-1, a number of biophysical studies were made of the wild type protein.

The first of these studies was an analysis of the secondary structure content of TIMP-1 using CD and FTIR spectroscopy. Both methods showed that TIMP-1 is comprised mostly of anti-parallel β -sheet with 20-25% of the structure as α -helix. Evidence from NMR spectra of the wild type protein also indicated that there were a substantial number of backbone alpha protons in regions of β -conformation. This was the first study to provide any data on the structural content of a TIMP.

In the initial absence of any other structural data for comparison, the experimental results obtained for the secondary structure content of TIMP-1 were compared with the theoretical contents obtained using a number of structure prediction programs. This exercise demonstrated that, although structure prediction programs are becoming increasingly sophisticated, it is still possible to obtain results that bear little resemblance to experimental data. The relatively high homology of the TIMPs, and the constraints imposed on the structure by the presence of the disulphide bonds, suggest that the overall fold of all members of the family is likely to be similar. This appears to be borne out by the recent publication of the solution structure of the N-terminal domain of TIMP-2 which also shows a molecule with a high proportion of β -sheet. However, since only the N-terminus has been studied and no tertiary structural data exists for TIMP-1 the two proteins may yet prove to have substantial differences.

One of the notable features of TIMP-1 is its high thermal stability, which has been so well documented that it is often used as one of the criteria for identifying a TIMP. Much of this stability has been attributed to the six disulphide bonds which presumably prevent the complete unfolding, and subsequent aggregation at higher temperatures. The effect of temperature on the secondary structure of TIMP-1 was studied by both CD and FTIR. This showed that the secondary structure was also heat stable, with no dramatic changes seen in the spectrum until the protein aggregated. This high structural stability might indicate that much of the structure of TIMP-1 is in a compact form, with an extensive hydrogen bonding network that requires relatively high temperature to disrupt. For the high concentrations of protein used in this study, thermal denaturation is accompanied by rapid, irreversible aggregation. When biological assays have been performed after heating TIMP-1 in more dilute solutions, some activity has been restored on cooling. It is possible that TIMP-1 can undergo complete denaturation at high temperatures and only intermolecular interactions prevent the full restoration of inhibitory activity.

A number of different surface features of TIMP-1 have been described here. Although TIMP-1 is a glycoprotein, very little is known about the attached carbohydrate chains (at Asn-30 and Asn-78). They do not appear to have any function in the inhibitory activity of TIMP-1, but may have some other role *in vivo*. This function is unknown but may be involved with the stability of the protein.

Concanavalin A is sensitive not only to the composition, but the structure of a carbohydrate, making it fairly selective. During purification CAB and NCAB forms were identified. These were analysed by iso-electric focusing to identify any differences in the charge composition, and by HPLC to quantify the relative concentrations of monosaccharides present in each form. It was already known that human TIMP-1 had a range of pIs [134]. This study showed that for CAB and NCAB TIMP-1, different subgroups of charged molecules appeared to be distinguished by the Concanavalin A lectin. Monosaccharide analysis has also shown that the composition of the two pools is different. The two are very similar, with only a small quantity of mannose, and the majority made up from glucosamine. The primary difference is that the CAB forms have relatively more galactose than the NCAB forms. This compositional difference may be responsible for the differential Concanavalin A binding. It would be desirable to obtain the structure of the polysaccharide to explain the differential binding in terms of the accessibility of carbohydrate ligands.

This study has identified an additional carbohydrate feature. By probing a Western blot with biotinylated Concanavalin A it is possible to detect those glycoproteins which bind the Concanavalin A lectin. Unsurprisingly wild type TIMP-1 was revealed on development of the blot. More unexpected was the observation of a 21 kDa band associated with TIMP-1 that had been treated with an endoglycosidase. The nature of this small additional glycosylation was not explored further and its function is unknown. It may be possible to identify it by acid hydrolysis of PNGase treated TIMP-1 and HPLC analysis of the products.

To accompany the biochemical analysis of the TIMP-1 carbohydrate, some of the carbohydrate features in a COSY NMR spectrum were analysed. By comparison with tables of published chemical shift data tentative assignments were made of some sugar anomeric protons, which have chemical shifts separating them from the rest of the sugar resonances. The inferred composition is close to the biochemical observations, with little evidence of mannose present. Since the use of chemical shift data alone is not a reliable method of confirming the identity of peaks in a spectrum, this data serves only to support the HPLC analysis.

NMR was also used to identify surface residues of TIMP-1. The titration using MnCl_2 shows a large number of peaks broadening with increasing Mn concentration. The Mn ion binds to negative charges on the proteins surface. In this sample it may also interact with the sugar groups. Information from this titration can aid the assignment of the TIMP-1 spectrum by identifying peaks from acidic residues.

A number of side chain methyls and the side chains of two aromatic residues (probably a tyrosine, and either a phenylalanine or tryptophan) showed line broadening caused by binding of the spin probe OH-TEMPO. This is a particularly interesting observation indicating that the surface of TIMP-1 has one or more exposed hydrophobic regions. The majority of hydrophobic residues are normally found at the protein core. Exposed regions may be involved in protein-protein interactions.

The evidence for an exposed hydrophobic region was strengthened by a study using the fluorescent probe ANS. A titration of TIMP-1 against ANS was used to determine the number of ANS binding sites and the average K_a . A single binding site with a low K_a ($3.3 \times 10^4 \text{ M}^{-1}$) was identified. Further studies using the N- and C-terminal domains of TIMP-1 may help to locate this site. Although the N-terminal fragment of collagenase did not bind ANS, when TIMP-1 was added the fluorescence increased. In a titration experiment identical to that performed for TIMP-1 alone very similar results were obtained. Because the fraction of enzyme-inhibitor complex is not known it is not

possible to determine whether this represents a small change occurring across the entire population, or a more extensive change restricted to a few molecules.

A role for a hydrophobic, or aromatic, residue in the interaction between TIMP-1 and the MMPs has been suggested by kinetic data of TIMP-1 mutants [330]. This suggested that Trp-105 may be part of a large interface between TIMP-1 and matrilysin. This residue (Trp-107) is seen at the edge of a large concave region in the N-terminus of TIMP-2 [141] along with a tyrosine (Tyr-122) and a phenylalanine (Phe-103). The data presented in this study provides additional evidence for the exposure of hydrophobic and/or aromatic residues in TIMP-1.

The inhibition of the MMPs by the TIMPs is of enormous interest to those wishing to design novel therapeutics for the treatment of those diseases where MMP activity is unchecked. Identifying the residues involved in the interaction and their conformation will provide an important aid to drug development. A useful key to functionally important residues is the extent of conservation both within members of the TIMP family and between TIMPs in different species. The homology between all TIMPs identified at the time of compilation is shown in Appendix 3. The regions of high homology are likely to be important for function or for the maintenance of the overall structure of the protein. Substitution, or deletion mutants of TIMP-1 may identify structurally or functionally important residues. A reduction in the amount of protein produced can indicate that the mutation has affected the structure of the protein. If the inhibitory activity of TIMP-1 is reduced, the mutant or absent residues may be involved in the inhibition of the MMPs.

In this way, the N-termini of the TIMPs have been indicated as potentially important for inhibition. Subsequently a peptide based on the sequence of TIMP-1 was produced. Some weak inhibitory activity was observed towards gelatinase at high concentrations of peptide. NMR studies of this peptide showed that it had a structure entirely unlike that found for TIMP-2. The inhibitory activity seen may be due to a weak

interaction with the active site of the enzyme, possibly involving the histidine in the peptide.

NMR studies of this peptide in H₂O found that it adopted a large number of slowly interconverting conformations as a result of the isomerisation of the three prolines present. The most interesting feature of this was that the *cis* form of all three prolines had been stabilised sufficiently for the isomerisation to be observed in the NMR timescale. Also interesting was the extensive effect of the isomerisation on residues some distance away in the sequence. In TFE-d₂, the structure seen was entirely different to that observed in H₂O. TFE is often used as a structure inducing solvent. Sometimes the structure produced is very similar to that of the peptide in the context of its parent protein. It is also possible for TFE to induce structure that is entirely unlike the parent.

Interestingly, the stabilisation of the *cis* form of Pro-6 was retained when the peptide was studied in TFE-d₂. This feature has been observed in other peptides and may prove to be a common feature of proline-proline units under certain conditions. It may be present in whole TIMP-1 and have a function in the structure of this region of the protein. Since TIMP-2 does not have this unit no predictions can be made by comparison with the known structure.

Further experiments may be able to provide data of sufficient quality to identify individual conformers and determine their structures. From this it may be possible to explain the increased stability of the *cis* form of the prolines in Cys-3 - Cys-13.

The complete structure of TIMP-1 remains to be solved. Some of the work presented here is a preliminary study of wild type TIMP-1 to determine how it behaves under the conditions required for NMR spectroscopy. The evidence so far indicates that wild type human TIMP-1 is very stable at high concentrations and low pH for many months. Although it is possible that the non-glycosylated, recombinant protein may be destabilised it is unlikely since mutants of human TIMP-1, without the essential

asparagine residues have been shown to crystallise successfully. Once the structure is known a great deal may be revealed about the mechanism of MMP inhibition.

In the future our knowledge will be greatly enhanced by a complete structure for each enzyme and inhibitor. The difficulty of producing sufficient quantities of enzyme or inhibitor has hampered the study of structure-function in the MMPs and TIMPs. As solutions to the difficulties presented by instability and complex folding are found more structural data for individual proteins will become available. More information will come from studies of enzyme-inhibitor complexes and dynamics measurements. It might also be possible to use synthetic substrates that are held at the active site but are either uncleaved, or partially cleaved allowing a dissection of the cleavage reaction.

The matrix metalloproteinases and their specific inhibitors are an extremely important and expanding area of study. The many roles they have to play in both normal and disease processes make them of interest to researchers in many fields from cancer and arthritis to dentistry and reproductive biology. Many of these proteins are relatively recent discoveries and there is still much to be learnt about their regulation, structure and function.

References.

1. Birkedal-Hansen, H., Moore, W.G.I., Bodden, M.K., Windsor, L.J., Birkedal-Hansen, B., DeCarlo, A., Engler, J.A. Matrix Metalloproteinases: A Review. (1993) *Crit. Rev. Oral. Biol. Med.* 4, 197-250.
2. Matrisian, L.M. Metalloproteinases and their inhibitors in matrix remodelling. (1990) *Trends Genet.* 6, 121-125.
3. Arthur, M.J.P., Iredale, J.P. Hepatic Lipocytes, TIMP-1 and liver fibrosis. (1994) *J Royal College Physicians London* 28, 200-208.
4. Gross, J., Lapierre, C.M. Collagenolytic activity in amphibian tissues: A tissue culture assay. (1962) *Proc. Natl. Acad. Sci. USA.* 48, 1014-1022.
5. Murphy, G., Willenbrock, F., Ward, R., O'Shea, M., Docherty, A.J.P. (1993). Studies on the structure and function of the matrix metalloproteinases and their inhibitors. Proteolysis and protein turnover. Eds. J.S. Bond and A.J. Barrett. Portland Press Proceedings.
6. Ennis, B.W., Matrisian, L.M. Matrix degrading metalloproteinases. (1994) *J. Neuro-Onc.* 18, 105-109.
7. Huhtala, P., Chow, L.T., Tryggvason, K. Structure of the human type IV collagenase gene. (1990) *J. Biol. Chem.* 265, 11077-11082.
8. Grant, G.A., Eisen, A.Z., Marmer, B.L., Roswit, W.T., Goldberg, G.I. The activation of human skin fibroblast procollagenase. (1987) *J. Biol. Chem.* 262, 731-741.
9. Vallee, B.L., Auld, D.S. Active zinc binding sites of metalloenzymes. (1992) *Matrix special supplement* 1, 5-19.
10. Lepage, T., Gache, C. Early expression of a collagenase like hatching enzyme gene in sea urchin embryo (1990) *EMBO J.* 9, 3993-4012.
11. Tryggvason, K., Huhtala, P., Tuutilla, A., Chow, L., Keski-Oja, J., Lohi, J. Structure and expression of type IV collagenase genes. (1990) *Cell. Diff. Develop.* 32, 307-312.

12. Quantin, B., Murphy, G., Breathnach, R. Pump-1 cDNA codes for a protein with characteristics similar to those of the classical collagenase family members. (1989) *Biochemistry* 29, 5327-5334.
13. Jongeneel, C. V., Bouvier, J., Bairoch, A. A unique signature identifies a family of zinc-dependant metalloproteinases. (1989) *FEBS Lett.* 242, 211-214.
14. Bode, W., Gomis-Rüth, F., Stöckler, W. Astacins, serralytins, snake venom and matrix metalloproteinases exhibit identical zinc-binding environments (HEXXHXXGXXH and Met turn) and topologies and should be grouped into a common family, the 'metzincins'. (1993) *FEBS Lett.* 331, 134-140.
15. Evanson, J. M., Jeffrey, J.J., Krane, S.M. Studies on collagenase from rheumatoid synovium in tissue culture. (1968) *J. Clin. Invest.* 47, 2639-2651.
16. Evanson, J. M., Jeffrey, J.S., Krane, S.M. Human collagenase: Identification and characterisation of an enzyme from rheumatoid cell culture. (1967) *Science* 158, 499-502.
17. Church, R.L., Bauer, E.A., Eisen, A.Z. Human skin collagenase: Assignment of the structural gene to chromosome 11 in both normal and recessive dystrophic epidermolysis bullosa using human-mouse somatic cell hybrids. (1983) *Collagen Rel. Res.* 3, 115-124.
18. Campbell, E. J., Davis-Cury, J., Lazarus, C.I., Welgus, H.G. Monocyte procollagenase and tissue inhibitor of metalloproteinases. Identification, characterisation and regulation of secretion. (1987) *J. Biol. Chem.* 262, 15862-15868.
19. Goldberg, G.I., Wilhelm, S.M. Human fibroblast collagenase. Complete primary structure and homology to an oncogene transformation induced rat protein. (1986) *J. Biol. Chem.* 261, 6600-6605.
20. Hasty, K. A., Pourmotabbed, T.F., Goldberg, G.I., Thompson, J.P., Spinello, D.G., Stevens, R.M., Mainardi, C.L. Human neutrophil collagenase. (1990) *J. Biol. Chem.* 265, 11421-11424.
21. Freije, J.M.P., Diez-Itza, I., Balbín, M., Sánchez, L.M., Blasco, R., Tolivia, J., López-Otin, C. Molecular cloning and expression of collagenase-3, a novel human matrix

- metalloproteinase produced by breast carcinomas. (1994) *J. Biol. Chem.* 269, 16766-16773.
22. Quinn, C.O., Scott, D.K., Brinckerhoff, C.E., Matrisian, L.M., Jeffrey, J.J., Partridge, N.C. Rat collagenase. Cloning, amino acid sequence comparison and parathyroid hormone regulation in osteoblastic cells. (1990) *J. Biol. Chem.* 265, 22342-22347.
23. Henriot, P., Rousseau, G.G., Eeckhout, Y. Cloning and sequencing of mouse collagenase cDNA. Divergence of mouse and rat collagenases from the other mammalian collagenases. (1992) *FEBS Lett.* 310, 175-178.
24. Wu, H., Byrne, M.H., Stacey, A., Goldring, M.B., Birkhead, J.R., Jaenisch, R., Krane, S.M. Generation of collagenase resistant collagen by site directed mutagenesis of murine $\alpha 1(I)$ collagen gene. (1990) *Proc. Natl. Acad. Sci. USA.* 87, 5888-5892.
25. Fields, G.B., Van Wart, H.E., Birkedal-Hansen, H. Sequence specificity of human skin fibroblast collagenase. (1987) *J. Biol. Chem.* 262, 6221-6226.
26. Murphy, G., Allan, J.A., Willenbrock, F., Cockett, M.I., O'Connell, J.P., Docherty, A.J.P. The role of the C-terminal domain in collagenase and stromelysin specificity. (1992) *J. Biol. Chem.* 267, 9612-9618.
27. Sanchez-Lopez, R., Alexander, C.M., Behrendtsen, O., Breathnach, B., Werb, Z. Role of zinc-binding and hemopexin domain encoded sequences in the substrate specificity of collagenase and stromelysin-2 as revealed by chimeric proteins. (1993) *J. Biol. Chem.* 257, 7238-7247.
28. Clark, I. M., Cawston, T.E. Fragments of human fibroblast collagenase. (1989) *Biochem. J.* 263, 201-206.
29. Hirose, T., Patterson, C., Pourmotabbed, T., Mainardi, C., Hasty, K.A. Structure function relationship of human neutrophil collagenase: Identification of regions responsible for substrate specificity and general proteinase activity. (1993) *Proc. Natl. Acad. Sci. USA.* 90, 2569-2573.

30. Mookhtiar, K., Wang, F., Van Wart, H.E., Functional constituents of the active site of human neutrophil collagenase. (1986) *Arch. Biochem. Biophys.* 246, 645-649.
31. Murphy, G., McAlpine, C.G., Poll, C.T., Reynolds, J.J. Purification and characterisation of a bone metalloproteinase that degrades gelatin and types IV and V collagen. (1985) *Biochim. Biophys. Acta.* 831, 49-58.
32. Collier, I.E., Wilhelm, S.M., Eisen, A.Z., Marmer, B.L., Grant, G.A., Seltzer, J.L., Kronenberger, A., He, C., Bauer, E.A., Goldberg, G.I. H-ras oncogenic transformed human bronchial epithelial cells (TBE-1) secrete a single metalloproteinase capable of degrading basement membrane collagen. (1988) *J. Biol. Chem.* 263, 6579-6587.
33. Kalebic, T., Garbisa, S., Glaser, B., Liotta, L.A. Basement membrane collagen: Degradation by migrating endothelial cells. (1983) *Science* 221, 281-283.
34. Seltzer, J.L., Adams, S.A., Grant, G.A., Eisen, A.Z. Purification and properties of a gelatin-specific neutral protease from human skin. (1981) *J. Biol. Chem.* 256, 4662-4669.
35. Wilhelm, S.M., Collier, I.E., Marmer, B.L., Eisen, A.Z., Grant, G.A., Goldberg, G.I. SV40 transformed human lung fibroblasts secrete a 92 kDa type IV collagenase which is identical to that secreted by normal human macrophages. (1989) *J. Biol. Chem.* 264, 17213-17221.
36. Hibbs, M.S., Hasty, K.A., Seyer, J.M., Kang, A.H., Mainardi, C.M. Biochemical and immunological characterisation of the secreted forms of human neutrophil collagenase. (1985) *J. Biol. Chem.* 260, 2493-2500.
37. Mainardi, C.L., Hibbs, M.S., Hasty, K.A., Seyer, J.M. Purification of a type V collagen degrading metalloproteinase from rabbit alveolar macrophages. (1984) *Collagen. Rel. Res.* 4, 479-492.
38. Collier, I. E., Krasnov, P.E., Strongin, A.Y., Birkedal-Hansen, H., Goldberg, G.I. Alanine scanning mutagenesis and functional analysis of the fibronectin like collagen binding domain from human 92 kDa type collagenase. (1992) *J. Biol. Chem.* 267, 6776-6781.
39. Murphy, G., Nguyen, Q., Cockett, M.I., Atkinson, S.J. Allen, J.A., Knight, C.G., Willenbrock, F., Docherty, A.J.P. Assessment of the role of the fibronectin-like domain of gelatinase A by analysis of a deletion mutant. (1994) *J. Biol. Chem.* 269, 6632-6636.

40. Murphy, G., Ward, R., Hembry, R.M., Reynolds, J.J., Kühn, K., Tryggvason, K. Characterisation of gelatinase from pig polymorphonuclear leucocytes. (1989) *Biochem J.* 258, 463-472.
41. Hostikka, S.L., Tryggvason, K. The complete primary structure of the $\alpha 2$ chain of human type IV collagen and comparison with the $\alpha 1$ (IV) chain. (1988) *J. Biol. Chem.* 263, 19488-19493.
42. Murphy, G. J. P., Murphy, G., Reynolds, J.J. The origin of matrix metalloproteinases and their familial relationships. (1991) *FEBS Lett.* 289, 4-7.
43. Okada, Y., Nagase, H., Harris, E.D. Jr. A metalloproteinase from rheumatoid synovial fibroblasts that degrade connective tissue matrix components: Purification and characterisation. (1986) *J. Biol. Chem.* 261, 14245-14255.
44. Wu, J.J., Lark, M.W., Chun, L.E., Eyre, D.R. Sites of stromelysin cleavage in collagen types II, IX, X and XI of cartilage. (1991) *J. Biol. Chem.* 266, 5625-5628.
45. Murphy, G., Cockett, M.I., Ward, R.V., Docherty, A.J.P. Matrix metalloproteinases degradation of elastin, type IV collagen and proteoglycan. (1991) *Biochem. J.* 277, 277-279.
46. Basset, P., Bellocq, J.P., Wolf, C., Stoll, I., Hutin, P., Limacher, J.M., Podhajcer, O.L., Chenard, M.P., Rio, M.C., Chambon, P. A novel metalloproteinase gene specifically expressed in stromal cells of breast carcinomas. (1990) *Nature* 348, 699-704.
47. Levy, A., Zucman, J., Delattre, O., Matlei, M., Rio, M., Basset, P. Assignment of the human stromelysin (STMY 3) gene to the q11.2 region of chromosome 22. (1992) *Genomics* 13, 881-883.
48. Formstone, C. J., Byrd, P.J., Ambrose, H.J., Riley, J.H., Hernandez, D., McConville, C.M., Taylor, A.M.R. The order and orientation of a cluster of metalloproteinase genes, Stromelysin 2, Collagenase, and Stromelysin, together with D11S385, on chromosome 1q22-q23. (1993) *Genomics* 16, 289-291.
49. Murphy, G., Segain, J-P., O'Shea, M., Cockett, M., Ioannou, C., Lefebvre, O., Chambon, P., Basset, P. The 28 kDa N-terminal domain of mouse stromelysin-3 has the general properties of a weak metalloproteinase. (1993) *J. Biol. Chem.* 268, 15435-15441.

50. Woessner, F.J.Jr., Taplin, C.J. Purification and properties of a small matrix metalloproteinase inhibitor of the rat uterus. (1988) *J. Biol. Chem.* 263, 16918-16925.
51. Shapiro, S.D., Griffin, G.L., Gilbert, D.J., Jenkins, N.A., Copeland, N.G., Welgus, H.G., Senior, R.M., Ley, T.J. Molecular cloning, chromosomal location and bacterial expression of a murine macrophage metalloelastase. (1992) *J. Biol. Chem.* 267, 4664-4671.
52. Sato, H., Takino, T., Okada, Y., Cao, J., Shinagawa, A., Yamamoto, E., Seiki, M. A matrix metalloproteinase expressed on the cell surface of invasive tumour cells. (1994) *Nature* 370, 61-65.
53. Seltzer, J. L., Jeffrey, J.J., Eisen, A.Z. Evidence for mammalian collagenases as zinc ion metalloenzymes. (1977) *Biochim. Biophys. Acta.* 485, 179-187.
54. Salowe, S.P., Marcy, A.I., Cuca, G.C., Smith, C.K. Kopka, I.E., Hagmann, W.K., Hermes, J.D. Characterisation of zinc-binding sites in human stromelysin-1: Stoichiometry of the catalytic domain and identification of a cysteine ligand in the proenzyme. (1992) *Biochemistry* 31, 4535-4540.
55. Lovejoy, B., Cleasby, A., Hassell, A.M., Longley, M.A., Luther, M.A., Weigl, D., McGeehan, G., McElroy, A.B., Drewry, D., Lambert, M.H., Jordan, S.R. Structure of the catalytic domain of human fibroblast collagenase complexed with an inhibitor. (1994) *Science* 263, 375-377.
56. Lowry, C.L., McGeehan, G., LeVine H. Metal ion stabilization of the conformation of a recombinant 19 kDa catalytic fragment of human fibroblast collagenase (1992) *Proteins. Struct. Funct. Genet.* 12, 42-48.
57. Housely, T. J., Baumann, A.P., Braun, I.D., Davis, G., Seperack, P.K., Wilhelm, S.M. Recombinant chinese hamster ovary cell matrix metalloproteinase-3 (MMP-3, Stromelysin-1). (1993) *J. Biol. Chem.* 268, 4481-4487.
58. Stricklin, G.P., Eisen, A.Z., Bauer, E.A., Jeffrey, J.J. Human skin fibroblast collagenase: Chemical properties of precursor and active forms. (1978) *Biochemistry* 17, 2331-2337.
59. Sakamoto, S., Sakamoto, M., Matsumoto, A., Nagayama, M., Glimcher, M.J. Chick bone collagenase inhibitor and latency of collagenase. (1981) *Biochem. Biophys. Res. Commun.* 103, 339-346.

60. Stricklin, G. P., Jeffrey, J.J., Roswit, W.T., Eisen, A.Z. Human skin fibroblast procollagenase: Mechanisms of activation by organomercurials and trypsin. (1983) *Biochemistry* 22, 61-68.
61. Shinkai, H., Nagai, Y. A latent collagenase from human skin explants (1977) *J. Biochemistry*. 31, 1261-1268.
62. Birkedal-Hansen, H., Taylor, R.E. Detergent-activation of latent collagenase and resolution of its component molecules. (1982) *Biochem. Biophys. Res. Commun.* 107, 1173-1178.
63. Nagase, H., Enghild, J.J., Suzuki, K., Salvesen, G. Stepwise activation mechanisms of the precursor of matrix metalloproteinase 3 (stromelysin) by proteinases and (4-aminophenyl) mercuric acetate. (1990) *Biochemistry* 29, 5783-5789.
64. Vissers, M. C. M., Winterbourn, C.C. Activation of human neutrophil gelatinase by endogenous serine proteinases. (1988) *Biochem. J.* 249, 327-331.
65. Sorsa, T., Ingman, T., Suomaleinen, K., Haapasalo, M., Kontinen, Y.T., Lindy, O., Saari, H., Uitto, V. Identification of proteases from periodontopathogenic bacteria as activators of latent human neutrophil and fibroblast type interstitial collagenases. (1992) *Infection. Immunity.* 60, 4491-4495.
66. Wilhelm, S. M., Collier, I.E., Marmer, B.L., Eisen, A.Z., Grant, G.A., Goldberg, G.I. SV40-transformed human lung fibroblasts secrete a 92-kDa type IV collagenase which is identical to that secreted by normal human macrophages. (1989) *J. Biol. Chem.* 264, 17213-17221.
67. Saarinen, J., Kalkkinen, N., Welgus, H.G., Kovanen, P.T. Activation of human interstitial procollagenase through direct cleavage of the Leu83-Thr84 bond by mast cell chymase. (1994) *J. Biol. Chem.* 269, 18134-18140.
68. Azzam, H. S., Thompson, E.W. Collagen-induced activation of the Mr 72,000 type IV collagenase in normal and malignant human fibroblastoid cells. (1992) *Cancer. Res.* 52, 4540-4544.
69. Ogata, Y., Enghild, J.J., Nagase, H. Matrix metalloproteinase 3 (stromelysin) activates the precursor for the human matrix metalloproteinase 9. (1992) *J. Biol. Chem.* 276, 3581-3584.

70. Suzuki, K., Nagase, H., Ito, A., Enghild, J.J., Salvesen, G. The role of matrix metalloproteinase-3 in the stepwise activation of human rheumatoid synovial procollagenase. (1990) *Biol. Chem. Hoppe Seyler* 371 suppl, 305-310.
71. Stetler-Stevenson, W.G., Talano, J., Gallagher, M.E., Krutzch, H.C., Liotta, L.A. Inhibition of human type IV collagenase by a highly conserved peptide sequence derived from its pro segment. (1991) *Am. J. Med. Sci.* 302, 163-170.
72. Windsor, L. J., Birkedal-Hansen, H., Birkedal-Hansen, B., Engler, J.A. An internal cysteine plays a role in the maintenance of the latency of human fibroblast collagenase. (1991) *Biochemistry* 30, 641-647.
73. Springman, E.B., Angleton, E.L., Birkedal-Hansen, H., Van Wart, H.E. Multiple modes of action of latent human fibroblast collagenase: Evidence for the role of Cys73 active site zinc complex in latency and a cysteine switch mechanism for activation. (1990) *Proc. Natl. Acad. Sci. USA* 87, 364-368.
74. Bläser, J., Triebel, S., Reinke, H., Tschesche, H. Formation of a covalent Hg-Cys bond during mercurial activation of PMNL procollagenase gives evidence of a cysteine switch mechanism. (1992) *FEBS Lett.* 313, 59-61.
75. Chen, L., Noelken, M., Nagase, H. Disruption of the cysteine-75 and zinc ion coordination is not sufficient to activate the precursor of human matrix metalloproteinase-3 (stromelysin-1). (1993) *Biochemistry* 32, 10289-10295.
76. Crabbe, T., Willenbrock, F., Eaton, D., Hynds, P., Carne, A., Murphy, G., Docherty, A.J.P. Biochemical characterisation of matrilysin: Activation conforms to the stepwise mechanisms proposed for other matrix metalloproteinases. (1992) *Biochemistry* 31, 8500-8507.
77. Ito, A., Nagase, H. Evidence that human rheumatoid synovial matrix metalloproteinase 3 is an endogenous activator of procollagenase. (1988) *Arch. Biochem. Biophys.* 267, 211-216.
78. Suzuki, K., Enghild, J.J., Morodomi, T., Salvesen, G., Nagase, H. Mechanisms of the activation of tissue procollagenase by matrix metalloproteinase-3 (stromelysin) (1990) *Biochemistry* 29, 10261-10270.

79. Reinemer, P., Grams, F., Huber, R., Kleine, T., Schneirer, Piper, M., Tschesche, H., Bode W. Structural implications for the role of the N-terminus in the 'superactivation' of collagenases. (1994) *FEBS Lett.* 338, 227-233.
80. Stetler-Stevenson, W. G., Krutzch, H.C., Wachter, M.P., Margulies, I., Liotta, L.A. The activation of human type IV collagenase proenzyme. (1989) *J. Biol. Chem.* 264, 1353-1356.
81. Bläser, J., Knäuper, V., Osthues, A., Reinke, H. Mercurial activation of polymorphonuclear leucocyte procollagenase. (1991) *Eur. J. Biochem.* 202, 1223-1230.
82. Triebel, S., Bläser, J., Reinke, H., Knaüper, V., Tschesche, H. Mercurial activation of human PMN leukocyte type IV procollagenase (gelatinase). (1992) *FEBS Lett.* 298, 280-284.
83. Van Doren, S. R., Kurochkin, A.V., Ye, Q., Johnson, L.L., Hupe, D.J., Zuiderweg, E.R.P. Assignments for the main-chain nuclear magnetic resonances and delineation of the secondary structure of the catalytic domain of human stromelysin-1 as obtained from triple-resonance 3D NMR experiments. (1993) *Biochemistry* 32, 13109-13122.
84. Bode, W., Gomis-Rüth, F.X., Huber, R., Zwilling, R., Stöcker, W. Structure of astacin and implications for the activation of astacins and zinc ligation of collagenases. (1992) *Nature* 358, 164-167.
85. Bode, W., Reinemer, P., Huber, R., Kleine, T., Schnierer, S., Tschesche, H. The X-ray crystal structure of the catalytic domain of human neutrophil collagenase inhibited by a substrate analogue reveals the essentials for catalysis and specificity. (1994) *EMBO J.* 13, 1263-1269.
86. Spurlino, J.C., Smallwood, A.M., Carlton, D.D., Banks, T.M., Vavra, K.J., Johnson, J.S., Cook, E.R., Falvo, J., Waki, R.C., Pulvino, T.A., Wendoloski, J.J., Smith, D.L. 1.56 Å structure of mature truncated human fibroblast collagenase. (1994) *Proteins. Struct. Funct. Genet.* 19, 98-109.
87. Woolley, D.E., Roberts, D.R., Evanson, J.M. Small molecular weight β 1 serum protein which specifically inhibits human collagenases. (1976) *Nature* 261, 325-327.
88. Sellers, A., Reynolds, J.J. Identification and partial characterisation of an inhibitor of collagenase from rabbit bone. (1977) *Biochem. J.* 167, 353-360.

89. Murphy, G., Cartwright, E.C., Sellers, A., Reynolds, J.J. The detection and characterisation of collagenase inhibitors from rabbit tissues in culture. (1977) *Biochim. Biophys. Acta.* 483, 493-498.
90. Sellers, A., Cartwright, E., Murphy, G., Reynolds, J.J. Evidence that latent collagenases are enzyme-inhibitor complexes. (1977) *Biochem. J.* 163, 303-307.
91. Reynolds, J.J., Bunning, R.A.D., Cawston, T.E., Murphy, G. Tissue metallo-proteinase inhibitors and their role in matrix catabolism. (1981) *Cellular Interactions*. D. A. Gordon, 205-213.
92. Yasui, N. Hori, H., Nagai, Y. Production of collagenase inhibitor by the growth cartilage of embryonic chick bone: Isolation and partial characterisation. (1981) *Coll. Res.* 1, 59-72.
93. Nolan, J.C., Ridge, S., Oronsky, A.L., Slakey, L.L. Synthesis of a collagenase inhibitor by smooth muscle cells in culture. (1978) *Biochem. Biophys. Res. Commun.* 83, 1183-1190.
94. Pettigrew, D. W., Wang, H.M., Sodek, J., Brunette, D.M. Synthesis of collagenolytic enzymes and their inhibitors by gingival tissue in vitro. (1981) *J. Periodontal. Res.* 16, 637-645.
95. Roughley, P. J., Murphy, G., Barrett, A.J. Proteinase inhibitors of bovine nasal cartilage. (1978) *Biochem. J.* 169, 721-724.
96. Nolan, J. C., Ridge, S.C., Oronsky, A.L., Kerwar, S.S. Purification and properties of a collagenase inhibitor from cultures of bovine aorta. (1980) *Atherosclerosis.* 35, 93-102.
97. Welgus, H.G., Stricklin, G.P., Eisen, A.Z., Bauer, E.A., Jeffrey, J.J. Vertebrate collagenase produced by human skin fibroblasts. (1978) *Clin. Res.* 26, 489A.
98. Vater, C.A., Mainardi, C.L., Harris, E.D. Binding of latent rheumatoid synovial collagenase to collagen fibrils. (1978) *Biochim. Biophys. Acta.* 539, 238-247.
99. Vater, C.A., Mainardi, C.L., Harris, Jr. E.D. Inhibitor of collagenase from cultures of human tendon. (1979) *J. Biol. Chem.* 254, 3045-3053.
100. Simpson, J., Mailman, M.L. Synthesis of a collagenase inhibitor by gingival fibroblasts in culture. (1981) *Biochim. Biophys. Acta.* 673, 279-285.

101. Sakamoto, S., Sakamoto, M., Matsumoto, A., Nagayama, M., Glimcher, M.J. Chick bone collagenase inhibitor and latency of collagenase. (1981) *Biochem. Biophys. Res. Commun.* 103, 339-346.
102. Kerwar, S., Nolan, J.C., Ridge, S.C, Oronsky, A.L., Slakey, L.L. Properties of a collagenase inhibitor partially purified from smooth muscle cells. (1980) *Biochim. Biophys. Acta.* 632, 183-191.
103. Cawston, T. E., Galloway, W.A., Mercer, E., Murphy, G., Reynolds, J.J. Purification of rabbit bone inhibitor of collagenase. (1981) *Biochem. J.* 195, 159-165.
104. Bunning, R.A., Murphy, G., Kumar, S., Phillips, P., Reynolds, J.J. Metalloproteinase inhibitors from bovine cartilage and body fluids. (1984) *Eur. J. Biochem.* 139, 75-80.
105. DeClerck, Y.A., Laug, W.E. Inhibition of tumour cell collagenolytic activity by bovine endothelial cells (1986) *Cancer Res.* 46, 3580-3586.
106. Stetler-Stevenson, W.G., Krutzsch, H.C., Liotta, L.A. Tissue inhibitor of metalloproteinases-2 (TIMP-2) (1989) *J. Biol. Chem.* 264, 17374-17378.
107. DeClerck, Y.A., Yean, T., Ratzkin, B.J., Lu, H.S., Langley, K.E. Purification and characterisation of two related but distinct metalloproteinase inhibitors secreted by bovine aortic endothelial cells. (1989) *J. Biol. Chem.* 264, 17445-17453.
108. Murray, J.B., Allison, K., Sudhalter, J., Langer, R. Purification and partial amino acid sequence of a bovine cartilage derived collagenase inhibitor. (1986) *J. Biol. Chem.* 261, 4154-4159.
109. Blenis, J., Hawkes, S.P. Transformation sensitive protein associated with the cell substratum of chicken embryo fibroblasts. (1983) *Proc. Natl. Acad. Sci. USA.* 80, 770-774.
110. Pavloff, N., Staskus, P.W., Kishmani, N.S., Hawkes, S.P. A new inhibitor of metalloproteinases from chicken: Chimp-3. (1992) *J. Biol. Chem.* 267, 17321-17326.
111. Stricklin, G.P., Welus, H.G. Human skin fibroblast collagenase inhibitor. Purification and biochemical characterisation. (1983) *J. Biol. Chem.* 258, 12252-12258.

112. Docherty, A.J.P., Lyons, A., Smith, B.J., McWright, E., Stephens, P.E., Harris T.J.R., Murphy, G., Reynolds, J.J. Sequence of tissue inhibitor of metalloproteinases and its identity to erythroid -potentiating activity. (1985) *Nature* 318, 66-69.
113. Gewert, D.R., Coulcombe, B., Castelino, M., Skup, D., Williams, B.R.G. Characterisation and expression of a murine gene homologous to EPA/TIMP: A virus induced gene in the mouse. (1987) *EMBO J.* 6, 651-657.
114. DeClerck, Y.A., Yean, T.D., Ratzkin, B.J., Lu, H.S., Langley, K.E. Characterisation of two related, but distinct metalloproteinase inhibitors secreted by bovine aortic endothelial cells. (1989) *J. Biol. Chem.* 264, 17445-17453.
115. Smith, G.W., Goetz, T.L., Anthony, R.V., Smith, M.F. Molecular cloning of an ovine ovarian tissue inhibitor of metalloproteinases: Ontogeny of ribonucleic acid expression and in situ localisation within pre-ovulatory follicles and luteal tissue. (1994) *Endocrinology* 134, 344-352.
116. Okada, A., Garnier, J., Vicaire, S., Basset, P. Cloning of the cDNA encoding rat tissue inhibitor of metalloproteinase 1 (TIMP-1), amino acid comparison with other TIMPs, and gene expression in rat tissues. (1994) *Gene* 147, 301-302.
117. Horowitz, S., Dafni, N., Shapiro, D.L., Holm, B.A., Notler, R.H., Quible, D.J. Hyperoxic exposure alters gene expression in the lung. Induction of the tissue inhibitor of metalloproteinases messenger RNA and other RNAs. (1989) *J. Biol. Chem.* 264, 7092-7095.
118. Tanaka, T., Andoh, N., Takeya, T. Differential screening of the ovarian cDNA libraries detected the expression of the porcine collagenase inhibitor gene in the functional corpora lutea. (1992) *Mol. Cell. Endocrinol.* 83, 65-71.
119. Forough, R., Nikkari, S.T., Hasenstab, D., Clowes, A.W. Cloning and characterisation of baboon tissue inhibitor of metalloproteinases-1 (TIMP-1) (1994) Unpublished data lodged in the EMBL database.
120. Leco, K.J., Hayden, L.J., Sharma, R.E., Rocheleau, H., Greenberg, A.H., Edwards, D.R. Differential regulation of TIMP-1 and TIMP-2 expression in normal and Ha-ras transformed murine fibroblasts. (1992) *Gene* 17, 209-217.

121. Cook, T.F., Burke, J.S., Bergman, K.D., Quinn, C.O., Jeffrey, J.J., Partridge, N.C. Cloning and regulation of rat tissue inhibitor of metalloproteinases-2 in osteoblastic cells. (1994) *Arch. Biochem. Biophys.* 311, 313-320.
122. Pavloff, N., Staskus, P.W., Kishnani, N.S., Hawkes, S.P. A new inhibitor of metalloproteinases from chicken: Chimp-3 A third member of the TIMP family. (1992) *J. Biol. Chem.* 267, 17321-17326.
123. Apte, S.S., Mattei, M., Olsen, B.R. Cloning of the cDNA encoding human tissue inhibitor of metalloproteinases-3 (TIMP-3) and mapping of the human TIMP-3 gene to chromosome 22. (1994) *Genomics* 19, 86-90.
124. Apte, S.S., Hayashi, K., Seldin, M.F., Mattei, M.G., Hayashi, M., Olsen, B.R. Gene encoding a novel murine tissue inhibitor of metalloproteinases (TIMP), TIMP-3 is expressed in developing mouse epithelia, cartilage and muscle, and is located on mouse chromosome 10. (1994) *Developmental Dynamics* 200, 177-197.
125. Pearson, D.J., Lipman, W.R. Improved tools for biological sequence analysis. (1988) *Proc. Natl Acad. Sci. USA.* 85, 2444-2448.
126. Denhardt, D.T., Feng, B., Edwards, D.R., Cocuzzi, E.T., Malyankar, U.M. Tissue inhibitor of metalloproteinases (TIMP aka EPA). Structure, control of expression and biological function. (1993) *Pharmacol. Ther.* 59, 329-341.
127. Robinson, A.B., Robinson, L.R. Distribution of glutamine and asparagine residues and their near neighbours in peptides and proteins. (1991) *Proc. Natl. Acad. Sci. USA.*, 88, 8880-8884.
128. Cawston, T. E., Murphy, G., Galloway, W.A., Reynolds, J.J. The binding of rabbit bone inhibitor of collagenase to Concanavalin A Sepharose. (1980) *Biochem. Soc. Trans.* 8, 112-113.
129. Stricklin, G.P. Human fibroblast tissue inhibitor of metalloproteinases: Glycosylation and function. (1986) *Collagen Rel. Res.* 6, 219-228.
130. Carmichael, D.F., Sommer, A., Thompson, R.C., Anderson, D.C., Smith, C.G., Welgus, H.G, Stricklin G.P. Primary structure and cDNA cloning of human fibroblast collagenase inhibitor. (1986) *Proc. Natl. Acad. Sci. USA.* 83, 2407-2411.

131. Williamson, R. A., Smith, B.J., Angal, S., Freedman, R.B. Chemical modification of tissue inhibitor of metalloproteinases-1 and its inactivation by diethyl pyrocarbonate. (1992) *Biochim. Biophys. Acta.* 1203, 147-154.
132. Kishi, J., Hayakawa, T. Purification and characterisation of bovine dental pulp collagenase inhibitor. (1984) *J. Biochem.* 96, 395-404.
133. Cawston, T.E., Mercer, E., Mooney, C., Wright, J.K. Tissue inhibitor of metalloproteinases. (1986) *Proteinases in inflammation and tumour invasion* Ed. H. Tschesche. Walter de Gruyter & Co, Berlin. 189-210.
134. Andrews, H.J., Plumpton, T.A., Harper, G.P., Cawston, T.E. A synthetic peptide metalloproteinase inhibitor, but not TIMP, prevents the breakdown of proteoglycan within articular cartilage in vitro. (1992) *Agents Actions* 37, 147-154.
135. Clark, I.M., Powell, L.K., Wright, J.K., Cawston, T.E. Polyclonal and monoclonal antibodies against human tissue inhibitor of metalloproteinases (TIMP) and the design of an enzyme-linked immunosorbent assay to measure TIMP. (1991) *Matrix* 11, 76-85.
136. Williamson, R. A., Marston, F.A.C., Angal, S., Koklitis, P., Panico, M., Morris, H.R., Carne, A.F., Smith, B.J., Harris, T.J.R., Freedman, R.B. Disulphide bond assignment in human tissue inhibitor of metalloproteinases (TIMP). (1990) *Biochem. J.* 268, 267-274.
137. DeClerck, Y. A., Yean, T., Lee, Y., Tomich, J.M., Langley, K.E. Characterisation of the functional domain of tissue inhibitor of metalloproteinases-2 (TIMP-2). (1993) *Biochem. J.* 289, 65-69.
138. Okada, Y., Watanabe, S., Nakanishi, I., Kishi, J., Hayakawa, T., Watorek, W., Travis, J., Nagase, H. Inactivation of tissue inhibitor of metalloproteinases by neutrophil elastase and other serine proteinases. (1988) *FEBS Lett.* 229, 157-160.
139. Williamson, R.A., Smith, B.J., Angal, S., Murphy, G., Freedman, R.B. Structural analysis of tissue inhibitor of metalloproteinases-1 (TIMP-1) by tryptic peptide mapping. (1993) *Biochim. Biophys. Acta.* 1164, 8-16.
140. Blenis, J., Hawkes, S.P. Characterisation of a transformation sensitive protein in the extracellular matrix of chicken embryo fibroblasts. (1984) *J. Biol. Chem.* 259, 11563-11570.

141. Williamson, R.A., Martorell, G., Carr, M.D., Murphy, G., Docherty, A.J.P., Freedman, R.B., Feeney, J. Solution structure of the active domain of tissue inhibitor of metalloproteinases-2. A new member of the OB fold protein family. (1994) *Biochemistry* 33, 11745-11759.
142. Williamson, R.A., Bartels, H., Murphy, G., Freedman, R.B. Folding and stability of the active N-terminal domain of tissue inhibitor of metalloproteinases-1 and -2. (1994) *Protein Engineering* 7, 1035-1040.
143. Huebner, K. A., Rushdie, A., Griffin, C.A., Isobe, D.W., Croce, C.M. Localisation of the gene encoding human erythroid potentiating activity to chromosome region Xp11.1 → Xp11.1. (1986) *Am. J. Hum. Genet.* 38, 819-826.
144. Willard, H. F., Duffy, S.J., Mahtani, M.M., Dorkins, H., Davies, K.E., Williams, B.R.G. Regional localisation of the TIMP gene on the X chromosome. (1989) *Hum. Genet.* 81, 234-238.
145. Spurr, N. K., Goodfellow, P.N., Docherty, A.J.P. Chromosomal assignment of the gene encoding the human tissue inhibitor of metalloproteinases to Xp11.1-p11.4 (1987) *Ann. Hum. Genet.* 51, 189-194.
146. DeClerck, Y. A., Szpirer, C., Aly, M.S., Cassiman, J., Eeckhaut, Y., Rousseau, G. The gene for human tissue inhibitor of metalloproteinases-2 is localised on human chromosome arm 17q25. (1992) *Genomics* 14, 782-784.
147. Brown, C.J., Flenniken, A.M., Williams, B.G., Willard, H.F. X chromosome inactivation of the human TIMP gene. (1990) *Nucl. Acid. Res.* 18, 4191-4195.
148. Edwards, D. R., Waterhouse, P., Holman, M.L., Denhardt, D.T. A growth-responsive gene (16C8) in normal mouse fibroblasts homologous to a human collagenase inhibitor with erythroid-potentiating activity: evidence for inducible and constitutive transcripts. (1986) *Nucl. Acids Res.* 14, 8863-8878.
149. Gewert, D.R., Coulombe, B., Castelino, M., Skup, D., Williams, B.R.G. Characterisation and expression of a murine gene homologous to EPA/TIMP: A virus induced gene in the mouse. (1987) *EMBO J.* 6, 651-657.

150. Murphy, G., Reynolds, J.J., Werb, Z. Biosynthesis of tissue inhibitor of metalloproteinases by human fibroblasts in culture. (1985) *J. Biol. Chem.* 260, 3079-3088.
151. Coulombe, B., Ponton, A., Daigneault, L., Williams, B.R.G., Skup, D. Presence of transcription regulatory elements within an intron of the virus-inducible murine TIMP gene (1988) *Mol. Cell. Biol.* 8, 3227-3234.
152. Flenniken, A.M., Williams, B.G. Developmental expression of the endogenous TIMP gene and a TIMP-lacZ fusion gene in transgenic mice. (1990) *Genes Dev.* 4, 1094-1106.
153. Ponton, A., Coulombe, B., Steyeart, A., Williams, B.R.G., Skup, D. Basal expression of the gene (TIMP) encoding the murine tissue inhibitor of metalloproteinases is mediated through AP1- and CCAAT- binding factors. (1992) *Gene* 116, 187-194.
154. Campbell, C.E., Flenniken, A.M., Skup, D., Williams, B.R.G. Identification of a serum- and phorbol ester-responsive element in the murine tissue inhibitor of metalloproteinase gene (1991) *J. Biol. Chem.* 266, 7199-7206.
155. Edwards, D.R., Rocheleau, H., Sharma, R.R., Wills, A.J., Cowie, A., Hassell, J.A., Heath, J.K. Involvement of AP1 and PEA3 binding sites in the regulation of murine tissue inhibitor of metalloproteinases-1 (TIMP-1) transcription. (1992) *Biochim. Biophys. Acta.* 1171, 41-55.
156. DeClerck, Y.A., Darville, M.I., Eeckhout, Y., Rousseau, G.G. Characterisation of the promoter of the gene encoding tissue inhibitor of metalloproteinases-2 (TIMP-2). (1994) *Gene* 139, 185-191.
157. Uchijima, M., Sato, H., Fujii, M., Seiki, M. Tax proteins of human T-cell leukaemia virus type 1 and 2 induce expression of the gene encoding erythroid potentiating activity (tissue inhibitor of metalloproteinases -1, TIMP-1). (1994) *J. Biol. Chem.* 269, 14946-14950.
158. Shapiro, S. D., Doyle, G.A.R., Ley, T.J., Parks, W.C., Welgus, H.G. Molecular mechanisms regulating the production of collagenase and TIMP in U937 cells: Evidence for involvement of delayed transcriptional activation and enhanced mRNA stability. (1993) *Biochemistry* 32, 4286-4292.

159. Andrews, H.J., Edwards, T.A., Cawston, T.E., Hazleman, B.L. Transforming growth factor- β causes partial inhibition of interleukin-1 stimulated cartilage degradation in vivo. (1989) *Biochem. Biophys. Res. Commun.* 162, 144-150.
160. Lefebvre, V., Peeters-Joris, C., Vaes, G. Modulation by interleukin-1 and tumour necrosis factor α of production of collagenase, tissue inhibitor of metalloproteinases and collagen in differentiated and dedifferentiated articular cartilage. (1990) *Biochim. Biophys. Acta.* 1052, 366-378.
161. Legendre, P., Richards, C.D., Rafferty, J.A., Dew, G.W., Reynolds, J.J. The expression of matrix metalloproteinases and their inhibitors by pig synovial cells and their regulation by combinations of cytokines and growth factors. (1993) *Comp. Biochem. Physiol.* 106B, 691-704.
162. MacNaul, K., Chartrain, N., Lark, M., Tocci, M.J., Hutchinson, N.I. Discoordinate expression of stromelysin, collagenase and tissue inhibitor of metalloproteinases-1 in rheumatoid human synovial fibroblasts. (1990) *J. Biol. Chem.* 265, 17238-17245.
163. Martel-Pelletier, J., Zafarullah, M., Kodama, S., Pelletier, J.-P. In vitro effect of interleukin 1 on the synthesis of metalloproteinases, TIMP, plasminogen activators and inhibitors in human articular cartilage. (1991) *J. Rheumatol.* 18, suppl 27, 80-84.
164. Ito, A., Goshwami, H., Sato, T., Mori, Y., Yamashita, K., Hayakawa, T., Nagase, H. Human recombinant interleukin-1- α -mediated stimulation of procollagenase production and suppression of biosynthesis of tissue inhibitor of metalloproteinases in rabbit uterine cervical fibroblasts. (1988) *FEBS Lett.* 234, 326-330.
165. Chua, C.C., Chua, B.H.L. Tumour necrosis factor- α induces mRNA for collagenase and TIMP in human skin fibroblasts. (1990) *Conn. Tiss. Res.* 25, 161-170.
166. Lefebvre, V., Peeters-Joris, C., Vaes, G. Production of gelatin degrading matrix metalloproteinases ('type IV collagenases') and inhibitors by articular chondrocytes during their differentiation by serial subcultures and under stimulation by interleukin-1 and tumour necrosis factor- α (1991) *Biochim. Biophys. Acta.* 1094, 8-18.
167. Ito, A., Sato, T., Iga, T., Mori, Y. Tumour necrosis factor bifunctionally regulates matrix metalloproteinases and tissue inhibitor of metalloproteinases (TIMP) production by human fibroblasts. (1990) *FEBS Lett.* 269, 93-95.

168. Mawatari, M., Kohno, K., Mizoguchi, H., Matsuda, T., Asoh, K., Van Damme, J., Welgus, H.G., Kuwano, M. Effects of tumour necrosis factor α and epidermal growth factor on cell morphology, cell surface receptors and the production of tissue inhibitor of metalloproteinases and IL-6 in human microvascular epithelial cells. (1989) *J. Immunol.* 143, 1619-1627.
169. Roberts, A.B., Sporn, M.B., Assoian, R.K., Smith, J.M., Roche, N.S., Wakefield, L.M., Heine, U.I., Liotta, L.A., Falanga, V., Kerhl, J.H., Fauci, A.S. Transforming growth factor type β : Rapid induction of fibrosis and angiogenesis *in vivo* and stimulation of collagen formation *in vitro*. (1986) *Proc. Natl. Acad. Sci. USA* 83, 4167-4171.
170. Overall, C.M., Wrana, J.L., Sodek, J. Independent regulation of collagenase, 72 kDa progelatinase, and metalloproteinase inhibitor expression in human fibroblasts by transforming growth factor β . (1989) *J. Biol. Chem.* 264, 1860-1869.
171. Edwards, D.R., Murphy, G., Reynolds, J.J., Whitham, S.E., Docherty, A.J.P., Angel, P., Heath, J.K. Transforming growth factor beta modulates the expression of collagenase and metalloproteinase inhibitor. (1987) *EMBO J.* 6, 1899-1904.
172. Overall, C. M., Wrana, J.L., Sodek, J. Transforming growth factor- β regulation of collagenase, 72 kDa-progelatinase, TIMP and PAI-1 expression in rat bone cell populations and human fibroblasts. (1989) *Conn. Tiss. Res.* 20, 289-294.
173. Wright, J. K., Cawston, T.E., Hazleman, B.L. Transforming growth factor beta stimulates the production of the tissue inhibitor of metalloproteinases (TIMP) by human synovial and skin fibroblasts. (1991) *Biochim. Biophys. Acta.* 1094, 207-210.
174. Günther, M., Haubeck, H., Van De Leur, E., Bläser, J., Bender, S., Gütgemann, I., Fischer, D., Tschesche, H., Greiling, H., Heinrich, P.C., Graeve, L. Transforming growth factor β regulates tissue inhibitor of metalloproteinases-1 expression in differentiated human articular cartilage (1994) *Arthritis. Rheum.* 37, 395-405.
175. Meikle, M.C., McGarrity, A.M., Thomson, B.M., Reynolds, J.J. Bone derived growth factors modulate collagenase and TIMP (tissue inhibitor of metalloproteinases) activity and type I collagen degradation by mouse calvarial osteoblasts. (1991) *Bone Mineral* 12, 41-55.

176. Kordula, T., Güttgeman, I., Rose-John, S., Roeb, E., Osthues, A., Tschesche, H., Koj, A., Heinrich, P.C., Graeve, L. Synthesis of tissue inhibitor of metalloproteinases-1 (TIMP-1) in human hepatoma cells (HepG2). Upregulation by interleukin-6 and transforming growth factor β 1. (1992) *FEBS Lett.* 313, 143-147.
177. Sato, T., Ito, A., Mori, Y. Interleukin 6 enhances the production of tissue inhibitor of metalloproteinases (TIMP) but not that of matrix metalloproteinases by human fibroblasts. (1990) *Biochem. Biophys. Res. Commun.* 170, 824-829.
178. Lotz, M., Guerne, P. A. Interleukin-6 induces the synthesis of tissue inhibitor of metalloproteinases-1/erythroid potentiating activity (TIMP-1/EPA). (1991) *J. Biol. Chem.* 266, 2017-2020.
179. Houssiau, F.A., Devogelaer, J.-P., Van Damme, J., Nagant de Deuxchaisnes, C., Van Snick, J. Interleukin-6 in synovial fluid and serum of patients with rheumatoid arthritis and other inflammatory arthritides. (1988) *Arthritis. Rheum.* 31, 74-78.
180. Zhang, X., Gu, J.-J., Lu, Z.-Y., Yasukawa, K., Yancopoulos, G.D., Turner, K., Shoyab, M., Taga, T., Kishimoto, T., Bataille, R., Klein, B. Ciliary neurotropic factor, interleukin-11, eukaemia inhibitory factor and oncostatin M are growth factors for human cell lines using the interleukin 6 signal transducer GP130. (1994) *J. Exp. Med.* 177, 1337-1342.
181. Nishimoto, N., Ogata, A., Shima, Y., Tani, Y., Ogawa, H., Nakagawa, M., Sugiyama, H., Yoshizaki, K., Kishimoto, T. Oncostatin M, leukaemia inhibitory factor and interleukin 6 induce the proliferation of cells via the common signal transducer GP130. (1994) *J. Exp. Med.* 177, 1343-1347.
182. Richards, C. D., Shoyab, M., Brown, T.J., Gauldie, J. Selective regulation of metalloproteinase inhibitor (TIMP-1) by oncostatin M in fibroblasts in culture. (1993) *J. Immunol.* 150, 5596-5603.
183. Sakyo, K., Ito, A., Ogawa, C., Mori, Y. Hormonal control of collagenase inhibitor production in rabbit uterine cervical fibroblast like cells. (1986) *Biochim. Biophys. Acta.* 883, 517-522.
184. Imada, K., Ito, A., Itoh, Y., Nagase, H., Mori, Y. Progesterone increases the production of tissue inhibitor of metalloproteinases-2 in rabbit uterine cervical fibroblasts. (1994) *FEBS Lett.* 341, 109-112.

185. Morgan, A., Keeble, S.C., London, S.N., Muse, K.N., Curry, T.E., Jr. Antiprogestosterone (RU486) effects on metalloproteinase inhibitor activity in human and rat granulosa cells. (1994) *Fertil. Steril.* 61, 949-955.
186. Mann, J.S., Kindy, M.S., Hyde, J.F., Clark, M.R., Curry Jr, T.E. Role of protein synthesis, prostaglandins and estrogen in rat ovarian metalloproteinase inhibitor production. (1993) *Biol. Reprod.* 48, 1006-1013.
187. Hampton, A.L., Salamonsen, L.A. Expression of messenger ribonucleic acid encoding matrix metalloproteinases and their tissue inhibitors is related to menstruation. (1994) *J. Endocrinology* 141, R1-R3.
188. Mauviel, A., Halcin, C., Vasiloudes, P., Parks, W.C., Kurkinen, M., Uitto, J. Uncoordinate regulation of collagenase, stromelysin and tissue inhibitor of metalloproteinase genes by prostaglandin E2: Selective enhancement of collagenase gene expression by human dermal fibroblasts in culture. (1994) *J. Cell. Biochem.* 54, 465-472.
189. Partridge, N. C., Jeffrey, J.J., Ehrlich, E.H., Teitelbaum, S.L., Fliszar, C., Welgus, H.G., Kahn, A.J. Hormonal regulation of the production of collagenase and a collagenase inhibitor activity by rat osteogenic sarcoma cells. (1987) *Endocrinology.* 120, 1956-1962.
190. Wright, J. K., Clark, I.M., Cawston, T.E., Hazleman, B.L. The secretion of the tissue inhibitor of metalloproteinases (TIMP) by human fibroblasts is modulated by all-*trans*-retinoic acid. (1991) *Biochim. Biophys. Acta.* 1133, 25-30.
191. Welgus, H.G., Stricklin, G.P. Human skin fibroblast collagenase inhibitor. Comparative studies in human connective tissues, serum and synovial fluid. (1983) *J. Biol. Chem.* 258, 12259-12264.
192. Sottrup-Jensen, L., Birkedal-Hansen, H. Human fibroblast collagenase- α -macroglobulin interactions. (1988) *J. Biol. Chem.* 264, 393-401.
193. Millis, A. J. T., Hoyle, M., McCue, H.M., Martini, H. Differential expression of metalloproteinase and tissue inhibitor of metalloproteinase genes in aged human fibroblasts. (1992) *Exp. Cell. Res.* 201, 373-379.
194. Martin, J., Davies, M., Thomas, G., Lovett, D.H. Human mesangial cells secrete a GBM-degrading neutral proteinase and a specific inhibitor. (1989) *Kidney Int.* 36, 790-801.

195. Unemori, E. N., Bouhana, K.S., Werb, Z. Vectorial secretion of extracellular matrix proteins, matrix degrading proteinases and tissue inhibitor of metalloproteinases by endothelial cells. (1990) *J. Biol. Chem.* 265, 445-451.
196. Kishi, J., Hayakawa, T. Synthesis of latent collagenase and collagenase inhibitor by bovine aortic medial explants and cultured medial smooth muscle cells. (1989) *Conn. Tiss. Res.* 19, 63-76.
197. Welgus, H. G., Campbell, E.J., Bar-Shavit, Z., Senior, R.M., Teitelbaum, S.L. Human alveolar macrophages produce a fibroblast like collagenase and collagenase inhibitor. (1985) *J. Clin. Invest.* 76, 219-224.
198. Rifas, L., Halstead, L.R., Peck, W.A., Avidi, L.V., Welgus, H.G. Human osteoblasts in vitro secrete tissue inhibitor of metalloproteinases and gelatinase but not interstitial collagenase as major cellular products. (1989) *J. Clin. Invest.* 84, 686-694.
199. Flenniken, A. M., Williams, B.G. developmental expression of the endogenous TIMP gene and a TIMP-lac fusion gene in transgenic mice. (1990) *Genes Dev.* 4, 1094-1106.
200. Opbroek, A.M., Kenney, C., Brown, D. Characterisation of a human cornea metalloproteinase inhibitor (TIMP-1). (1993) *Curr. Eye. Res.* 12, 877-883.
201. Kawabe, T.T., Rea, T.J., Flenniken, A.M., Williams, B.R.G., Groppi, V.E., Buhl, A.E. Localisation of TIMP in cycling mouse hair (1991) *Development.* 111, 877-879.
202. Hoshino, T., Kishi, J., Kawai, T., Kobayashi, K., Hayakawa, T. Immunoelectron microscopic localisation of collagenase inhibitor on bovine dentin. (1986) *Coll. Rel. Res.* 6, 303-312.
203. Kryshtalskyj, E., Sodek, J. Nature of collagenolytic enzyme and inhibitor activities in crevicular fluid from healthy and inflamed periodontal tissues of beagle dogs. (1987) *J. Periodont. Res.* 22, 264-269.
204. Curry, T.E., Sanders, S.L., Pedigo, N.G., Estes, R.S., Wilson, E.A., Vernon, M.W. Identification and characterisation of metalloproteinase inhibitor activity in human ovarian follicular fluid. (1988) *Endocrinology* 123, 1611-1618.
205. Murphy, G., Cawston, T.E., Reynolds, J.J. An inhibitor of collagenase from amniotic fluid. (1981) *Biochem. J.* 195, 167-170.

206. Smith, G.W., Moor, R.M., Smith, M.F. Identification of a 30,000 Mr polypeptide secreted by cultured ovine granulosa cells and luteal tissue as tissue inhibitor of metalloproteinases. (1993) *Biol. Reprod.* 48, 125-132.
207. Zhu, C., Woessner, J.F.Jr., A tissue inhibitor of metalloproteinases and α -macroglobulins in the ovulating rat ovary: possible regulators of collagen matrix breakdown. (1991) *Biol. Reprod.* 45, 334-342.
208. Salamonsen, L.A. Matrix metalloproteinases and endometrial remodelling. (1994) *Cell. Biol. Int.* 18, 1139-1144.
209. Dean, D.D., Muniz, O.E., Woessner, J.F. Jr, Howell, D.S. Production of collagenase and tissue inhibitor of metalloproteinases (TIMP) by rat growth plates in culture. (1990) *Matrix* 10, 320-330.
210. Brenner, C.A., Adler, R.R., Rapolee, D.A., Pedersen, R.A., Werb, Z. Genes for extracellular matrix degrading metalloproteinases and their inhibitor, TIMP, are expressed during early mammalian development. (1989) *Genes Dev.* 3, 848-859.
211. Osthues, A., Knäuper, V., Oberhoff, R., Reinke, H., Tschesche, H. Isolation and characterisation of tissue inhibitors of metalloproteinases (TIMP-1 and TIMP-2) from human rheumatoid synovial fluid. (1992) *FEBS Lett.* 296, 16-20.
212. Cawston, T. E., McLaughlin, P., Coughlan, R., Kyle, V., Hazleman, B.L. Synovial fluids from infected joints contain metalloproteinase-tissue inhibitor of metalloproteinase complexes. (1990) *Biochim. Biophys. Acta.* 1033, 96-102.
213. Okada, Y., Gonoji, Y., Nakanishi, I., Nagase, H., Hayakawa, T. Immunohistochemical demonstration of collagenase and tissue inhibitor of metalloproteinases (TIMP) in synovial lining cells of the rheumatoid synovium. (1990) *Virch. Arch. B.* 59, 305-312.
214. Hembry, R. M., Ehrlich, H.P. Immunolocalisation of collagenase and tissue inhibitor of metalloproteinases (TIMP) in hypertrophic scar tissue. (1986) *Brit. J. Dermatol.* 115, 409-420.
215. Urbanski, S.J., Edwards, D.R., Maitland, A., Leco, K.J., Watson, A., Kossakowska, A.E. Expression of metalloproteinases and their inhibitors in primary pulmonary carcinomas. (1992) *Br. J. Cancer.* 66, 1188-1194.

216. Hewitt, R. E., Leach, I.H., Powe, D.G., Clark, I.M., Cawston, T.E., Turner, D.R. Distribution of collagenase and tissue inhibitor of metalloproteinases (TIMP) in colorectal tumours. (1991) *Int. J. Cancer*. 49, 666-672.
217. Kossakowska, A.E., Urbanski, S.J., Edwards, D.R. Tissue inhibitor of metalloproteinases-1 (TIMP-1) RNA is expressed at elevated levels in malignant non-Hodgkins lymphoma. (1991) *Blood* 177, 2475-2481.
218. Stetler-Stevenson, W.G., Brown, P.D., Onisto, M., Levy, A.T., Liotta, L.A. Tissue inhibitor of metalloproteinases-2 (TIMP) mRNA expression in tumour cell lines and human tumour tissues. (1990) *J. Biol. Chem.* 265, 13933-13938.
219. Goldberg, G.I., Strongin, A., Collier, I.E., Genrich, T., Marmer, B.L. Interaction of the 92-kDa type IV collagenase with the tissue inhibitor of metalloproteinases prevents dimerization, complex formation with interstitial collagenase and activation of the proenzyme with stromelysin. (1992) *J. Biol. Chem.* 267, 4583-4591.
220. Goldberg, G. I., Marmer, B.L., Grant, G.A., Eisen, A.Z., Wilhelm, S., He, C. Human 72 kilodalton type IV collagenase forms a complex with a tissue inhibitor of metalloproteinases designated TIMP-2. (1989) *Proc. Natl. Acad. Sci. USA*. 86, 8207-8211.
221. Cawston, T. E., Curry, V.A., Clark, I.M., Hazleman, B.L. Identification of a new metalloproteinase inhibitor that forms a tight binding complex with collagenase. (1990) *Biochem. J.* 269, 183-187.
222. Ward, R. V., Hembry, R.M. Reynolds, J.J., Murphy, G. The purification of tissue inhibitor of metalloproteinases-2 from its 72 kDa progelatinase complex. (1991) *Biochem. J.* 278, 179-187.
223. Miyazaki, K., Umenishi, F., Funahashi, K., Koshikawa, N., Yasumitsu, H., Umeda, M. Activation of TIMP-2/progelatinase A complex by stromelysin. (1992) *Biochem. Biophys. Res. Commun.* 185, 852-859.
224. Ward, R. V., Atkinson, S.J., Slocombe, P.M., Docherty, A.J.P., Reynolds, J.J., Murphy, G. Tissue inhibitor of metalloproteinases-2 inhibits the activation of 72 kDa progelatinase by fibroblast membranes. (1991) *Biochim. Biophys. Acta.* 1079, 242-246.

225. Brown, P. D., Kleiner, D.E., Unsworth, E.J., Stetler-Stevenson, W.G. Cellular activation of the 72 kDa type IV procollagenase/TIMP-2 complex. (1993) *Kidney Int.* 43, 163-170.
226. Kleiner, D.E., Unsworth, E.J., Krutsch, H.C., Stetler-Stevenson, W.G. Higher order complex formation between the 72-kilodalton type IV collagenase and tissue inhibitor of metalloproteinases-2. (1992) *Biochemistry* 31, 1665-1672.
227. Curry, V. A., Clark, I.M., Bigg, H., Cawston, T.E. Large inhibitor of metalloproteinases (LIMP) contains tissue inhibitor of metalloproteinases-2 (TIMP)-2 bound to 72000-Mr progelatinase. (1992) *Biochem. J.* 285, 143-147.
228. Howard, E. W., Banda, M.J. Binding of tissue inhibitor of metalloproteinases-2 to two distinct sites on human 72 kDa gelatinase. (1991) *J. Biol. Chem.* 266, 17972-17977.
229. Kolkenbrock, H., Orgel, D., Hecker-Kia, A., Noack, W., Ulbrich, N. The complex between a tissue inhibitor of metalloproteinases (TIMP-2) and 72 kDa progelatinase is a metalloproteinase inhibitor. (1991) *Eur. J. Biochem.* 198, 775-781.
230. Murphy, G., Houbrechts, A., Cockett, M.I., Williamson, R.A., O'Shea, M., Docherty, A.J.P. The N-terminal domain of tissue inhibitor of metalloproteinases retains metalloproteinase inhibitory activity. (1991) *Biochemistry* 30, 8097-8102.
231. Murphy, G., Willenbrock, F., Ward, R.V., Cockett, M.I., Eaton, D., Docherty, A.J.P. The C-terminal domain of 72 kDa gelatinase A is not required for catalysis, but is essential for membrane activation and modulates interactions with tissue inhibitor of metalloproteinases. (1992) *Biochem. J.* 283, 637-641.
232. Fridman, R., Fuerst, T.R., Bird, R.E., Hoyhyya, M., Oelkuet, M., Kraus, S., Komarek, D., Liotta, L.A., Berman, M.A., Stetler-Stevenson, W.G. Domain structure of the human 72 kDa gelatinase/ type IV collagenase. (1992) *J. Biol. Chem.* 267, 15398-15405.
233. Kleiner, D.E.J., Tuutilla, A., Tryggvason, K., Stetler-Stevenson, W.G. Stability analysis of latent and active 72-kDa type IV collagenase: The role of tissue inhibitor of metalloproteinases-2 (TIMP-2). (1993) *Biochemistry* 32, 1583-1592.
234. Baragi, V.M., Fliszar, C.J., Conroy, M.C., Ye, Q., Shipley, J.M., Welgus, H.G. Contribution of the C-terminal domain of metalloproteinases to binding by tissue inhibitor of metalloproteinases. (1994) *J. Biol. Chem.* 269, 12692-12697.

235. Nguyen, Q., Willenbrock, F., Cockett, M.I., O'Shea, M., Docherty, A.J.P., Murphy, G. Different domain interactions are involved in the binding of tissue inhibitors of metalloproteinases to stromelysin-1 and gelatinase A. (1994) *Biochemistry* 33, 2089-2095.
236. Cawston, T. E., Murphy, G., Mercer, E., Galloway, A., Hazleman, B.L., Reynolds, J.J. The interaction of purified rabbit bone collagenase with purified rabbit bone metalloproteinase inhibitor. (1983) *Biochem. J.* 211, 313-318.
237. Bodden, M.K., Harber, G.J., Birkedal-Hansen, B., Windsor, L.J., Caterina, N.C.M., Engler, J.A., Birkedal-Hansen, H. Functional domains of human TIMP-1 (Tissue inhibitor of metalloproteinases). (1994) *J. Biol. Chem.* 269, 18943-18952.
238. Cawston, T. E., Mercer, E. Preferential binding of collagenase to α -2 macroglobulin in the presence of tissue inhibitor of metalloproteinases. (1986) *FEBS Lett.* 209, 9-12.
239. Lelièvre, Y., Bouboutou, R., Boiziau, J., Faucher, D., Achard, D., Cartwright, T. Low molecular weight, sequence based, collagenase inhibitors selectively block the interaction between collagenase and TIMP (tissue inhibitor of metalloproteinases). (1990) *Matrix* 10, 292-299.
240. McLaughlin, B. M., Cawston, T.E., Weiss, J.B. Activation of the matrix metalloproteinase inhibitor complex by a low molecular weight angiogenic factor. (1991) *Biochim. Biophys. Acta.* 1073, 295-298.
241. Willenbrock, F., Crabbe, T., Slocombe, P.M., Sutton, C.W., Docherty, A.J.P., Cockett, M.I., O'Shea, M., Brocklehurst, K., Phillips, I.R., Murphy, G. The activity of the tissue inhibitors of metalloproteinases is regulated by the C-terminal domain interactions: A kinetic analysis of the inhibition of gelatinase A. (1993) *Biochemistry* 32, 4330-4337.
242. Crabbe, T., Zucker, S., Cockett, M.I., Willenbrock, F., Tickle, S., O'Connell, J.P., Scothern, J., Murphy, G., Docherty, A.J.P. Mutation of the active site glutamic acid of human gelatinase A: Effects on latency, catalysis, and the binding of tissue inhibitor of metalloproteinases -1. (1994) *Biochemistry* 33, 6684-6690.
243. Williamson, R. A., Freedman, R.B. Chemical modifications of tissue inhibitor of metalloproteinases-1 (TIMP-1). (1992) *Biochem. Soc. Trans.* 20, 255 (s).

244. O'Shea, M., Willenbrock, F., Williamson, R.A., Cockett, M.I., Freedman, R.B., Reynolds, J.J., Docherty, A.J.P., Murphy, G. Site-directed mutations that alter the inhibitory activity of the tissue inhibitor of metalloproteinases-1: Importance of the N-terminal region between cysteine 3 and cysteine 13. (1993) *Biochemistry* 31, 10146-10152.
245. Miyazaki, K., Funahashi, K., Numata, Y., Koshikawa, N., Akaogi, K., Kikkawa, Y., Yasumitsu, H., Umeda, M. Purification and characterisation of a two-chain form of tissue inhibitor of metalloproteinases (TIMP) type 2 and a low molecular weight TIMP-like protein. (1993) *J. Biol. Chem.* 268, 14387-14393.
246. Westbrook, C.A., Gasson, J.C., Gerber, S.E., Selsted, M.E., Golde, D.W. Characterisation of human T-lymphocyte-derived erythroid-potentiating activity (1984) *J. Biol. Chem.* 259, 9992-9996.
247. Avalos, B.R., Kaufman, S.E., Tomonaga, M., Williams, R.E., Golde, D.W., Gasson, J.C. K562 cells produce and respond to human erythroid potentiating activity. (1988) *Blood* 71, 1720-1725.
248. Gasson, J.C., Golde, D.W., Kaufman, S.E., Westbrook, C.A., Hewick, R.M., Kaufman, R.J., Wong, G.G., Temple, P.A., Leary, A.C. Brown, E.L., Orr, E.C., Clark, S.C. Molecular characterisation and expression of the gene encoding human erythroid-potentiating activity. (1985) *Nature* 315, 768-771.
249. Hayakawa, T., Yamashita, K., Kishi, J., Harigaya, K. Tissue inhibitor of metalloproteinases from human bone marrow stromal cell line KM102 has erythroid potentiating activity, suggesting its possibly bifunctional role in the haematopoietic environment. (1990) *FEBS Lett.* 268, 125-128.
250. Hayakawa, T., Yamashita, K., Tanzawa, K., Uchijima, E., Iwata, K. Growth Promoting activity of tissue inhibitor of metalloproteinases-1 (TIMP-1) for a wide range of cells. (1992) *FEBS Lett.* 298, 29-32.
251. Bertaux, B., Hornbeck, W., Eisen, A.Z., Dubertret, L. Growth stimulation of human keratinocytes by tissue inhibitor of metalloproteinases. (1991) *J. Invest. Dermatol.* 97, 679-685.
252. Murate, T., Yamashita, Y., Ohashi, H., Kagami, Y., Tsushita, K., Kinoshita, T., Hotta, T., Saito, H., Yoshida, K., Mori, K.J., Haykawa, T. Erythroid potentiating

- activity of tissue inhibitor of metalloproteinases on the differentiation of erythropoietin-responsive mouse erythroleukaemia cell line ELM-I-1-3, is closely related to its cell growth potentiating activity. (1993) *Exp. Haematology*. 21, 169-176.
253. Patarca, R. Haseltine, W.A. A major retroviral core protein related to EPA and TIMP. (1985) *Nature* 318, 390.
254. Stetler-Stevenson, W. G., Bersch, N., Golde, D.W. Tissue inhibitor of metalloproteinases-2 (TIMP-2) has erythroid-potentiating activity. (1992) *FEBS Lett.* 296, 231-234.
255. Nemeth, J. A., Goolsby, C.L. TIMP-2, a growth-stimulatory protein from SV40-transformed human fibroblasts (1993) *Exp. Cell. Res.* 207, 376-382.
256. Hayakawa, T., Yamashita, K., Ohuchi, E., Shinagawa, A. Cell growth promoting activity of tissue inhibitor of metalloproteinases-2 (TIMP-2). (1994) *J. Cell. Sci.* 107, 2373-2379.
257. Martel-Pelletier, J., McCollum, R., Fujimoto, N., Obata, K., Cloutier, J., Martel-Pelletier, J. Excess of metalloproteinases over tissue inhibitor of metalloproteinase may contribute to cartilage degradation in osteoarthritis and rheumatoid arthritis. (1994) *Laboratory Investigation*. 70, 807-815.
258. Cawston, T.E., Mercer, E., de-Silvia, E., Hazleman, B.L. Metalloproteinases and collagenase inhibitors in rheumatoid synovial fluid. (1984) *Arthritis. Rheum.* 27, 285-290.
259. Firestein, G., Paine, M.M. Stromelysin and tissue inhibitor of metalloproteinases gene expression in rheumatoid arthritis synovium. (1992) *Am. J. Pathol.* 140, 1309-1314.
260. Khokha, R., Zimmer, M.J., Graham, C.H., Lala, P.K., Waterhouse, P. Suppression of invasion by inducible expression of tissue inhibitor of metalloproteinase-1 (TIMP-1) in B16-F10 melanoma cells. (1992) *J. Natl. Cancer. Inst.* 84, 1017-1022.
261. Albini, A., Melchiori, A., Santi, L., Liotta, L.A., Brown, P.D., Stetler-Stevenson, W.G. Tumour cell invasion inhibited by TIMP-2. (1991) *J. Natl. Cancer. Inst.* 83, 775-779.
262. Larivée, J., Sodek, J., Ferrier, J.M. Collagenase and collagenase inhibitor activities in crevicular fluid of patients receiving treatment for localised juvenile periodontitis. (1986) *J. Periodont. Res.* 21, 702-715.

263. McPhee, J.R., Van de Water, T.R., Gordon, M.A. Otosclerosis: Correlation of clinical incidence and abnormal TIMP gene expression. (1991) *Ann NY Acad. Sci.* 30, 319-321.
264. McPhee, J.R., Gordon, M.A., Ruben, R.J., Van De Water, T.R. Evidence of abnormal stromelysin mRNA expression in suspected carriers of otosclerosis. (1993) *Arch. Otolaryngol. Head Neck Surg.* 119, 1108-1116.
265. Abramson, S.B. Therapy and mechanisms of nonsteroidal anti-inflammatory drugs. (1989) *Curr. Opinion Rheumatol.* 1, 61-67.
266. Simon, L.S. Nonsteroidal anti-inflammatory drug toxicity. (1993) *Curr. Opinion. Rheumatol.* 5, 265-275.
267. Conaghan, P.G., Brooks, P. Disease-modifying anti-rheumatic drugs, including methotrexate, sulfasalazine, gold, antimalarials, and D-penicillamine. (1993) *Curr. Opinion. Rheumatol.* 5, 276-281.
268. McCune, W.J., Friedman, A.W. Immunosuppressive drug therapy for rheumatic disease. (1993) *Curr. Opinion. Rheumatol.* 5, 282-292.
269. Sewell, K.L. Immunotherapy and other novel therapies, including biologic response modifiers, apheresis and dietary modifications. (1993) *Curr. Opinion. Rheumatol.* 5, 293-298.
270. Isaacs, J. D., Watts, R.A., Hazleman, B.L., Hale, G., Keogan, M.T., Cobbold, S.P., Waldmann, H. Humanised monoclonal antibody therapy for rheumatoid arthritis. (1992) *Lancet* 340, 748-752.
271. Moore, W. M., Spilburg, C.A. Peptide hydroxamic acids inhibit skin collagenase. (1986) *Biochem. Biophys. Res. Commun.* 136, 390-395.
272. Grobelny, D., Ponez, L., Galardy, R.E. inhibition of human skin fibroblast collagenase, thermolysin and pseudomonas aeruginosa elastase by peptide hydroxamic acids. (1992) *Biochemistry* 31, 7152-7154.
273. Mookhtiar, K.A., Marlowe, C.K., Bartlett, P.A., Van Wart, H.E. Phosphoramidate inhibitors of human neutrophil collagenase. (1987) *Biochemistry* 26, 1962-1965.
274. Kortylewicz, Z.P., Galardy, R.E. Phosphoramidate peptide inhibitors of human skin fibroblast collagenase. (1990) *J. Med. Chem.* 33, 263-273.

275. Schwartz, M. A., Venkataraman, S., Ghaffiri, M.A., Libby, A., Mookhtiar, K.A., Mallya, S.K., Birkedal-Hansen, H., Van Wart, H.E. Inhibition of human collagenase by sulfur based substrate analogs. (1991) *Biochem. Biophys. Res. Commun.* 176, 173-179.
276. Nixon, J. S., Bottomley, K.M.K., Broadhurst, M.J., Brown, P.A., Johnson, W.H., Lawton, G., Marley, J., Sedgwick, A.D., Wilkinson, S.E. Potent collagenase inhibitors prevent interleukin-1 induced cartilage degradation in vitro. (1991) *Int. J. Tiss. Res.* XIII 5, 237-243.
277. Sorbi, D., Fadly, M., Hicks, R., Alexander, S., Arbeit, L. Captopril inhibits the 72 kDa and 92 kDa matrix metalloproteinases. (1993) *Kidney. Int.* 44, 1266-1272.
278. Tolley, S.P., Davies, G.J., O'Shea, M., Cockett, M.I., Docherty, A.J.P., Murphy, G. Crystallisation and preliminary X-ray analysis of nonglycosylated tissue inhibitor of metalloproteinases-1, N₃₀QN78Q TIMP-1. (1993) *Proteins Struct. Funct. Genet.* 17, 435-437.
279. Cawston, T. E. Barrett, A.J. A rapid and reproducible assay for collagenase using [1-¹⁴C] acetylated collagen. (1979) *Anal. Biochem.* 99, 340-345.
280. Clark, I.M., Mitchell, R.E., Powell, L.K., Bigg, H.F., Cawston, T.E., O'Hare, M.C. Recombinant porcine collagenase: Purification and autolysis. (1995) *Arch. Biochem. Biophys.* 316, 123-127.
281. Smith, P.K., Krohn, R.I., Hermanson, G.T., Mallia, A.K., Gartner, F.H., Provenzano, M.D., Fujimoto, E.K., Goeke, N.M., Olson, B.J., Klenk, D.C. Measurement of protein using bicinchoninic acid. (1985) *Analytical Biochem.* 150, 76-85.
282. Laemmli, U.K., Favre, M. Maturation of the head of the bacteriophage T4. (1973) *J. Mol. Biol.* 80, 575-599.
283. Clark, I.M., Powell, L.K., Wright, J.K., Cawston, T.E., Hazleman, B.L. Monoclonal antibodies against human fibroblast collagenase and the design of an enzyme-linked immunosorbent assay to measure total collagenase. (1992) *Matrix* 12, 475-480.
284. Hayflick, L., Moorhead, P.S. The serial cultivation of human diploid cell strains. (1961) *Exp. Cell. Res.* 25, 585-621

285. Cocuzzi, E.T., Walther, S.E., Rajan, S., Denhardt, D.T. Expression and purification of mouse TIMP-1 from E.Coli. (1992) FEBS Lett. 307, 375-378.
286. Kleine, T., Bartsch, S., Bläser, J., Schnierer, S., Triebel, S., Valentin, M., Gote, T., Tschesche, H. Preparation of native recombinant TIMP-1 from *escherichia coli* inclusion bodies and complex formation with the recombinant catalytic domain of PMNL collagenase. (1993) Biochemistry 32, 14125-14131.
287. Kohno, T., Carmichael, D.F., Sommer, A., Thompson, R.P. Refolding of recombinant proteins. (1990) Methods in Enzymology 185, 187-195.
288. Cocuzzi, E.T., Walther, S.E., Denhardt, D.T. Expression and secretion of active mouse TIMP-1 using a baculovirus expression vector. (1994) Inflammation 18, 35-43.
289. Cockett, M.I., Bebbington, Yarranton, G.T. High level expression of tissue inhibitor of metalloproteinases in chinese hamster ovary cells using glutamine synthase gene amplification. (1990) Biotechnology 8, 662-667.
290. Nilsson, B., Moks, T., Jansson, B., Abarahmsén, L., Elmblad, A., Holmgren, E., Heinrichson, C., Jones, T.A., Uhlén, M. A synthetic IgG-binding domain based on staphylococcal protein A. (1987) Protein Eng. 1, 107-113.
291. Shevchik, V.E., Condemine, G., Robert-Baudouy, J. Characterisation of DsbC, a periplasmic protein of *Erwinia chrysanthemi* and *Escherichia coli* with disulphide isomerase activity. (1994) EMBO J. 13, 2007-2012.
292. Missiakas, D., Georgopoulos, C., Raina, S. The *Escherichia coli* dsbC (xprA) gene encodes a periplasmic protein involved in disulphide bond formation. (1994) EMBO J. 13, 2013-2020.
293. Maniatis, T., Fritsch, E.F., Sambrook, J. (1992) Molecular Cloning. A Laboratory Manual. Cold Spring Harbour Laboratory Press, N.Y.
294. Chou, P.Y., Fasman, G.D. Prediction of secondary structure of proteins from their amino acid sequences. (1978) Adv Enzymol. 47, 45-148.
295. Gibrat, J.F., Garnier, J.O., Robson, B. Further developments of protein secondary structure prediction using information theory. New parameters and consideration of residue pairs. (1987) J. Mol. Biol. 198, 425-433.

296. Lee, D.C., Haris, P.I., Chapman, D., Mitchell, R.C. Determination of protein secondary structure using factor analysis of infrared spectra. (1990) *Biochemistry* **29**, 9185-9193.
297. Provencher, S.W., Glöckner, J. Estimation of globular protein secondary structure from circular dichroism. (1981) *Biochemistry* **20**, 33-37.
298. Piantini, U., Sorensen, O.W., Ernst, R.R. Multiple quantum filters for elucidating NMR coupling networks. (1982) *J. Am. Chem. Soc.* **104**, 6800-6801.
299. Shaka, A.J., Freeman, R. Simplification of NMR spectra by filtration through multiple quantum coherence. (1983) *J. Magn. Reson.* **51**, 169-173.
300. Rance, M., Sorensen, O.W., Bodenhausen, G., Wagner, G., Ernst, R.R., Wüthrich, K. Improved spectral resolution in COSY H-1 NMR spectra of proteins via double quantum filtering. (1983) *Biochem. Biophys. Res. Commun.* **117**, 479-485.
301. Müller, N., Ernst, R.R., Wüthrich, K. Multiple quantum filtered two-dimensional NMR spectroscopy of proteins. (1986) *J. Am. Chem. Soc.* **108**, 6482-6492.
302. Rost, B., Sander, C. Prediction of protein secondary structure at better than 70% accuracy. (1993) *J. Mol. Biol.* **232**, 584-599.
303. Geourjon, C., Deleage, G. SOPM, a self optimised prediction method for protein secondary structure prediction (1994) *Protein Engineering*, **7**, 157-164
304. Kneller, D.G., Cohen, F.E., Langridge, R. Improvements in protein secondary structure prediction by an enhanced neural network. (1990) *J. Mol. Biol.* **214**, 171-182.
305. Fuchs, R., MSU - a mail server utility. (1993) Published electronically on the Internet. Available from <ftp.embl-heidelberg.de>.
306. Dalgarno, D.C., Levine, B.A., Williams, R. J. P. Structural information from NMR secondary chemical-shifts of peptide alpha-C-H protons in proteins. (1983) *Bioscience Reports* **3**, 443-452.
307. Hodges, D.J. Lee, D.C., Salter, C.J., Reid, D.G., Harper, G.P., Cawston. T.E. Purification and secondary structural analysis of tissue inhibitor of metalloproteinases-1. (1994) *Biochim. Biophys. Acta.* **1208**, 94-100.

308. Cawston, T.E., Mercer, E., Mooney, C., Wright, J.K. (1986) Proteinases in inflammation and tumour invasion (Walter de Gruyter and Co, Berlin) 189-210.
309. Ismail, A.A., Mantsch, H.M., Wong, P.T.T. Aggregation of chymotrypsinogen: portrait by infrared spectroscopy, (1992) *Biochim. Biophys. Acta* 1121, 183-188.
310. Hounsell, E.F., Wright, D.J., Donald, A.S.R., Feeney, J. A computerised approach to the analysis of oligosaccharide structure by high resolution proton NMR. (1984) *Biochem. J.* 223, 129-143.
311. Van Halbeek, H., Poppe, L. Conformation and dynamics of glycoprotein oligosaccharides as studied by ¹H NMR spectroscopy. (1992) *Magn. Reson. Chem.* 30, s74-s86.
312. Petros, A.M., Mueller, L., Kopple, K.D. NMR identification of protein surfaces using paramagnetic probes. (1990) *Biochemistry*, 29, 10041-10048.
313. Lepre, C.A., Cheng, J., Moore, J.M. Dynamics of a receptor bound ligand by heteronuclear NMR: FK506 bound to FKBP-12. (1993) *J. Am. Chem. Soc.* 115, 4929-4930.
314. Cardamone, M., Puri, N.K. Spectrofluorimetric assessment of the surface hydrophobicity of proteins. (1992) *Biochem. J.* 282, 589-593.
315. O' Hare, M.C., Clarke, N.J., Cawston, T.E. Production in *Escherichia coli* of porcine type-1 collagenase as a fusion protein with β -galactosidase. (1992) *Gene* 111, 245-248.
316. Scatchard, G., Coleman, J.S., Shen, A.L. Physical chemistry of protein solutions VII. The binding of some small anions to serum albumen. (1957) *J. Am. Chem. Soc.* 79, 12-20.
317. Klotz, I.M., Hunston, D.L. Properties of graphical representation of multiple classes of binding sites. (1971) *Biochemistry* 10, 3065-3069.
318. Werner, M.H., Wemmer, D.E. Three dimensional structure of soybean/chymotrypsin Bowman-Birk inhibitor in solution. (1992) *Biochemistry* 31, 999-1010.

319. Nishino, N., Aoyagi, H., Kato, T., Izumiya, N. Studies on the synthesis of proteinase inhibitors I. Synthesis and activity of nanopeptide fragments of soybean Bowman-Birk inhibitor. (1977) *J. Biochem.* 82, 901-999.
320. Wüthrich, K. *NMR of Proteins and Nucleic Acids.* (1986) John Wiley, New York.
321. Shaka, A.J., Lee, C.J., Pines, A. Iterative schemes for bilinear operators - Application to spin decoupling. (1988) *J. Magn. Reson.* 77, 274-293.
322. Bax, A., Davis, D.G. Practical aspects of two-dimensional transverse NOE spectroscopy. (1985) *J. Magn. Reson.* 63, 207-213.
323. Jeener, J., Meier, B.H., Bachmann, P., Ernst, R.R. Investigation of exchange processes by 2-dimensional NMR spectroscopy. (1979) *J. Chem. Phys.* 71, 4546-4553.
324. Kumar, A., Ernst, R.R., Wüthrich, K. A 2-dimensional nuclear overhauser enhancement experiment for the elucidation of complete proton-proton cross-relaxation networks in biological macromolecules. (1980) *Biochem. Biophys. Res. Commun.* 95, 1-6.
325. Brandts, J.F., Halvorsen, H.R., Brennan, M. Consideration of the possibility that the slow step in protein denaturation reactions is due to *cis-trans* isomerisation of proline residues. (1975) *Biochemistry* 14, 4953-4963.
326. Zanotti, G., Maione, A., Rossi, F., Saviano M., Pedone, C., Tancredi, T. Bioactive peptides: Conformational study of a cystinyl cycloheptapeptide in its free and calcium complexed forms. (1993) *Biopolymers* 33, 1083-1091.
327. Leatherbarrow, R.J., Salacinski, H.J. Design of a small peptide-based proteinase inhibitor by modelling the active site region of barley chymotrypsin inhibitor-2. (1991) *Biochemistry* 30, 10717-10721.
328. Wagner, G. Prospects for NMR of large proteins (1993) *J. Biomolecular NMR.* 3, 375-385.

329. Clore, G.M., Gronenborn, A.M. Structures of larger proteins in solution: Three and four dimensional heteronuclear NMR spectroscopy. (1991) *Science* 252, 1390-1399

330. Willenbrock, F., Murphy, G. Structure function relationships in the tissue inhibitors of metalloproteinases. (1994) *Am. J. Respir. Crit. Care Med.* 150, S165-170.

Appendix 1.

CLUSTAL V multiple sequence alignment of nine human MMPs and one mouse MMP.

```
MMP-1      MH-----SFP-----PL-LLLI.FWGVVSHSFPATLET---Q----EQDV
MMP-3      KM-----HPG-----VLAAFLFLSWTHCRALPLPSGG---D----EDDL
MMP-8      MF-----SLK-----TLPFLLLLHVQISKAFP--VSS---K----EKNT
MMP-9      M-----SLWQPL---VLVLLVLGCCFAAPRQRQSTLVLFP----GDLR
MMP-2      ME-----ALMARGALTGPLRALCLLGCLLSHAAAAPSPIIKFP----GDVA
MMP-3      M-----K-----SLPILLLLCVAVCSAYPLDGAA---R----GEDT
MMP-10     M-----M-----HLAFLVLLCLPVCSAYPI.SGAA---K----EEDS
MMP-11     M-----APAAWLRSAAARALLPPMLLLLLQPPPLLARALP-----
MMP-7      M-----RLTVLCAV-CLLPGSLALPLPQ---E----AGGM
MMP-14     SSVPTEDKGAPREWRCDPRAWARPRSHTARLTRWSRTMSPA-PRPSRCLLLPLLTLTAL
MMP-12 (murine) KF-----TMK-----FL-LILLQATASGALPLNSST-----SL
```

MMP-1 -----DLV-----QKYLEKYYNLKNDRQVEKRRNSGPVV-EKCLKQMQE FFGLKVTGKPD
 MMP-3 SE-EDLQFA----ERYLRSYYH-PTNLAGILKENAASSMT-ERLREMQS FFGLEVTGKLD
 MMP-8 -----KTV-----QDYLEKIFYQLPSNQYQSTRKNGTNVIV-EKCLKEMQRFFGLNVTGKPN
 MMP-9 TNLTDRQLA----EEYLRY-----GYTRVAEMRGESKSLGPALLLLQKQLSLPETGELD
 MMP-2 PK-TDKEI A----VQYLNTFYGCPKESCNLF-----VLKDTLKKMQKFFGLPQTGDLD
 MMP-3 S----MNLV----QKYLENYDDLKDVKQFVRRKDSGPVV-KKIREMQKFLGLEVTGKLD
 MMP-10 N----KDLA----QYLEKYYNLEKDVKQF-RRKDSNLIV-KKIQGMQKFLGLEVTGKLD
 MMP-11 PDVHHLHAERRGPQPW-----HAALPSSPAPAPATQEAPRPASS-----
 MMP-7 SE-LQWEQA----QDYLRFYLYDSETKNAN-----SLEAKLKEMQKFFGLPITGMLN
 MMP-14 ASLGSAQSSSFPEAWLQQYGYLPPGDLRTHTQKSPQS-LSAAIAAMQKIFYGLQVTGKAD
 MMP-12 (murine) EK-NNVLFG----ERYLEKIFYGLEINKLPVTKMKYSGNLMKEKI QEMQHFLGLKVTGQLD

MMP-1 AETLKVMKQPRCGVPD-----VAQFVLTEGNPRWEQTHLTYRIENYTPDLPRADVD
 MMP-3 DNTLDVMKKPRCGVPD-----VGEYNVFPRTLKWSKMNLTYRIVNYTPDMTHSEVE
 MMP-8 EETLDMKKPRCGVPD-----SGGFMLTPGNPKWERTNLTYRIRNYTPQLSEAEVE
 MMP-9 SATLKAMRTPRCGVPD-----LGRFQTFEGDLKWHHHNITYWIQNYSEDLPRAVID
 MMP-2 QNTIETMRKPRCGNPD-----VANYNFFPRKPKWDKNQITYRIIGYTPDLDPETVD
 MMP-3 SDTLEVMRKPRCGVPD-----VGHFRTFPGIPKWRKTHLTYRIVNYTPDLPKDAVD
 MMP-10 TDTLEVMRKPRCGVPD-----VGHFSSFPGMPKWRKTHLTYRIVNYTPDLPRDAVD
 MMP-11 -----LRPPRCGVPDP-SDGLSARNRQKRFVLSGGRWEKTDLTYRI LRFPWQLVQEQVR

MMP-8 AFQPGQGI GGDAHFDAEETWTNTSA-----
MMP-9 AFPPGPGIQGDAHFDDDELWSLGKGVVVPTRFGNADGAACHFPFI FEGRSYSACTTDGRS
MMP-2 AFAPGTGVGGDSHFDDDELWTLGEGQVVRVKYGNADGEYCKFPFLFNGKEYNSCTDTGRS
MMP-3 AYAPGPGINGDAHFDDDEQWTKLDTT-----
MMP-10 AYPPGPGLYGDIHFDDDEKWTEDAS-----
MMP-11 AFFPKTHREGDVHFDYDETWTIGD-----
MMP-7 AFAPGTGLGGDAHFDEDERWTDGSSLGIN-----FLYA-----
MMP-14 AYFPGPNIIGGDTHFDSAEPWTV-----RN
MMP-12 (murine) AFGPGSGI GGDAHFDEDEFWTT HSG-----
* . * ** *** * * .

MMP-1 -----
MMP-3 -----
MMP-8 -----
MMP-9 DGLPWCSTTANYDTDDRFGFCPSERLYTRDGNADGKPCQFPFI FQGQSYSACTTDGRSDG
MMP-2 DGFLWCSTTYNFEKDGKYGFCPHEALFTMGGNAEGQPCKFPFRFQGT SYDSCTTEGRTDG
MMP-3 -----
MMP-10 -----
MMP-11 -----
MMP-7 -----
MMP-14 EDL-----
MMP-12 (murine) -----

MMP-1 -----
 MMP-3 -----
 MMP-8 -----
 MMP-9 YRWCATTANYDRDKLFGFCPTRADSTVMGGNSAGELCVFPFTFLGKEYSTCTSEGRGDGR
 MMP-2 YRWC GTTEDYDRDKKYGFCEPETAMSTV-GGNSEGAPCVFPFTFLGNKYESCTSAGRSDGK
 MMP-3 -----
 MMP-10 -----
 MMP-11 -----
 MMP-7 -----
 MMP-14 -----
 MMP-12 (murine) -----

MMP-1 -----EYNLHRVAAHELGHSLGLSHSTDIGALMYPSTY-TF--SG
 MMP-3 -----GYNLFLVAAHEFGHSLGLDHSDPGALMFPIY-TYTGKS
 MMP-8 -----NYNLFLVAAHEFGHSLGLAHSSDPGALMYPNY-AFRETS
 MMP-9 LWCATTSNFDSDKKWGFCPDQGYSLFLVAAHEFGHALGLDHSSVPEALMYPMYR-FTEGP
 MMP-2 MWCATTANYDDDRKWGFCPDQGYSLFLVAAHEFGHAMGLEHSQDPGALMAPIY-TYT--K
 MMP-3 -----GTNLFLVAAHEIGHSLGLFHSANTEALMYPLYHSLTDLT
 MMP-10 -----GTNLFLVAAHELGHSLGLFHSANTEALMYPLYNSFTELA

MMP-11 -----DQGTDLLQVAAHEFGHVLGLQHTTAAKALMSAFY-TFR--Y
MMP-7 -----ATHELGHSLGMGHSSDPNAVMYPTY-GNGDPQ
MMP-14 -----NGNDIFLVAVHELGHALGLEHSSDPSAIMAPFYQ-WMDTE
MMP-12 (murine) -----GTNLFLTAVHEIGHSLGLGHSSDPKAVMEPTYK-YVDIN

* * * . * * . * . * . * . * . *

MMP-1 DVQLAQDDIDGIIQAIYGRSQNPVQ-----
MMP-3 HFMLPDDDDVQGIQSLYGPGE-----DP-----
MMP-8 NYSLPQDDIDGIIQAIYGLSSNPIQ-----
MMP-9 --PLHKDDVNGIRHLYGPRPEPEPRPPTTTTPQPTAPPTVCPTGPPTVHPSERPTAGPTG
MMP-2 NFRLSQDDIKGIQELYGASPDID----LGTGP-----
MMP-3 RFRLSQDDINGIQSLYGPPPDSPETPLVPTEP-----
MMP-10 QFRLSQDDVNGIQSLYGPPPASTEEPLVPTKS-----
MMP-11 PLSLSPDDCRGVQHLYG-----QPWPTVTSRTPALGP-----QAGIDTNE
MMP-7 NFKLSQDDIKGIQKLYG-----
MMP-14 KFVLPHYDPRGIQQLYGGKQGS-----PPRCP-----LNPGLPPGLLFLI
MMP-12 (murine) TFRLSADDIRGIQSLYGDPKENQRLP-----

* * * . * * . * *

MMP-1 -PI-GPQTPKACDSKLT-----FDAIT TIRGEVMFFKDRFYMR TN-PFY
 MMP-3 NPK-HPKTPDKCDPSLS-----LDAITSLRGETMI FKDRFFWRLH-PQQ
 MMP-8 -PT-GPSTPKPCDPSLT-----FDAIT TLRGEILFFKDRYFWRRH-PQL
 MMP-9 PPSAGPTGPPTAGPSTATTVPLSPVDDACNVNI FDAIAEIGNQLYLFKDGKYWRFSEGRG
 MMP-2 TPTLG PVTPEICKQDIV-----FDGIAQIRGEI FFFKDRFIWRTVTPRD
 MMP-3 VPP-EPGTPANCDPALS-----FDAVSTLRGEILI FKDRHFWRKS-LRK
 MMP-10 VPS-GSEMPAKCDPALS-----FDAISTLRGEYL FFKDRYFWRRS-HWN
 MMP-11 IAPLEPDAPP-----DACEAS-FDAVSTIRGEL FFFKAGFVWRLRGGQL
 MMP-7 -----
 MMP-14 NPKNPTYGPNICDGN-----FDTVAMLRGEMFD FKKRWFWRVRNQV
 MMP-12 (murine) -NP-DNSEPALCDPNLS-----FDAVTTVGNKI FFFKDRFFWLKV-SER

MMP-1 PEVE-LNFISVFWPQLPNGLEAAYEFADRDEVRF FKG NKYWAVQGQNVLHGYPKDIYSSF
 MMP-3 VDAE-LFLT KSFWPEL PNRIDAAYEHPSHDLI FIFRGRKFWALNGYDILEGYPKKI-SEL
 MMP-8 QRVE-MNFISLFWPSLPTGIQAAYEDFDRDLI FLFKGNQYWALSGYDILQGYPKDI-SNY
 MMP-9 SRPQGPFLIADKWPALPRKLD SVFEEPLSKKL FFFSGRQVWVYTGASVLG--PRRLD-KL
 MMP-2 KPMG-PLL VATFWPELPEKIDAVYEAPQEEKAVFFAGNEYWIYSASTLERGYPKPL-TSL
 MMP-3 LEPE-LHLISSFWPSLPSGVDAAYEVT SKDLVFI FKG NQFWAIRGNEVRAGYPRGIHT-L
 MMP-10 PEPE-FHLISAFWPSLPSYLDAAAYEVNSRDT VFI FKG NEFWAIRGNEVQAGYPRGIHT-L
 MMP-11 QPGYPA-LASRHWQGLPSVDAAFEDAQ-GHIWFFQGAQYWVYDGEKPV LG-PAPL-TEL

MMP-7 -----
 MMP-14 MDGYMP-IGQFWRGLPASINTAYERKDGKVFV-FKGDKHWFDEASLEPGYPKHIK-EL
 MMP-12 (murine) PKTS-VNLISSLWPTLPSGIEAAYEIEARNQVFLFKDDKYWLISNLRPEPNYPKSIHS-F

MMP-1 GFPRTVKHI DAALSE-ENTGKTYFFVANKYWRYDEYKRSMDPGYPKMIAHDFPGIGHKVD
 MMP-3 GLPKEVKKISAAVHF-EDTGKTLFSGNQVWRYDDTNHIMDKDYPRLIEEDFPGIGDKVD
 MMP-8 GFPSSVQAIDA AVF---YRSKTYFFVNDQFWRYDNQRQFMEPGYPKSISGAFFPGIESKVD
 MMP-9 GLGADVAQVTGAL-R-SGRGKMLLFSGRRLWRFDVKAQMVDPRSASEVDRMFPGVPLDTH
 MMP-2 GLPPDVQRVDAAFNW-SKNKTYIFAGDKFWRYNEVKKKMDPGFPKLIADAWNAIPDNLD
 MMP-3 GFPPTVRKIDAAISD-KEKNKTYFFVEDKYWRFDEKRNSMEPGFPKQIAEDFPGIDSKID
 MMP-10 GFPPTIRKIDAAVSD-KEKKKTYFFAADKYWRFDENQSMEQGFPRLIADDFPGVEPKVD
 MMP-11 GLVRF--PVHAALVWGPEKNKIYFFRGRDYWRFHPSTRRVDSVPVPRR-ATDWRGVPSEID
 MMP-7 -----KR-SNSRKK-----
 MMP-14 GRGLPTDKIDAALFW-MPNGKTYFFFRGNKYRFNEELRAVDSEYPKNI-KVWEGIPESPR
 MMP-12 (murine) GFPNFVKKIDA AVFN-PRFYRTYFFVDNQYWRYDERRQMMDPGYPKLITKNFQGIGPKID

MMP-1 AVF--MKDGGF----YFFHGTRQYKFDPKTKRILTLQKANS---WFNCRKN-----
 MMP-3 AVY--EKNGYI----YFFNGPIQFEYSIWSNRIVRVMPANS---ILWC-----

MMP-8	AVF--QQEHFF----HVFSGPRYYAFDLIAQRVTRVARGNK---WLNCRYG-----
MMP-9	DVFQYREKAYFCQDRFYWRVSSRSELN----QVDQVGIVTY--DILQCPED-----
MMP-2	AVVDLQGGGHS----YFFKGAYYLKLENQSLKSVKFGSIKS--DWLGC-----
MMP-3	AVF--EEFGFF----YFFTGSSQLEFDPNAKKVTHTLKSNS---WLNC-----
MMP-10	AVL--QAFGFF----YFFSGSSQFEFDPNARMVTHILKSNS---WLHC-----
MMP-11	AAFQ-DADGY----AYFLRGRLYWKFDPVKVKALEGFPRLVGPDDFFGCAEPANT-----
MMP-7	-----
MMP-14	GSFMGSDEVF----TYFYKGNKYWKFNQKLKVEPGYPKSALRDWMGCPSGGKRPDEGTEE
MMP-12 (murine)	AVF-YSKNKYY----YFFQGSNQFEYDFLLQRITKTLKSNS---WFGC-----
MMP-1	-----
MMP-3	-----
MMP-8	-----
MMP-9	-----
MMP-2	-----
MMP-3	-----
MMP-10	-----
MMP-11	-----FL-----
MMP-7	-----
MMP-14	ETEVI I IIEVDEEGGAVSAAAVVLPVLLLLLVAVGLAVFFFRRHGTPRRLLYCQRSLLD
MMP-12 (murine)	-----

MMP-1 --
MMP-3 --
MMP-6 --
MMP-9 --
MMP-8 --
MMP-5 --
MMP-10 --
MMP-11 --
MMP-7 --
MMP-14 KV
MMP-12 (murine) --

All sequences were downloaded from the EMBL database.

Appendix 2.

CLUSTAL V multiple sequence alignment for all three human TIMP sequences.

```
t1h human CTCVPPHPQTAFCNSDLVIRAKFVGTPEVNQTT-LYQR-----YEIKMTKMYKGFQALGDAADIRFVYT
t2h human CSCSPVHPQQAFCNADVIRAKAVSEKEVDSGNFIYGNPIKRIQYEIKQIKMFKGPEK-----DIEFIYT
t3h human CTCSPSHPQDAFCNSDIVIRAKVVGKLVKEG-----PFGTLVYTIKQMKMYRGFTKM---PHVQYIHT
      *.* * *** *****.*.***** *          * ** **..*          .. .. *

t1h human PAMESVCGYFHRSHNRSEEFLLIAGKLQ-DGLLHITTCSEFVAPWNSLSLAQRRGFTKTYTVGCEECTVFPC
t2h human APSSAVCGVSLDVGGKKE-YLIAGKAEGDGKMHITLCDFIVPBDTLSTTQKKSLSLNHRYQMGCE-CKITRC
t3h human EASESLCGLKLEVN-KYQ-YLLTGRVY-DGKMYTGLCNFVERWDQLTSLQRKGLNYRYHLGCN-CKIKSC
      . ..**          . . .*..* . ** . * * . * . * . * . . . * .** . * . *

t1h human LSIPCKLQSGTHCLWTDQLLQGSEKGFQSRHLACLPREPGLCTW-----QSLRSQIA
t2h human PMIPCYISSPDECLWMDWVTEKKNINGHQAKFFACIKRSDGSCAWYRGAAPPKQEFLDIEDP
t3h human YYLPCFVTSKNECLWTDMLSNFGYPGYQSKHYACIRQKGGYCSWYRGWAPPDKSIINATDP
      .** . * .*** * . . * *.. ** . * *.*          . .
```

All sequences were downloaded from the EMBL database.

Appendix 3.

CLUSTAL V multiple sequence alignment of all known TIMP sequences to date.

```

:.....: : : : : : : : : : :
human  timp-1  CTCVPPHPQTAF CNSDLVIRAKFVGTPEVNQTT-LYQ-----RYEIKMTKMYKGFQALG
mouse  timp-1  CSCAPPHPQTAF CNSDLVIRAKFMGSPEINETT-LYQ-----RYKIKMTKMLKGFKA VG
rabbit timp-1  CTCVPPHPQTAF CNSDLVIRAKFVGAPEVNHTT-LYQ-----RYEIKTTKMFKGF DALG
rat     timp-1  CSCAPTHPQTAF CNSDLVIRAKFMGSPEI IETT-LYQ-----RYEIKMTKMLKGFDA VG
bovine timp-1  CTCVPPHPQTAF CNSDVVIRAKFVGTAEVNETA-LYQ-----RYEIKMTKMFKGFSA LR
porcine timp-1  CTCVPPHPQTAF CSSDLVIRAKFVGAPEFNQTA-SYQ-----RYEIKMTKMFKGFNA LG
sheep  timp-1  CTCVPPHPQTAF CNSEVVIRAKFVGTAEVNETA-LYQ-----RYEIKMTKMFKGFSA LR
baboon timp-1  CTCVPPHPQTAF CNSDLVIRAKFVGTPEVNQTT-LYQ-----RYEIKMTKMYKGFQALG

:.....: : : : : : : : : : :
human  timp-2  CSCSPVHPQQAFCNADVIRAKAVSEKEVDSGNDIYGNPIKRIQYEIKQIKMFKGPEK--
bovine timp-2  CSCSPVHPQQAFCNADIVIRAKAVNKKEVDSGNDIYGNPIKRIQYEIKQIKMFKGPDQ--
mouse  timp-2  CSCSPVHPQQAFCNADVIRAKAVSEKEVDSGNDIYGNPIKRIQYEIKQIKMFKGPDK--
rat     timp-2  CSCSPVHPQQAFCNADVIRAKAVSEKEVDSGNDIYGNPIKRIQYEIKQIKMFKGPDK--

```



```

          ::::: :::::  :::  ::::::::::::::::::::::::::::  : : :::::..  :
human    timp-3  RKGLNYRYHLGCN-CKIKSCYYLPCFVTSKNECLWTDMLSNGYPGYQSKHYACIRQKGG
mouse    timp-3  RKGLNYRYHLGCN-CKIKSCYYLPCFVTSKNECLWTDMLSNGYPGYQSKHYACIRQKGG
chick    timp-3  RKGLNHRYHLGCG-CKIRPCYYLPCFATSKNECIWTDMLSNGHSGHQAKHYACIQRVEG

```

```

. . . * ** * . * .** * .** * . * .** . . .

```

```

          :::::
human    timp-1  LCTWQSLRSQI-----A
mouse    timp-1  LCTWRSLGAR-----
rabbit   timp-1  LCAWESLRPRK-----D
rat      timp-1  LCTWQYLGVSMTRSLPLAKAEA
bovine   timp-1  LCTWQSLRAQM-----A
porcine  timp-1  MCTWQSLRPRV-----A
sheep    timp-1  MCTWQSLRPRG-----A
baboon   timp-1  LCTWQSLRTRI-----A

```

```

          ::::::::::::::: :::::
human    timp-2  SCAWYRGAAPPKQEF-LDIEDP
bovine   timp-2  SCAWYRGAAPPKQEF-LDIEDP
mouse    timp-2  SCAWYRGAAPPKQEF-LDIEDP
rat      timp-2  SCAWYRGAAPPKQEF-LDIEDP

```

```

          ::::::::::::::: :::::
human   timp-3  YCSWYRGWAPPDKSI-INATDP
mouse   timp-3  YCSWYRGWAPPDKSI-SNATDP
chick   timp-3  YCSWYRGWAPPDKTI-INATDP

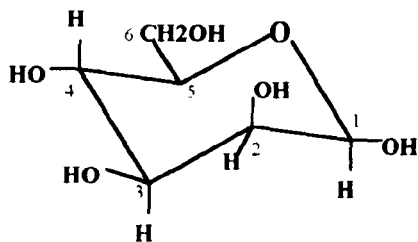
```

.

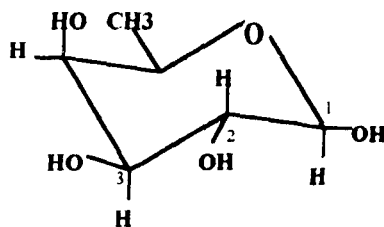
All sequences were downloaded from either Genbank, Swissprot or EMBL databases. The overall homology as calculated by ClustalV is marked by stars and dots under the complete set of 15 sequences. '*' indicates complete conservation and '.' indicates that conservative substitutions have occurred. The homology between the individual TIMP families is shown above the group of sequences. A colon indicates total conservation and a dot indicates a conservative substitution.

Appendix 4

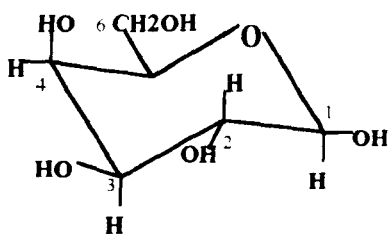
Structures of Some Common Sugars.



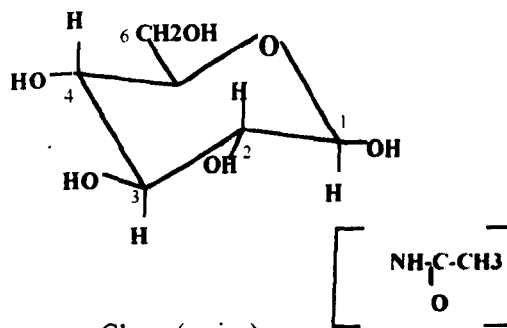
Mannose.



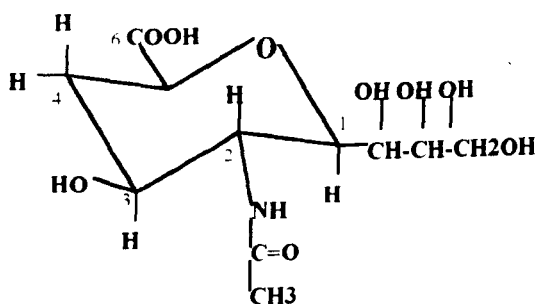
Fucose



Galactose.



Glucos(amine).



Sialic Acid.

Appendix 5
Random Coil Shifts.

Residue	Structure	NH	α H	β H	Others
Gly	-H	8.39	3.97		
Ala	-CH ₃	8.25	4.35	1.39	
Val	-CH(CH ₃) ₂	8.44	4.18	2.13	γ CH ₃ 0.97, 0.94
Ile	-CH(CH ₃)CH ₂ CH ₃	8.19	4.23	1.90	γ CH ₂ 1.48, 1.19 γ CH ₃ 0.95 δ CH ₃ 0.89
Leu	-CH ₂ CH(CH ₃) ₂	8.42	4.38	1.65	γ CH ₂ 1.64 δ CH ₃ 0.94, 0.90
tPro	-CH ₂ CH ₂ CH ₂ -	na	4.44	2.28, 2.02	γ CH ₂ 2.03 δ CH ₂ 3.68, 3.65
Ser	-CH ₂ OH	8.38	4.50	3.88	
Thr	-CH(OH)CH ₃	8.24	4.35	4.22	γ CH ₃ 1.23
Asp	-CH ₂ COOH	8.41	4.76	2.84, 2.75	
Glu	-CH ₂ CH ₂ COOH	8.37	4.29	2.09, 1.97	γ CH ₂ 2.31, 2.28
Lys	-CH ₂ CH ₂ CH ₂ CH ₂ NH ₃	8.41	4.36	1.85, 1.76	γ CH ₂ 1.45, 1.45 δ CH ₂ 1.70, 1.70 ϵ CH ₂ 3.02, 3.02 ϵ NH ₃ 7.52
Arg	-CH ₂ CH ₂ CH ₂ NHCONH ₂	8.27	4.38	1.89, 1.79	γ CH ₂ 1.70, 1.70 δ CH ₂ 3.32, 3.32 NH 7.17, 6.62
Asn	-CH ₂ CONH ₂	8.75	4.75	2.83, 2.75	γ NH ₂ 7.59, 6.91
Gln	-CH ₂ CH ₂ CONH ₂	8.41	4.37	2.13, 2.01	γ CH ₂ 2.38, 2.38

					δ NH2 6.87, 7.59
Met	-CH ₂ CH ₂ SCH ₃	8.42	4.52	2.15, 2.01	γ CH ₂ 2.64, 2.64 ϵ CH ₃ 2.13
Cys	-CH ₂ SH	8.31	4.69	3.28, 2.96	
Trp	-CH ₂ -indole-Ar	8.09	4.70	3.32, 3.19	2H 7.24 4H 7.65 5H 7.17 6H 7.24 7H 7.50 NH 10.22
Phe	-CH ₂ -Ar	8.23	4.66	3.22, 2.99	2,6H 7.30 3,5H 7.39 4H 7.34
Tyr	-CH ₂ -Ar-OH	8.18	4.60	3.13, 2.92	2,6H 7.15 3,5H 6.86
His	-CH ₂ -indole	8.41	4.63	3.26, 3.20	2H 8.12 4H 7.14

Appendix 6. Tabulated NOE data for C₃-C₁₃ in H₂O.

proton	ppm	strength	proton
V4dHN	0.888	w	V4dHy
V4dHN	4.455	w	V4dH α
V4cH α	0.867	w	V4cHy'
V4bH α	0.830	w	V4bHy'
V4cH α	3.813	w	P5tH δ
V4bH α	1.957	w	V4bH β
V4bH β	0.885	w	V4bHy
P5tH α	2.274	w	P6cH β
P5tH α	1.916	w	V4a/bH β
P5tH α	1.084	w	T10a/bHy /A11aH β
P5cH α	3.681	w	P6cH δ
P6tH α	3.677		
P6tH α	2.284	w	
P6tH α	2.184	w	P6tH β
P6tH α	2.104	w	P6tH β '
P6tH α	1.017	w	V4cHy
P6tH α	0.944	w	V4cHy'
H7aHN	1.104	w	A11eH β
H7aHN	3.065	s	H7aH β
H7aHN	3.237	m	F12bH β
H7aHN	4.228	w	T10cH β
H7aHN	4.329	w	P8tH α
H7aHN	4.632	w	F12a/bH α
H7bHN	1.096		
H7bHN	1.197		A11c/dH β
H7bHN	2.977		H7bH β
H7bHN	3.187		F12aH β
H7bHN	4.220		T10cH β
H7cHN	1.104	s	A11aH β
H7cHN	1.214	s	T10cHy/A11c H β

H7cHN	3.002	m	H7cH β
H7cHN	3.187	w	F12aH β
H7cHN	4.094	m	A11aH β /A11c H α
H7cHN	4.279	s	Q9cH α
H7cHN	4.422	w	P6cH α /P8cH α / T10bH α
P8tH α	2.289		P8tH β
P8tH α	4.070		A11a/eH β
P8tH α	1.947		P8tH β
P8cH α	3.164		H7b/cH β
P8cH α	1.084	m	T10a/bH γ
Q9aHN	4.368	m	P8tH α
Q9aHN	4.238	m	T10cH β
Q9aHN	2.372	m	Q9aH γ
Q9aHN	2.136	w	Q9aH β
Q9aHN	1.975	w	Q9aH β
Q9bHN	4.361		P8tH α
Q9bHN	4.220		Q9bH α
Q9cHN	4.30		Q9cH α
Q9cHN	2.378		Q9cH γ
Q9cHN	4.455		T10dH α
Q9dHN	4.290		Q9dH α
T10bH α	1.084		T10bH γ
T10bH α	2.281		P8t/cH β /P6H β
T10cHN	1.146		T10cH α
T10cHN	2.381		Q9a/cH γ
T10cHN	4.000		T10cH β
T10cHN	4.464		V4dH α
A11aHN	1.099		A11aH β
A11bHN	4.209		A11bH α
A11bHN	4.410		T10bH α
A11bHN	4.132		Q9dH α
A11cHN	1.198		A11cH β
A11cHN	3.062		??
A11cHN	4.093		T10bH β

A11cHN	4.279		A11cH α
A11cHN	4.410		T10bH α
A11cHN	4.475		V4??
A11gHN	2.128	w	V4cH β /Q9bH β
A11gHN	2.230	w	?
A11gHN	2.376	w	H7cH??
A11gHN	4.408	w	??
A11gHN	4.092		A11gH α
F12aHN	1.121		T10Hy
F12aHN	1.247		T10cHy
F12aHN	2.910		F12aH β
F12aHN	3.221		F12aH β '
F12aHN	4.119		T10aHb
F12aHN	4.304		H7aH α
F12bHN	4.103	w	T10a/bH β
F12bHN	1.096	w	T10a/bHy
F12cHN	2.986		C13aH β '
F12cHN	3.137	m	H7b/cH β /C13c H β
F12cHN	3.187		F12cH β
F12cHN	4.245		A/T H α /H β ???
C13bHN	4.293		H7aH α
C13bHN	3.062		C13bH β
C13bHN	1.137		T10dHy
C13aHN	4.279		H7aH α
C13aHN	3.737		P8tH δ /P8cH δ / A11fH α
C13aHN	3.263		C13aH β
C13aHN	3.070		C13aH β
C13aHN	1.840		P5tHy
C13aHN	1.096		T10d/aHy

Appendix 7. Tabulated NOE data for C₃-C₁₃ in TFE-d₂.

proton	ppm	strength	proton
V4HN	1.071	s	V4H γ '
V4HN	1.196	m	V ϵ H γ
V4HN	2.067	s	V4H β
V4HN	3.054	s	P8H δ '
V4HN	3.140	w	H7H β '
V4HN	3.342	w	H7H β
V4HN	4.244	s	P5H δ
V4HN	4.314	s	V4H γ
H7HN	4.525	s	P5H α
H7HN	4.458	m	H7H α
H7HN	4.384	m	P6H α
H7HN	3.462	m	P6H δ
H7HN	3.348	s	H7H β
H7HN	3.146	m	H7H β '
H7HN	1.162	w	V4aH γ
H7HN	2.070	w	V4aH β
H7HN	2.500	w	P6H β
H7HN	3.032	w	P8H δ '
Q9HN	4.439	s	P8H α
Q9HN	4.353	w	Q9H α
Q9HN	2.510	m	Q9H γ
Q9HN	2.175	w	Q9H β
Q9HN	2.020	m	Q9H β '
Q9HN	1.919	w	P8H β '
T10HN	1.273	s	T10H γ
T10HN	1.942	w	P8H β '
T10HN	2.036	w	Q9H β '
T10HN	2.16	w	Q9H β
T10HN	4.337	s	Q9H α
T10HN	4.579	s	T10H α
A11HN	4.136	s	A11H α
F12HN	4.773	m	F12H α

F12HN	3.350	m	F12H β
F12HN	3.116	s	F12H β '
C13HN	4.773	s	F12H α
C13HN	4.431	s	C13H α
C13HN	4.127	w	A11H α
C13HN	3.319	m	F12H β
C13HN	3.085	m	F12H β '
C13HN	1.297	w	T10H γ